Profiling MicroRNAs To Identify Candidate Posttranscriptional Regulators of Hepatic Glucose Metabolism in Rainbow Trout (*Oncorhynchus mykiss*)

Daniel Kostyniuk

Thesis submitted to the
Faculty of Science of the
University of Ottawa
in partial fulfillment of the requirements for the
MSc degree in Biology

Department of Biology
Faculty of Science
University of Ottawa

Abstract

Rainbow trout are an important salmonid species whose poor utilization of dietary carbohydrates spurred research investigating molecular and physiological components of its glucoregulation. Among the environmental factors described to exert robust changes in glucose metabolism in rainbow trout, nutrition and social stress are among the most studied: Diets exceeding 20% of carbohydrates and chronic social stress induce hyperglycemia in adult and juvenile rainbow trout, respectively. Common to both responses is a contribution of hepatic *de novo* gluconeogenesis, which has been described to evade repression in response to high dietary carbohydrate content and to be stimulated in subordinate rainbow trout. Compared to previous studies investigating the regulation of hepatic gluconeogenesis at the molecular level, the recent publication of the annotated rainbow trout genome has opened novel possibilities to investigate paralogue-specific and posttranscriptional regulation of gluconeogenesis. In this thesis, I identify and describe the regulation of the novel phosphoenolpyruvate carboxykinase paralogue *pck2b* in rainbow trout and identify specific miRNA candidates predicted to contribute to gene paralogue-specific regulation of gluconeogenesis in nutritional and social contexts using small RNA next generation sequencing, *real-time* RT-PCR and *in silico* target prediction approaches. In nutritional and social status experiments, *in silico* predicted targets of differentially expressed hepatic miRNAs are enriched for gluconeogenesis regulation, suggesting a posttranscriptional component in regulating gluconeogenic transcript abundance. Differentially expressed hepatic miRNAs in both experiments comprise evolutionarily conserved and teleost-specific miRNAs, and are indicative of both environmental factor-specific and common regulation of gluconeogenesis transcripts in rainbow trout liver. Together this work provides novel comparative insight into hepatic miRNA-

dependent glucoregulation and identifies several specific candidate miRNAs for future functional validation in hepatic glucoregulation in rainbow trout.

Résumé

La truite arc-en-ciel est une espèce importante de salmonidés dont la faible utilisation des glucides alimentaires a stimulé la recherche sur les composantes moléculaires et physiologiques de sa glucorégulation. Parmi les facteurs environnementaux décrits pour exercer des changements robustes dans le métabolisme du glucose chez la truite arc-en-ciel, la nutrition et le stress social sont parmi les plus étudiés : Les régimes dépassant 20 % des glucides et le stress social chronique provoquent l'hyperglycémie chez la truite arc-en-ciel adulte et juvénile, respectivement. Les deux réponses ont en commun une contribution de la gluconéogenèse hépatique de novo, qui a été décrite comme un évitement de la répression en réponse à une teneur élevée en glucides alimentaires et comme étant stimulée chez la truite arc-en-ciel de niveau inférieur. Par rapport aux études antérieures sur la régulation de la gluconéogenèse hépatique au niveau moléculaire, la publication récente du génome annoté de la truite arc-en-ciel a ouvert de nouvelles possibilités pour étudier la régulation paralogique et post-transcriptionnelle de la gluconéogenèse. Dans cette thèse, j'identifie et décrit la régulation du nouveau paralogue de phosphoénolpyruvate carboxykinase pck2b chez la truite arc-en-ciel et j'identifie des candidats miRNA spécifiques qui devraient contribuer à la régulation de la gluconéogenèse paralogue génétique dans les contextes nutritionnel et social en utilisant les approches de séquençage des petits ARN nouvelle génération, RT-PCR temps réel et de prédiction *in silico* des cibles. Dans les expériences sur l'état nutritionnel et social, les cibles prévues *in silico* des miARNs hépatiques à expression différentielle sont enrichies en régulation de la gluconéogenèse, ce qui suggère un composant post-transcriptionnel

dans la régulation de l'abondance de la transcription gluconéogénique. Dans les deux expériences, le miARN hépatique exprimé différemment comprend le miARN conservé au cours de l'évolution et le miARN spécifique à la téléostéose, et indique une régulation à la fois spécifique des facteurs environnementaux et commune des transcrits de la gluconéogenèse dans le foie de la truite arc-en-ciel. L'ensemble de ces travaux fournit un nouvel aperçu comparatif de la glucorégulation hépatique miRNA-dépendante et identifie plusieurs miARN candidats spécifiques pour une validation fonctionnelle future de la glucorégulation hépatique chez la truite arc-en-ciel.

Acknowledgements

To begin I would like to express my sincerest gratitude to my supervisor, Dr. Jan Mennigen, for his enthusiasm, guidance and support throughout the course of my Master's. His positivity, patience and energy propelled me through this project. He helped me develop a greater understanding and appreciation for research and science, and I am grateful to him for this opportunity and am proud of the research we have published together. Second, I would like to thank my committee members, Dr. Kathleen Gilmour, Dr. Tom Moon and Dr. Ken Storey, for their time, feedback and comments on my project. I am fortunate to have been able to work with such knowledgeable scientists. Additionally, I am extremely grateful for my experience at INRA in Saint-Pée-sur-Nivelle in France under the supervision of Dr. Lucie Marandel and Vincent Veron. I learned valuable lessons in trouble shooting and the experiences and connections I made are invaluable. Thanks also to Jingwei Liu for helping me get to know the other students and researchers so I had people to eat lunch with. I would also like to extend my thanks to the Mennigen and Gilmour labs. Your support the past three years collectively has been amazing, and I am lucky to be a part and collaborate with a great group of people. A special thank you to Carol Best for her

help all the way back to when I was doing my coop and honours project, Jon Tea for also working at the lab at ridiculous hours of the night, Mais Jubouri for helping kickstart the Mennigen lab and everyone else who has helped along the way. To all those that I have been fortunate enough to collaborate with over my time at UOttawa who have not already been mentioned, Rubén Francisco Martínez López, Johnathon Forbes, Elie Farhat, and Dr. Wenqing Tu, you all made coming into the lab enjoyable and interesting. Additionally, I am very appreciative of Bill Fletcher, Christine Archer and ACVS for their help with animal care, answering my questions and making it possible to run the experiments.

To my family and friends, for all your support and understanding of my long days, late nights and all-nighters when the qPCR machine was available. Especially my parents Tim and Ambra Kostyniuk who supported me throughout and picked me up from the bus stop many times late at night; and my sisters Anna and Laura Kostyniuk for being my confidants and making me laugh in my times of struggle while being the greatest hypewomen when things were going well, thank you. Finally, thank you Sarah Best for your support and understanding throughout this process, it's been a long one.

Table of Contents

List of Figures

Chapter 1

Chapter 2

Chapter 3

Chapter 4

Chapter 5

List of Tables

Chapter 2

Chapter 3

Chapter 4

Chapter 5

List of Abbreviations

AGO2 argonaute-2
AMPK AMP-activated protein kinase
ANOVA Analysis of variance
ATP Adenosine triphosphate
ADP-GK ADP-specific glucokinase
AKT Protein kinase B
BSA bovine serum albumin
CAD Canadian dollar
CDNA Complementary deoxyribonucleic acid
CHO Carbohydrate
CCR *Cyprinus carpio*
CPTA carnitine palmitoyltransferase
DNA deoxyribonucleic acid
DNL de novo lipogenesis
DRE *Danio rerio*
DROSHA RNase III
EDTA Ethylenediaminetetraacetic acid
EGTA Egtazic acid
FBP Fructose-1,6-bisphosphatase
FDR False discovery rate
FIS1 Mitochondrial fission 1 protein

FASN fatty acid synthase
FRU *Fugu rubripes*
G6PC Glucose 6-phosphatase
GD Genome duplication
GEO Gene expression Omnibus
GI Glucose Intolerant
GO Gene ontology
GP Glycogen phosphorylase
GLUT9 glucose transporter 9
HSL Hormone-sensitive lipase
IPU *Ictalurus punctatus*
IR Insulin receptor
MRNA Mature Ribonucleic acid
MS-222 Tricaine mesylate
MTOR Mammalian target of rapamycin
MYA Million years ago
MFN Mitofusin
MIR MicroRNA
MIRNA microRNA
NADH Nicotinamide adenine dinucleotide + hydrogen
NCBI National Center for Biotechnology Information
NT Nucleotide
OLA *Oryzias latipes*
PAGE Parametric analysis of gene expression
PBS Phosphate-buffered saline
PCA Principal components analysis
PCK Phosphoenolpyruvate Carboxykinase
PCR Polymerase chain reaction
POL *Paralichthys olivaceus*
PRE-MIRNA Precursor-miRNA
PRI-MIRNA Primary miRNA
PYGB Glycogen Phosphorylase Brain
PYGL Glycogen Phosphorylase Liver
RIP-CHIP RNA immunoprecipitation-microarray
RISC RNA-induced silencing complex
RNA Ribonucleic acid
RT Reverse transcriptase
RT-PCR reverse transcription polymerase chain reaction
RA Rate of appearance
S6 Ribosomal protein S6
SD Socially dominant
SDS-PAGE Sodium dodecyl sulfate-Polyacrylamide gel electrophoresis
SEM Standard error of the mean
SI Socially isolated
SS Socially subordinate
SAGD Salmonid-specific genome duplication

SOGA Suppressor Of Glucose
SSA S*almo salar*
TCA Tricarboxylic acid
TGD Teleostspecific genome duplication
TORC1 Insulin-target of rapamycin complex 1
TMG Resorption maximum for glucose
UNG Uracil N-Glycosylase
UTR Untranslated region
XPO5 Exportin-5
ΔG Gibbs free energy

Chapter 1: Introduction

This chapter is partially based on my contribution to the following review paper: Best C, Ikert H, ***Kostyniuk DJ****, Craig PM, Navarro-Martin L, Marandel L, Mennigen JA. 2018. Epigenetics in teleost fish: From molecular mechanisms to physiological phenotypes. Comp. Biochem. Physiol. B Biochem. Mol. Biol. 224: 210-244.*

1.1. Rainbow trout as a research model in the comparative physiology of metabolism and its economic importance

Rainbow trout (*Oncorhynchus mykiss*) are a salmonid species which are native to Pacific drainages of North America but has been introduced to water systems on all continents except Antarctica since 1874. Rainbow trout are an important fish species in the field of comparative physiology (Best *et al.* 2018). Research in the field of rainbow trout energy metabolism has received increased attention, owing to the fact that rainbow trout have global economic importance as an aquaculture and angling species. Indeed, the economic importance of rainbow trout has experienced significant growth since the 1960s, reaching, according to the Food and Agriculture Organization of the United Nations, an estimated global production volume of more than 800,000 t at an economic value exceeding 2 billion CAD (www.fao.org). Metabolically, carnivorous rainbow trout exhibit a 'glucose intolerant' phenotype (Phillips *et al.* 1948, Bergot 1979, Marandel *et al.* 2015, Marandel, Lepais, *et al.* 2016), and exhibit pronounced postprandial hyperglycemia in response to dietary carbohydrate amounts which exceed 20% of the diet's macronutrient composition (Legate *et al.* 2001). Because current rainbow trout aquaculture operations rely on the ecologically and economically unsustainable practice of using fish meal as the principal protein ingredient in dietary formulations (Naylor *et al.* 2009, Panserat *et al.* 2013), significant research efforts have been geared towards the determination of underlying molecular and physiological mechanisms of glucose intolerance in this species. One particular goal is to gain insight into molecular and physiological constraints of carbohydrate utilization in rainbow trout in order to develop novel diets which to large extents replace dietary proteins with sustainable carbohydrate-rich alternatives such as, for example, plant-based diets (Panserat *et al.* 2013).

Aspects of rainbow trout energy metabolism in general (Gilmour *et al.* 2005, 2017, Kostyniuk *et al.* 2018), and glucose metabolism in particular (DiBattista *et al.* 2006, Gilmour *et al.* 2012, Culbert and Gilmour 2016) have also been investigated in social status experiments, as small groups of juvenile rainbow trout establish hierarchies with dominant and subordinate fish that incur different metabolic costs (Metcalfe 1986). While utilization of metabolic fuels such as lipids and amino acids play a predominant role in rainbow trout energy metabolism, a number of specific rainbow trout tissues, including the brain, spleen, kidney and hindgut, have comparatively high rates of glucose utilization compared with other tissues (Blasco *et al.* 2001). While these demands can be met entirely by endogenous *de novo* production of glucose in the absence of dietary carbohydrates (Panserat *et al.* 2013), both chronical activation of the endocrine stress axis and fasting experienced by socially subordinate trout have been shown to affect glucose metabolism by increasing systemic circulating glucose concentrations (DiBattista *et al.* 2006, Gilmour *et al.* 2012, Culbert and Gilmour 2016). In sum, among environmental factors shown to affect rainbow trout glucose homeostasis (reviewed by Polakof *et al.* 2011, 2012, Panserat *et al.* 2013), both nutritional and social factors have repeatedly been shown to exert robust effects.

1.2. Hepatic gluconeogenesis in rainbow trout and its regulation in response to dietary carbohydrates and social stress

Glucose metabolism in response to high amounts of dietary carbohydrates has been comparatively well-described at different levels of biological organization due to the rainbow trout's particular 'glucose intolerant' (GI) phenotype. At the organismal level (**Fig. 1A**), the physiology of glucose ingestion and excretion has been described, and evidence suggests a role for gastrointestinal absorption of digestible carbohydrates in diet-induced glucose intolerance in rainbow trout, as intestinal glucose absorption may be higher compared to amino acids in rainbow

trout (Mannerstrom *et al.* 2001, Subramaniam *et al.* 2016). Conversely, at the level of excretion, evidence points to an involvement of the kidney: At the resorption maximum for glucose (TmG), plasma glucose concentration is 22 mmol/l in rainbow trout (Bucking and Wood 2005), twice the estimated amount of the 11 mmol/l in healthy humans and matching the rate observed in diabetic humans (Wilding 2014). This suggests that increased resorption capacity of glucose in the kidney also contributes to the GI phenotype in rainbow trout. In addition to net ingestion and excretion, several tissues act in concert to regulate glucose homeostasis, and tissue-specific mechanisms have been described to contribute to the glucose intolerant phenotype in rainbow trout muscle and liver.

Briefly, glucoregulatory pathways in the liver (**Fig. 1B**) can be separated into catabolic (glycolysis) and anabolic pathways (gluconeogenesis), which are linked to short term storage and release of glycogen via glycogen synthase and glycogen phosphorylase. Both glycolysis and gluconeogenesis are linked to the Krebs cycle. Under aerobic conditions, the Krebs cycle mediates complete oxidation of glucose using acetyl-CoA derived from glycolysis. In this process, nicotinamide adenine dinucleotide + hydrogen (NADH) generated in the Krebs cycle fuels mitochondrial oxidative phosphorylation to yield 38 molecules of adenosine triphosphate (ATP) per molecule of glucose. In addition to aerobic conditions, the glycolytic pathway remains active under anaerobic conditions, producing lactate as metabolic end-product of a process which generates 2 ATP per molecule of glucose. Conversely, the Krebs cycle, under conditions such as fasting which favour *de novo* gluconeogenesis, also metabolizes gluconeogenic amino acids to fuel gluconeogenesis, complementing additional cellular sources such as lactate and glycerol in this process. Finally, the liver has the capacity to metabolize glucose into fatty acids (via acetyl CoA in the Krebs cycle) and triglycerides (via glycolysis). The regulation of these pathways is, to a

large extent, regulated by glucoregulatory endocrine factors, including insulin (Plagnes-Juan *et al.* 2008, Dai *et al.* 2013).

While a low peripheral glucose utilization by white and red muscle tissue, at least in part linked to reduced responses to insulin, has been hypothesized to contribute to glucose 'intolerance' in rainbow trout (Blasco *et al.* 2001, Forbes *et al.* 2019) on the one hand, the strong induction of glucokinase transcripts in response to dietary carbohydrates and insulin (Panserat *et al.* 2000), and the induction of glycogen synthase activity in response to insulin (Pereira *et al.* 1995) provides evidence of the rainbow trout liver's capacity to metabolize and store available glucose. Conversely, sustained *de novo* gluconeogenesis transcript abundance and enzymatic activity in rainbow trout following ingestion of dietary carbohydrates and amino acids in the liver, the most important site of gluconeogenesis (Haman *et al.* 1997), has been identified as a possible mechanism contributing to glucose 'intolerance' (Kirchner *et al.* 2003, Marandel, Dai, *et al.* 2016, Marandel *et al.* 2019). A role for hepatic gluconeogenesis in rainbow trout glucose 'intolerance' has also been confirmed at the flux level, as rainbow trout only moderately inhibit the rate of appearance (R_a) compared to humans/mammals when challenged with a high carbohydrate load (Choi and Weber 2015). Additionally, several lines of evidence have pointed to a reduced dietary carbohydrate-dependent stimulation of hepatic *de novo* lipogenesis and triglyceride synthesis in rainbow trout (Panserat *et al.* 2009, Skiba-Cassy *et al.* 2009, Mennigen, Martyniuk, *et al.* 2014, Dai *et al.* 2015), potentially limiting the metabolic utilization of dietary carbohydrates towards synthesis of fatty acids and its triesters via acetyl CoA and glycerol. Finally, hepatic insulin signaling in rainbow trout has been linked to hyperglycemia in response to dietary carbohydrates. Indeed, the rainbow trout hepatic insulin-target of rapamycin complex 1 (TORC1) pathway-dependent stimulation of the lipogenic fatty acid synthase and suppression of gluconeogenic gene

glucose-6-phosphatase is much more responsive to dietary protein compared to dietary carbohydrates (Seiliez *et al.* 2011, Dai *et al.* 2013, 2014).

In addition to nutritional factors, regulation of rainbow trout glucose metabolism has also been investigated in the context of social status, especially in juvenile rainbow trout. Small groups of juvenile rainbow trout establish linear dominance hierarchies as a result of competition for shelter and feeding territories (Metcalfe 1986). Socially dominant fish within these hierarchies monopolize preferred territories, displaying high levels of aggression towards their socially subordinate counterparts, which experience chronic stress and fasting responses (DiBattista *et al.* 2006, Gilmour *et al.* 2012, Kostyniuk *et al.* 2018). Previous studies revealed an increased potential for hepatic glucose liberation in socially subordinate trout compared to socially dominant fish. Socially subordinate trout not only display an increased mobilization of stored hepatic glycogen compared to socially dominant trout, as evidenced by lower glycogen concentrations and higher glycogen phosphorylase activity in subordinate fish (Gilmour *et al.* 2012), but also exhibit enhanced gluconeogenic and decreased glycolytic potential, supported by increased hepatic phosphoenolpyruvate carboxykinase activity and decreased pyruvate kinase activity (DiBattista *et al.* 2006). These changes are in part dependent on the glucocorticoid stress hormone cortisol and fasting, and mechanistically link chronically elevated cortisol levels in socially subordinate trout to reported increases in circulating glucose concentrations (Culbert and Gilmour 2016). While the carbohydrate utilization in rainbow trout muscle is comparatively poor, circulating glucose nevertheless represents an important fuel source for several specific rainbow trout tissues critically involved in the coping with stress, such as the brain, heart and erythrocytes which have high carbohydrate demands (Legate *et al.* 2001, Moon 2001, Polakof *et al.* 2011). Overall these studies therefore suggest a crucial role for gluconeogenesis in metabolic responses to chronic stress in

juvenile rainbow trout which is largely mediated by cortisol and/or fasting. While not investigated in a social hierarchy context, norepinephrine, a neuronal component of the stress response in rainbow trout has also been linked to increases in hepatic glucose production at the metabolic flux level (Weber and Shanghavi 2000). Together, both nutritional and social stress stimuli are robust regulators of hepatic trout gluconeogenesis at the transcript, enzyme and metabolite level, providing excellent systems to begin the investigate the role of novel emerging mechanisms which may be involved in their regulation in this species.

A

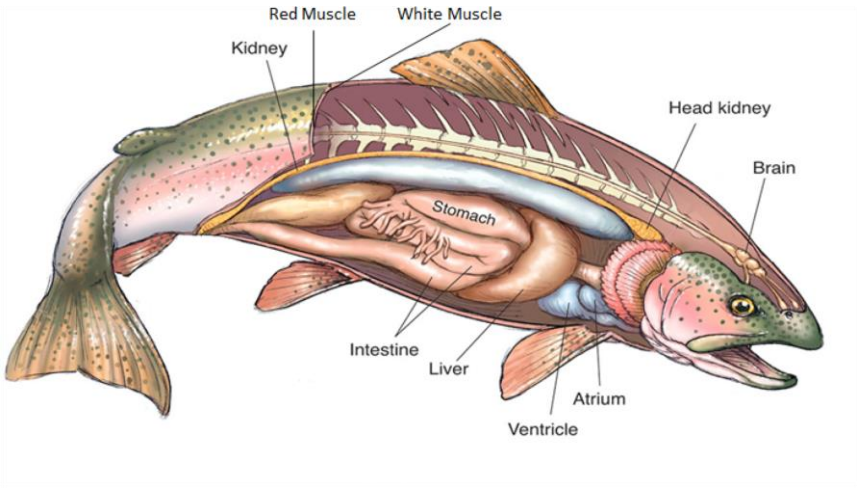

B

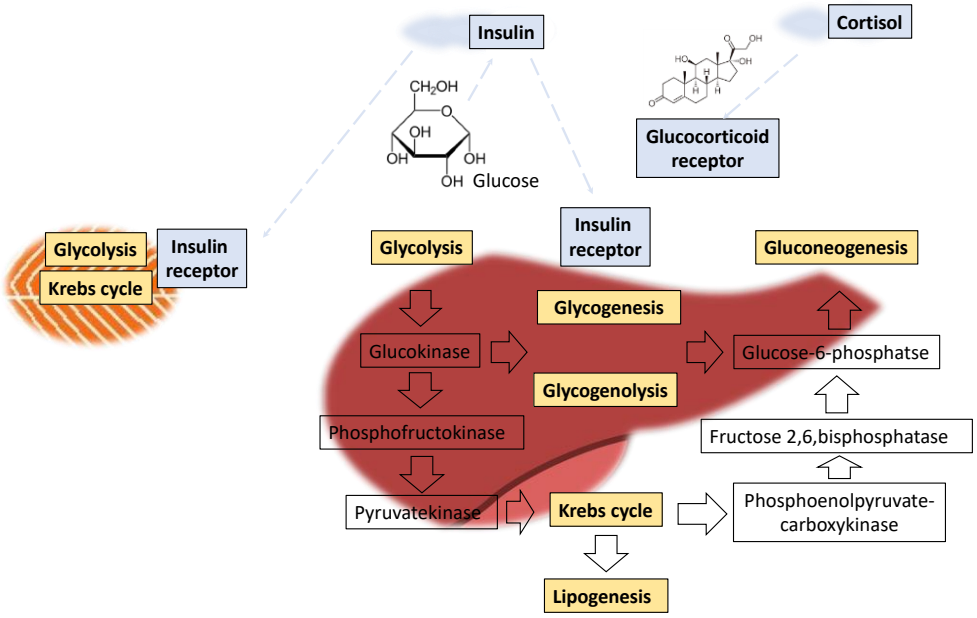

Figure 1. *Important tissues involved in rainbow trout glucose homeostasis* (**A**) *and hepatic cellular signaling and metabolic pathways* (**B**) *involved in rainbow trout glucoregulation. Key glucoregulatory pathways are indicated in yellow, endocrine regulators of these pathways are indicated in blue*.

1.3. Recent advances in rainbow trout genome resources: Implications for the study of epigenetic regulation of gluconeogenic gene expression in a complex genome

In 2014, the first draft of an annotated rainbow trout genome was published, making it the first published salmonid genome (Berthelot *et al.* 2014). This initially annotated genome draft allowed for the identification of several gluconeogenic gene paralogues in the complex rainbow trout genome (Marandel *et al.* 2015). Several gluconeogenic gene paralogues exist, as rainbow trout have, in addition to a vertebrate- and teleost-specific genome duplications, undergone another, salmonid-specific genome duplication 80 million years ago which has resulted in the presence of additional paralogues differentially retained in the genome (Berthelot *et al.* 2014, Lien *et al.* 2016). Notably, the first rainbow trout genome draft allowed for the identification of a novel teleost-specific description of glucose-6-phosphatase b2 genes, of which two paralogues, glucose-6-phosphatase b2a and glucose-6-phosphatase b2b, exist (Marandel, Dai, *et al.* 2016). In addition, the identification of novel gluconeogenic gene paralogues allowed, for the first time, the specific quantification of individual gluconeogenic transcript abundances under experimental conditions. This is in contrast to previously reported unspecific and simultaneous quantification of multiple paralogue mRNAs by single *real-time* reverse transcription polymerase chain reaction (RT-PCR) assays. These previously used unspecific approaches potentially masked important paralogue-specific gluconeogenic transcript regulation. This is important, as both temporal and spatial

(tissue) differences in gluconeogenic transcript abundance may be indicative of the fate and functional role of gluconeogenic gene paralogues retained in the rainbow trout genome following the salmonid-specific genome duplication event. Following genome duplication, paralogues may undergo different fates: Duplicated genes can either be lost or fixed and maintained with three distinct outcomes, i.e. neofunctionalization, sub-functionalization, and conservation of function (Hahn 2009). Gene duplication via genome duplication is thus a source of genetic novelty and can lead to adaptive innovation. In this context, the study of duplicated gluconeogenic genes has led to novel hypothesis towards a better understanding of the glucose intolerant phenotype in rainbow trout. Indeed, while glucose-6 phosphatase 1a and glucose-6 phosphatase 1b paralogues in rainbow trout have been shown to be suppressed in response to dietary carbohydrates (Marandel *et al.* 2015) and insulin (Marandel, Dai, *et al.* 2016) similar to the situation in glucose tolerant mammals, the newly described glucose-6-phosphatase b2a and glucose-6-phosphatase b2b paralogues exhibited an atypical induction in response to these stimuli, providing evidence for a paralogue specific role in the observed lack of suppression of *de novo* gluconeogenesis reported at the enzymatic (Kirchner *et al.* 2003, Panserat *et al.* 2013) and glucose flux level (Choi and Weber 2015). Therefore, a major advantage in terms of molecular resources provided by the sequencing and annotation of the rainbow trout genome is the possibility to investigate the mRNA abundance of specific paralogues of gluconeogenic genes in salmonids in experimental contexts.

A second major advantage of the published rainbow trout genome is the possibility to use positional genome information to address epigenetic mechanisms in the context of the complex rainbow trout genome (Bobe *et al.* 2016, Best *et al.* 2018). Indeed, in the context of gluconeogenic gene regulation, DNA level epigenetic mechanisms, specifically histone modification marks associated with chromatin accessibility and DNA methylation, have been profiled in newly

available putative promoter regions of rainbow trout gluconeogenic gene paralogues (Marandel, Lepais, *et al.* 2016). At the post-transcriptional level, the rainbow trout genome sequence opens up the possibility to investigate microRNA-dependent (miRNA-dependent) regulation of gluconeogenic gene expression (Mennigen 2016): Firstly, the publication of the rainbow trout genome allows for the identification of conserved and teleost- or salmonid-specific miRNA loci (Juanchich *et al.* 2016), which in turn permits the profiling of specific miRNAs using next generation sequencing and/or targeted PCR based methods. Secondly, the rainbow trout genome, in addition to next generation sequencing transcript data, allows for the extraction of gluconeogenic paralogue specific 3'UTR sequence information (Mennigen and Zhang 2016). This is important, as it enables the utilization of *in silico* prediction tools to identify relationships between differentially regulated miRNAs and gluconeogenic target transcripts and to subsequently test functional interactions between miRNA and 3'UTRs *in vitro*. Indeed, while specific hepatic miRNAs have been shown to be functionally involved in the regulation of organismal level glucose homeostasis in rainbow trout prior to the publication of the rainbow trout genome (Mennigen, Martyniuk, *et al.* 2014), knowledge of the miRNA and 3'UTR repertoires facilitate the prediction of functional consequences in an integrative manner at the pathway level, an important feature given the promiscuity of miRNA-mRNA interactions.

1.4. miRNA biogenesis, function and roles in the regulation of hepatic glucose metabolism

MicroRNAs are short, non-protein coding RNA molecules which are ~22 nucleotides (nt) in length and are produced mostly via the canonical pathway (He and Hannon 2004). Canonical miRNA biogenesis (**Fig. 2**) is initiated in the nucleus, where primary miRNAs (pri-miRNAs) are transcribed from genes by polymerase II. The resulting pri-mRNA transcripts often form hairpin

loops, which are several hundred nucleotides long. The pri-miRNAs are then further processed by the RNase III DROSHA to yield precursor miRNA (pre-miRNA), which possesses a characteristic stem-loop structure which is ~70-100 nt long, as well as a 3'overhang (Lee *et al.* 2006). The pre-miRNA is subsequently recognized and transported from the nucleus to the cytoplasm by exportin 5, a process that is dependent on ATP. In the cytoplasm, pre-miRNAs are further processed by the RNAse III DICER to yield mature miRNA (Tijsterman and Plasterk 2004). Mature miRNA is able to bind to the 3'UTR of mRNA through complementary base pairing as part of the RNA-induced silencing complex (RISC). The most critical component of the RISC is the argonaute 2 protein, which mediates miRNA-target mRNA binding (Pratt and MacRae 2009). The key sequence in the miRNA in terms of binding to an mRNA target is generally considered to be the so-called seed region, which span nucleotides 2-8 of the 5' end. Functionally, binding of the RISC results in either RNA degradation, inhibition of translation initiation or decreased translation efficiency (Bartel 2009, Fabian *et al.* 2010), thus ultimately resulting in a reduction of functional protein. Recent *in vitro* knock-down studies have identified DROSHA as the rate-limiting step in the canonical miRNA biogenesis pathway. Canonically processed miRNAs are generally transcribed by Polymerase II, and are located in intergenic regions, where they may occur as clusters, defined as two or more miRNA which are transcribed from miRNA genes that are physically adjacent (Lai and Vera 2013). While quantitatively less important compared to the canonical pathway, RNA splicing events can give rise to miRNAs, which are often encoded in gene introns and act to support the host gene's biological function (Horie *et al.* 2010). Recent evidence suggests that biological activity of miRNAs is regulated not only at the biogenesis level, but also at the level of their stability and half-life. As revealed by pulse-chasing experiments, miRNA half-lives vary widely (Marzi *et al.* 2016), ranging from short lived miRNAs (4h-14h turn-

over time) to long-lived miRNAs (>24h turn-over time). The cellular environment, the nature and abundance of the target mRNA binding sites (Chen *et al.* 2011, Rüegger and Großhans 2012, Wightman *et al.* 2018) all appear to regulate specific miRNA turnover rates, which are mediated by a diverse array of degrading enzymes (Best *et al.* 2018). However, in contrast to the canonical miRNA biogenesis pathway, these enzymes appear to be highly selective in their regulation of targets, the governing principles of which remain poorly understood (Best *et al.* 2018).

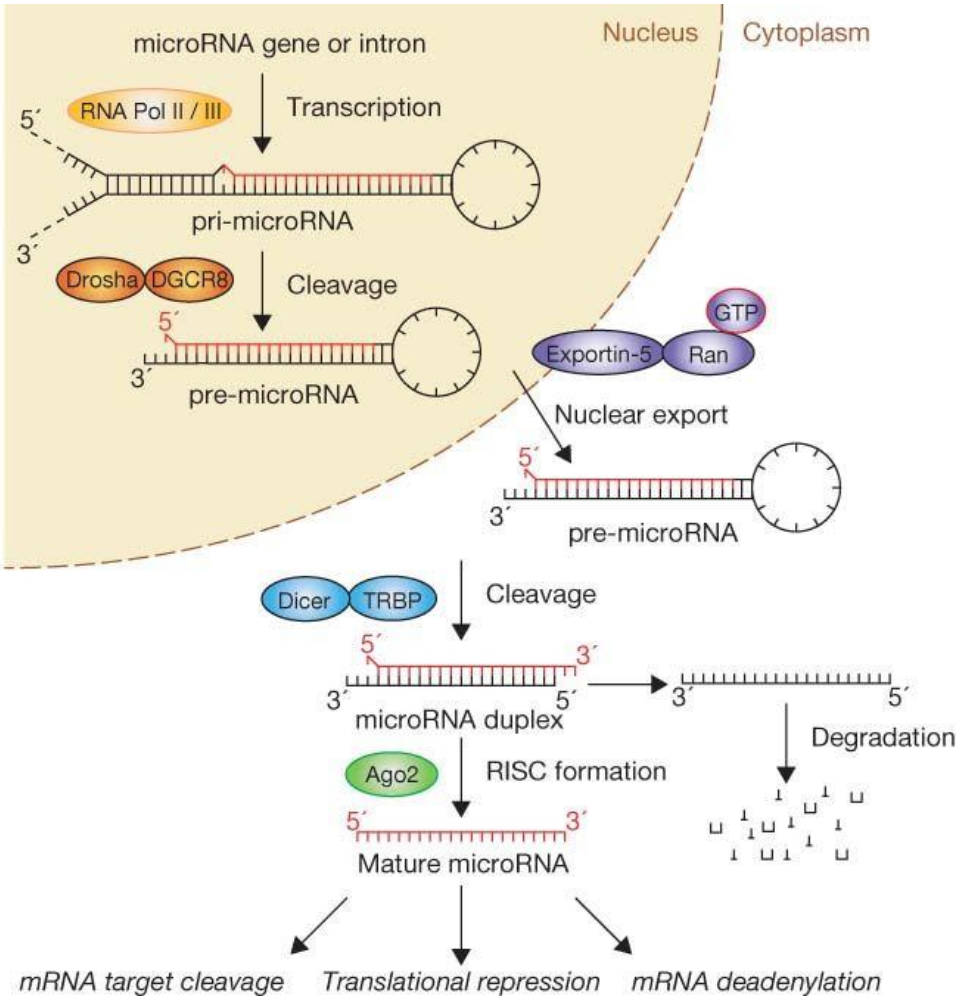

Figure 2. *Schematic illustration of the canonical miRNA biogenesis pathway as described by Winter et al. 2009.*

Functionally, miRNAs mode of action is, similarly to transcription factors, uniquely suited to coordinate gene expression within or between metabolic pathways by acting on both multiple or individual target gene transcripts (**Fig. 3**). Because important metabolic pathways have long been known to be regulated, albeit by no means exclusively, at the transcriptional level (Desvergne *et al.* 2006), the important roles as posttranscriptional regulators of metabolism (Rottiers and Näär 2012), which emerged following the discovery of miRNAs, are not completely surprising. Indeed, following the identification of hepatic miRNA dysregulation in rodent models of diabetes (Li *et al.* 2009, Zhao *et al.* 2009, Herrera *et al.* 2010), specific roles for miRNAs in hepatic glucoregulation have rapidly emerged. Together, these studies have shown that hepatic miRNAs may either directly regulate individual or multiple gluconeogenic gene to control *de novo* synthesis of glucose (Li *et al.* 2015, Zhuo *et al.* 2016) or may (additionally) affect upstream signaling of important metabolic pathways, such as the insulin pathway (reviewed by Mirra *et al.* 2018, Nigi *et al.* 2018), which is involved in the regulation of gluconeogenesis. Regardless of the specific mode of action these studies clearly show a role for miRNAs in hepatic glucoregulation via action on hepatic gluconeogenesis. However, with the exception of a proof of principle study confirming a minor, evolutionarily conserved role of the liver specific and abundant miRNA-122 in glucoregulation in rainbow trout compared to mammals presumably linked to its well described lipogenic role (Tsai *et al.* 2012, Mennigen, Martyniuk, *et al.* 2014), glucoregulatory function of miRNAs in comparative models remain essentially unstudied. Because meaningful miRNA-mRNA target relationships are often identified by the criteria of deep evolutionary conservation (Mennigen 2016, Best *et al.* 2018), such comparative studies offer potential insight into evolutionary old and therefore important miRNA-mRNA target relationships important in hepatic control of glucose metabolism. On the other hand, comparative studies may provide insight into

extensive rewiring of miRNA-mRNA relationships and the role of species-specific miRNAs in specific glucoregulatory phenotypes. The latter consideration is potentially a very important mechanisms in different phenotypes investigated in comparative physiology, as only 10% of miRNA-mRNA relationship are estimated to be evolutionarily conserved between fish and relatively well studied mammalian species (Xu *et al.* 2013).

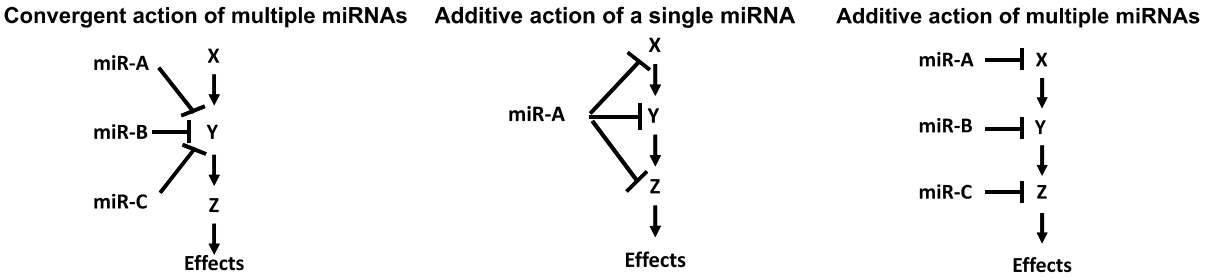

Figure 3. *Conceptual view of miRNA dependent regulation of metabolic pathways. Adapted from* Dumortier *et al.* 2013 .

1.5. Thesis objectives and approach

The overall objective of the thesis is to identify candidate miRNA-mRNA pairs which may play a functional role in the regulation of the gluconeogenic pathway in rainbow trout. In addition to advancing our knowledge on the evolution of miRNA-mRNA networks regulating this evolutionarily ancient and important metabolic pathway (Miyamoto and Amrein 2017), this work will also provide the basis to functionally explore potential posttranscriptional mechanisms related to specific hepatic origins of glucose 'intolerance' in rainbow trout. Given that the rainbow trout genome is complex and contains many gluconeogenic paralogues, this thesis will also provide the necessary framework to probe specific miRNA dependent regulation of gluconeogenic paralogues, which may specifically be linked to hepatic origins of glucose intolerance observed in this species

(Marandel, Dai, *et al.* 2016). The thesis is divided into three published data chapters and a discussion, which correspond to four specific objectives as follows.

(1) Since the original publication of the rainbow trout genome (Berthelot *et al.* 2014), extensive progress has been made to update the annotation of the rainbow trout genome (Macqueen *et al.* 2017). Because both the ability to profile specific gluconeogenic gene paralogues as well as knowledge of their 3'UTRs are critical to investigate miRNA dependent regulatory mechanisms, the first objective was to verify that all gluconeogenic paralogues had indeed been identified in rainbow trout, and that 3'UTRs had been correctly annotated. Because this search revealed the presence of a novel, yet uncharacterized phosphoenolpyruvate 2 paralogue, I characterized its regulation compared to other paralogues in physiological conditions known to regulate hepatic gluconeogenic pathway activity.

(2) The following chapters sought to identify differentially regulated miRNAs in the liver of rainbow trout which, following a short-term fast, had been refed diets with different carbohydrates contents known to differentially affect circulating glucose concentrations and gluconeogenic paralogue expression. Based on this expression profile, I identified predicted miRNA-gluconeogenic gene relationships using an *in silico* approach.

(3) Using the same strategy described under Objective 2, I profiled miRNAs and quantified gluconeogenic gene paralogue expression in livers of dominant and subordinate rainbow

trout to identify predicted miRNA-gluconeogenic gene relationships using an *in silico* approach.

(4) The final objective of the thesis was to integrate findings from both previous studies to establish consistent relationships between differentially regulated miRNAs and gluconeogenic paralogue expression. This approach was used to gain insight into potentially important posttranscriptional regulatory switches consistently involved in posttranscriptional regulation of gluconeogenic paralogue expression in the rainbow trout liver under physiological conditions known to affect hepatic gluconeogenesis on the one hand, and to identify potential stimulus-specific posttranscriptional regulation of the gluconeogenic pathway on the other. Based on these analyses, specifically identified miRNA gluconeogenic paralogue transcript target pairs are proposed for future mechanistic physiological study in (atypical) hepatic rainbow trout glucoregulation.

Chapter 2: The salmonid-specific molecular evolution of phosphoenolpyruvate carboxykinase paralogues and their regulation in response to dietary carbohydrates and social status

This chapter has been published as Marandel L, **Kostyniuk DJ***, Best C, Forbes JLI, Liu J, Panserat S, Mennigen JA Pck-ing up steam: Widening the salmonid gluconeogenic gene duplication trail. Gene. 2019 698:129-140. Authors indicated by asterisk share first authorship of the published manuscript.*

***Statement of contribution**: The work in this chapter at uOttawa and during a research visit to INRA, St.Pée-sur-Nivelle France, financed through a MITACS Globalink scholarship. First authorship of the resulting manuscript is shared between Dr. Lucie Marandel (host at INRA) and myself. I identified the novel paralogue, and conducted all real-time RT-PCR assays with the exception of assays for the juvenile hypoxia experiment in larvae, which was conducted by Dr. Jingwei Liu at INRA. RNA samples from different exposures were obtained at OttawaU in collaboration with Dr. Gilmour (social status experiment; fasting and cortisol implant experiment), or INRA France (dietary carbohydrate experiment, hypoxia experiment). Phylogenetic analyses were constructed under the guidance of Dr. Lucie Marandel.*

Publisher allows the reproduction of the manuscript in full within the context of my MSc thesis.

https://www.elsevier.com/about/policies/copyright/permissions

Contents lists available at ScienceDirect

Gene

journal homepage: www.elsevier.com/locate/gene

Research paper

Pck-ing up steam: Widening the salmonid gluconeogenic gene duplication trail

L. Marandel[a,1], D.J. Kostyniuk[b,1], C. Best[b], J.L.I. Forbes[b], J. Liu[a], S. Panserat[a], J.A. Mennigen[b,*]

[a] INRA, Université de Pau et Pays d'Adour, UMR 1419, Nutrition, Metabolism and Aquaculture, Saint Pée-sur-Nivelle F-64310, France
[b] Department of Biology, University of Ottawa, Ottawa, Ontario K1N 6N5, Canada

ARTICLE INFO

Keywords:
Rainbow trout
Teleost
Phosphoenolpyruvate carboxykinase
Duplicated genes
Gluconeogenesis glucose intolerance

ABSTRACT

Rainbow trout have, as salmonid fish species, undergone sequential genome duplication events in their evolutionary history. In addition to a teleost-specific whole genome duplication approximately 320–350 million years ago, rainbow trout and salmonids in general underwent an additional salmonid lineage-specific genome duplication event approximately 80 million years ago. Through the recent sequencing of salmonid genome sequences, including the rainbow trout, the identification and study of duplicated genes has become available. A particular focus of interest has been the evolution and regulation of rainbow trout gluconeogenic genes, as recent molecular and gene expression evidence points to a possible contribution of previously uncharacterized gluconeogenic gene paralogues to the rainbow trout long-studied glucose intolerant phenotype. Since the publication of the initial rainbow trout genome draft, resequencing and annotation have further improved genome coverage. Taking advantage of these recent improvements, we here identify a salmonid-specific genome duplication of ancestral mitochondrial phosphoenolpyruvate carboxykinase 2 isoenzyme, we termed *pck2a* and *pck2b*. Cytosolic phosphoenolpyruvate carboxykinase (*Pck1*) and, more recently mitochondrial *Pck2*, are considered to be the rate-limiting enzymes in *de novo* gluconeogenesis. Following *in silico* confirmation of salmonid *pck2a* and *pck2b* evolutionary history, we simultaneously profiled cytosolic *pck1* and mitochondrial *pck2a* and *pck2b* expression in rainbow trout liver under several experimental conditions known to regulate hepatic gluconeogenesis. Cytosolic *pck1* abundance was increased by nutritional (diets with a high protein to carbohydrate ratio compared to diets with a low carbohydrate to protein ratio) and glucoregulatory endocrine factors (glucagon and cortisol), revealing that the well-described transcriptional regulation of *pck1* in mammals is present in rainbow trout. Conversely, and in contrast to mammals, we here describe endocrine regulation of *pck2a* (decrease in abundance in response to glucagon infusion), and nutritional, social-status-dependent and hypoxia-dependent regulation of *pck2b*. Specifically, *pck2b* transcript abundance increased in trout fed a diet with a low protein to carbohydrate ratio compared to a diet with a high protein to carbohydrate ratio, in dominant fish compared to subordinate fish as well as hypoxia. This specific and differential expression of rainbow trout *pck2* ohnologues is indicative of functional diversification, and possible functional consequences are discussed in light of the recently highlighted gluconeogenic roles of mitochondrial *pck2* in mammalian models.

1. Introduction

Over the last decade, whole genome sequencing of model and non-model species has increased dramatically, especially in teleost fishes and salmonid species in particular (Berthelot et al., 2014; Chen et al., 2014; Hu and Chen, 2015; Lien et al., 2016). The availability of these genome sequences has opened up novel avenues to better understand species diversification at the genome and gene expression level. Indeed, in animal evolution, several whole genome duplications (GD) have occurred, two before or around the vertebrate radiation (termed VGD1 and VGD2 for vertebrate genome duplication events 1 and 2, respectively), one at the radiation of teleost fishes (termed TGD for teleost-specific genome duplication), and finally one at the radiation of salmonids (called SaGD for salmonid-specific genome duplication), which

Abbreviations: pck1, phosphoenolpyruvate carboxykinase 1 (cytosolic); pck2, phosphoenolpyruvate carboxykinase 2 (mitochondrial); SaGD, salmonid specific genome duplication; GD, genome duplication; PEP, phosphoenolpyruvate; GTP, guanosine triphosphate

* Corresponding author.
E-mail address: jan.mennigen@uottawa.ca (J.A. Mennigen).

[1] These authors contributed equally to the present work.

https://doi.org/10.1016/j.gene.2019.02.079
Received 3 December 2018; Received in revised form 3 February 2019; Accepted 21 February 2019
Available online 05 March 2019
0378-1119/

gave rise to new genetic raw material for (molecular) evolution. Indeed, after a GD event, several scenarios can occur, and duplicated genes can either be lost or fixed and maintained with three distinct outcomes, *i.e.* neofunctionalization, subfunctionalization, and conservation of function (Hahn, 2009). Gene duplication *via* GD is thus a source of genetic novelty and can lead to adaptive innovation. In this context, the study of duplicated genes can lead to a better understanding of phenotypes in species. Salmonid species in particular are good models to study the fate of duplicated genes, because the recent nature of the SaGD event approximately 80 million years ago (MYA) (Berthelot et al., 2014; Chen et al., 2014; Hu and Chen, 2015; Lien et al., 2016; Macqueen and Johnston, 2014), resulted in salmonid genomes with an increased level of complexity and number of duplicated genes. One area of research in salmonid physiology that has particularly benefitted from these recent advances in molecular resources is the investigation of the glucose intolerant (GI) metabolic phenotype in rainbow trout. Research aiming to determine molecular underpinnings of this phenotype is of particular importance in the race to improve the sustainability of salmonid production, with the long term goal to use understanding of the phenotype to substitute high fishmeal based proteins contents with environmentally and ecologically sustainable dietary carbohydrates (Naylor et al., 2009; Polakof et al., 2012). Indeed, the sequencing of the rainbow trout (*Oncorhynchus mykiss*) genome in 2014, the first salmonid genome sequence (Berthelot et al., 2014), allowed the discovery of new gluconeogenic glucose-6-phosphatase encoding genes which were atypically regulated by high dietary carbohydrates (Marandel et al., 2015) and insulin (Marandel et al., 2016). These discoveries led to the novel hypothesis that genome duplication and atypical regulation of paralogous gluconeogenic genes may, at least partially, be involved in GI phenotype in rainbow trout. The rainbow trout genome sequence published in 2014 also allowed the identification of a cytosolic phosphoenolpyruvate carboxykinase (*pck1*) encoding gene, whose expression was found to be down-regulated by high dietary carbohydrates (Marandel et al., 2015). This challenged the view that rainbow trout *pck* gene expression is unresponsive to carbohydrates, as this finding had been based on the only previously known rainbow trout *pck2* sequence cloned in 2001 (Panserat et al., 2001b). Even though the sequencing of the whole trout genome did allow for major gene discoveries with respect to gluconeogenic paralogues, the first version of the rainbow trout genome (Berthelot et al., 2014) displayed sequencing gaps and suffered from comparatively poor genome annotation. In an effort to improve the rainbow trout reference genome sequence, the United States Department of Agriculture re-sequenced the doubled haploid Swanson line using longer Illumina technology reads (NCBI accession number: PRJNA335610) in 2017, opening doors to identify new genes that had previously been unidentified in the originally published genome sequence. Exploring this new assembly, we identified a new *pck*-like sequence which is the main subject of the present study.

The first step of the present work was to establish the identity and the origin of this new gene which turned out to be a *pck2* (mitochondrial *pck*). In mammals, both cytosolic and mitochondrial PCK catalyze the reaction that converts oxaloacetate into phosphoenolpyruvate (PEP) and CO_2 by consuming guanosine triphosphate (GTP) as co-factor. PEP can then re-enter the tricarboxylic acid (TCA) cycle or be used as precursor for several cellular processes, including gluconeogenesis, for which it is the rate-limiting step (Yang et al., 2009). The function of mitochondrial PCK2 has long been regarded to be limited to ensuring continuous cataplerotic PEP production and regulating mitochondrial metabolism-mediated insulin secretion in pancreatic beta-cell without any major relevance for the hepatic glucose production, a function largely linked to PCK1 (Stark and Kibbey, 2014). However, PCK2 has recently been proven to have a crucial metabolic role in PEP production in rodents *in vivo*, where it contributes to up to a third of hepatic gluconeogenesis (Méndez-Lucas et al., 2014; Stark et al., 2014). One reason for the only recent acknowledgement of physiological importance of mitochondrial PCK2 is the fact that in rodent models (mice and rats), cytosolic PCK1 is the principally expressed enzyme (Stark et al., 2014), and studies focusing on the regulation of rodent *Pck1* and *Pck2* gene expression have subsequently revealed that nutrients or glucoregulatory hormones that are known to regulate hepatic gluconeogenesis induce large transcription changes in cytosolic *Pck1* (Hanson and Reshef, 1997), but do not affect transcript abundance of constitutively expressed mitochondrial *Pck2* (Modaressi et al., 1998). Conversely, in trout, hepatic mRNA abundance of the initially cloned *pck2* (Panserat et al., 2001b) was shown to be down-regulated by intraperitoneally (i.p.) injected insulin (Plagnes-Juan et al., 2008), but upregulated by i.p. injected glucose (Jin et al., 2014). Hepatic mRNA abundance of this *pck2* gene as well as mitochondrial PCK2 enzyme activity (Marandel et al., 2015) were however neither sensitive to the nutritional status (Kirchner et al., 2008; Marandel et al., 2015; Panserat et al., 2001a; Panserat et al., 2001b), nor regulation by dietary carbohydrates in trout (Marandel et al., 2015; Panserat et al., 2001b). Finally, hepatic *pck2* expression has been shown to be regulated by lipids (Ducasse-Cabanot et al., 2007; Jin et al., 2014) *in vivo* and by amino acids *in vitro* (Lansard et al., 2010).

The discovery of a new *pck2* encoding gene in trout raised new questions concerning the regulation and role/function of this duplicate. Following the first part of the work which demonstrated the identity and evolutionary origin of the newly identified gene, we investigated the potentially differential regulation of the gene expression of the newly discovered *pck2* gene we termed *pck2b*, as well as *pck1,* for which only few data were available, and the previously well-characterized *pck2* gene, now termed *pck2a.* Specifically we used several experimental conditions linked to altered hepatic gluconeogenesis in rainbow trout, the major contributor of *de novo* glucose production in this and other species (Haman et al., 1997). The first experiment comprised a short term fast and a refeeding regime with two different diets which were either devoid of (0%) or contained a high amount (> 20%) of dietary carbohydrates (Marandel et al., 2015), allowing to profile *pck* paralogues in the rainbow trout liver in response to different nutritional stimuli. In a second experiment, we profiled hepatic *pck* paralogue transcript abundance in fasted rainbow trout that had been infused with key glucoregulatory hormones glucagon and insulin in order to address endocrine regulation of *pck* paralogues predicted to decrease (insulin) or increase (glucagon) hepatic gluconeogenesis. In a third experiment, we investigated hepatic *pck* paralogue expression in rainbow trout housed either individually or in a dyad that led to the clear establishment of social hierarchies of consisting of a dominant and a subordinate fish (Kostyniuk et al., 2018), the latter of which is characterized by a prolonged fasted state and persistent increases in the glucoregulatory hormone cortisol (Kostyniuk et al., 2018), and increased global hepatic Pck activity (DiBattista et al., 2006). To investigate individual contributions of fasting and cortisol individually and to identify potentially synergistic effects of nutritional and hormonal parameters on *pck* transcript regulation in subordinate trout, we also profiled hepatic transcript abundance of *pck* paralogues in trout subjected to a short term fast and cortisol levels that matched these parameters experienced with regard to time and concentration (Kostyniuk et al., 2018). In a fourth experiment, we profiled *pck* paralogue transcript abundance in whole rainbow trout embryos that had been exposed to hypoxia (Liu et al., 2017a), an environmental stimulus known to increase hepatic production of glucose in trout and mammals (Omlin et al., 2010; Choi and Weber, 2015). Together, profiling of all three *pck* transcript in rainbow trout liver and whole embryos across a variety of environmental (nutrition, conspecific interaction, hypoxia) and endogenous endocrine factors involved in glucoregulation (glucagon, insulin, cortisol), will allow for a potential differential regulation of *pck* paralogues in conditions affecting gluconeogenesis in rainbow trout.

R_norvegicus(ENSRNOG00000018536)	1																		
M_musculus(ENSMUSP00000038555)	0,808	1																	
H_sapiens(ENSP00000216780)	0,808	0,883	1																
C_Familiaris(ENSCAFG00000011868)	0,715	0,839	0,836	1															
X_laevis(ENSXETP00000031961)	0,626	0,707	0,732	0,664	1														
D_rerio(ENSDARP00000005448)	0,574	0,615	0,647	0,576	0,687	1													
O_latipes(ENSORLP00000007889)	0,583	0,633	0,659	0,587	0,699	0,855	1												
T_rubripes(ENSTRUP00000011092)	0,574	0,632	0,657	0,587	0,678	0,844	0,887	1											
T_nigoviris(ENSTNIP00000008046)	0,574	0,632	0,656	0,582	0,681	0,822	0,872	0,926	1										
G_aculaetus(ENSGACP00000002900)	0,577	0,633	0,658	0,587	0,683	0,841	0,896	0,886	0,861	1									
O_mykiss(NM_001124275.1)	0,58	0,633	0,656	0,593	0,695	0,866	0,864	0,86	0,847	0,867	1								
S_alpinus(XP_023855596.1)	0,541	0,596	0,625	0,56	0,656	0,792	0,775	0,772	0,771	0,779	0,878	1							
O_tshawytscha(XP_024229996.1)	0,578	0,632	0,655	0,591	0,695	0,866	0,864	0,86	0,847	0,867	0,995	0,877	1						
S_salar(XM_014159685.1)	0,539	0,593	0,622	0,557	0,654	0,784	0,772	0,764	0,767	0,773	0,878	0,98	0,876	1					
O_mykiss(XM_021562670.1)	0,578	0,627	0,651	0,587	0,691	0,865	0,86	0,859	0,843	0,866	0,96	0,851	0,959	0,849	1				
S_alpinus(XP_023828293.1)	0,569	0,625	0,642	0,587	0,687	0,834	0,831	0,834	0,818	0,837	0,927	0,832	0,926	0,832	0,953	1			
O_tshawytscha(XP_024248492.1)	0,58	0,628	0,653	0,588	0,693	0,866	0,86	0,859	0,84	0,868	0,96	0,851	0,959	0,849	0,996	0,953	1		
S_Salar(XM_014181078.1)	0,546	0,594	0,624	0,56	0,657	0,784	0,773	0,766	0,763	0,775	0,857	0,959	0,855	0,956	0,88	0,858	0,88	1	

pck2a vs pck2b within a salmonid species
pck2a
pck2b

Fig. 1. Matrix protein identity of *pck2* genes. Accession numbers are given in parentheses.

2. Material and methods

2.1. In silico characterization of a novel salmonid pck2 paralogue

All *pck* sequences used in the *in silico* analysis were collected from either the Ensembl database (http://useast.ensembl.org/index.html) or the NCBI Genome assembly database (https://www.ncbi.nlm.nih.gov/assembly). All specific accession numbers are provided in Fig. 1. Phylogenetic analysis was performed using the MEGA package version 6 software (Tamura et al., 2013). The phylogenetic tree (Fig. 2), based on full-length gene sequence-deduced amino acid sequences, was built by the neighbor-joining method and confirmed by the minimum evolution method (data not shown). The reliability of the inferred trees was estimated by the bootstrap method with 1000 replicates. New gene annotations were chosen according to the ZFIN Nomenclature guidelines (http://zfin.org/). Percentage identity matrix established among paralogous derived Pck2 sequences (Fig. 2) and sequence alignments were performed with Clustal 2.1 using the MUSCLE interface (Edgar, 2004).

Comparison of *pck2*-deduced amino acid sequences between mammals and teleosts was also performed by aligning proteins sequences (Fig. 3), and important functional protein domains were highlighted based on the description of Schein et al. (2004). Tissue expression profiles of *pck* genes (Fig. 4) were identified in the PhyloFish database using the Blast tool (Pasquier et al., 2016). The *pck2* ohnologues possess highly similar sequences, and we considered fragments that included SNPs specific to each gene in the PhyloFish database to distinguish the expression of each of them from the longest sequences that showed the highest percent identity and lowest BLAST e-value.

2.2. Experimental designs to profile regulation of pck paralogue transcript

2.2.1. Refeeding experiment

Details concerning this experiment can be accessed in a previous publication (Marandel et al., 2015). Juvenile rainbow trout (70 g body mass) were reared at 17 °C at INRA experimental facilities at Saint-Pée-sur-Nivelle, France and were distributed in six tanks (15 fish per tank). After 4 days of total fasting, two fish from each tank were sacrificed (fasted group). Rainbow trout were then fed with either a control diet devoid of digestible carbohydrates (NoCHO) or a diet containing 30% of dietary carbohydrates (HighCHO) twice a day at 2.5% live weight for 4 days. A table detailing dietary composition can be found in Supplementary File 1. 6 h following last feed, nine rainbow trout (3 per tank, 3 replicate tanks per dietary treatment) were sampled. To ensure that sampled fish had effectively consumed the diets, gut content of the sampled animals was systematically checked. The fresh liver of each fish was dissected and immediately frozen in liquid nitrogen and then stored at −80 °C. Investigations were conducted according to the guiding principles for the use and care of laboratory animals and in compliance with French and European regulations on animal welfare (Décret 2001-464, 29 May 2001 and Directive 2010/63/EU, respectively). This protocol and the project were approved by the French National Consultative Ethics Committee.

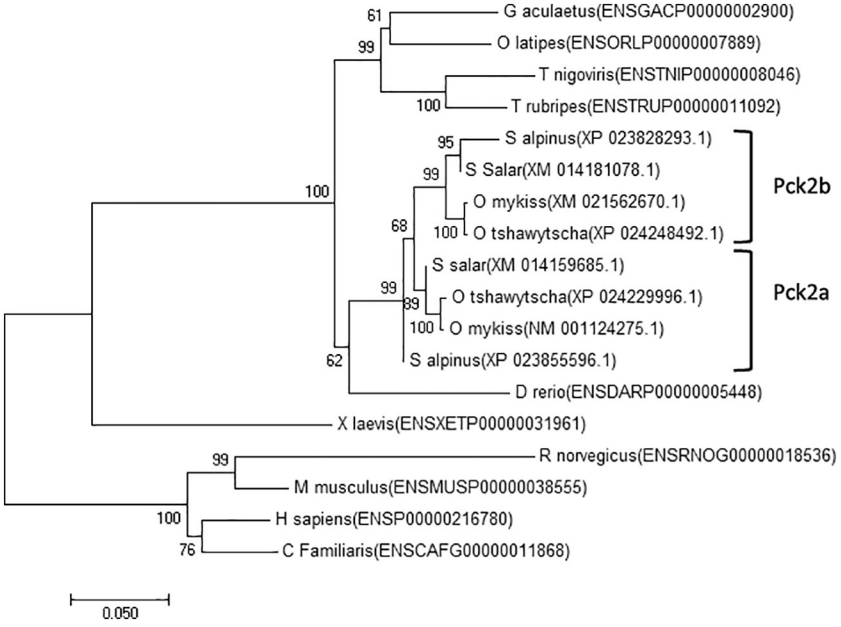

Fig. 2. Phylogenetic analysis of phosphoenol-pyruvate carboxykinase 2. The phylogenetic analyze was performed using MEGA package version 6 software. The phylogenetic tree was built by the neighbor-joining (NJ) method. The reliability of the inferred trees was estimated by the bootstrap method with 1000 replications. All accession numbers (from NCBI or Ensembl databases) are specified in parentheses.

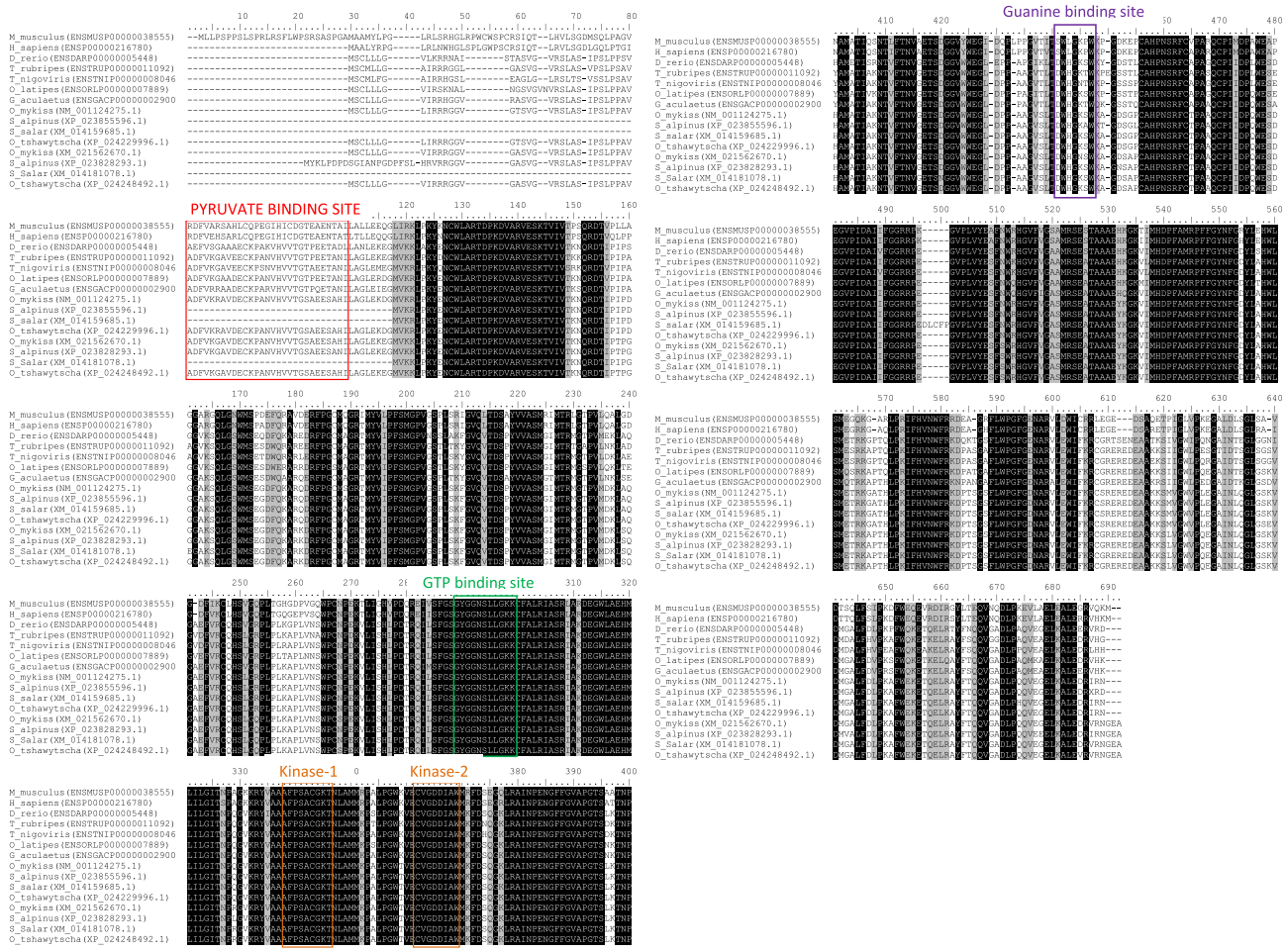

Fig. 3. Comparison of pck2 deduced amino acid sequences between mammals and teleosts. Important functional domains are highlighted based on the description of Schein et al. (2004).

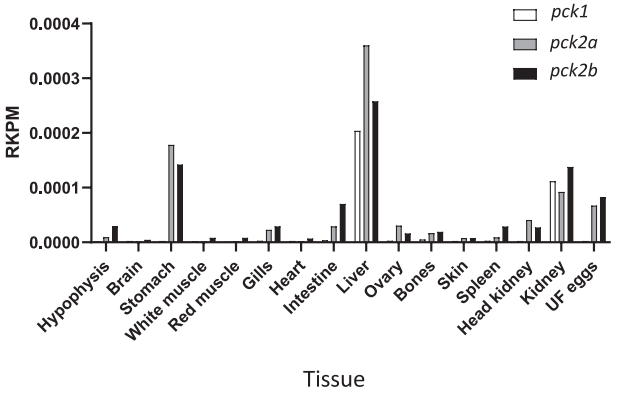

Fig. 4. PhyloFish-based tissue abundance of pck1, pck2a and pck2b transcripts. Data retrieved from Pasquier et al. (2016).

2.2.2. Infusion experiments of glucoregulatory hormones insulin and glucagon

Details concerning this experiment can be accessed in a previous publication (Forbes et al., 2019). Rainbow trout were purchased from Linwood Acres Trout Farm (Campbellcroft, Ontario, Canada). The fish were held in a 1200 l flow-through tank supplied with dechloraminated Ottawa tap water at 13 °C, on a 12 h:12 h light:dark photoperiod and were fed Profishnet floating fish pellets (Martin Mills, Elmira, ON, Canada) 5 days per week. They were acclimated to these conditions for a minimum of 2 weeks before experiments. Prior to surgery, the fish were anesthetized with ethyl 3-aminobenzoate methanesulfonate (60 mg l^{-1} MS-222 buffered with 0.2 g l^{-1} sodium bicarbonate) and then singly cannulated with BTPE-50 catheters (Instech Laboratories, Plymouth Meeting, PA, USA) in the dorsal aorta (Haman et al., 1997). The catheters were kept patent by flushing with Cortland saline containing 50 U ml^{-1} heparin (Sigma-Aldrich, St Louis, MO, USA). Fish were left to recover overnight in a 90 l swim-tunnel (Loligo Systems, Tjele, Denmark) where resting animals where maintained at a water velocity of 0.5 body length per second (BL s^{-1}). The catheters were made accessible through the swim tunnel lid by channeling them through a watertight port. Physiological saline (control group), bovine glucagon (Sigma-Aldrich; 8.3 µg kg^{-1} min^{-1}) or bovine insulin (Sigma-Aldrich; 1.5 µg insulin kg^{-1} min^{-1}) were administered at 1 ml/h through the catheter for 4 h using a standard infusion syringe pump (Harvard Apparatus, Holliston, MA, USA). The animals were then euthanized by a sharp blow on the head before collecting the liver, which was flash frozen in liquid nitrogen and stored at −80 °C until analyses. All the procedures were approved by the Animal Care Committee under animal care protocol BL-1625 of the University of Ottawa and adhered to the guidelines established by the Canadian Council on Animal Care.

2.2.3. Social status experiments

A detailed description of experimental procedures has been published elsewhere (Kostyniuk et al., 2018). Briefly, juvenile rainbow trout were held at the University of Ottawa in a 1275 l fiberglass tank. Tanks were supplied with flowing, aerated, dechloraminated 13 °C city of Ottawa tap water. Fish were fed a ration of 0.5% body mass daily and

acclimated to holding conditions which minimize hierarchy formation (*e.g.* the use of scatter feeding, homogenous tanks with a mild current) for a minimum two weeks before experimentation. Juvenile rainbow trout were confined in pairs or handled identically but held individually (sham-treated controls), for four days (n = 12 pairs, 13 shams). Paired fish were initially separated from one another overnight by an opaque, perforated divider in a 40 l flow-through Plexiglas observation tank which was supplied with flowing, aerated dechloraminated city of Ottawa tap water at 13 °C. The divider was then removed the following morning, and fish were allowed to interact for four days. Social status was assessed using a scoring system that awards more points for more dominant behaviors; specifically, patrolling the water column in the tank, aggressive behavior, first to feed, and absence of fin damage. Within a pair, the fish with the higher score was assigned dominant status, while the fish with the lower score was subordinate. Parameters associated with social status were also measured, where plasma cortisol levels were significantly increased (27-fold) in dominants over subordinate and sham fish, and food intake was significantly decreased (28-fold) in subordinates compared to dominant fish (Kostyniuk et al., 2018). All experimental protocols complied with the guidelines of the Canadian Council on Animal Care for the use of animals in research and teaching and were approved by the University of Ottawa's Animal Care Committee. After the interaction period, both fish in a pair were rapidly euthanized *via* terminal anesthesia (0.5 g l^{-1} ethyl-p-aminobenzoate). Liver tissue was freeze clamped and stored at −80 °C for later analysis.

To further assess the contributions of specific subordinate-associated traits, particularly increased cortisol and decreased food intake to *pck* transcript abundance, a subsequent experiment was conducted to assess the contributions of elevated cortisol and fasting. Juvenile trout were randomly allocated into one of three 115 l holding tanks in groups of 10–12 fish per tank and were either maintained as controls, injected with cortisol implants or fasted over a period of 4 days. Cortisol-treated fish were lightly anesthetized and given an intraperitoneal implant of cocoa butter (5 ml/kg body mass) containing hydrocortisone 21-hemisuccinate (22 mg ml^{-1}; Sigma-Aldrich). A dosage of 110 mg kg^{-1} body mass, was shown to raise circulating cortisol levels to those of subordinate fish in previous studies (Gilmour et al., 2017; Jeffrey et al., 2012). The fasted treatment group was not fed for 4 days. A random subset of five to six fish from each set was sampled as described above. All experimental protocols complied with the guidelines of the Canadian Council on Animal Care for the use of animals in research and teaching and were approved by the University of Ottawa's Animal Care Committee.

2.2.4. Embryonic hypoxia exposure

Detailed descriptions of experimental approaches can be accessed in a recent publication (Liu et al., 2017b). Briefly, rainbow trout embryos were maintained in 8 °C source water at the INRA experimental facilities in Lees-Athas, France. Triplicate tanks for both normoxia and hypoxia groups were used. 152 °d (degree day) trout embryos at stage 21 (Vernier, 1969), were either kept under continuously normoxic conditions (11.0 mg l^{-1} dissolved oxygen, normoxic group) or exposed to a 24 h-acute hypoxic stimulus (2.5 mg l^{-1} dissolved oxygen, hypoxia group). Samples (30 embryos per tank) from both groups were collected during the last hour of the hypoxic stimulus, directly snap-frozen in liquid nitrogen and stored at −80 °C until further analysis. The protocol was approved by the French National Consultative Ethics Committee.

2.3. Circulating glucose and cortisol concentrations across experiments

Throughout experiments, circulating glucose and cortisol concentrations are provided where possible, in order to provide a context for the described transcriptional regulation of rainbow trout *pck1*, *pck2a* and *pck2b*. These values are summarized in Table 2. Briefly, plasma cortisol concentrations were measured using a commercially available radioimmunoassay (MP Biomedicals, Santa Ana, CA) that had previously been validated for trout plasma (Kostyniuk et al., 2018). The kit has a detection limit of 0.17 μg/dl. Intra-assay variation was 9.6% (% coefficient variation). Plasma glucose concentrations were quantified spectrophotometrically using a Spectra Max Plus384 Absorbance Microplate Reader (Molecular Devices, Sunnyvale, CA, USA) following a NAD+/NADH-coupled enzymatic assay at 340 nm with hexokinase and glucose-6-phosphate dehydrogenases, as previously reported (Forbes et al., 2019).

2.4. Total RNA extraction and cDNA synthesis

For the refeeding, glucoregulatory hormone infusion, social status and short term fast and cortisol implantation experiments, total RNA was extracted from 20 to 100 mg of liver using TRIzol reagent (Invitrogen, Burlington, ON, Canada) following the manufacturer's protocol. Tissue homogenization was performed by forcing the solution of TRIzol and tissue through 18- and 23-G needles using a syringe until the solution passed easily through the needle. Extracted RNA was quantified using a NanoDrop 2000c UV–Vis Spectrophotometer (Thermo-Fisher Scientific, Ottawa, ON, Canada) and cDNA was generated using a QuantiTech Reverse Transcription Kit (Qiagen, Toronto, ON, Canada) following the manufacturer's protocol. For the embryonic hypoxia experiment, samples were homogenized using a Precellys® 24 homogenizer (Bertin Technologies, Montigny-le-Bretonneux, France). 7 ml tubes containing 30 pooled embryos per sample in TRIzol reagent (Invitrogen, Carlsbad, CA, USA) as well as 2.8 mm ceramic beads were agitated at 5500 rpm for 2 × 30 s, separated by a pause of 15 s. Ten picograms of luciferase control RNA (Promega, Charbonniéres, France) per 1.9 mg of embryo was added to each sample to allow for data normalization during early development as previously described (Desvignes et al., 2011; Marandel et al., 2012). Extracted total RNA (1 μg) was used for the Super-Script III RNAse H–Reverse transcriptase kit (Invitrogen) and random primers (Promega) to synthesise cDNA according to the manufacturer's protocol.

2.5. SYBR Green real-time RT-PCR assays

For the refeeding, glucoregulatory hormone infusion, social status and short term fast and cortisol implantation experiments, a standard curve consisting of serial dilutions of pooled hepatic cDNA, a negative no-RT control, and individual samples were run in duplicate for each experiment. For each individual reaction, the total volume was 20 μl, which consisted of 4 μl of diluted cDNA template, 0.5 μl of each 10 nM specific forward and reverse primer (Integrated DNA technologies, Skokie, IL, USA), 10 μl of SsoAdvanced Universal Inhibitor-Tolerant SYBR Green Supermix (Bio-Rad, Montréal, QC, Canada), and 5 μl of DNAse/RNAse-free water (VWR International, Mississauga, ON, Canada). Cycling parameters were a 5 min activation step at 95 °C, followed by 40 cycles consisting of a 20 s denaturation step at 95 °C and a combined 30 s annealing and extension step at primer specific temperatures (Table 1). After each run, melting curves were produced by gradually increasing temperature where the final curves were monitored for single peaks to confirm the specificity of the reaction and the absence of primer dimers. In cases where primers were newly designed (*pck2b*), pooled samples were sent for sequencing (Ottawa Hospital Research Institute, Ottawa, ON, Canada), followed by BLAST search (National Center for Biotechnology Information), to confirm amplicon specificity. The acceptable range for amplification efficiency calculated from serially diluted standard curves was 90–110%, with R^2 values > 0.95. Assays were subsequently normalized using the NORMA Gene approach (Heckmann et al., 2011). Finally, mRNA fold changes were calculated relative to the control group.

For the embryonic hypoxia experiment, SYBR Green realtime RT-PCR assays were performed with the Roche Lightcycler 480 system (Roche Diagnostics, Neuilly-sur-Seine, France). Each assay included replicate samples (duplicate of reverse transcription and PCR

Table 1
Primer sequences and annealing temperatures used for mRNA quantification by real-time RT-PCR.

Target	Forward primer sequence (5′3′)	Reverse primer sequences (3′5′)	Annealing temperature [°C]	Reference
pck1	ACAGGGTGAGGCAGATGTAGG	CTAGTCTGTGGAGGTCTAAGGGC	55	Marandel et al., 2015
pck2a	ACAATGGAGATGATGTGACTGCA	TGCTCCATCACCTACAACCT	56	Marandel et al., 2015
pck2b	AGTAGGAGCAGGGACAGGAT	CCGTTCAGCAAAGGTTAGGC	59	Primer3 newly designed
ef1a	CATTGACAAGAGAACCATTGA	CCTTCAGCTTGTCCAGCAC	56	Birceanu et al., 2015

amplification) and negative controls (reverse transcriptase and cDNA template free samples). The reaction mix was 6 µl per sample, including 2 µl of diluted cDNA template (1:25), 0.12 µl of each primer (10 µmol l^{-1}), 3 µl of Light Cycler 480 SYBR® Green I Master mix and 0.76 µl of DNAse/RNAse-free water (5 Prime GmbH, Hamburg, Germany). The realtime RT-PCR protocol was initiated at 95 °C for 10 min for the initial denaturation of the cDNA and hot-start Taq-polymerase activation, followed by 45 cycles of a two-step amplification programme (15 s at 95 °C; 10 s at 60 °C). Melting curves were monitored systematically (temperature gradient 0.11 °C per second from 65 to 97 °C) at the end of the last amplification cycle to confirm the specificity of the amplification reaction. Data were subsequently normalized to the exogenous luciferase transcript abundance in samples diluted at 1:25 using the E method (Light Cycler software) as previously described (Marandel et al., 2012).

2.6. Statistical analysis

Data were tested for normality and homoscedasticity using the Shapiro-Wilk test and Bartlett's test, respectively. If these assumptions were met, data were tested for single outliers using Grubb's test and subsequently analyzed using a one-way ANOVA, followed by Tukey's post-hoc test for multiple comparisons or a Student's *t*-test and significance level was $p < 0.05$ for all tests. When data did not meet these assumptions, data were either transformed to meet the assumptions or were analyzed using the nonparametric Kruskal-Wallis test followed by Bonferroni-adjusted Mann-Whitney *U* tests or a Welch's *t*-test. All statistical analysis and graphing were carried out using Prism, Version 8 (Graphpad software, La Jolla, CA).

3. Results

3.1. In silico analysis of salmonid pck2 genes

By analyzing the new assembly of the rainbow trout genome in the NCBI database (GCA_002163495.1), we identified, for the first time, two gene loci which both share high sequence homology with the gluconeogenic *pck2* gene, which are located on separate chromosomes (chromosome 11 and chromosome 15). Two distinct genomic loci for *pck2* paralogues were also identified in other salmonid species with available genome assemblies in NCBI (*Salvelinus alpinus*, GCA_002910315.2; *Oncorhynchus tshawytscha*, GCA_002872995; *Salmo salar*, GCA_000233375.4). Conversely, non-salmonid teleost species with available genomes in NCBI or Ensembl databases only contain a single *pck2* sequence. The two salmonid *pck2* sequences shared < 60% nucleotide sequence identity with *pck1* in other teleost species (data not shown) but shared between 77% and 87% identity with teleost *pck2* (Fig. 1). Within individual salmonid species, both *pck2* sequences identified shared between 83% and 96% identity depending on the species (Fig. 1). A phylogenetic analysis using full-length Pck2/PCK2 protein sequences of several non-salmonid teleost (*Danio rerio*, *Takifugu rubripes*, *Tetraodon nigroviridis*, *Gasterosteus aculeatus*, *Oryzias latipes*) and mammalian (*Homo sapiens*, *Mus musculus*, *Rattus norvegicus*, *Canis familiaris*) species was then computed to clarify the origin and identity of these salmonid sequences. This phylogenetic analysis showed that both sequences identified in salmonids grouped together with other Pck teleost sequences (Fig. 2). In addition, within the salmonids, the two derived Pck2 amino acid sequences formed two distinct groups (Fig. 2). We subsequently employed our proposed nomenclature of *pck2a*, which designates the previously characterized *pck2* form initially cloned and described by Panserat et al. (2001b), and *pck2b*, which designates the *pck2* ohnologue described for the first time in the current study. We then aligned (predicted) Pck2/PCK2 sequences from the phylogenetic analysis to identify conservation of important regions involved in protein function (*i.e.* catalytic and binding sites, co-factor binding sites) based on the description provided by Schein et al. (2004). The annotated sequences are depicted in Fig. 3. Finally, *in silico* analysis of RNA-sequencing data from the PhyloFish database (Pasquier et al., 2016), reveals that all rainbow trout *pck* genes are preferentially expressed in the liver (Fig. 4). RNA abundance of *pck1* was like in mammals, specific to gluconeogenic tissues, while both *pck2a* and *pck2b* reveal a more ubiquitous tissue expression, again similar to the situation in mammals.

3.2. Pck paralogue expression patterns under experimental conditions linked to altered rainbow trout hepatic gluconeogenesis

3.2.1. Refeeding short-term fasted trout diets devoid of or with high amount of carbohydrate content differentially affects hepatic pck paralogue transcript abundance

The mRNA abundance of *pck1* changed significantly between fasted, NoCHO and HighCHO refed groups (Fig. 5A; Kruskal-Wallis, $H_{2,26} = 8.903$, $p < 0.0117$). Tukey's post-hoc comparison revealed a significantly higher *pck1* transcript abundance in the group refed with NoCHO diet compared to the group refed a HighCHO diet ($p < 0.01$), while refeeding itself did not significantly change *pck1* mRNA abundance in either dietary group compared to fasted animals ($p > 0.05$). A significant difference in *pck2a* transcript abundance between fasted, NoCHO and HighCHO groups was identified (Fig. 5B; 1-way ANOVA, $F_{2,26} = 3.708$, $p = 0.0402$), but could not be resolved by Tukey's post-hoc tests ($p > 0.05$). A significant difference (Fig. 5B; 1-way ANOVA, $F_{2,27} = 7.659$, $p = 0.0027$) in the transcript abundance of *pck2b* was identified between treatment groups, and Tukey's post-hoc comparison revealed a significant induction of *pck2b* transcript abundance in HighCHO diet fed trout compared to fasted animals ($p < 0.01$).

3.2.2. Infusion of the glucoregulatory hormones glucagon, but not insulin, alters pck paralogue transcript abundance

Glucagon infusion significantly increased hepatic *pck1* mRNA abundance compared to saline infused control fish (Fig. 6A; 2-tailed *t*-test with unequal variances, df = 6.009, t = 5.216, $p = 0.0020$). Conversely, glucagon infusion significantly decreased the mRNA abundance of *pck2a* compared to saline infusion (Fig. 6B; 2-tailed *t*-test with unequal variances, df = 11.99, t = 2.707, $p = 0.0191$). Finally, no significant difference in *pck2b* mRNA abundance was observed between glucagon and saline infused fish (Fig. 6C; 2-tailed *t*-test with unequal variances, df = 7.275, t = 1.602, $p = 0.1517$). The mRNA abundance of *pck1* (Fig. 6D; 2-tailed *t*-test with unequal variances, df = 7.545, t = 1.456, $p = 0.1858$), *pck2a* (Fig. 6E; 2-tailed *t*-test with unequal variances, df = 9.511, t = 0.2507, $p = 0.8074$) and *pck2b* (Fig. 6F, 2-tailed *t*-test with unequal variances, df = 7.127, t = 0.6854, $p = 0.5148$) did not change with insulin infusion compared to saline infusion.

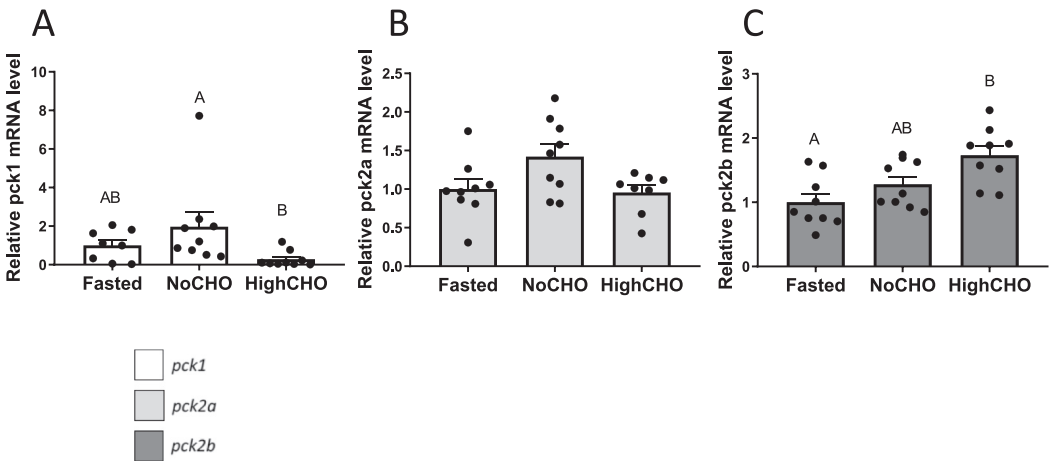

Fig. 5. mRNA abundance of the three *pck* paralogues, a rate limiting enzyme in gluconeogenesis, with cytosolic *pck1* (A) and mitochondrial *pck2a* and *pck2b* (B, C) in fasted, NoCHO and HighCHO fish. Values are presented as means ± SE with n = 8–9 for all groups; values for individuals included in the means are indicated by the symbols. Bars that share a letter are not significantly different from one another (A, B and C).

3.2.3. Social status-dependent differential regulation of pck transcript abundance is partially mimicked by cortisol or short term fasting

The hepatic mRNA abundance of *pck1* differed significantly with social status (Fig. 7A; 1-way ANOVA, $F_{2,18} = 132.1$, $p < 0.0001$), with a > 400-fold increase in mRNA abundance in subordinate trout compared to both sham ($p < 0.01$) and dominant fish ($p < 0.01$). Conversely, no significant differences in hepatic *pck2a* mRNA abundance were observed among sham control, dominant and subordinate fish (Fig. 7B, 1-way ANOVA, $F_{2,19} = 1.313$, $p = 0.2966$). Finally, hepatic mRNA abundance of *pck2b* differed significantly with social status (Fig. 7C, 1-way ANOVA, $F_{2,19} = 2.199$, $p = 0.0445$) revealing a decreased mRNA abundance in subordinate fish compared with dominant fish ($p < 0.05$).

When investigating the possible contribution of cortisol and/or fasting to hepatic *pck1* transcript abundance (Fig. 7D, 1-way ANOVA, $F_{2,16} = 12.19$, $p = 0.001$), we found that cortisol implanted fish exhibited significantly increased *pck1* transcript abundance compared to control fish ($p < 0.01$) and fasted fish ($p < 0.01$). There were no

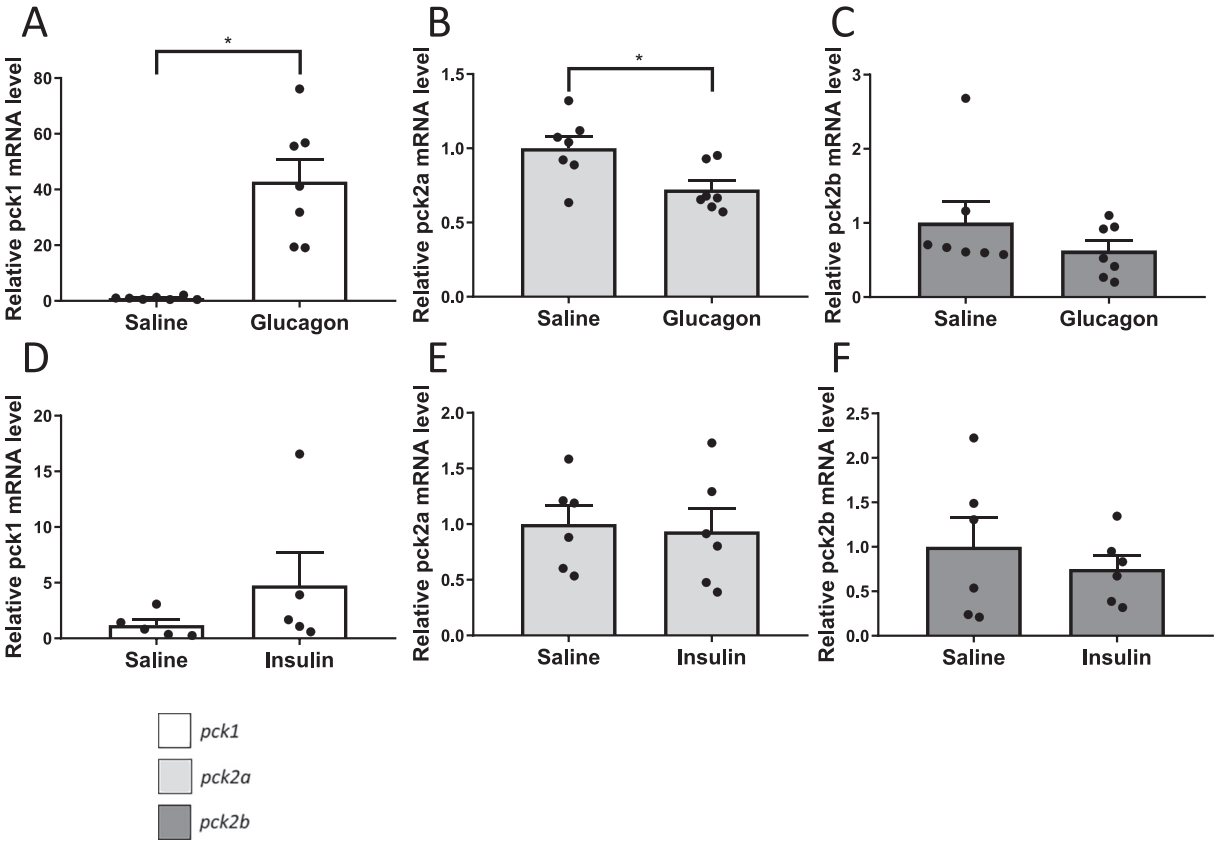

Fig. 6. mRNA abundance of the three *pck* paralogues, a rate limiting enzyme in gluconeogenesis, with cytosolic *pck1* (A and D) and mitochondrial *pck2a* (B and E) and *pck2b* (C and F) in saline and glucagon infused fish (A, B and C) and saline and insulin infused fish (D, E and F). Values are presented as means ± SE with n = 7 for all groups for the saline and glucagon infused fish and n = 5–6 for the saline and insulin infused fish; values for individuals included in the means are indicated by the symbols. Bars annotated with an * are significantly different from each other.

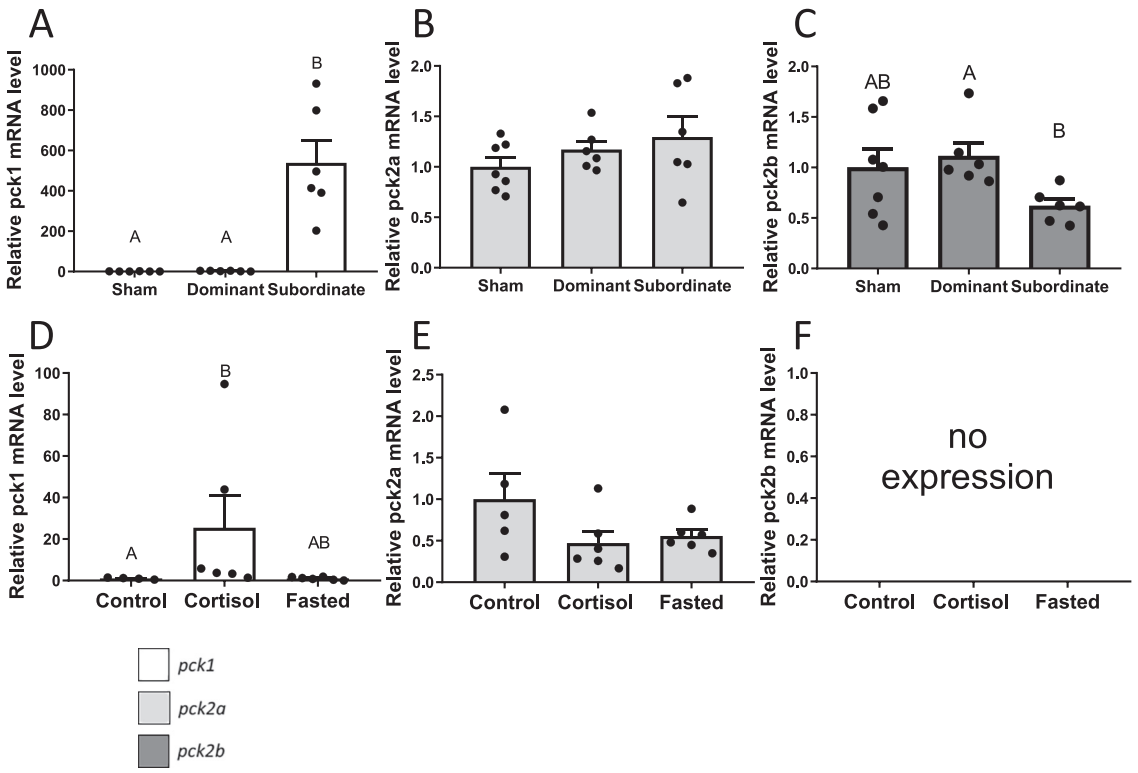

Fig. 7. mRNA abundance of the three *pck* paralogues, a rate limiting enzyme in gluconeogenesis, with cytosolic *pck1* (A and D) and mitochondrial *pck2a* (B and E) and *pck2b* (C and F) in sham, dominant and subordinate fish (A, B and C) and control, cortisol injected and fasted fish (D, E and F). Values are presented as means ± SE with n = 5–7 for the sham, dominant and subordinate fish and n = 4–6 for the control, cortisol and fasted fish; values for individuals included in the means are indicated by the symbols. Bars that share a letter are not significantly different from one another.

significant differences in the hepatic mRNA abundance of *pck2a* (Fig. 7E, 1-way ANOVA, $F_{2,17} = 2.258$, $p = 0.1412$). Regarding this experiment, there was no detected expression of *pck2b*.

3.2.4. Embryonic hypoxia

The whole embryo mRNA abundance of *pck1* (Fig. 8A; 2-tailed *t*-test with unequal variances, df = 6.5588, t = 0.9966, $p = 0.3543$) and *pck2a* (Fig. 8B; 2-tailed *t*-test with unequal variances, df = 7.906, t = 1.109, $p = 0.3002$) were unaffected by 24 h acute hypoxia, however hypoxia caused a four-fold increase in mRNA abundance of *pck2b* relative to normoxia (Fig. 8C; 2-tailed *t*-test with unequal variances, df = 5.6, t = 7.191, $p = 0.0078$.

3.2.5. Circulating cortisol and glucose concentration measurements

Wherever possible, glucose and cortisol concentrations for all experiments were obtained either form previously published studies (Marandel et al., 2015; Forbes et al., 2019; Kostyniuk et al., 2018), or through additional measurements conducted for the purpose of the current study. Briefly, plasma glucose concentration was, with regard to nutritional stimuli, significantly elevated by dietary HighCHO compared to Fasted and NoCHO groups. Infusion of the glucoregulatory hormones insulin and glucagon significantly increased and decreased plasma glucose concentrations, respectively. Finally, subordinate social status increased circulating glucose concentrations compared to dominant fish and sham fish. Similarly, cortisol treated fish exhibited higher

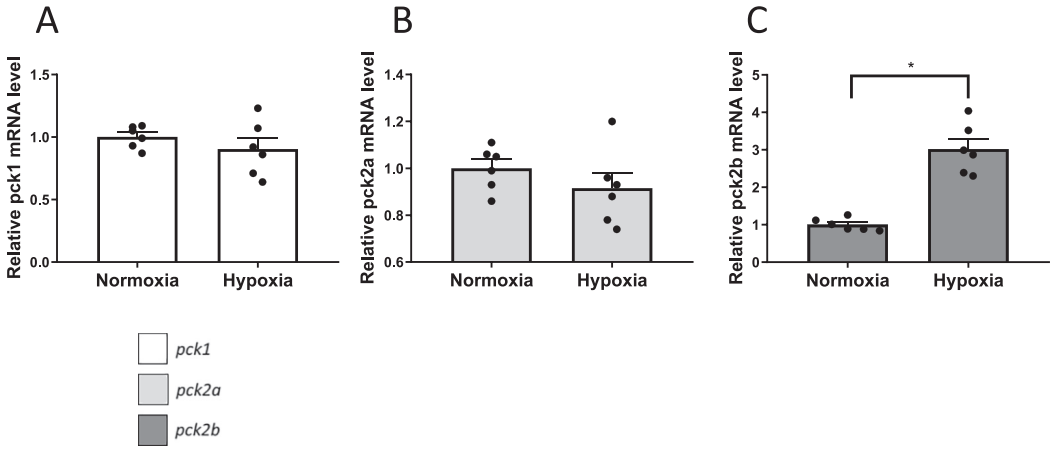

Fig. 8. mRNA abundance of the three *pck* paralogues, a rate limiting enzyme in gluconeogenesis, with cytosolic *pck1* (A) and mitochondrial *pck2a* and *pck2b* (B, C) in fish embryos exposed to normoxia and hypoxia. Values are presented as means ± SE with n = 6 for all groups; values for individuals included in the means are indicated by the symbols. Bars annotated with an * are significantly different from each other.

Table 2
Circulating glucose and cortisol condition in experiments used to profile relative pck paralogue transcript abundance in rainbow trout.

Experiment	Circulating glucose [mmol]	Circulating cortisol [nmol]	Reference
Nutritional stimulus Fasted trout compared to trout refed diets with different carbohydrate:protein content	Fasted: 3.30 ± 0.22 (a) NoCHO: 3.33 ± 0.16 (a) HighCHO: 8.43 ± 0.60 (b) One-way ANOVA: $p < 0.01$ Post-hoc: Fasted, NoCHO < High CHO $p < 0.01$	Not available	Marandel et al., 2015
Glucoregulatory hormone infusion Insulin and glucagon infusion	Insulin experiment Sal: 5.5 ± 0.05 (a) Ins: 3.9 ± 0.03 (b) *t*-Test: $p < 0.05$ Glucagon experiment Sal: 8.863 ± 0.43 (a) Glu: 11.67 ± 0.42 (b) *t*-Test: $p < 0.05$	Insulin experiment Sal: 7.84 ± 1.31 (a) Ins: 48.34 ± 12.80 (b) *t*-Test: $p < 0.01$ Glucagon experiment Sal: 19.90 ± 6.55 (a) Glu: 39.94 ± 4.84 (b) *t*-Test: $p < 0.01$	Forbes et al., 2019
Social status experiment Isolated sham fish and dyad paired dominant and subordinate trout and fasted and cortisol treated fish	Isolated and dyad paired trout Sham: 7.25 ± 1.13 (a,b) Dom: 5.30 ± 0.85 (a) Sub: 8.84 ± 0.51 (b) One-way ANOVA: $p < 0.05$ Post-hoc: Dom < Sub $p < 0.05$ Fasted and cortisol treated fish Control: 25.04 ± 2.71 (a) Cortisol: 36.24 ± 1.91 (b) Fasted: 23.89 ± 1.86 (a) One-way ANOVA $p < 0.01$ Control, fasted < CORT, $p < 0.01$	Isolated and dyad paired trout Sham: 11.04 ± 2.48 (a) Dom: 6.90 ± 1.38 (a) Sub: 307.34 ± 69.52 (b) One-way ANOVA: $p < 0.01$ Post-hoc: Sham, Dom < Sub: $p < 0.01$ Fasted and cortisol treated fish Control: 27.86 ± 4.19 (a) Cortisol: 1211.70 ± 197.04 (b) Fasted: 21.79 ± 14.98 (a) One-way ANOVA $p < 0.01$ Fasted, NoCHO < High CHO, $p < 0.01$	Kostyniuk et al., 2018
Hypoxia Alevin exposure to hypoxia	Not available	Not available	Liu et al., 2017a

circulating glucose concentrations compared to control and fasted fish. No glucose concentrations were measured in alevins in the acute hypoxia study.

With regard to plasma cortisol concentrations, a significant increase was measured in insulin and glucagon infused fish compared to controls, in subordinate trout compared to dominant and sham trout and in cortisol treated trout compared to control and fasted trout. No plasma cortisol concentrations were obtained for the nutritional and hypoxic stimuli studies. A summary of all plasma glucose and cortisol concentration is given in Table 2.

4. Discussion

Over the last decade, several genomes of model and non-model teleost species have been sequenced (Brawand et al., 2014; Xu et al., 2014), which include salmonid genomes (Berthelot et al., 2014; Lien et al., 2016). The quality of their assembly and annotation is continually improved and updated (Samy et al., 2017). These advances allow for the identification of duplicated genes which constitute raw genetic materials for evolution. In this context, it is now accepted that the outcome of duplicated genes arising from salmonid specific genome duplication (SaGD) in rainbow trout can lead to adaptive innovation (Sato et al., 2009), depending on whether these genes are lost or fixed and maintained (Hahn, 2009). Elucidating the evolutionary history of such genes and studying their expression patterns may help to reveal new molecular underpinnings involved in adaptive behavior in rainbow trout, including its GI phenotype (Marandel et al., 2015). In the present study we describe a new gluconeogenic pck encoding gene in rainbow trout. Following the clarification of its identify and evolutionary history, we subsequently provide first insight on possible sub- or neo-functionalization of the *pck2* paralogues in physiological contexts linked to regulation of (hepatic) gluconeogenesis in rainbow trout.

4.1. The duplication of teleost mitochondrial pck2 before or around the SaGD and fixation of pck2a and pck2b in salmonids

Our *in silico* analysis indicated that the newly identified *pck* sequence in the updated rainbow trout genome in NCBI was related to *pck2* in teleost fishes and mammals. Because of (1) the presence of only a single *pck2* gene in the genome of non-salmonid teleost species which did not undergo an additional whole genome duplication even following the teleost specific genome duplication event, (2) the distinct clustering of the two individual *pck2* salmonid sequences in the phylogenetic tree, and (3) the high similarity between nucleotides and derived amino acid sequences between the both salmonid *pck2* genes, we postulate that, in all likelihood, both *pck2* genes arose from the SaGD event. In this context, the two retained salmonid *pck2* genes should be considered as ohnologous genes and annotated as *pck2a* (NM_001124275.1) and *pck2b* (XM_021562670.1), according to the ZFIN Nomenclature guidelines (https://wiki.zfin.org/display/general/ZFIN+Zebrafish+Nomenclature+Conventions). By analyzing the deduced protein sequences of both, the *pck2a* gene and the *pck2b* gene, we showed that amino acid sequences previously described to play a critical role in the function of the mammalian PCK2 protein (Schein et al., 2004), such as ligand or co-factor binding sites, were highly conserved. This finding may point to a conservation of the Pck2a and Pck2b protein function after duplication of the ancestral teleost PCK2 encoding gene.

4.2. Evidence for differential regulation of pck1 and pck2 ohnologues

In our study we comparatively investigated the hepatic expression of *pck1* as well as the *pck2a* and *pck2b* ohnologues. With regard to *pck1*, our study reveals a strong regulation of *pck1* transcript abundance of *pck1* in response to both nutritional and endocrine factors. Following a short term fast, postprandial hepatic *pck1* mRNA abundance is significantly reduced in fish fed a hyperglycemia- inducing, high carbohydrate diet compared to a protein rich diet devoid of carbohydrates.

With regard to endocrine factors, glucagon infusion and cortisol implantation strongly induces *pck1* mRNA abundance, while no changes were observed in response to insulin infusion. This observed strong regulation of *pck1* is in line with the well-characterized and strong transcriptional regulation of hepatic *pck1* in mammals, which is strongly induced by glucagon and cortisol, and inhibited by glucose (Chakravarthy et al., 2005; Cournarie et al., 1999; Hanson and Reshef, 1997; Iynedjian and Salavert, 1984). In contrast to mammalian observations in which *pck1* mRNA abundance is rapidly reduced by insulin, we did not observe a decrease in *pck1* in response to 4 h infusion of insulin. However, the experimental infusion design did only result in muscular, but not hepatic activation of the Akt signaling pathway and induced a counterregulatory increase in circulating glucagon (Forbes et al., 2019). A lack of activation of chronic insulin infusion as opposed to acute insulin injection has been previously reported (Polakof et al., 2010), and may explain the lack of *pck1* regulation at the mRNA level in our experiment. Additionally, infusion of both insulin and glucagon led to a significant increase in circulating cortisol, which, given the clearly shown cortisol dependent induction of *pck1*, may have attenuated a possible insulin dependent inhibition of *pck1* transcripts. On the other hand, the induction in response to glucagon may be slightly overestimated, given glucagon and cortisol not only independently stimulate *pck1* transcription (Chakravarthy et al., 2005), but also act synergistically to stimulate *pck1* transcription (Iynedjian and Salavert, 1984)).

When considering socially subordinate fish, we observed a very strong (~400-fold) induction of hepatic *pck1* transcript abundance. Because subordinate fish are characterized by a sustained increase in circulating cortisol and fast over a period of 4 d, these mechanisms may be indicative of well described synergistic action of cortisol and glucagon, a fasting hormone on hepatic *pck1* gene expression described in mammalian hepatocytes (Iynedjian and Salavert, 1984). Finally, in whole body embryos, we did not observe significant changes in *pck1* transcript in response to acute hypoxia. Conversely, in fetal sheep subjected to anemic hypoxia, a significant increase in hepatic *pck1* was observed (Culpepper et al., 2016). However, given that whole embryos were investigated the specific contribution of hepatic *pck1* remains unknown in trout larvae and renders comparisons to hepatic *pck1* mRNA abundance under developmental hypoxia difficult. Nevertheless, our data collectively reveal a strongly conserved nutritional and endocrine regulation of *pck1* and the transcript level, which is likely mediated at the transcriptional and promotor level, although post-transcriptional regulation, for example by miRNAs, cannot be excluded and warrant investigation (Mennigen, 2016).

With regard to *pck2*, the current manuscript is the first to describe differential regulation of salmonid *pck2* ohnologues under experimental conditions known to modify gluconeogenesis in different organisms. Generally, a stronger regulation of the newly described *pck2b* compared to *pck2a* was observed across conditions. Specific *pck2b* upregulation was observed postprandially in response to hyperglycemia inducing high carbohydrate diets compared to fasted rainbow trout, as well as in whole embryos exposed to acute hypoxia. A specific decrease in *pck2b* was observed in subordinate rainbow trout liver. Conversely, glucoregulatory hormones only affected *pck2a* transcript abundance, as evidenced by a significant decrease in this transcript in response to glucagon perfusion. In contrast to *Pck1*, the transcriptional regulation of *Pck2* in mammals is largely unstudied, due to the fact that it is considered constitutively expressed in hepatic, but also extrahepatic tissues and appears to be largely unresponsive to glucoregulatory hormones such as glucagon (Modaressi et al., 1998; Stark and Kibbey, 2014). Because of this notion, mammalian Pck2 has long been considered to principally exert anaplerotic functions in the mitochondrial TCA. However, this notion has recently been challenged by rodent model knock out studies of *pck2* both *in vivo* and in primary hepatocytes *in vitro* (Méndez-Lucas et al., 2014; Stark et al., 2014), which revealed a physiological role for PCK2 to modulate *de novo* gluconeogenesis in response to mitochondrial substrate or energy availability, at least in part *via* amplification of PCK1-dependent gluconeogenesis. PCK2 knock down in primary hepatocytes also resulted in a shift of gluconeogenic substrates from lactate, glutamine and alanine metabolized by PCK2 to glycerol and pyruvate (Stark et al., 2014). Our results reveal, in contrast to mammalian studies, evidence for both endocrine and nutritional regulation of *pck2* ohnologue transcript abundance. Interestingly, and in direct contrast to the situation in mammals (Modaressi et al., 1998; Stark and Kibbey, 2014), *pck2a* transcript abundance appears to be regulated by glucoregulatory hormones in rainbow trout, as evidenced by a decrease in response to glucagon infusion in the current study, and a previous report of inhibition of this transcript by acute insulin administration *in vivo* and in primary hepatocytes *in vitro* (Plagnes-Juan et al., 2008). While differences in long term perfusion and i.p. injection likely account for differences between studies, the evidence to-date suggests that mitochondrial hepatic mitochondrial *pck2a* is responsive to glucoregulatory hormones in rainbow trout. The magnitude and directionality of *pck2a* expression is, at least in the case of glucagon, in contrast to the conserved regulation of *pck1* between trout and mammals. Our results also reveal evidence for nutritional and environmental regulation of mitochondrial *pck2*, which is, however, specific to *pck2b*. High dietary carbohydrates significantly increase *pck2b* mRNA abundance, suggesting a possible contribution to the glucose intolerant phenotype in rainbow trout, similarly to the proposed roles for the glucose-6-phosphatase 2b paralogues (Marandel et al., 2015). In mammals, a notable exception to the widely reported lack of transcriptional regulation of *Pck2* is a reported increase in both PCK2 mRNA and protein abundance in livers of rats that are chronically glucose-infused (Vincent et al., 2015). We furthermore observed specific increases in *pck2b* transcripts in whole embryos exposed to acute hypoxia. At least in adult rainbow trout, hypoxia exposure results in increased lactate concentration (Omlin et al., 2010). Because mitochondrial PCK2 preferentially metabolizes oxaloacetate derived from lactate (Modaressi et al., 1998), it is tempting to speculate that hepatic *pck2b* abundance may be controlled by its substrate; however, this scenario remains to be tested directly, especially given the comparatively small role of the rainbow trout liver in blood lactate regulation compared to mammals (Milligan and Girard, 1993).Interestingly, an increase in both mRNA level and enzymatic activity of Pck2 was also previously described in the hepatopancreas of shrimp exposed to acute hypoxia (Reyes-Ramos et al., 2018). A specific decrease in *pck2b* transcript abundance was observed in the liver of subordinate rainbow trout. This effect was not explained by a 4 day fast or cortisol increase alone, as evidenced by the lack of significant suppression in subsequent experiments examining key physiological correlates of subordinate trout status independently. When considering significantly increased circulating glucose concentration as an indicator of gluconeogenesis (which does not, however, take into account glucose fluxes - see Forbes et al., 2019), it appears that experimental conditions expected to increase and to inhibit gluconeogenesis were successful (Table 2), allowing for the interpretation of *pck* transcript changes in the context of altered hepatic gluconeogenesis. From a nutritional point of view, it appears that the increase of *pck2b* in trout fed a carbohydrate rich diet compared to fasted trout may, at least in part contribute to the observed 'glucose-intolerant' phenotype in this species. Indeed, transcripts of the previously identified novel glucose-6-phosphatase paralogues in rainbow trout (*g6pc2a* and *g6pc2b*) exhibit a similar increase in response to high carbohydrate diets, suggesting that the paradoxical upregulation of gluconeogenic enzyme paralogue transcripts is coordinated in this species (Marandel et al., 2015). With regard to endocrine factors, it appears that glucagon and cortisol contribute to increased *de novo* gluconeogenesis by inducing *pck1* in rainbow trout, similarly to the situation in mammals. Since subordinate trout exhibit high cortisol and increased PCK total enzyme activity (DiBattista et al., 2006), our study suggests that the cortisol-dependent stimulation of hepatic gluconeogenesis in subordinate trout is, at least in part, mediated by

transcriptional stimulation of *pck1*.

While the functional implications of the presence of *pck2* ohnologues and their differential regulation at the transcript level warrant future study in glucose intolerant rainbow trout and salmonids in general, the differential regulation of *pck2* ohnologues in itself is indicative of functional divergence. Functional divergence is largely considered to occur *via* three distinct mechanisms in teleost fishes (Glasauer and Neuhauss, 2014): neo-functionalization (assigning a novel function to one of the duplicates), sub-functionalization (partitioning of ancestral gene function on the duplicates), or dosage selection (preserving genes to maintain dosage balance between interconnected components). While the functional regulation of *pck2* in species ancestral to the SaGD event, such as zebrafish, are currently unknown, the differential regulation pattern of both ohnologous *pck2* transcripts in rainbow trout is reflective of possible neo- or sub-functionalization. Based on the largely conserved derived PCK2 amino sequences, which include an N-terminal sequence rich in positively charged amino acids which form part of the mitochondrial targeting sequence (Fukasawa et al., 2015), as well as high conservation of key catalytic and regulatory domains, it is likely that both Pck2a and Pck2b enzymes are functionally similar and that differential regulation occurred at the transcriptional/post-transcriptional level. It is currently unknown how differential expression, and more importantly, differential enzymatic activity, of mitochondrial Pck2a and Pck2b in conjunction with Pck1 affects hepatic *de novo* gluconeogenesis in rainbow trout. The recent acknowledgement for important gluconeogenic roles of PCK2 in mammals has led to the hypothesis that a dual regulation of hepatic gluconeogenesis by cytosolic PCK1 and mitochondrial PCK2 allows for increased metabolic plasticity. This is especially true in conditions of fasting and exercise, during which PCK2 is able to promote gluconeogenesis with greater efficiency and less dependence on oxygen consumption (Stark and Kibbey, 2014). Rainbow trout and salmonids are particularly interesting models to probe functional plasticity of gluconeogenic gene duplication, because as aquatic species they are subject to periodic hypoxia exposures, and are capable of long-term fasting and migration (Davidson, 2013). Indeed, unique metabolic phenotypes have evolved in rainbow trout, which include a pronounced inability to effectively utilize carbohydrates (Marandel et al., 2015) and muscle retention of lactate (Milligan and Girard, 1993). Future comparative studies in salmonids and ancestral non-salmonid species are therefore warranted to explore the nature of functional divergence of *pck2* genes and possible biological roles.

5. Conclusions

Our study identifies a previously undescribed salmonid-specific mitochondrial *pck2* paralogue, termed *pck2b* which arose from the SaGD. In rainbow trout exposed to experimental conditions, hepatic *pck1* exhibits strong expression changes in line with the reported strong transcriptional control of cytosolic *Pck1* reported in mammalian models. Conversely, rainbow trout exhibit differential regulation of *pck2* ohnologues, with endocrine regulation of *pck2a* and nutritional, social status-dependent and hypoxia dependent regulation of *pck2b*. Together, these differential transcript changes are indicative of sub- or neo-functionalization, and future studies probing the potential functional role of these ohnologues in the light of the glucose intolerant and fasting and exercise tolerant phenotype are warranted.

Supplementary data to this article can be found online at https://doi.org/10.1016/j.gene.2019.02.079.

Declaration of competing interests

No conflicts of interest, financial or otherwise, are declared by the author(s).

Funding

This work benefited from the financial support of the INRA PHASE Department. This research was carried out under the E2S UPPA supported by the “Investissements d'Avenir” managed by ANR (ANR-16-IDEX-0002). LM received EU support under the FP7 People: Marie-Curie Actions through an AgreenSkills+ fellowship (#609398). DJK gratefully acknowledges funding through a Mitacs Globalink grant, and JAM support from the Canada Foundation for Innovation (148035) and a NSERC Discovery grant (2114456-2017). The funding agencies had no role in the design, execution or interpretation of the study.

Author contributions

LM and JAM designed the study. LM performed *in silico* analysis. DJK identified the *pck2b* gene in NCBI *O. mykiss* database. DJK, JLIF and JL conducted experiments and analyzed gene expression data and provided specific graphs. DJK and JLIF conducted glucose assays, and CB conducted cortisol assays. LM, DJK and JAM wrote and edited the manuscript. DJK, JLIF, JL, CB, SP and JAM reviewed the final version of the manuscript and all authors approved the manuscript.

References

Berthelot, C., Brunet, F., Chalopin, D., Juanchich, A., Bernard, M., Noël, B., Bento, P., Da Silva, C., Labadie, K., Alberti, A., et al., 2014. The rainbow trout genome provides novel insights into evolution after whole-genome duplication in vertebrates. Nat. Commun. 5, 3657.

Birceanu, O., Servos, M.R., Vijayan, M.M., 2015. Bisphenol A accumulation in eggs disrupts the endocrine regulation of growth in rainbow trout larvae. Aquat. Toxicol. 161, 51–60.

Brawand, D., Wagner, C.E., Li, Y.I., Malinsky, M., Keller, I., Fan, S., Simakov, O., Ng, A.Y., Lim, Z.W., Bezault, E., et al., 2014. The genomic substrate for adaptive radiation in African cichlid fish. Nature 513, 375–381.

Chakravarthy, M.V., Pan, Z., Zhu, Y., Tordjman, K., Schneider, J.G., Coleman, T., Turk, J., Semenkovich, C.F., 2005. “New” hepatic fat activates PPARα to maintain glucose, lipid, and cholesterol homeostasis. Cell Metab. 1, 309–322.

Chen, S., Zhang, G., Shao, C., Huang, Q., Liu, G., Zhang, P., Song, W., An, N., Chalopin, D., Volff, J.-N., et al., 2014. Whole-genome sequence of a flatfish provides insights into ZW sex chromosome evolution and adaptation to a benthic lifestyle. Nat. Genet. 46, 253–260.

Choi, K., Weber, J.-M., 2015. Pushing the limits of glucose kinetics: how rainbow trout cope with a carbohydrate overload. J. Exp. Biol. 218, 2873–2880.

Cournarie, F., Azzout-Marniche, D., Foretz, M., Guichard, C., Ferre, P., Foufelle, F., 1999. The inhibitory effect of glucose on phosphoenolpyruvate carboxykinase gene expression in cultured hepatocytes is transcriptional and requires glucose metabolism. FEBS Lett. 460, 527–532.

Culpepper, C., Wesolowski, S.R., Benjamin, J., Bruce, J.L., Brown, L.D., Jonker, S.S., Wilkening, R.B., Hay, W.W., Rozance, P.J., 2016. Chronic anemic hypoxemia increases plasma glucagon and hepatic *PCK1* mRNA in late-gestation fetal sheep. Am. J. Physiol. Integr. Comp. Physiol. 311, R200–R208.

Davidson, W.S., 2013. Understanding salmonid biology from the Atlantic salmon genome. Genome 56, 548–550.

Desvignes, T., Fauvel, C., Bobe, J., 2011. The nme gene family in zebrafish oogenesis and early development. Naunyn Schmiedeberg's Arch. Pharmacol. 384, 439–449.

DiBattista, J.D.D., Levesque, H.M.M., Moon, T.W.W., Gilmour, K.M.M., 2006. Growth depression in socially subordinate rainbow trout *Oncorhynchus mykiss*: more than a fasting effect. Physiol. Biochem. Zool. 79, 675–687.

Ducasse-Cabanot, S., Zambonino-Infante, J., Richard, N., Medale, F., Corraze, G., Mambrini, M., Robin, J., Cahu, C., Kaushik, S., Panserat, S., 2007. Reduced lipid intake leads to changes in digestive enzymes in the intestine but has minor effects on key enzymes of hepatic intermediary metabolism in rainbow trout (Oncorhynchus mykiss). Animal 1, 1272–1282.

Edgar, R.C., 2004. MUSCLE: multiple sequence alignment with high accuracy and high throughput. Nucleic Acids Res. 32, 1792–1797.

Forbes, J.L.I., Kostyniuk, D.J., Mennigen, J.A., Weber, J.M., 2019. Unexpected effect of insulin on glucose disposal explains glucose intolerance in trout. Am. J. Physiol. Regul. Integr. Comp. Physiol., accepted. https://doi.org/10.1152/ajpregu.00344.2018.

Fukasawa, Y., Tsuji, J., Fu, S.-C., Tomii, K., Horton, P., Imai, K., 2015. MitoFates: improved prediction of mitochondrial targeting sequences and their cleavage sites. Mol. Cell. Proteomics 14, 1113–1126.

Gilmour, K.M., Craig, P.M., Dhillon, R.S., Lau, G.Y., Richards, J.G., 2017. Regulation of energy metabolism during social interactions in rainbow trout: a role for AMP-activated protein kinase. Am. J. Physiol. Regul. Integr. Comp. Physiol. 313, R549–R559.

Glasauer, S.M.K., Neuhauss, S.C.F., 2014. Whole-genome duplication in teleost fishes and its evolutionary consequences. Mol. Gen. Genomics. 289, 1045–1060.

Hahn, M.W., 2009. Distinguishing among evolutionary models for the maintenance of

gene duplicates. J. Hered. 100, 605–617.
Haman, F., Powell, M., Weber, J., 1997. Reliability of continuous tracer infusion for measuring glucose turnover rate in rainbow trout. J. Exp. Biol. 200.
Hanson, R.W., Reshef, L., 1997. Regulation of phosphoenolpyruvate carboxykinase (GTP) gene expression. Annu. Rev. Biochem. 66, 581–611.
Heckmann, L.-H., Sørensen, P.B., Krogh, P., Sørensen, J.G., 2011. NORMA-Gene: a simple and robust method for qPCR normalization based on target gene data. BMC Bioinformatics 12, 250.
Hu, W., Chen, J., 2015. Whole-genome sequencing opens a new era for molecular breeding of grass carp (Ctenopharyngodon idellus). Sci. China Life Sci. 58, 619–620.
Iynedjian, P.B., Salavert, A., 1984. Effects of glucagon, dexamethasone and triiodothyronine on phosphoenolpyruvate carboxykinase (GTP) synthesis and mRNA level in rat liver cells. Eur. J. Biochem. 145, 489–497.
Jeffrey, J.D., Esbaugh, A.J., Vijayan, M.M., Gilmour, K.M., 2012. Modulation of hypothalamic-pituitary-interrenal axis function by social status in rainbow trout. Gen. Comp. Endocrinol. 176, 201–210.
Jin, J., Médale, F., Kamalam, B.S., Aguirre, P., Véron, V., Panserat, S., 2014. Comparison of glucose and lipid metabolic gene expressions between fat and lean lines of rainbow trout after a glucose load. PLoS One 9, e105548.
Kirchner, S., Panserat, S., Lim, P.L., Kaushik, S., Ferraris, R.P., 2008. The role of hepatic, renal and intestinal gluconeogenic enzymes in glucose homeostasis of juvenile rainbow trout. J. Comp. Physiol. B. 178, 429–438.
Kostyniuk, D.J., Culbert, B.M., Mennigen, J.A., Gilmour, K.M., 2018. Social status affects lipid metabolism in rainbow trout, *Oncorhynchus mykiss*. Am. J. Physiol. Integr. Comp. Physiol. 315, R241–R255.
Lansard, M., Panserat, S., Plagnes-Juan, E., Seiliez, I., Skiba-Cassy, S., 2010. Integration of insulin and amino acid signals that regulate hepatic metabolism-related gene expression in rainbow trout: role of TOR. Amino Acids 39, 801–810.
Lien, S., Koop, B.F., Sandve, S.R., Miller, J.R., Kent, M.P., Nome, T., Hvidsten, T.R., Leong, J.S., Minkley, D.R., Zimin, A., et al., 2016. The Atlantic salmon genome provides insights into rediploidization. Nature 533, 200–205.
Liu, J., Dias, K., Plagnes-Juan, E., Veron, V., Panserat, S., Marandel, L., 2017a. Long-term programming effect of embryonic hypoxia exposure and high-carbohydrate diet at first feeding on glucose metabolism in juvenile rainbow trout. J. Exp. Biol. 220, 3686–3694.
Liu, J., Plagnes-Juan, E., Geurden, I., Panserat, S., Marandel, L., 2017b. Exposure to an acute hypoxic stimulus during early life affects the expression of glucose metabolism-related genes at first-feeding in trout. Sci. Rep. 7, 363.
Macqueen, D.J., Johnston, I.A., 2014. A well-constrained estimate for the timing of the salmonid whole genome duplication reveals major decoupling from species diversification. Proceedings. Biol. Sci. 281, 20132881.
Marandel, L., Labbe, C., Bobe, J., Le Bail, P.-Y., 2012. Nanog 5′-upstream sequence, DNA methylation, and expression in gametes and early embryo reveal striking differences between teleosts and mammals. Gene 492, 130–137.
Marandel, L., Seiliez, I., Véron, V., Skiba-Cassy, S., Panserat, S., 2015. New insights into the nutritional regulation of gluconeogenesis in carnivorous rainbow trout (*Oncorhynchus mykiss*): a gene duplication trail. Physiol. Genomics 47, 253–263.
Marandel, L., Véron, V., Surget, A., Plagnes-Juan, É., Panserat, S., 2016. Glucose metabolism ontogenesis in rainbow trout (Oncorhynchus mykiss) in the light of the recently sequenced genome: new tools for intermediary metabolism programming. J. Exp. Biol. 219, 734–743.
Méndez-Lucas, A., Hyroššová, P., Novellasdemunt, L., Viñals, F., Perales, J.C., 2014. Mitochondrial phosphoenolpyruvate carboxykinase (PEPCK-M) is a pro-survival, endoplasmic reticulum (ER) stress response gene involved in tumor cell adaptation to nutrient availability. J. Biol. Chem. 289, 22090–22102.
Mennigen, J.A., 2016. Micromanaging metabolism—a role for miRNAs in teleost energy metabolism. Comp. Biochem. Physiol. Part - B Biochem. Mol. Biol. 199, 115–125.
Milligan, C.L., Girard, S.S., 1993. Lactate metabolism in rainbow trout. J. Exp. Biol. 180.
Modaressi, S., Brechtel, K., Christ, B., Jungermann, K., localization, chromosomal, 1998. Human mitochondrial phosphoenolpyruvate carboxykinase 2 gene. Structure, chromosomal localization and tissue-specific expression. Biochem. J. 333 (Pt 2), 359–366.
Naylor, R.L., Hardy, R.W., Bureau, D.P., Chiu, A., Elliott, M., Farrell, A.P., Forster, I., Gatlin, D.M., Goldburg, R.J., Hua, K., et al., 2009. Feeding aquaculture in an era of finite resources. Proc. Natl. Acad. Sci. U. S. A. 106, 15103–15110.
Omlin, T., Weber, J.-M.J.-M., Weber, J.-M.J.-M., Randall, D., 2010. Hypoxia stimulates lactate disposal in rainbow trout. J. Exp. Biol. 213, 3802–3809.
Panserat, S., Plagnes-Juan, E., Kaushik, S., 2001a. Nutritional regulation and tissue specificity of gene expression for proteins involved in hepatic glucose metabolism in rainbow trout (Oncorhynchus mykiss). J. Exp. Biol. 204, 2351–2360.
Panserat, S., Plagnes-Juan, E., Brèque, J., Kaushik, S., 2001b. Hepatic phosphoenolpyruvate carboxykinase gene expression is not repressed by dietary carbohydrates in rainbow trout (Oncorhynchus mykiss). J. Exp. Biol. 204, 359–365.
Pasquier, J., Cabau, C., Nguyen, T., Jouanno, E., Severac, D., Braasch, I., Journot, L., Pontarotti, P., Klopp, C., Postlethwait, J.H., et al., 2016. Gene evolution and gene expression after whole genome duplication in fish: the PhyloFish database. BMC Genomics 17, 368.
Plagnes-Juan, E., Lansard, M., Seiliez, I., Médale, F., Corraze, G., Kaushik, S., Panserat, S., Skiba-Cassy, S., 2008. Insulin regulates the expression of several metabolism-related genes in the liver and primary hepatocytes of rainbow trout (Oncorhynchus mykiss). J. Exp. Biol. 211, 2510–2518.
Polakof, S., Alvarez, R., Soengas, J.L., 2010. Gut glucose metabolism in rainbow trout: implications in glucose homeostasis and glucosensing capacity. AJP Regul. Integr. Comp. Physiol. 299, R19–R32.
Polakof, S., Skiba-Cassy, S., Kaushik, S., Seiliez, I., Soengas, J.L., Panserat, S., 2012. Glucose and lipid metabolism in the pancreas of rainbow trout is regulated at the molecular level by nutritional status and carbohydrate intake. J. Comp. Physiol. B. 182, 507–516.
Reyes-Ramos, C.A., Peregrino-Uriarte, A.B., Cota-Ruiz, K., Valenzuela-Soto, E.M., Leyva-Carrillo, L., Yepiz-Plascencia, G., 2018. Phosphoenolpyruvate carboxykinase cytosolic and mitochondrial isoforms are expressed and active during hypoxia in the white shrimp Litopenaeus vannamei. Comp. Biochem. Physiol. Part B Biochem. Mol. Biol. 226, 1–9.
Samy, J.K.A., Mulugeta, T.D., Nome, T., Sandve, S.R., Grammes, F., Kent, M.P., Lien, S., Våge, D.I., 2017. SalmoBase: an integrated molecular data resource for Salmonid species. BMC Genomics 18, 482.
Sato, Y., Hashiguchi, Y., Nishida, M., 2009. Temporal pattern of loss/persistence of duplicate genes involved in signal transduction and metabolic pathways after teleost-specific genome duplication. BMC Evol. Biol. 9, 127.
Schein, V., Waché, Y., Etges, R., Kucharski, L.C., van Wormhoudt, A., Da Silva, R.S., 2004. Effect of hyperosmotic shock on phosphoenolpyruvate carboxykinase gene expression and gluconeogenic activity in the crab muscle. FEBS Lett. 561, 202–206.
Stark, R., Kibbey, R.G., 2014. The mitochondrial isoform of phosphoenolpyruvate carboxykinase (PEPCK-M) and glucose homeostasis: has it been overlooked? Biochim. Biophys. Acta - Gen. Subj. 1840, 1313–1330.
Stark, R., Guebre-Egziabher, F., Zhao, X., Feriod, C., Dong, J., Alves, T.C., Ioja, S., Pongratz, R.L., Bhanot, S., Roden, M., et al., 2014. A role for mitochondrial phosphoenolpyruvate carboxykinase (PEPCK-M) in the regulation of hepatic gluconeogenesis. J. Biol. Chem. 289, 7257–7263.
Tamura, K., Stecher, G., Peterson, D., Filipski, A., Kumar, S., 2013. MEGA6: molecular evolutionary genetics analysis version 6.0. Mol. Biol. Evol. 30, 2725–2729.
Vernier, M.J., 1969. Table chronogique du development embryonnaire de la truite arc-en-ciel, Salmo gairdneri Rich. Ann. Embryol. Morphog. 2, 495–520.
Vincent, E.E., Sergushichev, A., Griss, T., Gingras, M.-C., Samborska, B., Ntimbane, T., Coelho, P.P., Blagih, J., Raissi, T.C., Choinière, L., et al., 2015. Mitochondrial phosphoenolpyruvate carboxykinase regulates metabolic adaptation and enables glucose-independent tumor growth. Mol. Cell 60, 195–207.
Xu, P., Zhang, X., Wang, X., Li, J., Liu, G., Kuang, Y., Xu, J., Zheng, X., Ren, L., Wang, G., et al., 2014. Genome sequence and genetic diversity of the common carp, Cyprinus carpio. Nat. Genet. 46, 1212–1219.
Yang, J., Kalhan, S.C., Hanson, R.W., 2009. What is the metabolic role of phosphoenolpyruvate carboxykinase? J. Biol. Chem. 284, 27025–27029.

Chapter 3: Dietary carbohydrate content differentially regulate miRNAs and their predicted gluconeogenic gene paralogue targets

*This chapter has been published as **Kostyniuk DJ***, Marandel L*, Jubouri M, Dias K, de Souza RF, Zhang D, Martyniuk CJ, Panserat S, Mennigen JA. 2019. Profiling the rainbow trout hepatic miRNAome under diet-induced hyperglycemia. Physiol Genomics. 2019;51(9):411-431. Authors indicated by asterisk share first authorship of the published manuscript.*

***Statement of contribution**: The experimental samples were generated at INRA St.Pée-sur-Nivelle, France. I conducted and analyzed all real-time RT-PCR and protein assays, as well as in silico target prediction analysis of small RNA next generation sequence data.*

Publisher allows the reproduction of the manuscript in full within the context of my MSc thesis.

https://www.physiology.org/author-info.permissions

Reuse by Authors of Their Work Published by APS

The APS Journals are copyrighted for the protection of authors and the Society. The Mandatory Submission Form serves as the Society's official copyright transfer form. Author's rights to reuse their APS-published work are described below:

Theses and Dissertations	Authors may reproduce whole published articles in dissertations and post to thesis repositories without charge and without requesting permission. Full citation is required.

RESEARCH ARTICLE | *Genomics of Metabolic and Tumor/Cancer Traits*

Profiling the rainbow trout hepatic miRNAome under diet-induced hyperglycemia

Daniel J. Kostyniuk,[1]* Lucie Marandel,[2]* Mais Jubouri,[1] Karine Dias,[2] Robson F. de Souza,[3] Dapeng Zhang,[4] Christopher J. Martyniuk,[5] Stéphane Panserat,[2] and Jan A. Mennigen[1]

[1]*Department of Biology, University of Ottawa, Ottawa, Ontario, Canada;* [2]*INRA, Université de Pau et Pays d'Adour, UMR 1419, Nutrition, Metabolism and Aquaculture, E2S UPPA, Saint Pée-sur-Nivelle, France;* [3]*Microbiology Department, Institute of Biomedical Sciences, University of São Paulo, São Paulo, Brazil;* [4]*Department of Biology, Saint Louis University, Saint Louis, Missouri; and* [5]*Department of Physiological Sciences and Center for Environmental and Human Toxicology, UF Genetics Institute, College of Veterinary Medicine, University of Florida, Gainesville, Florida*

Submitted 4 April 2019; accepted in final form 28 June 2019

Kostyniuk DJ, Marandel L, Jubouri M, Dias K, de Souza RF, Zhang D, Martyniuk CJ, Panserat S, Mennigen JA. Profiling the rainbow trout hepatic miRNAome under diet-induced hyperglycemia. *Physiol Genomics* 51: 411–431, 2019. First published July 8, 2019; doi:10.1152/physiolgenomics.00032.2019.—Carnivorous rainbow trout exhibit prolonged postprandial hyperglycemia when fed a diet exceeding 20% carbohydrate content. This poor capacity to utilize carbohydrates has led to rainbow trout being classified as "glucose-intolerant" (GI). The metabolic phenotype has spurred research to identify the underlying cellular and molecular mechanisms of glucose intolerance, largely because carbohydrate-rich diets provide economic and ecological advantages over traditionally used fish meal, considered unsustainable for rainbow trout aquaculture operations. Evidence points to a contribution of hepatic intermediary carbohydrate and lipid metabolism, as well as upstream insulin signaling. Recently, microRNAs (miRNAs), small noncoding RNAs acting as negative posttranscriptional regulators affecting target mRNA stability and translation, have emerged as critical regulators of hepatic control of glucose-homeostasis in mammals, revealing that dysregulated hepatic miRNAs might play a role in organismal hyperglycemia in metabolic disease. To determine whether hepatic regulatory miRNA networks may contribute to GI in rainbow trout, we induced prolonged postprandial hyperglycemia in rainbow trout by using a carbohydrate-rich diet and profiled genome-wide hepatic miRNAs in hyperglycemic rainbow trout compared with fasted trout and trout fed a diet devoid of carbohydrates. Using small RNA next-generation sequencing and real-time RT-PCR validation, we identified differentially regulated hepatic miRNAs between these groups and used an in silico approach to predict bona fide mRNA targets and enriched pathways. Diet-induced hyperglycemia resulted in differential regulation of hepatic miRNAs compared with fasted fish. Some of the identified miRNAs, such as *miRNA-27b-3p* and *miRNA-200a-3p*, are known to be responsive to hyperglycemia in the liver of hyperglycemic glucose-tolerant fish and mammals, suggesting an evolutionary conserved regulation. Using Gene Ontology term-based enrichment analysis, we identify intermediate carbohydrate and lipid metabolism and insulin signaling as potential targets of posttranscriptional regulation by hyperglycemia-regulated miRNAs and provide correlative expression analysis of specific predicted miRNA-target pairs. This study identifies hepatic miRNAs in rainbow trout that exhibit differential postprandial expression in response to diets with different carbohydrate content and predicts posttranscriptionally regulated target mRNAs enriched for pathways involved in glucoregulation. Together, these results provide a framework for testable hypotheses of functional involvement of specific hepatic miRNAs in GI in rainbow trout.

glucose; liver; microRNA; nutrition; rainbow trout

INTRODUCTION

Rainbow trout is a carnivorous species that is considered to be "glucose intolerant" (GI) due to its poor utilization of carbohydrates and pronounced hyperglycemia following the ingestion of carbohydrates that exceed 20% of dietary macronutrients (3, 41, 42, 59). While the pronounced and prolonged high carbohydrate diet-induced hyperglycemia has led to the description of rainbow trout as GI (34), it is important to note that the long-term consequences of diet-induced hyperglycemia in rainbow trout may differ compared with well-described phenotypes of GI in diabetic mammals (78). While high-carbohydrate diets have been described to consistently increase the hepatosomatic index in rainbow trout (2, 28, 52), both inhibitory (2, 28) and stimulatory (52) effects on body weight gain have been described, as well as a lack of glucotoxic responses (52) associated with prolonged hyperglycemia in diabetic humans and animal models of diabetes (78).

Because of the rainbow trout's prominent role as a fish model in comparative physiology (12) and its commercial importance in freshwater aquaculture (54), the investigation of the molecular and cellular basis of GI in different tissues has been a research focus over the last two decades (49, 60, 61). In the context of comparative physiology, the identification of mechanisms underlying rainbow trout GI at the molecular, cellular, tissue, and organismal level may yield important insights into the evolution of GI in this species. In the context of rainbow trout aquaculture today, increasing the utilization of dietary carbohydrates represents a sustainable and economical alternative to the traditionally used economically and ecologically unsustainable fish-meal based protein diets (50, 54).

Driven by these basic and applied research goals, investigators have put forward several hypotheses to explain molecular and cellular underpinnings of the GI phenotype in several tissues in rainbow trout. For example, evidence has been

* D. J. Kostyniuk and L. Marandel contributed equally to this work.

Address for reprint requests and other correspondence: J. A. Mennigen, Dept. of Biology, Univ. of Ottawa, Ottawa, Ontario, K1N 6N5, Canada (e-mail: jan.mennigen@uottawa.ca).

reported for a role for gastrointestinal absorption of digestible carbohydrates in diet-induced GI in rainbow trout, which may be higher compared with amino acids in trout (40, 71). Conversely, at the level of excretion, evidence points to an involvement of the kidney. At the resorption maximum for glucose, plasma glucose concentration is 22 mmol/L in rainbow trout (9), twice the estimated amount of the 11 mmol/L in healthy humans and matching the rate observed in diabetic humans (76), suggesting that increased resorption capacity of glucose in the rainbow trout kidney also contributes to the GI phenotype in rainbow trout.

When one considers the metabolic fate of postprandial circulating glucose in rainbow trout in between absorption and excretion by metabolic tracing studies (6, 8, 21, 40) and calculation of metabolic flux (23), it is evident that the liver plays a particularly important role in intermediary glucose metabolism following the ingestion of dietary carbohydrates. The liver participates in the systemic regulation of circulating glucose concentrations specifically via regulation of glucose uptake, glycolysis, and glycogen deposition (6, 21) or de novo lipogenesis (DNL) (8, 21) on the one hand and de novo gluconeogenesis on the other (23). Molecular components of these pathways and their regulation have been interrogated over the past decade and have led to integrative hypotheses to include cellular and molecular components that underlie the contribution of the described intermediary metabolic pathways to GI in rainbow trout. First, while the rainbow trout liver efficiently responds to dietary carbohydrates as evidenced by strong induction of glucokinase expression and activity (55), the transcript abundance and/or activity of gluconeogenic enzymes are not inhibited in response to high dietary carbohydrates (32, 56). This suggests a contribution of hepatic gluconeogenesis to rainbow trout GI. Second, induction of transcripts encoding transcription factors and enzymes involved in hepatic DNL in genetically selected high-fat rainbow trout lines (32, 41, 42, 56) and pharmacologically treated (metformin) rainbow trout (57) correlates with improved responses to diet-induced hyperglycemia. This suggests that DNL may be limiting glucose utilization and hence contribute to persistent postprandial hyperglycemia in rainbow trout.

In addition to these key glucose and lipid metabolic pathways investigated at the gene transcript and activity level, upstream analysis of hepatic insulin signaling pathway has also been investigated comparatively in rainbow trout liver in vitro (15, 35) and in vivo (13, 14). These studies have revealed that gene expression and activity of hepatic lipogenic (fatty acid synthase) and gluconeogenic (glucose-6-phosphatase) enzymes are mediated via target of rapamycin (Tor) signaling, which is more responsive to proteins and amino acids than carbohydrates. These results indicate that nutrient-dependent activation of insulin/Tor signaling and downstream regulation of gene expression of intermediary metabolic genes involved in glucose and lipid metabolism have evolved to respond to dietary proteins, rather than carbohydrates in this carnivorous species. While this hepatic regulation in response to dietary proteins ensures suitable production of lipids preferably used as fuel by rainbow trout muscles compared with carbohydrates (10, 39) and sufficient amounts of de novo produced glucose to sustain tissues with high requirements for carbohydrates, including the brain, kidney, and spleen (10, 39), the reviewed literature reveals that such hepatic molecular, cellular, and metabolite-level regulation may underlie rainbow trout GI and poor carbohydrate utilization.

The recent sequencing of the rainbow trout genome and its annotation (4, 66) now allow for additional layers of investigation into hepatic mechanisms of GI in this species, first by allowing a more precise characterization of (possibly subfunctionalized) paralogs present in salmonid genomes (42), and second by enabling the study of the involvement of molecular epigenetic mechanisms, including DNA methylation and histone modifications at the DNA level (41) and posttranscriptional mechanisms, especially the microRNA (miRNA or miR)-based mRNA transcript regulation via 3′-untranslated region (UTR) binding (30, 43, 46). Indeed, the lack of suppression of hepatic G6pc activity has been linked to the atypical induction of two *g6pcb2* paralogs in rainbow trout in response to dietary carbohydrates, suggesting that paralogs retained following genome duplication events may contribute to GI in rainbow trout (41, 42). In addition to global hypomethylation, reduction in methylation of specific CpG sites in proximity to transcription state sites was determined for both *g6pcb2* paralogs, suggesting a potential role for DNA methylation dynamics in the differential regulation of these paralogs (41).

In contrast, while a functional proof-of-principle study revealed a role for the liver-specific *miRNA-122* in the regulation of postprandial circulating glucose in trout (44), possibly via reduced hepatic DNL capacity consistent with described effects in mammalian knockout models (74), the possible involvement of hepatic miRNAs in the GI phenotype in rainbow trout has not been systematically investigated at the transcriptome level following the publication of the rainbow trout genome. Given that hepatic miRNAs have emerged as important regulators of hepatic glucose metabolism (37, 48) and are indeed markers (26, 27, 36, 82) and functional contributors (22, 63, 65) of GI in mammalian models of metabolic disease by targeting intermediary metabolic pathways of glucose and lipid metabolism and/or upstream insulin signaling pathways (22, 63, 65), the current study aims to comparatively assess a possible role for hepatic miRNAs in GI in rainbow trout by a multitiered approach. First, we globally determine a possible involvement for hepatic miRNAs in diet-induced GI by profiling key components of the canonical miRNA biogenesis machinery in fasted trout compared with trout refed a diet devoid of carbohydrates and enriched in carbohydrates that induces GI. Second, to identify specific hepatic miRNAs that may be implicated in GI in rainbow trout, we identify differentially expressed hepatic miRNAs between fasted trout and two groups of trout: one fed a diet devoid of carbohydrates and the other fed a diet enriched in carbohydrates that induces GI, using a transcriptome level sequencing approach. Lastly, to infer possible functional posttranscriptional consequences at the genome-wide level, we use an in silico approach to predict whether differential expressed hepatic miRNAs target genes and enriched pathways relevant to GI in rainbow trout, and assess the activity of these pathways by using molecular markers. In doing so, we prioritize specific hepatic miRNAs for future functional study in the rainbow trout liver.

METHODS

Experimental Design, Diets, and Tissue Sampling

The liver samples used to profile miRNAs in the current study were obtained from an experiment originally described by Marandel et al. (41, 42). In brief, juvenile rainbow trout (70 g body mass) were distributed in six tanks ($n = 15$ fish per tank) and reared at 17°C in the INRA experimental facilities at Saint-Pée-sur-Nivelle, France. After 4 days of total starvation (Fasted), two fish per tank were euthanized. Fish were then fed twice a day at a ratio of 2.5% body weight for 4 days with one of two diets (Fig. 1*A*): a NoCHO (diet without carbohydrate) and a HighCHO (diet with ~30% carbohydrates), prepared at INRA, Saint-Pée-sur-Nivelle, France, as pressed pellets. The two diets were isolipidic and isoenergetic. Gelatinized starch was included as carbohydrate source, protein was provided by fishmeal, and dietary lipid by fish oil and fish meal. Inclusion of carbohydrates (30%) in the HighCHO diet was compensated for by a decreased dietary protein level (40%), which was still above the 37% protein requirement of rainbow trout (49a). No carbohydrates were added to the NoCHO diet, which contained 60% crude protein. A detailed description of diet composition can be found in Additional File 1. (Supplemental material for this article can be found at https://figshare.com/s/d2939b753fc65b1455e7.)

Each dietary treatment was administered in three tanks, and neither body weight nor standard length changed between groups over the course of the experiment. Fish were euthanized 6 h after the last meal ($n = 9$ fish per diet, 3 per tank). Gut content of the sampled animals was systematically checked to confirm that the fish sampled had consumed the diet. Blood was removed from the caudal vein via heparinized syringes and centrifuged (3,000 *g*, 5 min). The plasma recovered was immediately frozen and kept at −20°C until analysis to confirm expected hyperglycemia in the HighCHO diet-fed group. The fresh liver of each fish was dissected and frozen immediately in liquid nitrogen and then kept at −80°C. A subset of $n = 4$ randomly selected samples per treatment group was used for miRNA profiling. The randomly selected samples maintained the different glucose profiles previously reported (Fig. 1*B*).

Ethics Approval and Consent to Participate

All investigations were conducted according to the guiding principles for the use and care of laboratory animals and in compliance with French and European regulations on animal welfare (Décret 2001-464, 29 May 2001 and Directive 2010/63/EU, respectively). Fish were killed by concussion/blow to the skull, and death was confirmed by exsanguination. No anesthetic was used to avoid bias in analysis of enzymatic activity. This protocol and the project as a whole were approved by the French National Consultative Ethics Committee.

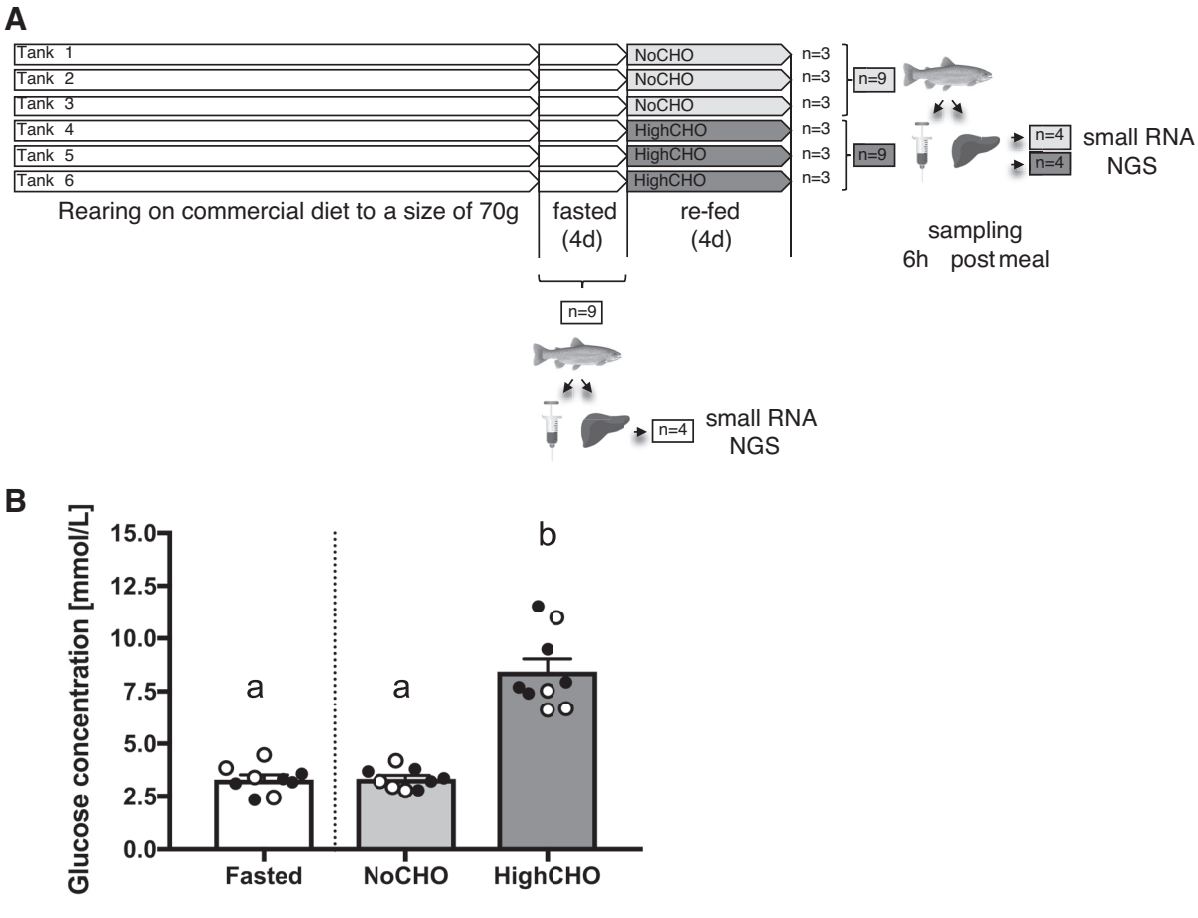

Fig. 1. Overview of the experimental design, tissue sampling and experimental end points (*A*). Mean serum/plasma glucose concentration (+SE) in rainbow trout fasted for 2 days and in rainbow trout 6 h after being refed either a NoCHO diet (devoid of carbohydrates) or a HighCHO diet (containing 30% carbohydrates) (*B*). Diets used were isoenergetic. Individual data are represented by dots, with open circles representing samples from individual fish that correspond to randomly selected liver samples ($n = 4$) used for next-generation sequencing (NGS). Two separate one-way ANOVAs followed by Tukey's post hoc ($P < 0.05$) tests revealed a significant induction of hyperglycemia 6 h after refeeding a carbohydrate-rich diet, both in the full sample set ($F_{2,27} = 74.89$, $P < 0.01$), as well as in the randomly selected subset of 4 samples per group ($F_{2,12} = 18.27$, $P < 0.01$). Different letters indicate significantly different glucose concentrations between groups.

Small RNA Next-generation Sequencing and Differential Expression Analysis

Total RNA was extracted by the Trizol method as previously described (41, 42), and the quality of total RNA was confirmed twice (before and after shipping of RNA samples) by RNA integrity numbers (RIN) >9.2 with an Agilent Technologies 2100 Bioanalyzer (Agilent, Mississauga, ON, Canada). Small RNA sequencing was performed by using services provided by LC Sciences (Houston, TX) using four randomly selected samples from each treatment group. Nucleotide fractions (15–50 nt) of small RNA were isolated from the total RNA by polyacrylamide gel electrophoresis and were ligated to a 30 nt adapter followed by a 50 nt adapter (TruSeq Small RNA Library Prep kit; Illumina, San Diego, CA). The small RNA ligated to the adaptors was reverse transcribed to cDNA, PCR amplified, and gel purified. The gel-extracted cDNA was used for library preparation, which was further used for cluster generation on Illumina's Cluster Station before sequencing using Illumina GAIIx. Raw sequence data were obtained from image data with Illumina's Sequencing Control Studio software version 2.8 (SCS v2.8) following real-time sequencing image analysis and base-calling by Illumina's Real-Time Analysis version 1.8.70 (RTA v1.8.70) and deposited in the National Center for Biotechnology Information (NCBI) Gene expression Omnibus (GEO) under accession number GSE112814 with specific files (n = 4) for fasted groups (GSM3084221-GSM3084224), refed NoCHO (GSM3084224-GSM3084228), and refed HighCHO (GSM3084229-GSM3084232).

Briefly, sequences were initially filtered with the proprietary LC Science ACGT10-miR v4.2 pipeline to remove low-quality sequences, low-complexity sequences, and sequences corresponding to common RNA families (mRNA, RFam, Repbase, piRNA), as described by Ma and colleagues (38). Retained high-quality sequences were then submitted to a bowtie search against all fish miRNA gene sequences deposited in miRbase v21.0 (1 mismatch allowed in the first 16 nt). In cases where unique sequences mapped to the miRbase-deposited fish miRNA genes, the obtained miRbase hits were subsequently mapped to the rainbow trout genome to determine genomic locations. Any alignment that had already previously been characterized as a genomic location for this specific microRNA in the rainbow trout genome (30) was identified as known rainbow trout miRNA (gp 1a). All miRNAs that were successfully aligned to miRbase deposited fish species miRNA genes, and had not been described in the rainbow trout miRNA repertoire but mapped to the rainbow trout genome, were retained as trout microRNAs (gp 1b). The remaining miRbase hits form both gp1a and gp1b that in addition to known miRNA loci also mapped to other rainbow trout genome loci were designated as gp1c.

High-quality sequences that could be matched to fish species miRNA genes in miRbase, which in turn could not be mapped to the rainbow trout genome, were further analyzed as follows: The high-quality short sequence was directly mapped onto the rainbow trout genome, and the locus further analyzed for its possibility to generate hairpin transcripts. This was achieved by retrieving 80 nt flanking sequences of mapped high-quality sequences. Retrieved sequence were then analyzed for their propensity to form hairpin structures by RNA-fold software (http://rna.tbi.univie.ac.at/cgi-bin/RNAfold.cgi) with the following criteria: *1*) ≤12 nt in one bulge in stem, *2*) ≥16 bp in the stem region of the predicted hairpin, *3*) ≤−15 kCal/mol cut-off of ΔG, *4*) ≥50 hairpin length that contains up and down stems and hairpin loop, *5*) a ≤200 nt hairpin loop length, *6*) ≤4 nt in one bulge in the mature miRNA region, *7*) ≤2 errors in one bulge in mature region, *8*) ≤2 biased bulges in mature region, *9*) ≤4 errors in the mature miRNA region, *10*) ≥12 bp in the mature region of the predicted hairpin, *11*) >80% of mature miRNA is in located in the stem. Sequences in located in loci predicted to form hairpins were grouped as gp2a, and sequences mapped to loci not predicted to form hairpins were designated as gp2b. High-quality sequences mapped to fish miRNA genes deposited in miRbase, which neither mapped to the rainbow trout genome as fish miRbase gene hit, nor as mature sequence, but had been identified as mature miRNA in rainbow trout were designated gp3a. Conversely, high-quality sequences mapped to fish miRNA genes deposited in miRbase, which neither mapped to the rainbow trout genome as fish miRbase gene hit, nor as mature sequence, and had not been identified as mature miRNA in rainbow trout were designated gp3b. Finally remaining sequences that could not be matched to miRbase fish species but could be mapped to the rainbow trout genome were again tested for the potential to form hairpin structures with flanking sequences. Sequences predicted to be able to form hairpins were designated as gp4a, sequences predicted to be unable to form hairpins were designated as gp4b. An overview of the bioinformatics pipeline and databases used are provided in Additional Files 2 and 3.

Differentially expressed miRNAs were identified with the statistical software R (version 3.2.2) package DESeq2 for one-way ANOVA comparison of all three treatment groups (fasted-NoCHO-HighCHO), and t-tests for specific between-group comparisons (fasted-NoCHO, fasted-HighCHO, NoCHO-HighCHO).

Relative mRNA quantification. Total RNA was extracted by the Trizol method as previously described (41, 42), and the QuantiTect reverse transcriptase kit (Qiagen) was used to generate mRNA cDNA with total RNA according to the manufacturer's protocol. The mRNA abundance levels of several specific targets (Table 1) were assessed by two-step real-time RT-PCR using the CFX96-Real-Time System-C1000 Thermal Cycler machine (Bio-Rad). Reactions were prepared in a total volume of 20 μL, containing 10 μL of SsoAdvanced Universal Inhibitor-Tolerant SYBR Green Supermix (Bio-Rad), 4 μL of diluted cDNA template, 0.5 μL of each specific forward and reverse primer at a concentration of 10 nM (IDT, Table 1), and 5 μL of H_2O. Elongation factor 1 (ef1α) mRNA abundance was used to normalize mRNA gene expression (51). A noRT and noTemp reaction was included to control for DNA contamination in each assay. Standard curves were generated for each primer pair from serially diluted (1:2) pooled cDNA to determine amplification efficiency and R^2 values. Following an enzyme activation step at 98°C (2 min), two steps were repeated for 40 cycles. These included a denaturation step at 95°C (20 s) and a combined annealing and extension step at primer-specific temperatures (Table 1). Following each run, melting curves were produced by gradual (0.5°C increase each 5 s) increase in temperature from 65 to 95°C and were monitored for single peaks suggesting specific amplicon production and absence of primer dimers. Specificity of newly designed primer pairs was furthermore confirmed by sequencing (OHRI, Ottawa, ON, Canada), and product sequences confirmed via NCBI Basic Local Alignment Search Tool search of the trout genome. The amplification efficiencies were between 92.3 and 112.8%, and the R2 was >0.98 (see Table 1). As for the miRNAs, normalized mRNA abundance (mRNA/ef1α) was calculated relative to the fasted group and presented as fold changes according to the ΔΔCT method (67). Data were analyzed with Prism Version 7 and transformed to fit normal distribution. In normally distributed data, Grubb's outlier test was used to identify and remove possible single outliers in a treatment group. Data were subsequently analyzed by a one-way ANOVA followed by Tukey's post hoc test. In cases where data did not meet normality and homoscedasticity criteria as assessed by Shapiro-Wilk and Bartlett's test, data were analyzed by a Kruskal-Wallis test followed by Dunn's multiple comparison test. Significance was determined at a $P < 0.05$ level.

Quantitative miRNA quantification. miRNA cDNA was synthesized by TaqMan MicroRNA Reverse Transcription Kit (Life Technologies, Burlington, ON, Canada) with 10 ng of total RNA per 15 μL RT reaction containing 0.15 μL 100 mM dNTPs (with dTTP), 1.00 μL MultiScribe Reverse Transcriptase 50 U/μL, 1.50 μL 10× Reverse Transcription Buffer, 0.19 μL RNase Inhibitor 20 U/ μL, 4.16 μL nuclease-free water, 5 μL total RNA, and 3 μL miRNA-specific 5× RT primer following the manufacturer's protocol. Two-step real-

Table 1. *Real-time RT-PCR assay primer sequences and reaction parameters*

Gene Target	Primer Pair (5′ to 3′)	Annealing Temperature, °C	Efficiency, %	R^2
	Canonical microRNA biogenesis pathway			
drosha	F: GAGGAGTCGGTGAAGGAATG	60	92.3	0.98
GSONMT00009052001	R: CATGTGGGAGAAGAGGGAGA			
xpo5a	F: ACTCTCGAACACGGCTGATG	59	103.3	0.99
GSONMT00065065001	R: CACACATATCAGCCACCGGT			
xpo5b	F: AGTCAACTGGGTGGGGATTC	55	108.6	0.98
GSONMT00007401001	R: TCCCACCTCAGACATGCTCA			
ago2a	F: GTGGTGGGGTGGACTCATTT	59	108.0	0.98
GSONMT00060791001	R: AAACCTTCAATCGGGCCCTT			
ago2b	F: TGTCGCACGGTGTTAACATG	58	101.3	0.99
GSONMT00025973001	R: AGCAATGCCGAGAAGAGCTA			
	miRNAs			
miR-200a-3p	TaqMan probe MIMAT0002981	60	98.1	0.97
miR-27b-3p	TaqMan probe MIMAT0001797	60	102.8	0.99
miR-122-5p	TaqMan probe MIMAT0001818	60	96.5	0.98
	Markers of hepatic lipid metabolism			
srebp1c	F: GACAAGGTGGTCCCAGTTGCT	58	98.8	0.99
n/a	R: CACACGTTAGTCCGCATCAC			
fasn	F: TGATCTGAAGGCCCGTGTCA	58	91.8	0.98
n/a	R: GGGTGACGTTGCGTGGTAT			
cpt1a	F: TCGATTTTCAAGGGTCTTCG	57	103.1	0.98
n/a	R: CACAACGATCAGCAAAGTGG			
	Other targets of interest			
ir	F: TCAGGAGCAGGAGGACTTTG	50	96.8	0.98
GSONMT00026581001	R: GTGTGTGTACGGGACGTGTT			
rac1	F: CGACCACTGTCCTATCCACA	54	112.8	0.98
GSONMT00034847001	R: TGATGGGGGTGAGTTTCTTC			
glut9	F: GTGTTCCTGGTGGTGTGTGT	58	106.9	0.99
GSONMT00066217001	R: CTTGATGGCAAGTTCGTTCTC			
adp-gk	F: GTTCTGCTGGCGTACTGGTT	50	96.3	0.99
GSONMT00073455001	R: TTCATCCCCACTTTGCTTTC			
soga1	F: GCTGCACCAGTACACAGGAA	58	92.8	0.99
GSONMT00057063001	R: GCAAAGCAGAAGGACAGGA			
mfn1	F: AGGGAGCTGGAGGGAGAAAT	55	108.2	0.99
GSONMT00027395001	R: CCAAGACAGGCTCCAGTGAA			
mfn2	F: ACTGCTCCGGAATAAGGCTG	55	98.4	0.99
GSONMT00004526001	R: GTGGTCTTTTCGCGGTCAAC			
Fis	F: GGTTTGGTTGGCATGGCAAT	55	103.2	0.99
GSONMT00039888001	R: TTCTCATCTTGGGGAACGGC			
	Reference genes			
ef1a	F: CATTGACAAGAGAACCATTGA	56	102.6	0.97
n/a	R: CCTTCAGCTTGTCCAGCAC			

F, forward; R, reverse, n/a, not available.

time RT-PCR was used to validate the abundance of *miR-122-5p, miR-27b-3p, miR-200a-3p, miR-21, miR-152, miR-722* using the CFX96-Real-Time System-C1000 Thermal Cycler machine (Bio-Rad, Mississauga, ON, Canada). Real-time RT-PCR reactions were prepared in a total volume of 20 μL per reaction, containing 1.00 μL TaqMan Small RNA Assay 20×, 1.33 μL Product from RT reaction, 10.00 μL TaqMan Universal PCR Master Mix (2×) with UNG, and 7.67 μL nuclease-free water. A no reverse transcriptase (noRT), where the RT was replaced with nuclease-free water, and a no template (noTemp), where product from RT reaction was replaced with nuclease-free water, were included during cDNA synthesis as controls for DNA contamination. Following an activation step at 50°C (2 min) to activate UNG and another activation step at 95°C (10 min) to activate the polymerase in the qPCR mix, two steps were repeated for 40 cycles including the denaturation at 95°C (15 s) and a combined annealing and extending step at 60°C (60 s). Assays were subsequently normalized by the NORMA-Gene approach as described by Heckman et al. (24) miRNA fold changes were calculated relative to the fasted group. Data were analyzed with Prism version 8 (GraphPad Software, La Jolla, CA) and transformed to fit normal distribution when necessary. In normally distributed data, Grubb's outlier test was used to identify and remove possible single outliers in a treatment group. Data were subsequently analyzed by a one-way ANOVA followed by Tukey's post hoc test. In cases were data did not meet normality and homoscedasticity criteria as assessed by Shapiro-Wilk and Bartlett's test, data were analyzed by a Kruskal-Wallis test followed by Dunn's multiple-comparison test. Significance was determined at a $P < 0.05$ level.

Protein Extraction and Cell Signaling Quantification

Fractions (~100 mg) of frozen livers ($n = 4$ per treatment group) were weighted into 1 mL of lysis buffer [150 mM NaCl, 10 mM Tris HCl, 1 mM EGTA, 1 mM EDTA (pH 7.4), 100 mM sodium fluoride, 4 mM sodium pyrophosphate, 2 mM sodium orthovanadate, 1% Triton X-100, 0.5% NP-40-IGEPAL, and a protease inhibitor cocktail (Roche, Basel, Switzerland)] and homogenized using a Precellys-Cryolys (Bertin Instruments, Montigny-le-Bretonneux, France). We centrifuged the homogenates at 1,000 *g* for 15 min at 4°C and then recovered the supernatant to centrifuge again at 20 000 *g* for 30 min

at 4°C. The resulting supernatant fractions were recovered and stored at −80°C. Protein concentrations were determined with the Bio-Rad protein assay kit (Bio-Rad Laboratories, Munich, Germany) with BSA (bovine serum albumin) as the standard. Lysates (20 μg of the total protein) were subjected to SDS-PAGE and wet-transfer blotting. Appropriate antibodies were obtained from Cell Signaling Technologies (Ozyme, Saint Quentin Yvelines, France). Anti-phospho-Akt (Ser473, #4060), anti-Akt (#9272), Anti-phospho-Tor (Ser2448, #5536), anti-Tor (#2972), Antiphospho-S6 (Ser235/236, #4858), anti-S6 (#2217) were used on the Western blots. All the antibodies have been shown to cross-react successfully with rainbow trout proteins of interest (13–16, 35, 44, 70). After being washed, membranes were incubated with an IRDye infrared secondary antibody (LI-COR Biosciences). The bands were visualized by infrared fluorescence using the odyssey Imaging System (LI-COR Biosciences) and quantified by Odyssey Infrared Imaging System software (version 3.0, LI-COR Biosciences). Data were analyzed with Prism version 7 and transformed to fit normal distribution. In normally distributed data, Grubb's outlier test was used to identify and remove possible single outliers in a treatment group. Data were subsequently analyzed by a one-way ANOVA followed by Tukey's post hoc test. In cases where data did not meet normality and homoscedasticity criteria as assessed by Shapiro-Wilk and Bartlett's test, data were analyzed by a Kruskal-Wallis test followed by Dunn's multiple-comparison test. Significance was determined at a $P < 0.05$ level.

In Silico miRNA-Target Analysis

To predict rainbow trout-specific mRNA targets of differentially regulated miRNAs, we utilized the miRanda package initially developed in the Enright laboratory (18). The miRanda algorithm places emphasis on seed match and free energy of the duplex structure, two of the most relevant aspects in miRNA-target interaction (1, 62). Among the available miRNA target prediction algorithms (20, 58), we chose the miRanda algorithm based on its increased sensitivity compared with other algorithms (77), as well as its previous application across several rainbow trout transcriptome-level miRNA target prediction studies (33, 46, 53), in an effort to facilitate comparison between studies. Since, increased sensitivity occurs at the cost of an increased rate of false-positive predictions, we used a stringent cut-off with a miRanda pairing score $S > 140$, and a free-energy score ΔG cut-off < -20, where S is the sum of single residue-pair match scores over the alignment trace, and ΔG is the free energy of duplex formation calculated by the Vienna package (29). Annotated 3′-UTRs were taken from the microTrout database (46).

Gene Ontology Enrichment, Pathway, and Subnetwork Enrichment Analysis

Gene Ontology (GO) enrichment analysis of mRNA targets predicted to be regulated by differentially expressed miRNAs is a widely used approach to infer possible biological consequence at the genome regulation level in rainbow trout and mammalian models (26, 33, 53). We performed GO enrichment analysis in JMP Genomics V8.1. Parametric analysis of gene expression (PAGE) was conducted to determine which GO terms were significantly enriched in the data set for each experiment based upon predicted targets of miRNAs. The rainbow trout genome was used as a background list for comparison. Genes were considered to be miRNA targets if transcript-miRNA predicted by the miRanda algorithm had cut-off values of $S > 140$ and $\Delta G < -20$. The *P* value for each GO term was corrected by false discovery rate (FDR). To build pathways for gene targets, we imported the short list of genes within a group of GO categories (i.e., those related to "glucose metabolism") into Pathway Studio 11.4 (Elsevier). The software uses known relationships (i.e., based on expression, binding, common pathways) between genes to create networks focused around a cell process. The miRNA targets were imported into the program using the "Name + Alias" and rainbow trout genes were mapped to their mammalian homologs. Lastly, the miRNA targets were subjected to a subnetwork enrichment analysis in Pathway Studio for "Cell Process." This approach was used to achieve a general overview of cell processes that may be relevant to hepatic regulation of glucose and intermediary metabolism in general, those that may be controlled posttranscriptionally by the regulated miRNA network.

Correlative Analysis of miRNA-mRNA Targets

Specific mRNA targets belonging to enriched pathways of interest predicted to be regulated by differentially expressed miRNAs were quantified to elucidate a potential involvement in GI in response to HighCHO in rainbow trout and to determine miRNA-mRNA relationships correlatively. While not indicative of functional relationship, such correlations may aid to prioritize specific miRNA-mRNA target pairs for future functional studies. Correlation of expression between differentially expressed miRNAs and specific targets were assessed by Pearson coefficient and its significance computed in Prism Version 7 (GraphPad Software).

RESULTS

Transcripts of the miRNA Biogenesis Pathway are Responsive to High Dietary Carbohydrates In Rainbow Trout

Responsiveness to dietary carbohydrates of key enzymes of the miRNA biogenesis pathway was probed at the mRNA abundance level in rainbow trout liver (Fig. 2). Specifically, *drosha* (Fig. 2*A*), which exists as single locus in the rainbow trout genome (5), and the two salmonid paralogs of *xpo5* (Fig. 2, *B* and *C*) and *ago2* (Fig. 2, *D* and *E*) were quantified in rainbow trout that were fasted or refed with either a NoCHO and a HighCHO diet. The mRNA abundance of *drosha* ($F_{2,24} = 6.459$, $P = 0.0057$; Fig. 2*A*) was significantly induced postprandially in trout fed HighCHO ($P = 0.0041$) but not NoCHO diets ($P = 0.1379$). Conversely, both *xpo5a* ($F_{2,24} = 5.332$, $P = 0.0121$; Fig. 2*B*) and *xpo5b* ($F_{2,24} = 3.995$, $P = 0.0318$; Fig. 2*C*) were induced by both NoCHO ($P = 0.0031$ and $P = 0.0004$, respectively) and HighCHO diets ($P = 0.0001$ and $P = 0.0001$, respectively) compared with fasting; the HighCHO also led to a stronger induction of the *xpo5b* paralog compared with NoCHO diet ($P = 0.0003$). With regard to *ago2* paralogs, *ago2a* ($F_{2,24} = 3.615$, $P = 0.0424$; Fig. 2*D*) was significantly induced in HighCHO diet-fed fish compared with fasted fish ($P = 0.0368$), while no induction was observed in NoCHO diet-fed fish compared with fasted fish ($P = 0.6585$). No change in mRNA abundance was observed between groups for the *ago2b* paralog ($F_{2,23} = 0.7908$, $P = 0.1578$; Fig. 2*E*).

Small RNA Next-generation Sequencing and Identification of Hepatic miRNAs in Rainbow Trout

Of the overall ~96.18 M raw reads, 55.56 M read (57.8%) were excluded first due a lack of 3′-adaptor or 3′-ADT (~44.85 M or 46.6%) and second because of nucleotide size outside the targeted range of 15–32 nt (~10.7 M or 11.2%) after 3′-ADT sequence screening, resulting in ~40.60 M mappable reads, of which a combined 78% exhibit a size between 19 and 23 nt (Additional File 4). The Phred Score distribution of reads was larger than 30 (Additional File 4), indicating a probability of incorrect base calls of less than 1 in 1,000 nucleotides (or

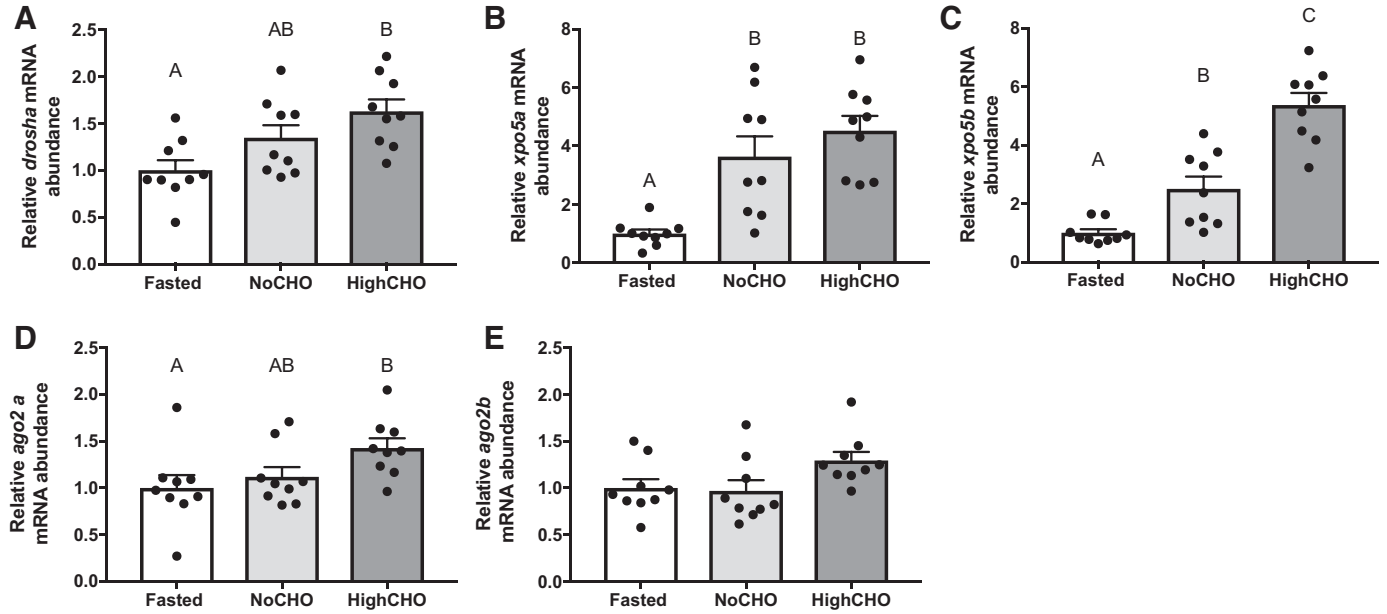

Fig. 2. Relative steady-state mRNA abundance (+SE) of hepatic canonical miRNA biogenesis components drosha (*A*), exportin 5 (*B, C*), and argonaute 2 (*D, E*) in rainbow trout 6 h after being refed either a NoCHO diet (devoid of carbohydrates) or a HighCHO diet (containing 30% carbohydrates) normalized to elongation factor 1α and expressed as relative fold change compared with rainbow trout fasted for 2 days. In cases where data were normally distributed and met the criteria of homoscedasticity, a one-way ANOVA followed by Tukey's post hoc was used for analysis, whereas a Kruskal-Wallis test followed by Dunn's multiple comparisons test was used in cases where data did not meet these criteria. A P value of $P < 0.05$ was used as cut-off for significant effects.

99.9% accuracy). With regard to individual sample sequencing depth, a range between ~6.4 M and ~9.4 M reads per sample was obtained (Additional File 5). Following quality assurance of small RNA sequencing, the total ~40.6 M mappable reads was annotated in specific groups according to the described pipeline. In this process, a total of ~23.42 M or 57.7% of reads were annotated as 604 known miRNAs (*group 1*), while ~2.64 M or 4.9% of reads were annotated as 1,278 predicted miRNAs (*groups 2–4*), summarized in Additional File 6. A total of ~12.44 M or 38.9% of mappable reads were annotated as other RNA species or did not yield any hit (Additional File 7). Thus, we identified a total of 1886 unique miRNAs, whose specific sequences are available in Additional File 5.

Trout Hepatic miRNAome Responds More Strongly to Diets High in Carbohydrates than Diets Devoid of Carbohydrates

Differential hepatic miRNA abundance was analyzed globally between fasted, NoCHO, and HighCHO groups by one-way ANOVA (Fig. 3*A*), which identified a total of 60 differentially expressed candidates between all three experimental groups. Pair-wise comparisons investigating differentially expressed hepatic miRNA between fasted and NoCHO (Fig. 3*B*) and fasted and HighCHO (Fig. 3*C*) identified 23 (17 up, 6 down) differentially regulated miRNAs in response to NoCHO diet, and 49 (20 up 29 down) in response to HighCHO diet. When we compared NoCHO and HighCHO by pairwise comparison (Fig. 3*D*), 30 miRNAs (14 up, 16 down) were differentially regulated. A summary of differentially regulated miRNAs across all pairwise comparisons is shown in Fig. 3*E*. All individual miRNA sequences, their normalized count numbers, and their differential regulation for all comparisons displayed in Fig. 3 can be accessed in detail in Additional File 8.

Real-time TaqMan RT-PCR Validation of Specific miRNAs

We quantified the expression of three specific miRNAs, *miR-200a-3p* (Fig. 4*A*), *miRNA-27-3p* (Fig. 4*B*), and hepatic miRNA abundance of *miRNA-122-5p* (Fig. 4*C*). Hepatic abundance of *miRNA-200a-3p* ($F_{2,26} = 6.394$ $P < 0.01$, Fig. 4*A*) was reduced in the NoCHO group ($P = 0.0048$) but not HighCHO group compared with the fasted group ($P = 0.4187$). A marginal, but nonsignificant increase in HighCHO compared with NoCHO was observed ($P = 0.0764$). Hepatic abundance of *miRNA-27b-3p* ($F_{2,26} = 17.83$, $P < 0.01$, Fig. 4*B*) was significantly decreased in response to NoCHO ($P = 0.0001$) but not HighCHO ($P = 0.6181$) compared with fasted fish, and significantly higher in HighCHO compared with NoCHO diets ($P = 0.0003$). No significant change in *miRNA-122-5p* was observed ($F_{2,26} = 17.83$, $P > 0.05$, Fig. 4*C*).

GO Term Analysis of In Silico-predicted Targets of Differentially Regulated miRNAs Identifies Glucose and Intermediary Metabolic Pathways as Targets for Posttranscriptional Regulation in Response to Dietary Carbohydrates

By applying the miRanda algorithm used in microTrout (46), we identified specific 3′-UTR targets for all differentially regulated miRNAs in specific comparisons, the results of which can be consulted in Additional File 9. Using the GO term annotations based on genes containing these 3′-UTRs, we generated GO-term enrichment analysis to identify diet-dependent postranscriptionally regulated pathways in silico. The complete list of enriched GO terms and their probability of being enriched are contained in Additional File 10. GO terms can be overrepresented or underrepresented in a data set compared with a reference data set. The overrepresented GO

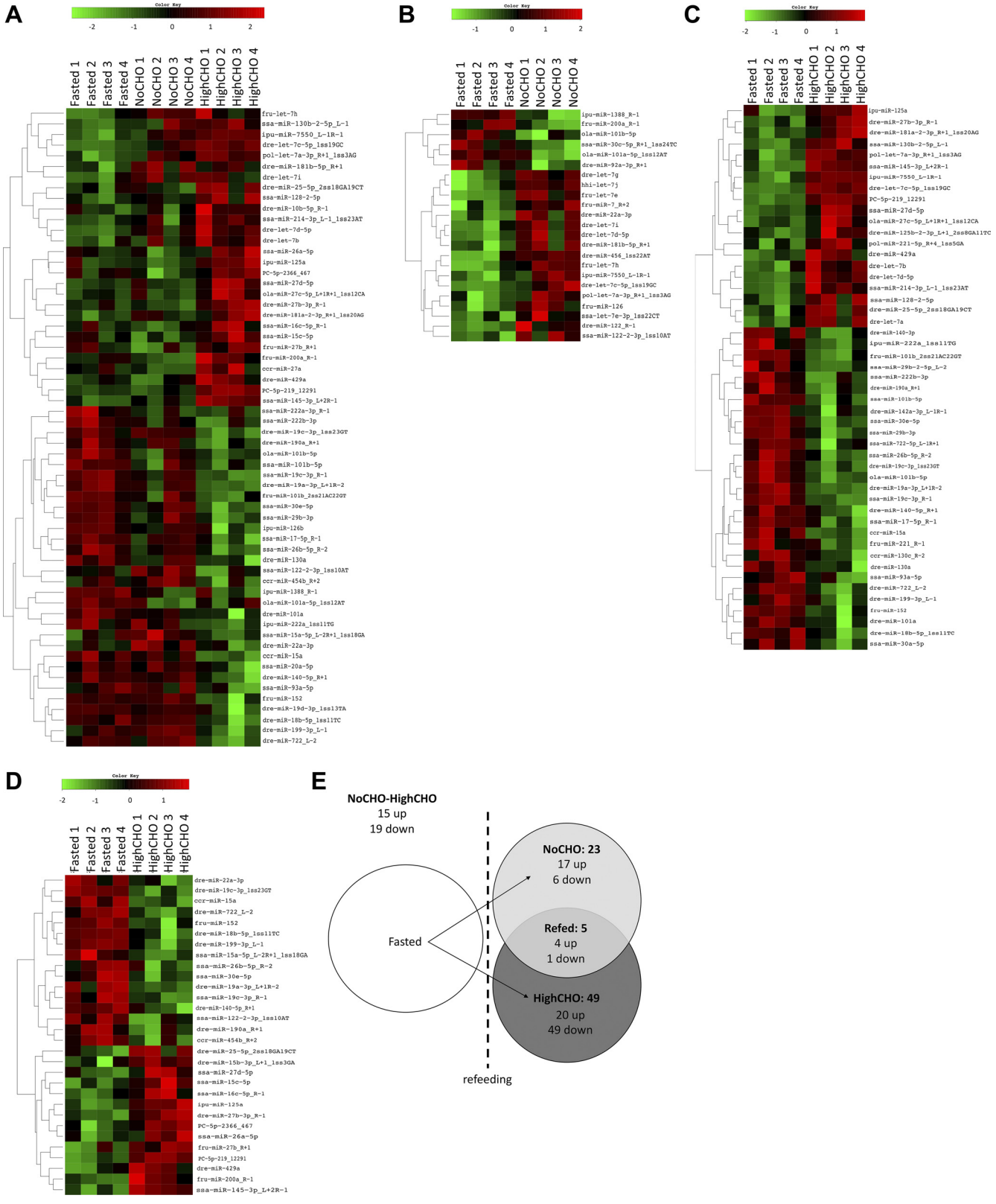

Fig. 3. Heat maps showing hierarchical clustering of differentially regulated miRNAs between Fasted, NoCHO, and HighCHO analyzed by one-way ANOVA (*A*) and between Fasted-NoCHO (*B*), Fasted-HighCHO (*C*), and NoCHO-HighCHO (*D*) analyzed by *t*-test. *E*: summary of differentially regulated miRNAs across all pairwise comparisons.

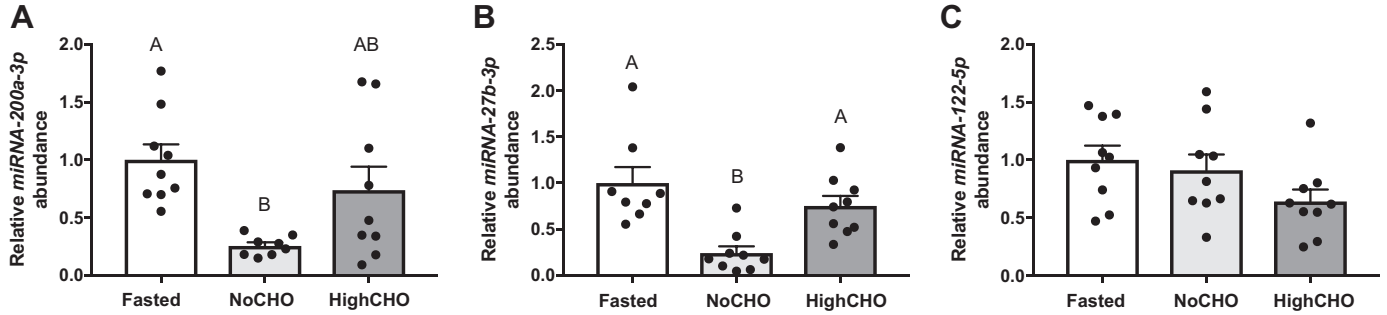

Fig. 4. Relative steady-state miRNA abundance (+SE) of *miRNA-200a-3p* (*A*), *miRNA-27b-3p* (*B*), and *miRNA-122-5p* (*C*) in rainbow trout 6 h after being refed either a NoCHO diet (devoid of carbohydrates) or a HighCHO diet (containing 30% carbohydrates) normalized with NORMA-Gene and expressed as relative fold change compared with fasted group analyzed by real-time TaqMan RT-PCR assay (n = 9 samples per group). In cases where data were normally distributed and met the criteria of homoscedasticity, a one-way ANOVA followed by Tukey's post hoc was used for analysis, whereas a Kruskal-Wallis test followed by Dunn's multiple-comparisons test was used in cases where data did not meet these criteria. A P value of $P < 0.05$ was used as cut-off for significant effects.

terms are indicated as "0," while the underrepresented GO terms are represented with "1" (Additional file 10). For figures and subsequent discussion, we focus exclusively on GO terms that were overrepresented in a predicted gene target list compared with the rainbow trout genome and are relevant to hepatic glucose and intermediary metabolism, summarized in Additional File 11. Specific miRNA-mRNA predictions within enriched metabolic pathways are listed in Additional File 12. A visual representation of immediate glucose metabolic pathways and their interactions predicted to be subject to posttranscriptional regulation by differential miRNAs between NoCHO and HighCHO groups obtained by SNEA analysis is shown in Additional Files 13 and 14.

Assessment of Hypotheses of Hepatic Cellular and Molecular Contributions to GI in Rainbow Trout

Following the identification of gluconeogenesis, lipogenesis, and insulin signaling as being regulated by differentially regulated miRNAs in response to dietary carbohydrates (Additional File 11), we assessed functional changes in these pathways using well-established rainbow trout markers at the molecular and cellular level. A lack of suppression of de novo gluconeogenesis, potentially linked to an induction of *g6pc2* paralogs that are induced by HighCHO, had previously already been reported for our tissue samples at the transcript and enzyme activity level (41). We therefore used well-established general gene expression markers of rainbow trout DNL (13–15, 70) and protein markers of insulin signaling (13–16, 35, 70) to address the additional hypotheses that limited hepatic DNL and/or insulin signaling is associated with GI in rainbow trout fed excess carbohydrates.

Hepatic markers of DNL are not induced by the carbohydrate-rich diet. Compared with fasted rainbow trout, hepatic expression of the lipogenic transcription factor *srebp1c* ($H_{2,27}$ = 15.62, P = 0.0004; Fig. 5*A*) and the lipogenic enzyme fatty acid synthase *fasn* ($F_{2,24}$ = 47.49, P = 0.0001; Fig. 5*B*) was induced by refeeding, irrespective of dietary carbohydrate content: In the case of *srebp1c*, an induction of mRNA abundance was observed in both rainbow trout refed NoCHO (P = 0.0108) and HighCHO diets (P = 0.0005) compared with fasted trout, while no difference between diets was observed (P = 0.9999). Similarly, *fasn* (P = 0.0001) mRNA abundance increased in rainbow trout refed both NoCHO (P = 0.0001) and HighCHO diets, while no difference was found between refed dietary treatment groups (P = 0.9107). Conversely, while the mRNA abundance of the mitochondrial transport protein *cpt1a* ($F_{2,19}$ = 4.814, P = 0.0203; Fig. 5*C*), the rate-limiting enzyme in fatty acid oxidation, was decreased in both NoCHO (P =

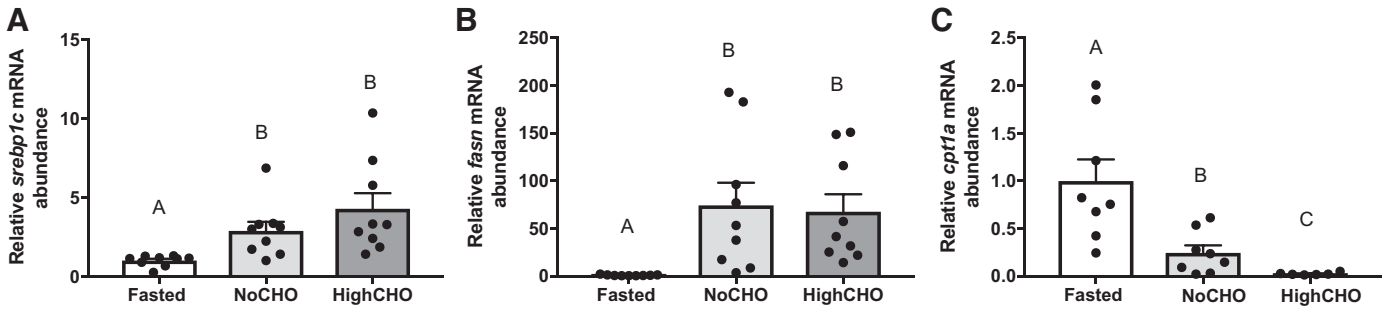

Fig. 5. Steady-state mRNA abundance (□SE) of general markers of hepatic lipid metabolism, including de novo lipogenesis (DNL) markers sterol regulatory element binding protein 1c (A), fatty acid synthase (B), and fatty acid oxidation pathway marker carnithine palmitoyltransferase 1a (C). Abundance of transcripts was measured in rainbow trout that were fasted and in rainbow trout 6 h after being refed either a NoCHO diet (devoid of carbohydrates) or a HighCHO diet (containing 30% carbohydrates) and normalized to elongation factor 1 and expressed as relative fold change compared with the fasted group. In cases where data were normally distributed and met the criteria of homoscedasticity, a one-way ANOVA followed by Tukey's post hoc was used for analysis, whereas a Kruskal-Wallis test followed by Dunn's multiple comparisons test was used in cases where data did not meet these criteria. A P value of P □ 0.05 was used as cut-off for significant effects.

0.0028) and HighCHO ($P = 0.0001$) diet groups compared with fasted fish, the inhibition response was also diet dependent, as it was stronger in HighCHO-fed trout compared with the NoCHO fed trout ($P = 0.0031$).

Activity of components of the hepatic insulin signaling pathway is increased by a carbohydrate-rich diet. Activity of Akt ($F_{2,12} = 5.44$, $P = 0.0283$), assessed as the quantified ratio of Ser^{437} phosphorylated Akt and total Akt (Fig. 6*A*), significantly increased in response to refeeding the HighCHO diet ($P = 0.0311$), but not the NoCHO ($P = 0.8423$) diet. No difference was observed between groups refed with NoCHO and HighCHO diets ($P = 0.0748$). A similar pattern was observed in the Tor target $Ser^{234/235}$ S6 phosphorylation ($F_{2,12} = 7.10$, $P = 0.0144$; Fig. 6*B*), which increased significantly in HighCHO-refed rainbow trout compared with fasted trout ($P = 0.0149$), but not in rainbow trout refed with NoCHO diet ($P = 0.0512$). Again, no differences between both refed groups were observed ($P = 0.7138$). Finally, the activity of Tor, as assessed by the ratio of Ser^{2448} phosphorylated and total Tor, did not change significantly between treatment groups ($F_{2,12} = 0.53$ $P = 0.7222$; Fig. 6*C*).

Additional targets of interest. In addition to quantifying aforementioned hepatic markers of gluconeogenesis, DNL, and insulin signaling hypothesized to play a role in GI in rainbow trout, we quantified additional specific transcripts related to glucose metabolism-related pathways (Fig. 7, *A* and *B*) and insulin signaling pathways (Fig. 7, *C* and *D*), because they first belong to enriched pathways predicted to be targeted by differentially regulated miRNAs and second are individually predicted to be targeted by several differentially regulated miRNAs (Additional Files 9 and 11). Hepatic mRNA abundance of the adp-dependent glucokinase (*adp-gk*; $F_{2,24} = 8.62$, $P = 0.015$; Fig. 7*A*) and glucose transporter 9 (*glut9*; $F_{2,22} = 6.495$, $P = 0.0061$; Fig. 7*B*) changed significantly between groups. In the case of *adp-gk*, the only significant change between groups was observed between NoCHO and HighCHO-fed fish ($P = 0.0041$). With regard to *glut9*, refeeding either NoCHO ($P = 0.0137$) or HighCHO ($P = 0.0120$) significantly increased mRNA abundance compared with fasted fish, but there was no difference in expression between fish refed either diet ($P = 0.9994$). Hepatic mRNA abundance of the insulin receptor subunit *ir* ($F_{2,22} = 5.456$, $P = 0.0119$; Fig. 7*C*) exhibited a similar reduction following refeeding both the NoCHO diet ($P = 0.0499$) and HighCHO diet ($P = 0.0147$), without a significant difference between both refeeding groups ($P = 0.8490$).

We furthermore quantified transcripts related to organelle dynamics, specifically autophagy and mitochondrial dynamics, because they first have been linked to glucoregulation in mammals (19, 64, 68, 72, 73) and, in the case of autophagy, also in rainbow trout (69). Second, these genes have been predicted to be regulated by differentially expressed miRNAs both at the pathway enriched level (Additional File 11) and specific transcript level (Additional File 12). Expression of suppressor of glucose autophagy-regulated 1 (*soga1*; $F_{2,22} = 25.12$ $P < 0.0001$; Fig. 7*D*) was significantly induced by refeeding NoCHO ($P = 0.0069$) and HighCHO ($P = 0.0001$), with a significantly higher induction in HighCHO compared with NoCHO ($P = 0.0046$). Finally, expression of mitofusin 1 (*mfn1*; $H_{2,27} = 17.75$, $P = 0.001$; Fig. 7*E*) and mitofusin2 (*mfn2*; $H_{2,27} = 17.40$**;** Fig. 7*F*) increased with both NoCHO ($P = 0.0003$ and $P = 0.0014$) and HighCHO ($P = 0.0029$ and $P = 0.0009$) compared with fasted fish. In neither case was there differential expression between refed groups ($P = 0.9999$ and $P = 0.9999$). Conversely, mitochondrial fission protein 1 (*fis1*; $F_{2,23} = 12.2$, $P = 0.0002$, Fig. 7*G*) changed significantly only in response to HighCHO compared with both fasted ($P = 0.0009$) and NoCHO-fed ($P = 0.0008$) fish.

Correlative Analysis of Differentially Regulated Hepatic miRNAs and Specific Transcripts of GO Term Enriched Pathways

Predicted targets involved in gluconeogenesis, glucose metabolism, insulin signaling, and organelle dynamics. Glucose metabolic pathways were predicted to be regulated by differentially regulated miRNAs in all comparisons (Additional File 11). Given that the gluconeogenesis pathway in general (Additional File 11) and *g6pcb2* paralogs in particular (Additional File 12) were identified as target of miRNAs in silico (Fig. 8) and that this pathway had been linked to GI in rainbow trout (41, 42), we investigated a potential role of differentially regulated miRNAs on this pathway by specific correlative analysis (Table 2). While not a proof of a causative relationship, significant negative correlations between miRNAs and their predicted target transcripts may allow investigators to prioritize specific predicted miRNA-mRNA pairs for future mechanistic studies. With regard to gluconeogenic transcripts whose expression had been previously described for this study, we observed significant negative correlations of miRNAs that are differentially expressed between fasted and HighCHO groups, specifically between *miR-27b-3p* and the glucose-6-phosphatase paralog b1a (*g6pcb1a*), significant negative correlations between *miR-126b-5p* and *miR-92a-3p* and glucose-6-phosphatase paralog b2a (*g6pcb2a*), and a significant negative correlation between *miR-101b-5p* and fructose 1,6 bisphosphatase 1b1 (*fbp1b1*). With regard to glycolytic transcripts, whose expression had been described previously for samples used in this study (42), we identified significant negative correlations for the abundance of *miR-126b-5p* and glucokinase a (*gcka*) and *miR-429a* and glucokinase b (*gckb*) when comparing fasted and HighCHO-fed fish.

Additional predicted targets involved in autophagy and mitochondria dynamics. Our in silico analysis predicted pathways related to autophagy and mitochondria organelle dynamics as being targets of posttranscriptional regulation by differentially expressed miRNAs in response to dietary carbohydrates (Additional File 11). Because hepatic autophagy and mitochondrial dynamics have been linked to glucoregulation in mammals (19, 64, 68, 72, 73) and, in the case of autophagy, in rainbow trout (69), we quantified predicted target transcripts of both GO-enriched pathways and correlatively investigated miRNA-target expression patterns (Table 3): Correlations in transcript abundance were also investigated for additional targets of interest involved in glucose metabolism, insulin signaling, and organelle dynamics (Table 3). Significant negative correlations in expression were identified between *miR-101-5p* and a paralog of adp-dependent glucokinase (*adp-gk*), *miR-30c-5p*, and an insulin receptor (*ir*) paralog, *miR-140* and suppressor of glucose autophagy associated1 (*soga1*), between *let7a*

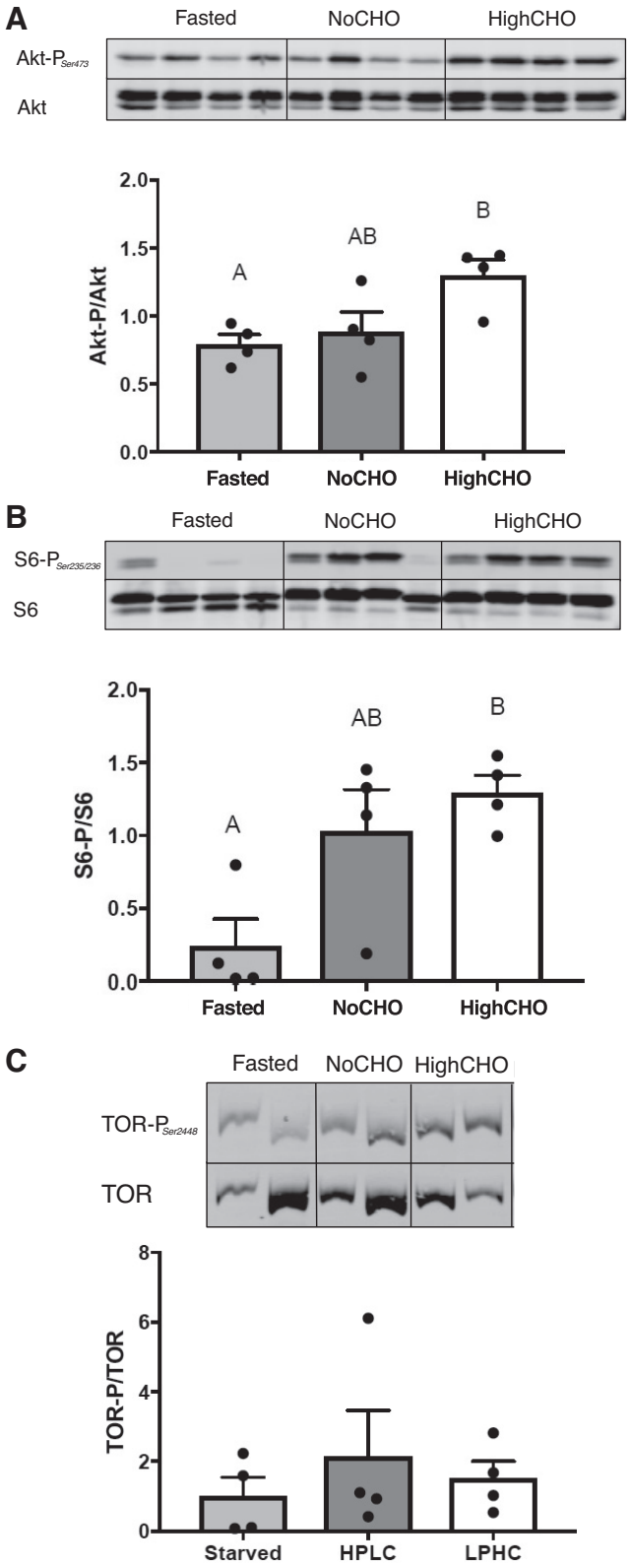

Fig. 6. Hepatic insulin signaling pathway activity assessed by ratios of phosphorylated and total protein (+SE) of Akt (*A*), S6 (*B*), and Tor (*C*) based on densitometry-based quantification of four samples per group by Western blots. In cases where data were normally distributed and met the criteria of homoscedasticity, a one-way ANOVA followed by Tukey's post hoc was used for analysis, whereas a Kruskal-Wallis test followed by Dunn's multiple comparisons test was used in cases where data did not meet these criteria. A P value of $P < 0.05$ was used as cut-off for significant effects.

and mitofusin1 (*mfn1*), and between *miR-15a-5p*, *miR-17-5p*, *miR-18b-5p*, *miR-152-5p*, and mitofusin 2 (*mfn2*).

DISCUSSION

Increased Dietary Carbohydrates Upregulate Expression of Canonical miRNA Biogenesis Pathway Components in Rainbow Trout

Our initial probing of a global role for the miRNA biogenesis pathway in response to dietary carbohydrates revealed that at least one paralog of components probed at different levels of the pathway was responsive to dietary carbohydrates. This is in contrast to hepatic responses to diets lacking dietary carbohydrates, which resulted in an induction of *xpo5* paralogs only. However, even with regard to *xpo5*, dietary carbohydrates induced a significantly higher mRNA abundance of the *xpo5b* paralog, suggesting an increase in pre-miRNA translocation out of the nucleus. Together, these data show that, at the level of gene expression, dietary carbohydrates concurrently induce the hepatic abundance of canonical miRNA biogenesis pathway components, suggesting a general stimulation of canonical miRNA biogenesis. As salmonids, rainbow trout are among the only species characterized to-date to possess paralogs of all components of this pathway with the exception of *drosha* (5). While their function in this species has not been probed, this pathway and its components are evolutionarily conserved (31), and recent siRNA-based functional studies targeting individual components of this pathway in a human cell line have revealed profound effects of *drosha* ablation on canonical miRNA biogenesis and only mild effects of *xpo5* ablation (31). Interestingly, rainbow trout and Atlantic salmon Xpo5 protein paralogs display specific AA substitutions in key sites involved in pre-mRNA binding, suggesting sub- or neofunctionalization of these paralogs to differentially affect miRNA export (5). The current study is the first to identify differential regulation of both paralogs *xpo5a* and *xpo5b* in response to dietary carbohydrates at the gene expression level, lending further support to possible sub- or neofunctionalization of these paralogs in rainbow trout and salmonids in general. While a working hypothesis at this point, regulation the *xpo5* paralogs may have contributed to differential miRNAs profiles between dietary groups via differential regulation of *pri-miRNA* nuclear export. It is important however to note that while isoenergetic diets were used that exclude secondary effects related to energy status, the increase in carbohydrates in the HighCHO diet was achieved by a corresponding reduction of protein content. It is therefore possible that the observed changes are related either to increased carbohydrate content and/or hyperglycemia or to a reduction in protein content and AA signaling. Future studies using different replacement of protein by undigestible carbohydrates to modulate protein content may be used to resolve this question.

In terms of nutritional regulation of key enzymes of the canonical miRNA biogenesis pathway, nutritional regulation of Drosha at the protein level and associated canonical miRNA biogenesis have recently been revealed to be dependent on signaling of the nutrient sensor mTor in C57/BL6 mice, which degrades Drosha to inhibit miRNA biogenesis under nutrient-rich conditions, while stabilizing Drosha to promote miRNA biogenesis under nutrient-poor conditions (79). While our current study only probed drosha mRNA abundance, it will be worthwhile to determine whether drosha and the miRNA pathway in trout respond to nutrient-poor

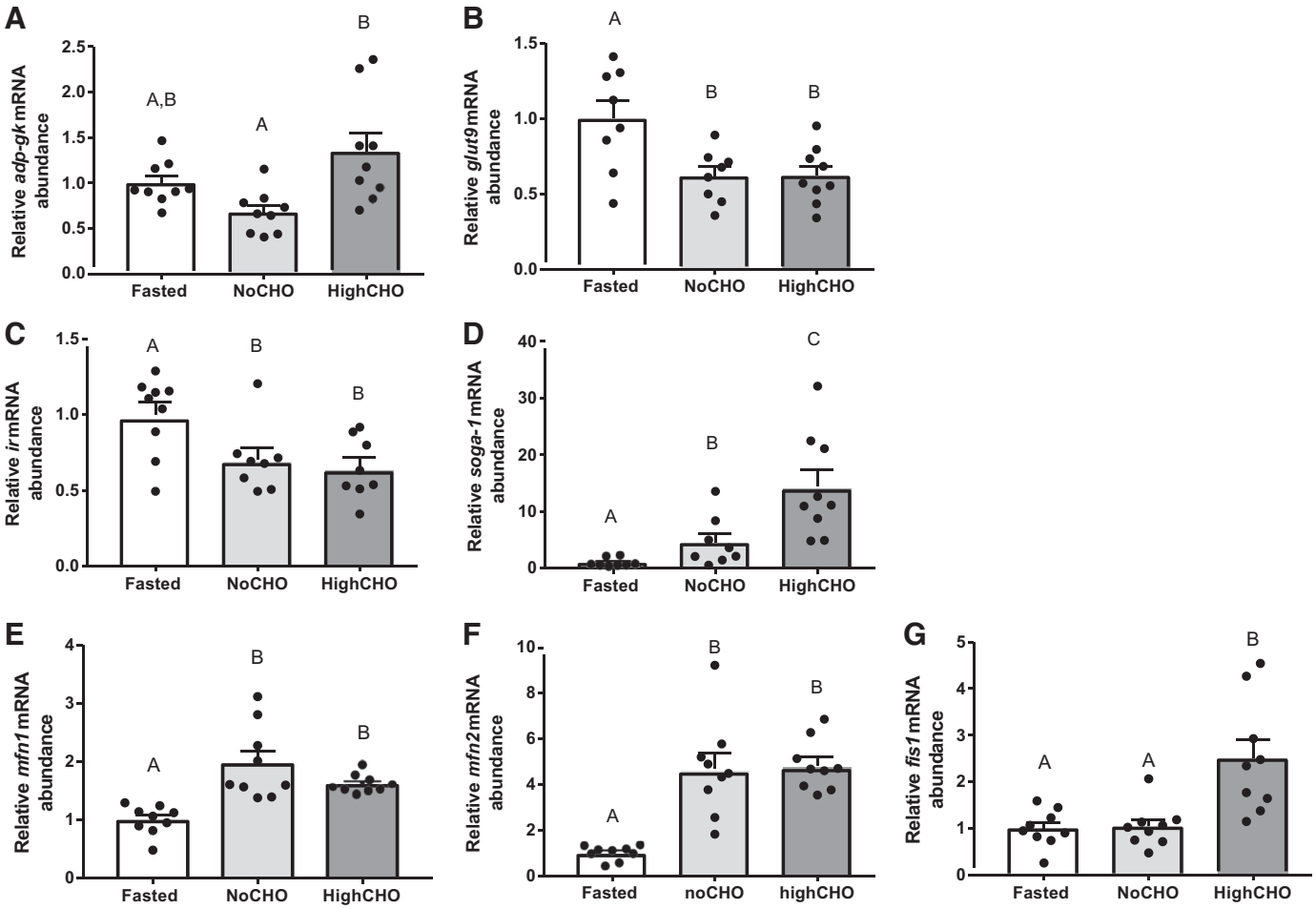

Fig. 7. Steady-state mRNA abundance (+SE) of adp-dependent glucokinase (*A*), glucose transporter 9 (*B*), insulin receptor (*C*), suppressor of glucose autophagy associated 1 (*D*), mitofusin 1 (*E*), mitofusin 2 (*F*), and mitochondrial fission protein 1 (*G*). In cases where data were normally distributed and met the criteria of homoscedasticity, a one-way ANOVA followed by Tukey's post hoc was used for analysis, whereas a Kruskal-Wallis test followed by Dunn's multiple comparisons test was used in cases where data did not meet these criteria. A P value of $P < 0.05$ was used as cut-off for significant effects.

conditions. In contrast to mammals, high dietary carbohydrate (and/or concurrent low protein content) represents poor nutrients for carnivorous rainbow trout, and the induction of *drosha* mRNA abundance and the canonical miRNA biogenesis pathway may represent a conserved mechanism to nutrient-poor conditions. The finding that activation of key components of the hepatic insulin pathway activity including upstream (Akt) and downstream (S6) components of Tor, but not Tor itself, increased in HighCHO-fed, but not NoCHO-fed trout compared with fasted trout in our study does suggest, however, that this mechanism may not be conserved between rainbow trout and C57/BL6 mice. However, whether Tor activation may play a role in observed significant induction of *drosha* and other components of the canonical miRNA biogenesis pathway in this study cannot be functionally answered, as experiments using pharmacological Tor inhibition in rainbow trout (4, 10, 39) would be needed to functionally link Tor signaling to the miRNA biogenesis pathway in rainbow trout.

The hepatic miRNAome is More Responsive to Carbohydrate Containing Diets Compared with Diets Devoid of Carbohydrates

In line with a more pronounced induction of miRNA biogenesis components in response to HighCHO diets compared with NoCHO diets, the global miRNAome is also more significantly altered with HighCHO diet compared with NoCHO diet. While the slightly higher number of upregulated miRNAs in trout refed a HighCHO diet, compared with trout fed a NoCHO diet, is indicative of an increase in miRNA biogenesis, an even stronger difference was observed for downregulated miRNAs, suggesting that in addition to increased miRNA biogenesis, specific hepatic miRNA processing, and/or miRNA turnover are also specifically increased by HighCHO diets. While components such as exonucleases are emerging to play a key role in miRNA turnover in mammals and are present in the trout genome (5), their functional roles remain poorly understood and appear to be very complex since they are, in contrast to the principal canonical miRNA biogenesis pathway, specific to individual miRNAs. Therefore, no general indexes of miRNA turnover could be quantified in our study.

The Regulated Hepatic miRNAome in Response to NoCHO and HighCHO after a Short-term Fast is Largely Different in Rainbow Trout

In addition to the described quantitative differences in the regulation of the hepatic miRNAome when comparing HighCHO and NoCHO refed trout compared with fasted trout, the

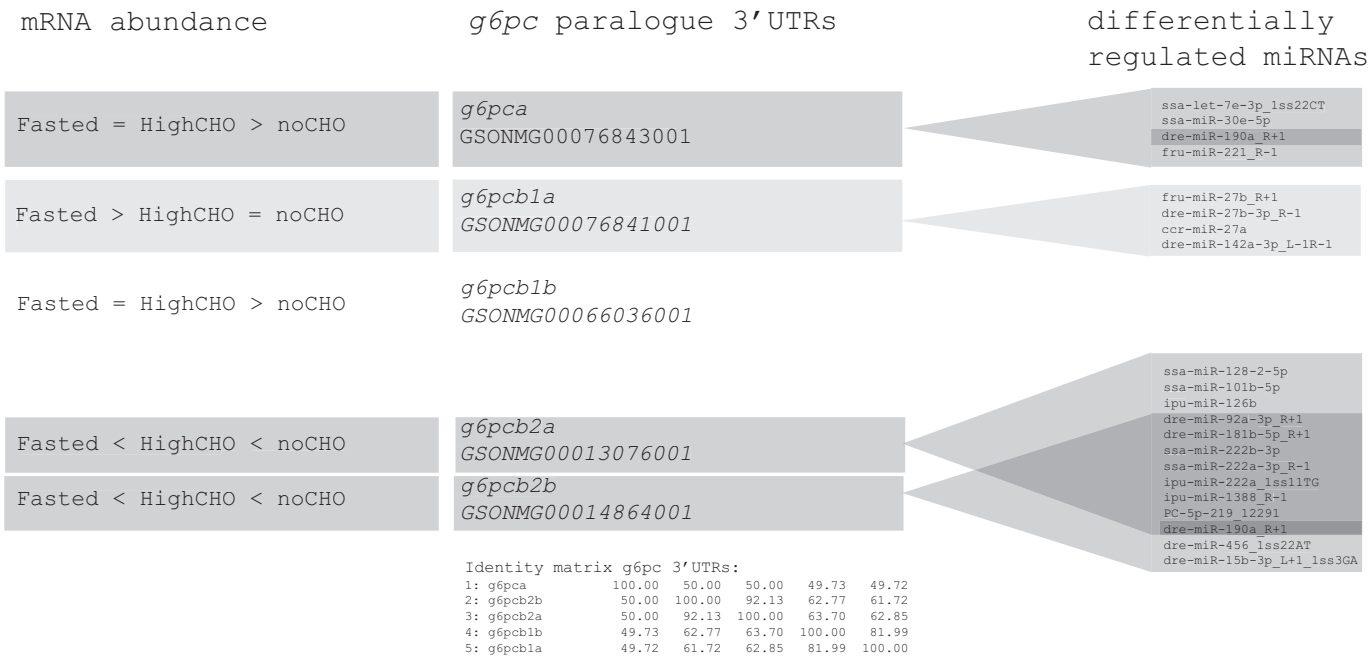

Fig. 8. Graphical representation of predicted differential and overlapping targeting of g6pc paralogs by differentially regulated miRNAs identified in the current study. An identity matrix of glucose 6 phosphatase paralog 3′-untranslated regions is presented.

miRNAome is also qualitatively different (Fig. 3*E*). Indeed, with the exception of four upregulated miRNAs (*let7a-3p*, *let7c-5p*, *let7d-5p*, *miR-7550-5p*) and one downregulated miRNA (*miR-101b-5p*) that significantly respond to refeeding irrespective of the nature of the diet when considering both pairwise comparisons between fasted fish and specific diets, all remaining miRNAs are differentially regulated. This pattern results in differential expression of 30 miRNAs when comparing HighCHO and NoCHO refed groups. Together, this suggests that the hepatic miRNAome is regulated more by specific diets than the process of refeeding isoenergetic meals itself. However, as previously stated, it is important to note that an increase in dietary carbohydrates is accompanied by an equivalent reduction of dietary protein content, and with the current experimental design it is impossible to dissociate the separate contribution of either parameter to the specific regulation of the hepatic miRNAome.

Identification of Evolutionarily Conserved and Divergent Regulation of Hepatic miRNAs in Response to Increased Circulating Glucose Concentrations

To assess whether the hepatic miRNA signature in GI rainbow trout in response to high dietary carbohydrate (30%)-induced hyperglycemia (~11 mmol) is largely species, class, or phenotype specific, we compared the hepatic miRNA profile obtained in our experiment to hepatic miRNA profiles identified in previous experiments. The first comparison included a recently published hepatic miRNA profiles in response to high dietary carbohydrates (50%) in blunt snout bream, *Megalobrama amblycephala* (47), which exhibited a significant but moderate increase in circulating glucose (~6 mmol), underlining its status as a glucose-tolerant species. The second comparisons included different genetic or pharmacological rodent models of hyperglycemia (26, 27, 36, 82): A GK rat strain exhibiting 25 mmol postprandial hyperglycemia compared with a normoglycemic BN strain (26, 27), C57BL/6 *ob/ob* mice, and streptozotocin-injected mice C57BL/6 mice exhibiting postprandial hyperglycemia at 13 and 19 mmol compared with normoglycemic C57BL/6 control mice (36), and BTBR *ob/ob* mice exhibiting hyperglycemia at 22 mmol compared with a normoglycemic B6 strain (82).

As shown in Fig. 9, we identified 11 miRNAs that include *miRNA-27-3p*, as being responsive to significant increases in circulating glucose in rainbow trout, blunt snout bream, and rodent models, revealing a core of miRNAs whose regulation may directly depend on circulating glucose across these species. Another subset of 11 miRNAs is regulated by high-carbohydrate diets and or increased circulating glucose in both rainbow trout and blunt snout bream with largely consistent directional expression changes, suggesting either dietary HighCHO-dependent responses or possible teleost-specific response to increased circulating glucose. These genes notably include the syn-expression of several components of the *miR-17-92* cluster. A subset of 16 miRNAs were identified when comparing glucose-tolerant species displaying increases in circulating glucose, the blunt snout bream (47) and rodent models (26, 27, 36, 82), opening up the possibility that a lack of regulation of these miRNAs in rainbow trout may contribute to its GI phenotype. Together, these findings suggest complex species and/or phenotype-specific patterns of miRNA regulation. Future studies probing the functional role of identified target miRNAs in GI in rainbow trout will allow us to answer several questions. First, it will be informative to investigate whether specific miRNAs identified as being regulated in dietary carbohydrate-induced hyperglycemia across species may still contribute to differences in glucose tolerance based on rewiring

Table 2. *Correlation of expression of differentially regulated miRNAs and predicted targets involved in pathways relevant to hepatic regulation of glucose metabolism*

	miRNA	Significantly Differentially Expressed	Pearson Correlation Coefficient	Significance
pck1	*ssa-miR-27d-5p*	All groups (ANOVA)	0.63	$P < 0.05$
GSONMT00082468001	*ssa-miR-27d-5p*	Fasted-HighCHO	0.62	n.s.
	ssa-miR-27d-5p	NoCHO-HighCHO	0.66	n.s.
	ola-miR-27c-5p_L+1R+1_1ss12CA	ANOVA	0.72	$P < 0.05$
	ola-miR-27c-5p_L+1R+1_1ss12CA	Fasted-HighCHO	0.72	$P < 0.05$
pck2	*ssa-miR-30e-5p*	All groups (ANOVA)	−0.41	n.s.
GSONMT00059643001	*ssa-miR-30e-5p*	Fasted-HighCHO	−0.46	n.s.
	ssa-miR-30e-5p	NoCHO-HighCHO	−0.43	n.s.
	ccr-miR-15a	All groups (ANOVA)	−0.32	n.s.
	ccr-miR-15a	Fasted-HighCHO	−0.22	n.s.
	ccr-miR-15a	NoCHO-HighCHO	−0.32	n.s.
	ssa-miR-30a-5p	Fasted-HighCHO	−0.28	n.s.
	ssa-miR-30c-5p_R+1_1ss24TC	Fasted-NoCHO	0.24	n.s.
g6pca	*dre-miR-190a_R+1*	All groups (ANOVA)	−0.42	n.s.
GSONMT00076843001	*dre-miR-190a_R+1*	Fasted-HighCHO	−0.29	n.s
	dre-miR-190a_R+1	NoCHO-HighCHO	−0.18	n.s.
	fru-miR-221_R-1	All groups (ANOVA)	−0.21	n.s.
	fru-miR-221_R-1	Fasted-HighCHO	−0.23	n.s.
	ssa-miR-30e-5p	All groups (ANOVA)	−0.13	n.s.
	ssa-miR-30e-5p	Fasted-HighCHO	−0.17	n.s.
	ssa-miR-30e-5p	NoCHO-HighCHO	−0.25	n.s.
	ssa-let-7e-3p_1ss22CT	Fasted-NoCHO	−0.61	n.s.
	ssa-miR-30a-5p	Fasted-HighCHO	0.78	$P < 0.05$
g6pcb1.a	*ccr-miR-27a*	All groups (ANOVA)	−0.25	n.s.
GSONMT00076841001	*dre-miR-27b-3p_R-1*	All groups (ANOVA)	−0.42	n.s.
	dre-miR-27b-3p_R-1	Fasted-HighCHO	−0.72	$P < 0.05$
	dre-miR-27b-3p_R-1	NoCHO-HighCHO	−0.42	n.s.
	dre-miR-142a-3p_L-1R-1	Fasted-HighCHO	0.03	n.s.
g6pcb1.b	none	n/a	n/a	n/a
GSNOMT00066036001				
g6pcb2.a	*dre-miR-181b-5p_R+1*	All groups (ANOVA)	0.12	n.s.
GSNOMT00013076001	*dre-miR-181b-5p_R+1*	Fasted-NoCHO	0.68	n.s.
	dre-miR-190a_R+1	All groups (ANOVA)	−0.45	n.s.
	dre-miR-190a_R+1	Fasted-HighCHO	−0.48	n.s.
	dre-miR-190a_R+1	NoCHO-HighCHO	−0.52	n.s.
	ipu-miR-1388_R-1	All groups (ANOVA)	−0.40	n.s.
	ipu-miR-1388_R-1	Fasted-NoCHO	−0.62	n.s.
	ipu-miR-222a_1ss11TG	All groups (ANOVA)	−0.43	n.s.
	ipu-miR-222a_1ss11TG	Fasted-HighCHO	−0.49	n.s.
	ssa-miR-222a-3p_R-1	All groups (ANOVA)	−0.29	n.s.
	ssa-miR-222b-3p	All groups (ANOVA)	−0.43	n.s.
	ssa-miR-222b-3p	NoCHO-HighCHO	−0.43	n.s.
	ssa-miR-101b-5p	All groups (ANOVA)	−0.47	n.s.
	ssa-miR-101b-5p	Fasted-HighCHO	−0.64	n.s.
	ola-miR-101b-5p	All groups (ANOVA)	−0.41	n.s.
	ola-miR-101b-5p	Fasted-NoCHO	−0.49	n.s.
	ola-miR-101b-5p	Fasted-HighCHO	−0.59	n.s.
	ssa-miR-128-2-5p	All groups (ANOVA)	0.66	$P < 0.05$
	ipu-miR-126b	All groups (ANOVA)	−0.72	$P < 0.05$
	dre-miR-92a-3p_R+1	Fasted-NoCHO	−0.73	$P < 0.05$
	PC-5p-219_12291	NoCHO-HighCHO	0.76	$P < 0.05$
g6pcb2.b	*dre-miR-181b-5p_R+1*	All groups (ANOVA)	0.23	n.s.
GSNOMT00014864001	*dre-miR-181b-5p_R+1*	Fasted-NoCHO	0.78	$P < 0.05$
	dre-miR-190a_R+1	All groups (ANOVA)	−0.59	n.s.
	dre-miR-190a_R+1	Fasted-HighCHO	−0.60	n.s.
	dre-miR-190a_R+1	NoCHO-HighCHO	−0.57	n.s.
	ipu-miR-1388_R-1	All groups (ANOVA)	−0.38	n.s.
	ipu-miR-1388_R-1	Fasted-NoCHO	−0.09	n.s.
	ipu-miR-222a_1ss11TG	All groups (ANOVA)	0.56	n.s.
	ipu-miR-222a_1ss11TG	Fasted-HighCHO	−0.64	n.s.
	ssa-miR-222a-3p_R-1	All groups (ANOVA)	−0.24	n.s.
	ssa-miR-222b-3p	All groups (ANOVA)	−0.48	n.s.
	ssa-miR-222b-3p	Fasted-HighCHO	−0.64	n.s.
	dre-miR-456_1ss22AT	Fasted-NoCHO	0.18	n.s
	PC-5p-219_12291	NoCHO-HighCHO	0.74	$P < 0.05$
	dre-miR-15b-3p_L+1_1ss3GA	NoCHO-HighCHO	0.70	$P < 0.05$

Continued

Table 2.—*Continued*

	miRNA	Significantly Differentially Expressed	Pearson Correlation Coefficient	Significance
fbp1a	none	n/a	n/a	n/a
GSNOMT00001932001				
fbp1b1	*dre-let-7c-5p_1ss19GC*	All groups (ANOVA)	0.05	n.s.
GSNOMT00063051001	*dre-let-7c-5p_1ss19GC*	Fasted-NoCHO	0.67	n.s.
	dre-let-7c-5p_1ss19GC	Fasted-HighCHO	0.11	n.s.
	dre-miR-130a	All groups (ANOVA)	0.01	n.s.
	dre-miR-130a	Fasted-HighCHO	−0.05	n.s.
	ola-miR-101b-5p	All groups (ANOVA)	−0.45	n.s.
	ola-miR-101b-5p	Fasted-NoCHO	−0.86	$P < 0.01$
	ssa-miR-101b-5p	Fasted-NoCHO	0.71	$P < 0.05$
fbp1b2	*ola-miR-101b-5p*	All groups (ANOVA)	0.13	n.s.
GSNOMT00015701001	*ola-miR-101b-5p*	Fasted-NoCHO	−0.03	n.s.
	ola-miR-101b-5p	Fasted-HighCHO	0.07	n.s.
	ssa-miR-101b-5p	Fasted-HighCHO	0.39	n.s.
gck1	*ipu-miR-126b*	All groups (ANOVA)	−0.56	n.s.
GSONMG00033781001	*ipu-miR-126b*	Fasted-NoCHO	−0.05	n.s.
gck2	*ipu-miR-126b*	Fasted-HighCHO	−0.71	$P < 0.05$
GSONMG00012878001	*dre-miR-429a*	All groups (ANOVA)	−0.60	n.s.
	dre-miR-429a	Fasted-NoCHO	−0.42	n.s.
	dre-miR-429a	Fasted-HighCHO	−0.71	$P < 0.05$

n/a, not available; n.s., Not significant; HighCHO, high-carbohydrate diet; NoCHO, no-carbohydrate diet.

of miRNA-target networks, which is estimated to differ by as much as 90% in targets between mammals and fish (43). Conversely, comparative identification of commonly regulated miRNA-target pairs with functions in glucoregulation may facilitate the identification of the biologically most relevant miRNA-mRNA target relationships in mammalian models, a major challenge in miRNA biology. Second, the identification of miRNAs that are specifically regulated in rainbow trout in response to HighCHO-induced glycemia will allow us to specifically and functionally probe the hypothesis that rainbow trout-specific miRNA regulation contributes to GI in this species. Third, by modulating specific expression of hepatic miRNAs that are only regulated in response to high dietary carbohydrates in GI species, but not rainbow trout, will allow us to test the hypothesis that, conversely, a lack of regulation of specific miRNAs in rainbow trout contributes to the GI phenotype in rainbow trout.

Enrichment of In Silico Predicted Targets of Differentially Expressed miRNAs Identifies Hepatic Metabolic and Cell Signaling Pathways Linked to GI in Rainbow Trout as Targets of Posttranscriptional Regulation

Glucose metabolism. Several pathways related to glucose metabolism were predicted to be posttranscriptionally regulated by differentially expressed miRNAs in pairwise comparisons between all experimental groups (Additional File 11). Interestingly, gluconeogenesis is enriched in all comparisons, suggesting that miRNAs differentially regulate this pathway in response to both NoCHO and HighCHO. Functionally, differential regulation of gene expression and enzymatic activity of components of the gluconeogenic pathway have been previously described in the same samples and revealed a possible contribution of the atypical induction of hepatic *g6pcb2* ohnologs in response to HighCHO to the lack of inhibition of gluconeogenesis (41). This differential regulation is, in turn, hypothesized to contribute to GI in rainbow trout (32, 41, 42, 56). Correlational analysis of specific miRNAs regulated in the HighCHO diet and their predicted target transcripts points to a possible role of *miRNA-27-3p* in regulating *g6pcb1*, but not *g6pcb2* paralogs. A recent study investigating overexpression of *miRNA-27b* in the mouse liver revealed a significant decrease in G6PC and PCK protein levels, suggesting an evolutionarily conserved response (81). Conversely, significant negative correlations between *miR-126b-5p* and *miR-92a-3p* and glucose-6-phosphatase b2a (*g6pcb2a*) suggest a specific role for these miRNAs in the atypical regulation of *g6pcb2* ohnologs. Together, these relationships raise the possibility that both rainbow trout *g6pcb2* paralogs escape from evolutionary conserved posttranscriptional *g6pc* regulation and/or that the evolution of novel miRNA-dependent regulation of *g6pcb2* paralogues may underlie their atypical regulation in response to dietary carbohydrates to contribute to GI in rainbow trout. Future functional studies using 3′-UTR luciferase reporter assays and miRNA modulation approaches in trout hepatocyte cell lines will be necessary to establish the first evidence of paralog-specific posttranscriptional regulation in salmonids and to functionally link these candidate miRNAs to paralog-specific regulation of gluconeogenic enzyme paralogs and their effect on de novo glucose production.

Lipid metabolism. DNL-related GO terms were predicted as being enriched in the NoCHO (positive regulation of triglyceride biosynthetic process) and HighCHO (fatty acid biosynthesis), respectively, indicative of a differential, miRNA-dependent posttranscriptional regulation of the hepatic DNL pathway in response to either diet. Functional markers at the gene expression level were not indicative of a differential activation of DNL in response to NoCHO and HighCHO diets, suggesting that a lack of carbohydrate-dependent induction of DNL, which is observed in glucose tolerant mammals, may contribute to GI in rainbow trout. Interestingly, the most abundant hepatic miRNA detected in our study, *miRNA-122*, was significantly induced in the liver only in response to the protein-rich NoCHO diet but not the carbohydrate-rich HighCHO diet, confirming the observed acute postprandial induction of this hepatic miRNA in response to a commercial,

protein rich diet (45). The induction of *miRNA-122*, which is lipogenic in trout as in mammals (17, 44), in response to dietary protein in the NoCHO, and the lack of induction in response to a HighCHO diet, is in line with reports that rainbow trout hepatic DNL is more responsive to dietary proteins than carbohydrates (13). Because *miRNA-122* regulation not only stimulates hepatic lipogenic pathways, but also secondarily improves glucose tolerance in rainbow trout, likely

Table 3. *Correlation of expression of differentially regulated miRNAs and predicted targets involved in pathways of interest relevant to hepatic regulation of glucose metabolism*

	miRNA	Significantly Differentially Expressed	Pearson Correlation Coefficient	Significance
		Glucose metabolism		
glut9	ssa-miR-222a-3p_R-1	All groups (ANOVA)	0.20	n.s.
GSONMT00066217001	ssa-miR-222a-3p_R-1	Fasted-HighCHO	0.15	n.s.
	ssa-miR-222b-3p	All groups (ANOVA)	0.33	n.s.
	pol-let-7a-3p_R+1_1ss3AG	All groups (ANOVA)	−0.37	n.s.
	pol-let-7a-3p_R+1_1ss3AG	Fasted-NoCHO	−0.63	n.s.
	dre-miR-722_L-2	All groups (ANOVA)	0.42	n.s.
	dre-miR-722_L-2	Fasted-NoCHO	0.04	n.s.
	dre-miR-722_L-2	Fasted-HighCHO	0.50	n.s.
adp-gk	ssa-miR-214-3p_L-1_1ss23AT	All groups (ANOVA)	0.34	n.s.
GSONMT00073455001	ssa-miR-214-3p_L-1_1ss23AT	Fasted-HighCHO	0.33	n.s.
	ssa-miR-27d-5p	All groups (ANOVA)	0.84	$P < 0.01$
	ssa-miR-27d-5p	Fasted-HighCHO	0.96	$P < 0.01$
	ssa-miR-27d-5p	NoCHO-HighCHO	0.95	$P < 0.01$
	ola-miR-27c-5p_L+1R+1 1ss12CA	All groups (ANOVA)	0.83	$P < 0.01$
	ola-miR-27c-5p_L+1R+1_1ss12CA	Fasted-HighCHO	0.98	$P < 0.01$
	ola-miR-101b-5p	All groups (ANOVA)	−0.27	n.s.
	ola-miR-101b-5p	Fasted-NoCHO	0.59	n.s.
	ola-miR-101b-5p	Fasted-HighCHO	−0.71	$P < 0.05$
	ssa-miR-30c-5p_R+1_1ss24TC	Fasted-NoCHO	−0.55	n.s.
	dre-miR-125b-2-3p_L+1_2ss8GA11TC	Fasted-HighCHO	0.77	$P < 0.05$
		Cell signaling		
ir	dre-miR-18b-5p_1ss11TC	All groups (ANOVA)	−0.03	n.s.
GSONMT00026581001	dre-miR-18b-5p_1ss11TC	Fasted-HighCHO	0.04	n.s.
	dre-miR-18b-5p_1ss11TC	noCHO-HighCHO	0.02	n.s.
	dre-miR-190a_R+1	All groups (ANOVA)	−0.18	n.s.
	dre-miR-190a_R+1	Fasted-HighCHO	−0.12	n.s.
	dre-miR-190a_R+1	noCHO-HighCHO	−0.33	n.s.
	ssa-miR-30e-5p	All groups (ANOVA)	−0.01	n.s.
	ssa-miR-30e-5p	Fasted-HighCHO	0.00	n.s.
	ssa-miR-30e-5p	noCHO-HighCHO	0.00	n.s.
	ssa-miR-30c-5p_R+1_1ss24TC	Fasted-NoCHO	−0.20	n.s.
	ssa-miR-30c-5p_R+1_1ss24TC	Fasted-HighCHO	−0.74	<0.05
	ssa-miR-30a-5p	Fasted-HighCHO	0.12	n.s.
	ssa-miR-722-5p_L-1R+1	Fasted-HighCHO	−0.04	n.s.
		Other pathways of interest		
Autophagy				
soga1	dre-miR-140-5p_R+1	All groups (ANOVA)	−0.80	$P < 0.01$
GSONMT00057063001	dre-miR-140-5p_R+1	Fasted-HighCHO	−0.86	$P < 0.01$
	dre-miR-140-5p_R+1	NoCHO-HighCHO	−0.77	$P < 0.05$
	dre-miR-214-5p_R+1	ANOVA	0.07	n.s.
	ssa-miR-214-3p_L-1_1ss23AT	Fasted-HighCHO	0.34	n.s.
Mitochondrial fusion				
fis1	fru-miR-200a_R-1	All groups (ANOVA)	0.20	n.s.
GSONMT00039888001	fru-miR-200a_R-1	Fasted-NoCHO	−0.25	n.s.
	fru-miR-200a_R-1	NoCHO-HighCHO	−0.18	n.s.
mfn1	dre-let-7d-5p	All groups (ANOVA)	0.74	$P < 0.01$
GSONMT00027395001	dre-let-7d-5p	Fasted-NoCHO	0.89	$P < 0.01$
	dre-let-7d-5p	Fasted-HighCHO	0.93	$P < 0.01$
	dre-let-7c-5p_1ss19GC	All groups (ANOVA)	0.57	n.s.
	dre-let-7c-5p_1ss19GC	Fasted-HighCHO	0.94	$P < 0.01$
	dre-let-7c-5p_1ss19GC	NoCHO-HighCHO	−0.21	n.s.
	dre-let-7a	Fasted-HighCHO	−0.72	$P < 0.05$
	ssa-miR-27d-5p	All groups (ANOVA)	−0.20	n.s.
	ssa-miR-27d-5p	Fasted-HighCHO	−0.54	n.s.
	ssa-miR-27d-5p	NoCHO-HighCHO	−0.40	n.s.
	ola-miR-27c-5p_L+1R+1_1ss12CA	All groups (ANOVA)	0.16	n.s
	ola-miR-27c-5p_L+1R+1_1ss12CA	Fasted-HighCHO	0.51	n.s
	fru-miR-7_R+2	Fasted-NoCHO	0.70	n.s

Continued

Table 3.—*Continued*

	miRNA	Significantly Differentially Expressed	Pearson Correlation Coefficient	Significance
mfn2	ssa-miR-214-3p_L-1_1ss23AT	All groups (ANOVA)	0.83	$P < 0.01$
GSONMT00004526001	ssa-miR-214-3p_L-1_1ss23AT	Fasted-HighCHO	0.87	$P < 0.01$
	ssa-miR-16c-5p_R-1	All groups (ANOVA)	0.16	n.s
	ssa-miR-16c-5p_R-1	noCHO-HighCHO	0.13	n.s
	fru-miR-152	All groups (ANOVA)	−0.57	n.s
	fru-miR-152	Fasted-HighCHO	−0.81	$P < 0.05$
	fru-miR-152	noCHO-HighCHO	−0.53	n.s.
	ccr-miR-15a	All groups (ANOVA)	−0.60	$P < 0.05$
	ccr-miR-15a	Fasted-HighCHO	−0.89	$P < 0.01$
	ccr-miR-15a	noCHO-HighCHO	−0.26	n.s.
	ssa-miR-17-5p_R-1	All groups (ANOVA)	−0.54	n.s.
	ssa-miR-17-5p_R-1	Fasted-HighCHO	−0.77	$P < 0.05$
	dre-miR-18b-5p_1ss11TC	All groups (ANOVA)	−0.53	n.s.
	dre-miR-18b-5p_1ss11TC	Fasted-HighCHO	−0.75	$P < 0.05$
	dre-miR-18b-5p_1ss11TC	noCHO-HighCHO	−0.40	n.s.
	ssa-miR-15b-5p	All groups (ANOVA)	−0.39	n.s.
	ssa-miR-15b-5p	noCHO-HighCHO	0.31	n.s.
	dre-miR-181b-5p_R+1	Fasted-NoCHO	0.91	$P < 0.01$
	ssa-miR-101b-5p	Fasted-HighCHO	−0.75	$P < 0.05$
	ssa-miR-29b-2-5p_L-2	Fasted-HighCHO	−0.55	n.s.

by increasing glucose flux toward the 'lipogenic sink', suggests that this specific nutritional regulation of the most abundant, functionally conserved hepatic miRNA may play a role in GI tolerance in rainbow trout (7, 44). However, real-time RT-PCR did not validate an increase in *miRNA-122* across all 9 samples, suggesting that the induction might have been observed only in a subset of $n = 4$ samples used for NGS small RNA sequencing.

Insulin signaling. In contrast to a previous study that revealed a significant increase in activity of specific components (Akt, S6) of the hepatic insulin signaling in response to a diet with low, but not high CHO content in response to a single meal following a short-term fast, the current study of rainbow trout refed for 4 days, provides contrasting evidence for an induction of Akt and S6 activity in response to the HighCHO, but not a the NoCHO diet. Together, this finding may suggest a time-dependent acclimation of the hepatic insulin signaling pathway to excess dietary carbohydrates, refuting, at least under our current experimental conditions, the hypothesis that diminished hepatic insulin pathway signaling activity may be linked to GI in rainbow trout. Therefore, the reported enrichment of insulin signaling in general, and Akt and Tor signaling pathways in particular, in response to HighCHO (Additional File 11) may be indicative of miRNA-dependent adaptive changes in the hepatic insulin signaling pathway in response to HighCHO. Interestingly, an enrichment for insulin signaling was equally predicted in targets of differentially regulated hepatic miRNAs in the glucose-tolerant blunt snout bream (47) and GI rodent models (26), suggesting that posttranscriptional regulation of the insulin pathway in response to dietary carbohydrates is widespread in GI and glucose-tolerant fish species as well as rodent models (26). At the specific transcript level, we identified a significant correlation of *miR-30c-5p* family member and the profiled insulin receptor (*ir*) when comparing fasted and HighCHO groups, suggesting a possible posttranscriptional role for *miR-30c-5p* posttranscriptional regulation of *ir* under these conditions. However, because the abundance of this *ir* paralog was similarly decreased by refeeding irrespective of diet, it does not explain the differential activation observed for the insulin signaling pathway.

Additional predicted targets of differentially expressed miRNAs: organelle dynamics. Additional hepatic pathways relevant to GI in rainbow trout that emerged as being regulated posttranscriptionally by differentially regulated miRNAs were related to specific hepatic organelle function, especially autophagy and mitochondrial dynamics, both of which have been linked to regulating systemic glucose homeostasis in trout (69) and/or in mammals (19, 64, 68, 72, 73). With regard to autophagy, analysis of transcript abundance of targeted markers involved in autophagy reveal an induction of a *soga1*, an inhibitor of autophagy and gluconeogenic AA-dependent de novo gluconeogenesis in response to HighCHO diets, indicative of an adaptive response to HighCHO diet-induced hyperglycemia. We identified a significant negative correlation in the expression of *miR-140-5p* and the *soga1* paralog, across all experimental groups, raising the possibility of a general posttranscriptional control of *soga1* and its regulated processes under different dietary conditions.

With regard to mitochondria fusion and fission dynamics, the induction of *mfn1* and *mfn2* paralogs did not differ between diets, in contrast to *fis1*, which was significantly induced in trout refed HighCHO compared with fasted and NoCHO-fed trout. Indeed, mitochondrial fission has been shown to be induced in response to oxidative stress and increased gluconeogenesis in a hepatoma cell line (25), suggesting that this process may play a role in HighCHO-induced GI in rainbow trout. However, significant negative correlations between miRNAs predicted to target these transcripts were only observed for mitofusins, but not *fis1*, suggesting that the differential regulation of *fis1* is likely dependent on factors other than miRNAs.

Additional Considerations

The current study is the first to identify differential global and specific regulation of hepatic miRNAs in rainbow trout in response to refeeding and reveals that the regulation of the miRNA biogenesis pathway and the miRNAome in general is more dependent on carbohydrate and protein content than the process of refeeding itself. We furthermore show that the

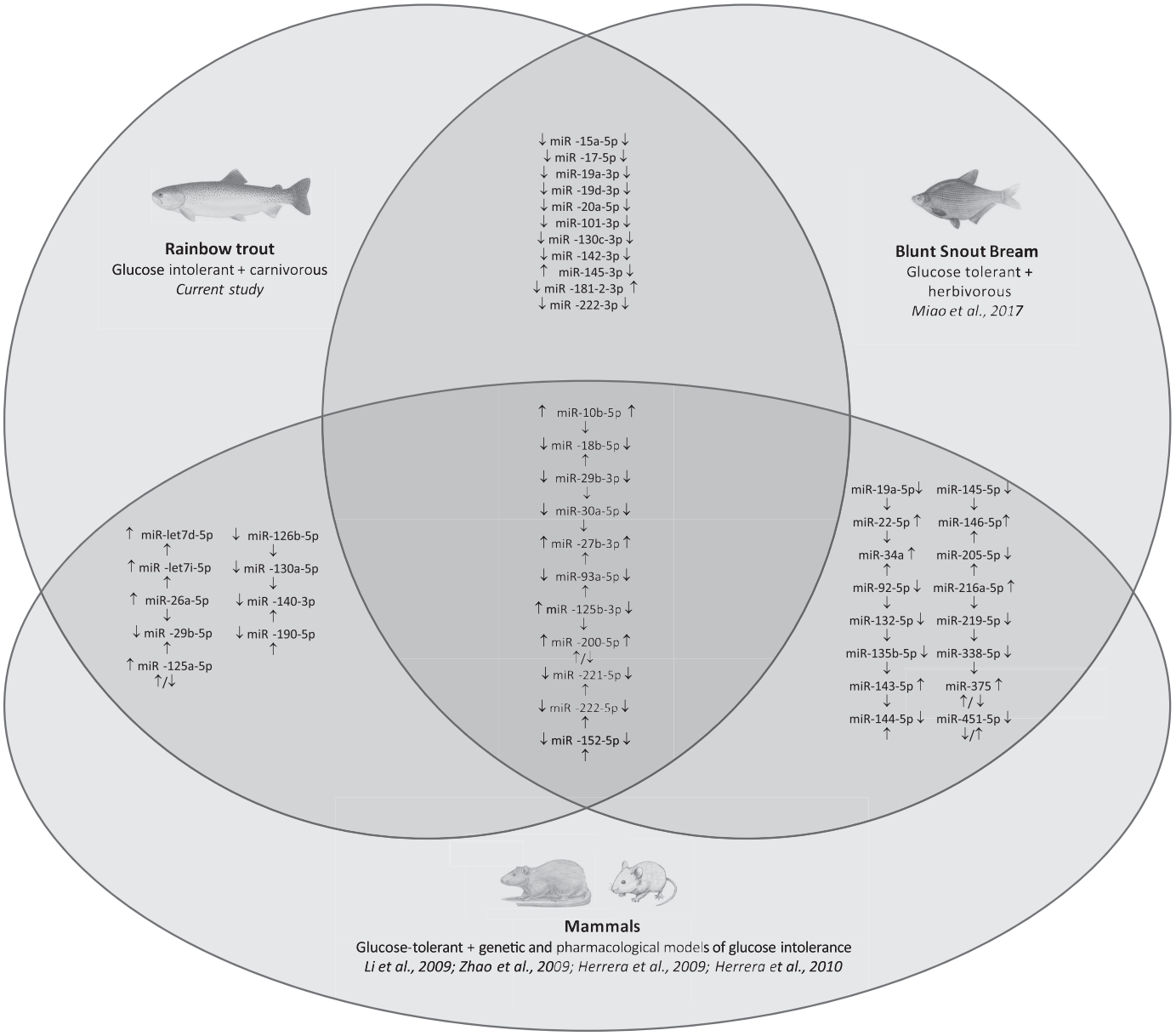

Fig. 9. Venn diagram-based representation of differentially regulated hepatic miRNAs in response to diet-induced hyperglycemia in glucose-intolerant rainbow trout (current study), glucose-tolerant blunt snout bream (47) and rodent models of diet-induced hyperglycemia (26, 27, 36, 82). The identification of common differentially regulated hepatic miRNAs in hyperglycemic conditions between these species is indicated in intersections of the Venn diagram. Differentially regulated miRNAs in response to hyperglycemic conditions identified in rainbow trout, blunt snout bream, and mammalian models are indicated in the center of the Venn diagram. The directional change of specific miRNA expression within specific studies is indicated as follows: For each individual miRNA, an arrow to its *left* indicates the observed miRNA expression change observed in rainbow trout in the current study, an arrow to its *right* the observed expression changes in the glucose-tolerant blunt snout bream and an arrow located *below* each specific miRNA indicates its expression change observed in mammalian studies.

regulation of several identified hepatic miRNAs in response to increases in circulating glucose may be evolutionarily conserved in vertebrates. The current study furthermore predicts hepatic pathways relevant to GI in rainbow trout and especially identifies gluconeogenesis, de novo lipogenesis, and insulin signaling as being subjected to posttranscriptional regulation. Because these hepatic pathways have previously been linked to GI in rainbow trout, our study opens up the possibility to specifically probe hepatic miRNA-target pairs underlying GI in rainbow trout for future functional studies.

However, there are some limitations of the study that should be pointed out. First, it is important to note that while the study establishes important qualitative and quantitative differences related to macronutrient composition of the isoenergetic diets, it is not possible to specify whether the HighCHO diet changes are related to an increase in dietary carbohydrates and/or hyperglycemia or a decrease in dietary protein content, which is replaced in favor of increased carbohydrate content. The fact that several identified differentially regulated miRNAs in response to HighCHO diet have equally been shown to be induced in response increases in circulating glucose suggests that this subset of miRNAs is evolutionarily conserved in its direct response to circulating glucose. However, the possibility some miRNAs are differentially regulated by altered protein

abundance remains a possibility. Diet preparation using non-digestible CHO to replace dietary protein content, as well as glucose injections, an/or in vitro studies of trout hepatocytes in response to medium glucose and AA will allow us to delineate the exact nutritional factors involved in this regulation further. Second, because of the large number of miRNA-mRNA target pairs, it remains challenging to infer specific biological consequences of differentially regulated miRNAs. Our study took advantage of the recently available rainbow trout genome resources (4, 43) to use an in silico approach to predict posttranscriptional regulation of transcripts at the genome level, similarly to previously published approaches in trout (33, 53), other fish species (47), and mammals (26). While not all 3′-UTRs are available, this approach represents a significant advancement compared with approaches used before genome publication, as previously discussed (46). The identification of particularly important individual miRNA-target relationships within these predicted pathways remains a particular challenge in miRNA biology, and expression between predicted miRNAs and targeted mRNA pairs remains correlative and now needs to be functionally tested. Despite a well-established negative posttranscriptional regulation as the principal mode of action of miRNAs, miRNA-mRNA target pairs do not necessarily correlate negatively. Several reasons account for this fact in addition to inherent limitations to in silico approaches (58). First, as in our study, samples analyzed for miRNAs and mRNAs are generally taken from a single time point, neglecting possible temporal factors in miRNA target interaction. Furthermore, miRNAs, in addition to acting to degrade mRNA abundance, may initially act at the protein level by inhibiting translation, thus without protein abundance data such effects may be missed (75). In general however, relatively good correlation in miRNA inhibition studies has been found at the protein and mRNA level, the inhibition of both of which is largely dependent on specific 3′-UTR seed binding sites (7, 17). Finally, miRNAs are one of several factors regulating gene expression, and indeed simple transcription factor and miRNA based gene regulation networks may result in negative or positive correlations, as well as stabilizing effect on mRNA abundance (11, 80). Nevertheless, the correlative expression between in silico predicted miRNA-mRNA pairs identifies interesting targets for functional in vitro assays in rainbow trout, which will delineate de facto regulation and metabolic functionality of specific proposed miRNA-mRNA target pairs in rainbow trout GI (43).

Conclusions

Overall, our study demonstrates that the hepatic miRNAs are more responsive to HighCHO diets compared with NoCHO diets in rainbow trout. This is evident from both end points related to the canonical pathway, as well as the number of differentially expressed miRNAs, which is higher in the HighCHO group compared with the NoCHO group. Specific comparative analyses identified a common set of miRNAs that increase in conditions of increased circulating glucose concentrations in GI rainbow trout, glucose-tolerant blunt snout bream, and rodent models of GI, as well miRNAs that are regulated under conditions of increased circulating glucose in both rainbow trout or glucose-tolerant species. These distinctions will aid in advancing our understanding of how specific miRNAs and/or evolutionary rewiring of miRNA-target networks may contribute to different phenotypes of glucose tolerance in the future. Genome-wide in silico analysis identified metabolic pathways (gluconeogenesis, DNL), cell signaling pathways (insulin signaling), and organelle dynamics (autophagy, mitochondrial fusion) as being subject to posttranscriptional regulation by miRNAs in response to HighCHO, providing specific targets for future studies probing the role of identified miRNAs in rainbow trout GI at a functional level in vitro.

ACKNOWLEDGMENTS

Availability of data and material: The data sets are available from the corresponding author upon reasonable request.

GRANTS

This work benefited from the financial support of the INRA PHASE Department. This research was carried out under the E2S UPPA supported by the "Investissements d'Avenir" managed by ANR (ANR-16-IDEX-0002). L. Marandel received EU support under the Marie-Curie FP7 COFUND People Program through an AgreenSkills+ fellowship (#609398). D. J. Kostyniuk gratefully acknowledge funding through a MITACS Globalink grant (IT-10852), and J. A. Mennigen support from the Canadian Foundation for Innovation (#35859) and an NSERC Discovery grant (#147476). The funding agencies had no role in the design, execution or interpretation of the study.

DISCLOSURES

No conflicts of interest, financial or otherwise, are declared by the authors.

AUTHOR CONTRIBUTIONS

D.J.K., L.M., M.J., and K.D. performed experiments; D.J.K., L.M., M.J., K.D., R.F.d.S., D.Z., C.J.M., and J.A.M. analyzed data; D.J.K., L.M., C.J.M., and J.A.M. interpreted results of experiments; D.J.K., L.M., C.J.M., and J.A.M. prepared figures; D.J.K. and J.A.M. drafted manuscript; D.J.K., L.M., M.J., K.D., D.Z., C.J.M., S.P., and J.A.M. edited and revised manuscript; D.J.K., L.M., M.J., K.D., R.F.d.S., D.Z., C.J.M., S.P., and J.A.M. approved final version of manuscript; L.M., S.P., and J.A.M. conceived and designed research.

REFERENCES

1. **Bartel DP.** MicroRNAs: target recognition and regulatory functions. *Cell* 136: 215–233, 2009. doi:10.1016/j.cell.2009.01.002.
2. **Beamish FW, Hilton JW, Niimi E, Slinger SJ.** Dietary carbohydrate and growth, body composition and heat increment in rainbow trout (Salmo gairdneri). *Fish Physiol Biochem* 1: 85–91, 1986. doi:10.1007/BF02290208.
3. **Bergot F.** Effects of dietary carbohydrates and of their mode of distribution on glycaemia in rainbow trout (Salmo gairdneri richardson). *Comp Biochem Physiol A Physiol* 64: 543–547, 1979. doi:10.1016/0300-9629(79)90581-4.
4. **Berthelot C, Brunet F, Chalopin D, Juanchich A, Bernard M, Noël B, Bento P, Da Silva C, Labadie K, Alberti A, Aury J-M, Louis A, Dehais P, Bardou P, Montfort J, Klopp C, Cabau C, Gaspin C, Thorgaard GH, Boussaha M, Quillet E, Guyomard R, Galiana D, Bobe J, Volff J-N, Genêt C, Wincker P, Jaillon O, Roest Crollius H, Guiguen Y.** The rainbow trout genome provides novel insights into evolution after whole-genome duplication in vertebrates. *Nat Commun* 5: 3657, 2014. doi:10.1038/ncomms4657.
5. **Best C, Ikert H, Kostyniuk DJ, Craig PM, Navarro-Martin L, Marandel L, Mennigen JA.** Epigenetics in teleost fish: From molecular mechanisms to physiological phenotypes. *Comp Biochem Physiol B Biochem Mol Biol* 224: 210–244, 2018. doi:10.1016/j.cbpb.2018.01.006.
6. **Blasco J, Marimón I, Viaplana I, Fernández-Borrás J.** Fate of plasma glucose in tissues of brown trout in vivo: effects of fasting and glucose loading. *Fish Physiol Biochem* 24: 247–258, 2001. doi:10.1023/A:1014084313207.
7. **Boutz DR, Collins PJ, Suresh U, Lu M, Ramírez CM, Fernández-Hernando C, Huang Y, Abreu Rde R, Le S-Y, Shapiro BA, Liu AM, Luk JM, Aldred SF, Trinklein ND, Marcotte EM, Penalva LOF.** Two-tiered approach identifies a network of cancer and liver disease-

related genes regulated by miR-122. *J Biol Chem* 286: 18066–18078, 2011. doi:10.1074/jbc.M110.196451.

8. **Brauge C, Corraze G, Médale F.** Effects of dietary levels of carbohydrate and lipid on glucose oxidation and lipogenesis from glucose in rainbow trout, Oncorhynchus mykiss, reared in freshwater or in seawater. *Comp Biochem Physiol A Physiol* 111: 117–124, 1995. doi:10.1016/0300-9629(95)98527-N.
9. **Bucking C, Wood CM.** Renal regulation of plasma glucose in the freshwater rainbow trout. *J Exp Biol* 208: 2731–2739, 2005. doi:10.1242/jeb.01668.
10. **Choi K, Weber J-M.** Coping with an exogenous glucose overload: glucose kinetics of rainbow trout during graded swimming. *Am J Physiol Regul Integr Comp Physiol* 310: R493–R501, 2016. doi:10.1152/ajpregu.00330.2015.
11. **Cora' D, Re A, Caselle M, Bussolino F.** MicroRNA-mediated regulatory circuits: outlook and perspectives. *Phys Biol* 14: 045001, 2017. doi:10.1088/1478-3975/aa6f21.
12. **Craig PM.** Why trout? in *Trout: From Physiology to Conservation* (Polakof S, Moon TW, editors). Nova Science Publishers, 2013, p. 1–8.
13. **Dai W, Panserat S, Kaushik S, Terrier F, Plagnes-Juan E, Seiliez I, Skiba-Cassy S.** Hepatic fatty acid biosynthesis is more responsive to protein than carbohydrate in rainbow trout during acute stimulations. *Am J Physiol Regul Integr Comp Physiol* 310: R74–R86, 2016. doi:10.1152/ajpregu.00281.2015.
14. **Dai W, Panserat S, Mennigen JA, Terrier F, Dias K, Seiliez I, Skiba-Cassy S.** Post-prandial regulation of hepatic glucokinase and lipogenesis requires the activation of TORC1 signalling in rainbow trout (Oncorhynchus mykiss). *J Exp Biol* 216: 4483–4492, 2013. doi:10.1242/jeb.091157.
15. **Dai W, Panserat S, Plagnes-Juan E, Seiliez I, Skiba-Cassy S.** Amino Acids Attenuate Insulin Action on Gluconeogenesis and Promote Fatty Acid Biosynthesis via mTORC1 Signaling Pathway in trout Hepatocytes. *Cell Physiol Biochem* 36: 1084–1100, 2015. doi:10.1159/000430281.
16. **Dai W, Panserat S, Terrier F, Seiliez I, Skiba-Cassy S.** Acute rapamycin treatment improved glucose tolerance through inhibition of hepatic gluconeogenesis in rainbow trout (Oncorhynchus mykiss). *Am J Physiol Regul Integr Comp Physiol* 307: R1231–R1238, 2014. doi:10.1152/ajpregu.00166.2014.
17. **Elmén J, Lindow M, Silahtaroglu A, Bak M, Christensen M, Lind-Thomsen A, Hedtjärn M, Hansen JB, Hansen HF, Straarup EM, McCullagh K, Kearney P, Kauppinen S.** Antagonism of microRNA-122 in mice by systemically administered LNA-antimiR leads to up-regulation of a large set of predicted target mRNAs in the liver. *Nucleic Acids Res* 36: 1153–1162, 2008. doi:10.1093/nar/gkm1113.
18. **Enright AJ, John B, Gaul U, Tuschl T, Sander C, Marks DS.** MicroRNA targets in Drosophila. *Genome Biol* 5: R1, 2003. doi:10.1186/gb-2003-5-1-r1.
19. **Ezaki J, Matsumoto N, Takeda-Ezaki M, Komatsu M, Takahashi K, Hiraoka Y, Taka H, Fujimura T, Takehana K, Yoshida M, Iwata J, Tanida I, Furuya N, Zheng D-M, Tada N, Tanaka K, Kominami E, Ueno T.** Liver autophagy contributes to the maintenance of blood glucose and amino acid levels. *Autophagy* 7: 727–736, 2011. doi:10.4161/auto.7.7.15371.
20. **Fan X, Kurgan L.** Comprehensive overview and assessment of computational prediction of microRNA targets in animals. *Brief Bioinform* 16: 780–794, 2015. doi:10.1093/bib/bbu044.
21. **Felip O, Ibarz A, Fernández-Borràs J, Beltrán M, Martín-Pérez M, Planas JV, Blasco J.** Tracing metabolic routes of dietary carbohydrate and protein in rainbow trout (Oncorhynchus mykiss) using stable isotopes ([^{13}C]starch and [^{15}N]protein): effects of gelatinisation of starches and sustained swimming. *Br J Nutr* 107: 834–844, 2012. doi:10.1017/S0007114511003709.
22. **Fernández-Hernando C, Ramírez CM, Goedeke L, Suárez Y.** MicroRNAs in metabolic disease. *Arterioscler Thromb Vasc Biol* 33: 178–185, 2013. doi:10.1161/ATVBAHA.112.300144.
23. **Haman F, Powell M, Weber JM.** Reliability of continuous tracer infusion for measuring glucose turnover rate in rainbow trout. *J Exp Biol* 200: 2557–2563, 1997.
24. **Heckmann L-H, Sørensen PB, Krogh PH, Sørensen JG.** NORMA-Gene: a simple and robust method for qPCR normalization based on target gene data. *BMC Bioinformatics* 12: 250, 2011. doi:10.1186/1471-2105-12-250.
25. **Hernández-Alvarez MI, Paz JC, Sebastián D, Muñoz JP, Liesa M, Segalés J, Palacín M, Zorzano A.** Glucocorticoid modulation of mitochondrial function in hepatoma cells requires the mitochondrial fission protein Drp1. *Antioxid Redox Signal* 19: 366–378, 2013. doi:10.1089/ars.2011.4269.
26. **Herrera BM, Lockstone HE, Taylor JM, Ria M, Barrett A, Collins S, Kaisaki P, Argoud K, Fernandez C, Travers ME, Grew JP, Randall JC, Gloyn AL, Gauguier D, McCarthy MI, Lindgren CM.** Global microRNA expression profiles in insulin target tissues in a spontaneous rat model of type 2 diabetes. *Diabetologia* 53: 1099–1109, 2010. doi:10.1007/s00125-010-1667-2.
27. **Herrera BM, Lockstone HE, Taylor JM, Wills QF, Kaisaki PJ, Barrett A, Camps C, Fernandez C, Ragoussis J, Gauguier D, McCarthy MI, Lindgren CM.** MicroRNA-125a is over-expressed in insulin target tissues in a spontaneous rat model of Type 2 Diabetes. *BMC Med Genomics* 2: 54, 2009. doi:10.1186/1755-8794-2-54.
28. **Hilton JW, Atkinson JL.** Response of rainbow trout (Salmo gairdneri) to increased levels of available carbohydrate in practical trout diets. *Br J Nutr* 47: 597–607, 1982. doi:10.1079/BJN19820071.
29. **Hofacker IL.** RNA secondary structure analysis using the Vienna RNA package. *Curr Protoc Bioinformatics* Chapter 12: Unit 12.2, 2004. doi:10.1002/0471250953.bi1202s04.
30. **Juanchich A, Bardou P, Rué O, Gabillard J-C, Gaspin C, Bobe J, Guiguen Y.** Characterization of an extensive rainbow trout miRNA transcriptome by next generation sequencing. *BMC Genomics* 17: 164, 2016. doi:10.1186/s12864-016-2505-9.
31. **Kim Y-K, Kim B, Kim VN.** Re-evaluation of the roles of DROSHA, Export in 5, and DICER in microRNA biogenesis. *Proc Natl Acad Sci USA* 113: E1881–E1889, 2016. doi:10.1073/pnas.1602532113.
32. **Kirchner S, Panserat S, Lim PL, Kaushik S, Ferraris RP.** The role of hepatic, renal and intestinal gluconeogenic enzymes in glucose homeostasis of juvenile rainbow trout. *J Comp Physiol B* 178: 429–438, 2008. doi:10.1007/s00360-007-0235-7.
33. **Koganti PP, Wang J, Cleveland B, Ma H, Weber GM, Yao J.** Estradiol regulates expression of miRNAs associated with myogenesis in rainbow trout. *Mol Cell Endocrinol* 443: 1–14, 2017. doi:10.1016/j.mce.2016.12.014.
34. **Krishnan J, Rohner N.** Sweet fish: Fish models for the study of hyperglycemia and diabetes. *J Diabetes* 11: 193–203, 2019. doi:10.1111/1753-0407.12860.
35. **Lansard M, Panserat S, Plagnes-Juan E, Seiliez I, Skiba-Cassy S.** Integration of insulin and amino acid signals that regulate hepatic metabolism-related gene expression in rainbow trout: role of TOR. *Amino Acids* 39: 801–810, 2010. doi:10.1007/s00726-010-0533-3.
36. **Li S, Chen X, Zhang H, Liang X, Xiang Y, Yu C, Zen K, Li Y, Zhang C-Y.** Differential expression of microRNAs in mouse liver under aberrant energy metabolic status. *J Lipid Res* 50: 1756–1765, 2009. doi:10.1194/jlr.M800509-JLR200.
37. **Lynn FC.** Meta-regulation: microRNA regulation of glucose and lipid metabolism. *Trends Endocrinol Metab* 20: 452–459, 2009. doi:10.1016/j.tem.2009.05.007.
38. **Ma H, Weber GM, Hostuttler MA, Wei H, Wang L, Yao J.** MicroRNA expression profiles from eggs of different qualities associated with post-ovulatory ageing in rainbow trout (Oncorhynchus mykiss). *BMC Genomics* 16: 201, 2015. doi:10.1186/s12864-015-1400-0.
39. **Magnoni L, Weber J-M.** Endurance swimming activates trout lipoprotein lipase: plasma lipids as a fuel for muscle. *J Exp Biol* 210: 4016–4023, 2007. doi:10.1242/jeb.007708.
40. **Mannerström M, Soivio A, Salama A.** Intestinal absorption and tissue distribution of glucose and isoleucine in rainbow trout (Oncorhynchus mykiss). *Aquacult Nutr* 7: 229–235, 2001. doi:10.1046/j.1365-2095.2001.00179.x.
41. **Marandel L, Lepais O, Arbenoits E, Véron V, Dias K, Zion M, Panserat S.** Remodelling of the hepatic epigenetic landscape of glucose-intolerant rainbow trout (Oncorhynchus mykiss) by nutritional status and dietary carbohydrates. *Sci Rep* 6: 32187, 2016. doi:10.1038/srep32187.
42. **Marandel L, Seiliez I, Véron V, Skiba-Cassy S, Panserat S.** New insights into the nutritional regulation of gluconeogenesis in carnivorous rainbow trout (Oncorhynchus mykiss): a gene duplication trail. *Physiol Genomics* 47: 253–263, 2015. doi:10.1152/physiolgenomics.00026.2015.
43. **Mennigen JA.** Micromanaging metabolism-a role for miRNAs in teleost energy metabolism. *Comp Biochem Physiol B Biochem Mol Biol* 199: 115–125, 2016. doi:10.1016/j.cbpb.2015.09.001.
44. **Mennigen JA, Martyniuk CJ, Seiliez I, Panserat S, Skiba-Cassy S.** Metabolic consequences of microRNA-122 inhibition in rainbow trout, Oncorhynchus mykiss. *BMC Genomics* 15: 70, 2014. doi:10.1186/1471-2164-15-70.

45. **Mennigen JA, Panserat S, Larquier M, Plagnes-Juan E, Medale F, Seiliez I, Skiba-Cassy S.** Postprandial regulation of hepatic microRNAs predicted to target the insulin pathway in rainbow trout. *PLoS One* 7: e38604, 2012. doi:10.1371/journal.pone.0038604.
46. **Mennigen JA, Zhang D.** MicroTrout: A comprehensive, genome-wide miRNA target prediction framework for rainbow trout, Oncorhynchus mykiss. *Comp Biochem Physiol Part D Genomics Proteomics* 20: 19–26, 2016. doi:10.1016/j.cbd.2016.07.002.
47. **Miao L-H, Lin Y, Pan W-J, Huang X, Ge X-P, Ren M-C, Zhou Q-L, Liu B.** Identification of Differentially Expressed Micrornas Associate with Glucose Metabolism in Different Organs of Blunt Snout Bream (Megalobrama amblycephala). *Int J Mol Sci* 18: E1161, 2017. doi:10.3390/ijms18061161.
48. **Mirra P, Nigro C, Prevenzano I, Leone A, Raciti GA, Formisano P, Beguinot F, Miele C.** The Destiny of Glucose from a MicroRNA Perspective. *Front Endocrinol (Lausanne)* 9: 46, 2018. doi:10.3389/fendo.2018.00046.
49. **Moon TW.** Glucose intolerance in teleost fish: fact or fiction? *Comp Biochem Physiol B Biochem Mol Biol* 129: 243–249, 2001. doi:10.1016/S1096-4959(01)00316-5.

49a. **National Research Council.** *Nutrient Requirements of Fish and Shrimp*. Washington, DC: National Academies Press, 2011. doi:10.17226/13039.

50. **Naylor RL, Hardy RW, Bureau DP, Chiu A, Elliott M, Farrell AP, Forster I, Gatlin DM, Goldburg RJ, Hua K, Nichols PD.** Feeding aquaculture in an era of finite resources. *Proc Natl Acad Sci USA* 106: 15103–15110, 2009. doi:10.1073/pnas.0905235106.
51. **Olsvik PA, Lie KK, Jordal A-EO, Nilsen TO, Hordvik I.** Evaluation of potential reference genes in real-time RT-PCR studies of Atlantic salmon. *BMC Mol Biol* 6: 21, 2005. doi:10.1186/1471-2199-6-21.
52. **Page GI, Hayworth KM, Wade RR, Harris AM, Bureau DP.** Non-specific immunity parameters and the formation of advanced glycosylation end-products (AGE) in rainbow trout, *Oncorhynchus mykiss* (Walbaum), fed high levels of dietary carbohydrates. *Aquacult Res* 30: 287–297, 1999. doi:10.1046/j.1365-2109.1999.00330.x.
53. **Paneru BD, Al-Tobasei R, Kenney B, Leeds TD, Salem M.** RNA-Seq reveals MicroRNA expression signature and genetic polymorphism associated with growth and muscle quality traits in rainbow trout. *Sci Rep* 7: 9078, 2017. doi:10.1038/s41598-017-09515-4.
54. **Panserat S, Kaushik SJ, Medale F.** Rainbow trout as a model for nutrition and nutrient metabolism studies, in *Trout: From Physiology to Conservation* (Polakof S, Moon TW, editors). Nova Science Publishers, 2013, p. 131–151.
55. **Panserat S, Médale F, Blin C, Brèque J, Vachot C, Plagnes-Juan E, Gomes E, Krishnamoorthy R, Kaushik S.** Hepatic glucokinase is induced by dietary carbohydrates in rainbow trout, gilthead seabream, and common carp. *Am J Physiol Regul Integr Comp Physiol* 278: R1164–R1170, 2000. doi:10.1152/ajpregu.2000.278.5.R1164.
56. **Panserat S, Plagnes-Juan E, Kaushik S.** Nutritional regulation and tissue specificity of gene expression for proteins involved in hepatic glucose metabolism in rainbow trout (Oncorhynchus mykiss). *J Exp Biol* 204: 2351–2360, 2001.
57. **Panserat S, Skiba-Cassy S, Seiliez I, Lansard M, Plagnes-Juan E, Vachot C, Aguirre P, Larroquet L, Chavernac G, Medale F, Corraze G, Kaushik S, Moon TW.** Metformin improves postprandial glucose homeostasis in rainbow trout fed dietary carbohydrates: a link with the induction of hepatic lipogenic capacities? *Am J Physiol Regul Integr Comp Physiol* 297: R707–R715, 2009. doi:10.1152/ajpregu.00120.2009.
58. **Peterson SM, Thompson JA, Ufkin ML, Sathyanarayana P, Liaw L, Congdon CB.** Common features of microRNA target prediction tools. *Front Genet* 5: 23, 2014. doi:10.3389/fgene.2014.00023.
59. **Phillipps A, Tunison A, Brockway DR.** The utilisation of carbohydrate by trout. *Fisheries Research Bulletin NY* 11: 1–44, 1948.
60. **Polakof S, Mommsen TP, Soengas JL.** Glucosensing and glucose homeostasis: from fish to mammals. *Comp Biochem Physiol B Biochem Mol Biol* 160: 123–149, 2011. doi:10.1016/j.cbpb.2011.07.006.
61. **Polakof S, Panserat S, Soengas JL, Moon TW.** Glucose metabolism in fish: a review. *J Comp Physiol B* 182: 1015–1045, 2012. doi:10.1007/s00360-012-0658-7.
62. **Rehmsmeier M, Steffen P, Hochsmann M, Giegerich R.** Fast and effective prediction of microRNA/target duplexes. *RNA* 10: 1507–1517, 2004. doi:10.1261/rna.5248604.
63. **Rottiers V, Näär AM.** MicroRNAs in metabolism and metabolic disorders. *Nat Rev Mol Cell Biol* 13: 239–250, 2012. [Erratum in *Nat Rev Mol Cell Biol* 13: 2012] 10.1038/nrm3313.
64. **Rovira-Llopis S, Bañuls C, Diaz-Morales N, Hernandez-Mijares A, Rocha M, Victor VM.** Mitochondrial dynamics in type 2 diabetes: Pathophysiological implications. *Redox Biol* 11: 637–645, 2017. doi:10.1016/j.redox.2017.01.013.
65. **Saliani N, Montazersaheb S, Montasser Kouhsari S.** Micromanaging Glucose Tolerance and Diabetes. *Adv Pharm Bull* 7: 547–556, 2017. doi:10.15171/apb.2017.066.
66. **Samy JKA, Mulugeta TD, Nome T, Sandve SR, Grammes F, Kent MP, Lien S, Våge DI.** SalmoBase: an integrated molecular data resource for Salmonid species. *BMC Genomics* 18: 482, 2017. doi:10.1186/s12864-017-3877-1.
67. **Schmittgen TD, Livak KJ.** Analyzing real-time PCR data by the comparative C(T) method. *Nat Protoc* 3: 1101–1108, 2008. doi:10.1038/nprot.2008.73.
68. **Schrepfer E, Scorrano L.** Mitofusins, from Mitochondria to Metabolism. *Mol Cell* 61: 683–694, 2016. doi:10.1016/j.molcel.2016.02.022.
69. **Seiliez I, Belghit I, Gao Y, Skiba-Cassy S, Dias K, Cluzeaud M, Rémond D, Hafnaoui N, Salin B, Camougrand N, Panserat S.** Looking at the metabolic consequences of the colchicine-based in vivo autophagic flux assay. *Autophagy* 12: 343–356, 2016. doi:10.1080/15548627.2015.1117732.
70. **Skiba-Cassy S, Lansard M, Panserat S, Médale F.** Rainbow trout genetically selected for greater muscle fat content display increased activation of liver TOR signaling and lipogenic gene expression. *Am J Physiol Regul Integr Comp Physiol* 297: R1421–R1429, 2009. doi:10.1152/ajpregu.00312.2009.
71. **Subramaniam M, Weber LP, Ching JC, Enns CB, Kilgour AB, Drew MD, Loewen ME.** Species Differences in Gastrointestinal Tract Glucose Transporters between Rainbow Trout (Oncorhynchus mykiss) and Nile Tilapia (Oreochromis niloticus). *FASEB J* 30, *Suppl*: 760.20, 2016.
72. **Theurey P, Rieusset J.** Mitochondria-Associated Membranes Response to Nutrient Availability and Role in Metabolic Diseases. *Trends Endocrinol Metab* 28: 32–45, 2017. doi:10.1016/j.tem.2016.09.002.
73. **Toledo M, Batista-Gonzalez A, Merheb E, Aoun ML, Tarabra E, Feng D, Sarparanta J, Merlo P, Botrè F, Schwartz GJ, Pessin JE, Singh R.** Autophagy Regulates the Liver Clock and Glucose Metabolism by Degrading CRY1. *Cell Metab* 28: 268–281.e4, 2018. doi:10.1016/j.cmet.2018.05.023.
74. **Tsai W-C, Hsu S-D, Hsu C-S, Lai T-C, Chen S-J, Shen R, Huang Y, Chen H-C, Lee C-H, Tsai T-F, Hsu M-T, Wu J-C, Huang H-D, Shiao M-S, Hsiao M, Tsou A-P.** MicroRNA-122 plays a critical role in liver homeostasis and hepatocarcinogenesis. *J Clin Invest* 122: 2884–2897, 2012. doi:10.1172/JCI63455.
75. **Wilczynska A, Bushell M.** The complexity of miRNA-mediated repression. *Cell Death Differ* 22: 22–33, 2015. doi:10.1038/cdd.2014.112.
76. **Wilding JPH.** The role of the kidneys in glucose homeostasis in type 2 diabetes: clinical implications and therapeutic significance through sodium glucose co-transporter 2 inhibitors. *Metabolism* 63: 1228–1237, 2014. doi:10.1016/j.metabol.2014.06.018.
77. **Witkos TM, Koscianska E, Krzyzosiak WJ.** Practical Aspects of microRNA Target Prediction. *Curr Mol Med* 11: 93–109, 2011. doi:10.2174/156652411794859250.
78. **Yan L-J.** Pathogenesis of chronic hyperglycemia: from reductive stress to oxidative stress. *J Diabetes Res* 2014: 137919, 2014. doi:10.1155/2014/137919.
79. **Ye P, Liu Y, Chen C, Tang F, Wu Q, Wang X, Liu C-G, Liu X, Liu R, Liu Y, Zheng P.** An mTORC1-Mdm2-Drosha axis for miRNA biogenesis in response to glucose- and amino acid-deprivation. *Mol Cell* 57: 708–720, 2015. doi:10.1016/j.molcel.2014.12.034.
80. **Zhang H-M, Kuang S, Xiong X, Gao T, Liu C, Guo A-Y.** Transcription factor and microRNA co-regulatory loops: important regulatory motifs in biological processes and diseases. *Brief Bioinform* 16: 45–58, 2015. doi:10.1093/bib/bbt085.
81. **Zhang W, Wang P, Chen S, Zhang Z, Liang T, Liu C.** Rhythmic expression of miR-27b-3p targets the clock gene *Bmal1* at the posttranscriptional level in the mouse liver. *FASEB J* 30: 2151–2160, 2016. doi:10.1096/fj.201500120.
82. **Zhao E, Keller MP, Rabaglia ME, Oler AT, Stapleton DS, Schueler KL, Neto EC, Moon JY, Wang P, Wang I-M, Lum PY, Ivanovska I, Cleary M, Greenawalt D, Tsang J, Choi YJ, Kleinhanz R, Shang J, Zhou Y-P, Howard AD, Zhang BB, Kendziorski C, Thornberry NA, Yandell BS, Schadt EE, Attie AD.** Obesity and genetics regulate microRNAs in islets, liver, and adipose of diabetic mice. *Mamm Genome* 20: 476–485, 2009. doi:10.1007/s00335-009-9217-2.

Chapter 4: Social status differentially regulates miRNAs and their predicted gluconeogenic gene paralogue targets

This chapter has been published as Kostyniuk DJ, Zhang D, Martyniuk CJ, Gilmour KM, Mennigen JA. 2019. Social status regulates the hepatic miRNAome in rainbow trout: Implications for posttranscriptional regulation of metabolic pathways. PLoS One. 14(6):e0217978.

***Statement of contribution**: The experimental samples were generated in a collaborative study with Dr. Gilmour at uOttawa. I conducted and analyzed all real-time RT-PCR and protein assays, as well as in silico target prediction analysis of small RNA next generation sequence data.*

PLOS ONE

RESEARCH ARTICLE

Social status regulates the hepatic miRNAome in rainbow trout: Implications for posttranscriptional regulation of metabolic pathways

Daniel J. Kostyniuk[1], Dapeng Zhang[2], Christopher J. Martyniuk[3], Kathleen M. Gilmour[1], Jan A. Mennigen[1]*

1 Department of Biology, University of Ottawa, Ottawa, Ontario, Canada, **2** Department of Biology, Saint Louis University, Saint Louis, Missouri, United States of America, **3** Department of Physiological Sciences and Center for Environmental and Human Toxicology, UF Genetics Institute, College of Veterinary Medicine, University of Florida, Gainesville, FL, United States of America

* jan.mennigen@uottawa.ca

Citation: Kostyniuk DJ, Zhang D, Martyniuk CJ, Gilmour KM, Mennigen JA (2019) Social status regulates the hepatic miRNAome in rainbow trout: Implications for posttranscriptional regulation of metabolic pathways. PLoS ONE 14(6): e0217978. https://doi.org/10.1371/journal.pone.0217978

Editor: José L. Soengas, Universidade de Vigo, SPAIN

Received: September 18, 2018

Accepted: May 21, 2019

Published: June 13, 2019

Data Availability Statement: Raw NGS sequence data were deposited in the NCBI Gene expression Omnibus (GEO) under accession number GSE112815 with specific files (n = 3) for subordinate (GSM3084233-GSM3084235) and dominant (GSM3084236-GSM3084238) rainbow trout liver samples.

Funding: Funding for this project was provided through the Canadian Network for Research and Innovation in Machining Technology, Natural Sciences and Engineering Research Council of

Abstract

Juvenile rainbow trout develop social hierarchies when held in dyads, and the development of socially subordinate (SS) and socially dominant (SD) phenotypes in this context has been linked to specific changes in the hepatic energy metabolism of all major macronutrients. Following our recently reported finding that transcript abundance of *drosha*, a key component of the microRNA (miRNA) biogenesis pathway, is increased in paired juvenile rainbow trout irrespective of social status compared to socially isolated (SI) controls, we here determined global changes of the hepatic miRNA pathway genes in detail at the transcript and protein level. Both SD and SS rainbow trout exhibited increased Ago2 protein abundance compared to SI rainbow trout, suggesting that hepatic miRNA function is increased in rainbow trout maintained in dyads. Given the well-described differences in hepatic intermediary metabolism between SD and SS rainbow trout, and the important role of miRNAs in the posttranscriptional regulation of metabolic pathways, we also identified changes in hepatic miRNA abundance between SS and SD rainbow trout using small RNA next generation sequencing. We identified a total of 24 differentially regulated miRNAs, with 15 miRNAs that exhibited increased expression, and 9 miRNAs that exhibited decreased expression in the liver of SS trout compared to SD trout. To identify potential miRNA-dependent posttranscriptional regulatory pathways important for social status-dependent regulation of hepatic metabolism in rainbow trout, we used an *in silico* miRNA target prediction and pathway enrichment approach. We identified enrichment for pathways related to metabolism of carbohydrates, lipids and proteins in addition to organelle-specific processes involved in energy metabolism, especially mitochondrial fusion and fission. Select predicted miRNA-mRNA target pairs within these categories were quantitatively analyzed by *real-time* RT-PCR to validate candidates for future studies that will probe the functional metabolic roles of specific hepatic miRNAs in the development of SD and SS metabolic phenotypes.

Canada (http://www.nserc-crsng.gc.ca) under the Discovery Grant program awarded to JAM under grant number NSERC-DG 147476, and an NSERC-DG grant to KMG. The Canadian Foundation of Innovation (https://www.innovation.ca) contributed to research infrastructure used in this research under (#35859) grants to JAM. The funders had no role in study design, data collection and analysis, decision to publish, or preparation of the manuscript.

Competing interests: The authors have declared that no competing interests exist.

1. Introduction

Juvenile salmonid fish establish linear dominance hierarchies as a result of competition for shelter and feeding territories [1–3]. Socially dominant (SD) fish within these hierarchies monopolize preferred territories, displaying high levels of aggression towards their socially subordinate (SS) counterparts [1,3]. These differences in behaviour are accompanied by a range of physiological responses, including changes in energy metabolism [4–7]. Previous studies revealed an increased potential for hepatic glucose liberation in SS compared to SD fish. SS trout displayed increased mobilization of stored glycogen compared to SD trout, as evidenced by lower hepatic glycogen concentrations and higher glycogen phosphorylase activity [6]. Furthermore, SS trout displayed enhanced gluconeogenic and decreased glycolytic potential [4], supported by increased hepatic phosphoenolpyruvate carboxykinase (Pck) activity and decreased pyruvate kinase (Pk) activity [4]. These changes are in part dependent on the glucocorticoid stress hormone cortisol [4–10], with chronically elevated cortisol levels in SS trout leading to increased circulating glucose concentrations [10]. However, although circulating glucose represents an important fuel source for specific rainbow trout tissues, such as the brain [11], glucose utilization for global energy metabolism in most other tissues is limited in rainbow trout [12]. In contrast, lipid metabolism is a key player in global energy metabolism in trout [7], and SS trout exhibit increased reliance on free fatty acids, as indicated by elevated circulating free fatty acid concentrations at the organismal level, and by increased expression of the mitochondrial free fatty acid transporter carnitine palmitoyltransferase (*cpt1a*) which is rate limiting to mitochondrial β-oxidation [7]. Conversely, SD trout reveal increased capacity for hepatic *de novo* lipogenesis, as indicated by increased abundance of the transcription factor sterol regulatory element binding protein 1c (*srebp1c*) and the enzyme fatty acid synthase (*fasn)* mRNA, which coincide with increased circulating levels of triglycerides [7]. Finally, recent circumstantial evidence suggests that hepatic protein metabolism may be affected by social status, because increased activated ribosomal protein S6, which is associated with increased protein translation, was observed in the liver of SS fish [7].

Over the last decade, posttranscriptional regulation has emerged as an important mechanism for control of hepatic energy metabolism largely in mammalian models [13], but also in teleost fishes, especially rainbow trout, where hepatic miRNAs have been shown to regulate carbohydrate and lipid metabolism [14,15]. In a recent study, we determined that the transcript abundance of *drosha*, a key component in canonical miRNA biogenesis [16], is upregulated in liver of both SD and SS trout relative to socially isolated (SI) fish, which were handled similarly but housed without a conspecific [7]. Here we investigated the expression of several key canonical miRNA biogenesis pathway components, including *ago2* and *xpo5* paralogues, in more detail. Following additional evidence that key components of the canonical miRNA biogenesis pathway were increased in both SD and SS rainbow trout compared to SI rainbow trout strongly suggesting a social status dependent function of hepatic miRNAs, we measured differential hepatic miRNA expression between SS and SD rainbow trout using a next generation sequencing (NGS) approach. By means of an *in silico* pipeline, we identified several metabolic pathways that potentially are post-transcriptionally regulated by the differentially expressed miRNAs, and measured expression of specific miRNAs-mRNA pairs to prioritize targets for future functional analysis.

2. Materials and methods

2.1 Experimental animals

All experimental animals used in the current study have been previously described [7]. Care was taken to use the same initial weight between SI fish (100.14 g ± 5.10 g) and paired fish

groups (100.92 g± 3.46 g). Briefly, juvenile rainbow trout, *Oncorhynchus mykiss*, were purchased from Linwood Acres Trout Farm (Campbellcroft, ON, Canada) and maintained in 1275 L fibreglass tanks at the University of Ottawa Aquatic Facility. All tanks were connected to flowing, aerated and dechloraminated 13˚C city of Ottawa tap water. Trout were held under a 12L:12D photoperiod and acclimated to these holding conditions for a minimum of 2 weeks prior to experimentation. All fish were fed a ration equivalent to 0.5% body mass daily by distributing commercial trout pellets (Zeigler Finfish Silver, Gardners, PA, USA) in the tank. The holding of large groups (>20 trout), as well as animal care procedures (e.g. use of scatter feeding, homogenous tanks with a mild current) were employed to minimize hierarchy formation prior to experimentation. To establish social status, fish were lightly anaesthetized in a solution of benzocaine (0.05 g L^{-1} ethyl-*p*-aminobenzoate; Sigma-Aldrich, Oakville, ON, Canada) and mass and fork length and fin damage were quantified as previously described [4–7,10]. In cases where morphological differences did not allow for identification of individual fish, a pectoral fin clip was used for identification. Fish dyads were then established taking care not to exceed 5% of fork length differences between fish in a pair. After the initial assessment, pairs were placed in a 40 L flow-through Plexiglas observation tank, in which individuals were separated by an opaque, perforated divider. Tanks were maintained with flowing aerated and dechloraminated 13˚C city of Ottawa tap water. The next morning, dividers were removed and fish were allowed to interact for a period of 4 d. At the end of the first day, a shelter in the form of a T-shaped PVC tube (11 x 13 cm long, 6 cm diameter) was added to the tanks. Behavioural observations were carried out twice per day between 9:00–11:00 h and 15:00–17:00 h, respectively. Each individual observation period within these time periods consisted of 5 min.

The group of SI rainbow trout was subjected to the same handling and treatment procedures as paired fish, but were housed individually in the Plexiglas observation tanks. All fish were offered 0.5% fish mass per tank daily following the final observation period (except on the initial day of interaction), and the mass of food consumed as well as the fish that consumed the food were noted. A summary of the experimental design is shown in **Fig 1**. Social status was assessed as previously described (4–7,10) by assigning points to each fish for position within the tank, food acquisition, aggressive acts, and fin damage acquired during the 4 d interaction period. The applied scoring system awards more points for more SD behaviours, specifically patrolling the water column in the tank, acts of aggressive behaviour, being the first to feed and absence of fin damage. A principle components analysis (SigmaPlot v13.0; Systat software, San Jose, CA, USA) was used to calculate behaviour scores for each fish based on the mean scores across observation periods of each parameter. Within a pair, the fish with the higher score was assigned SD status, while the fish with the lower score was SS.

Specific behaviour scores as well as additional endocrine parameters associated with social status (plasma cortisol concentrations) allowed to clearly distinguish SD and SS fish in dyads, and detailed measurements of these parameters can be consulted in a previous publication [7]. For the purpose of the current study, it is important to note that two factors with particular importance to the social status-dependent metabolic phenotype exhibited clear differences. Firstly, while all fish nominally received 0.5% food rations, SD fish generally monopolized all food offered in a dyad, resulting in 1% food ratio for the SD individual, and *de facto* fasting for the SS individual over the 4 day period. Secondly, SS fish displayed a chronic activation of the endocrine stress axis, as evidenced by significantly increased cortisol concentrations compared to SD and SI fish [7].

Following the 4 d observation period, all fish in a pair were rapidly euthanized via terminal anesthesia (0.5 g L^{-1} ethyl-*p*-aminobenzoate; Sigma-Aldrich). Final mass and fork length were measured, fin damage scored, and blood samples collected via caudal venipuncture into heparin-coated syringes (2500 IU mL^{-1} heparin sodium salt; Sigma-Aldrich). All blood samples

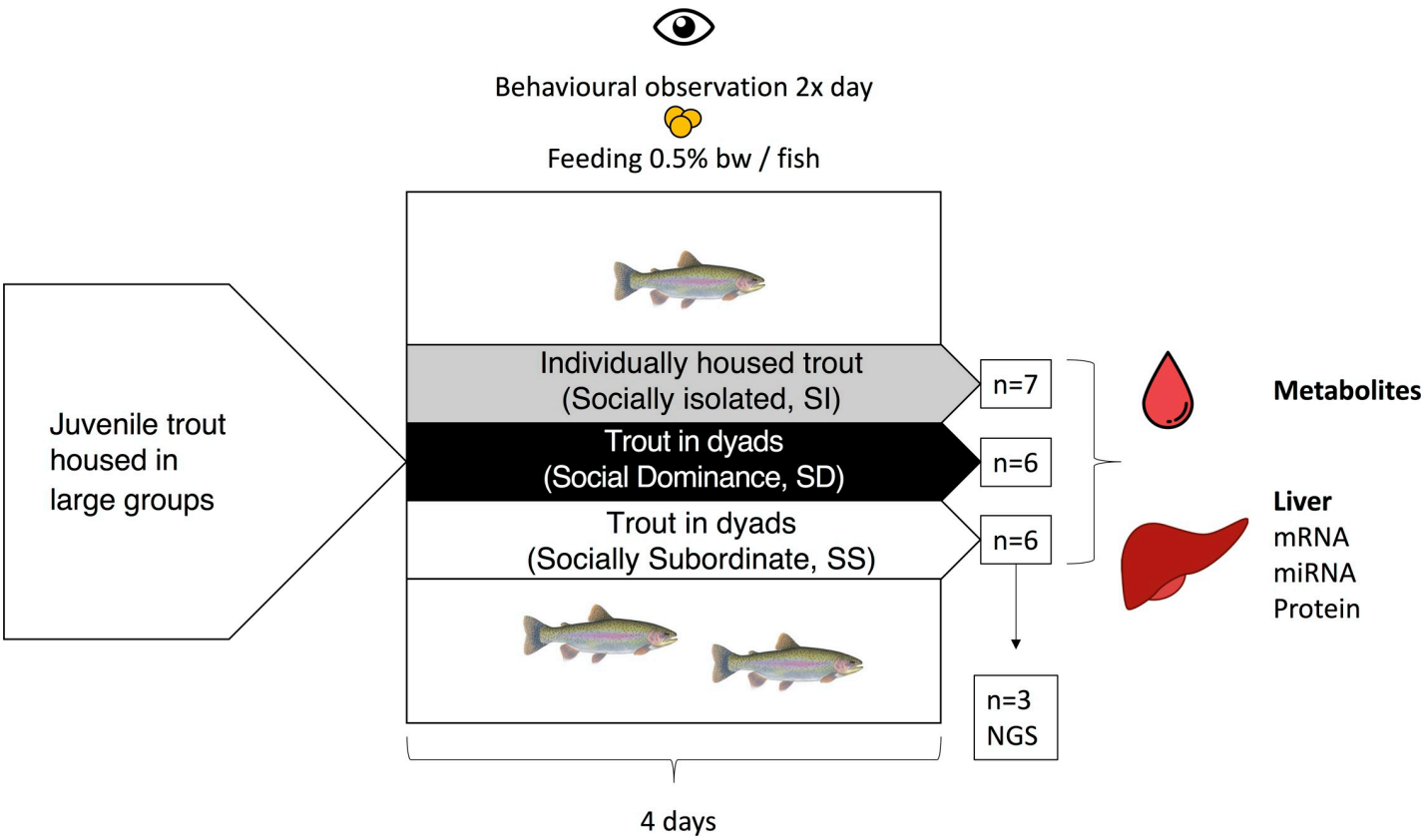

Fig 1. Schematic representation of the experimental design used to investigate the role of hepatic miRNAs in social status-dependent intermediary metabolism in juvenile rainbow trout, *Oncorhynchus mykiss*. *bw*, body weight; *NGS*, next generation sequencing.

https://doi.org/10.1371/journal.pone.0217978.g001

were centrifuged (10,000 *g* for 2 min) and plasma samples were flash frozen in liquid nitrogen before being stored at -80˚C. Liver tissue was collected, freeze clamped, and stored at -80˚C for subsequent analysis. All experimental protocols complied with the guidelines of the Canadian Council on Animal Care (CCAC) for the use of animals in research and teaching and were approved by the University of Ottawa's Animal Care Committee under protocol number BL-2118.

2.2. Real-time RT-PCR assays for mRNA and miRNA

2.2.1. Relative abundance mRNA quantification. Following the manufacturer's protocol, total RNA was extracted from 20 to 100 mg of liver using TRIzol reagent (Invitrogen, Burlington, ON, Canada). To homogenize the tissues, the solution of TRIzol and tissue was forced through 18-G and 23-G needles using a syringe until the solution passed easily through the needle. Extracted RNA was quantified using a NanoDrop 2000c UV-Vis Spectrophotometer (Thermo-Fisher Scientific, Mississauga, ON, Canada) and RNA integrity was assessed using a Bioanalyzer (model 2100, Agilent Technologies, Mississauga, ON, Canada). Next, cDNA was generated using a QuantiTech Reverse Transcription Kit (Qiagen, Toronto, ON, Canada) following the manufacturer's protocol which includes a DNA wipeout step before reverse transcription occurs. A noRT negative control sample containing water in place of the RT enzyme was also generated. Two-step relative abundance real-time RT-PCR assays were performed on a BioRad CFX96 instrument (Bio-Rad, Mississauga, ON, Canada) to quantify fold-changes in

relative hepatic mRNA abundances of key transcripts involved in canonical miRNA biogenesis (*xpo5a*, *ago2a*, *ago2b*) and metabolic target genes (*pck1*, *pck2*, *g6pca*, *g6pcb1a*, *g6pcb1b*, *g6pcb2a*, *g6pcb2b*,*pygl*, *pygb*, *hsl*, *mfn1*, *mfn2*, *fis1*) as well as two reference genes (*ef1a* and *18s*). A standard curve consisting of serial dilutions of pooled cDNA, as well as a negative no-RT control consisting of cDNA generated in a reaction that did not include reverse transcriptase, and individual samples were run in duplicate for each experiment. The total volume was 20 μl, which consisted of 4 μl of diluted cDNA template, 0.5 μl of 10 nM specific forward and 0.5 μl of 10 nM specific reverse primer (Table 1), 10 μl of SsoAdvanced Universal Inhibitor-Tolerant SYBR Green Supermix (Bio-Rad), and 5 μl of H_2O for each individual reaction. Real-time RT-PCR cycling parameters were a 5 min activation step at 95˚C, followed by 40 cycles consisting of a 20 s denaturation step at 95˚C and a 30 s annealing and extension step at a primer-specific temperature (Table 1). After each run, melting curves were produced and monitored for single peaks to confirm the specificity of the reaction and the absence of primer dimers. In cases where primers were newly designed (Table 1), purified and pooled PCR products were sent for sequencing (Ottawa Hospital Research Institute, Ottawa, ON, Canada), and a BLAST search (National Center for Biotechnology Information, Bethesda, MD, USA) was used to confirm amplicon specificity. All amplification efficiencies calculated from serially diluted 7-point standard curves were between 90–110%, with R^2 values > 0.98. Relative transcript abundance derived from standard curves was normalized using the NORMA-Gene approach as described by Heckman et al. [17]. Afterwards, mRNA fold changes were calculated relative to the SI group and data were analyzed and plotted using Prism Version 7 (GraphPad Software, San Diego, CA, USA) and transformed to fit a normal distribution. Grubb's outlier test was used to identify and remove single outliers in a treatment group. Data were subsequently analyzed using one-way analysis of variance (ANOVA) followed by Tukey's post-hoc test.

2.2.2. Relative abundance miRNA quantification. miRNA cDNA was synthesized using TaqMan MicroRNA Reverse Transcription Kit (Life Technologies Inc., Burlington, ON, Canada) with 10 ng of total RNA per 15 μl RT reaction containing 0.15 μl 100mM dNTPs (with dTTP), 1.00 μl MultiScribe Reverse Transcriptase 50 U/μl, 1.50ul 10X Reverse Transcription Buffer, 0.19 μl RNAse Inhibitor 20U/μl, 4.16ul nuclease free water, 5ul total RNA and 3ul miRNA specific 5X RT primer following the manufacturer's protocol. Two step real-time RT-PCR was used to validate the abundance of *fru-miRNA-21-5p*, *dre-miRNA-722*, *dre-miRNA-26a-5p*, *dre-let-7a*, *fru-miRNA-152* using the CFX96-Real-Time System- C1000 Thermal Cycler machine (BioRad, Mississauga, ON, Canada). Real-time RT-PCR reactions were prepared in a total volume of 20 μL per reaction, containing 1.00 μL Taqman Small RNA Assay 20X, 1.33 μL Product from RT reaction, 10.00 μL Taqman Universal PCR Master Mix (2X) with UNG and 7.67 μL nuclease free water. A no reverse transcriptase (noRT), where the RT was replaced with nuclease free water, and a no template (noTemp), where product from RT reaction was replaced with nuclease free water, were included during cDNA synthesis as controls for DNA contamination. Following an activation step at 50˚C (2 min) to activate UNG and another activation step at 95˚C (10 min) to activate the polymerase in the qPCR mix, two steps were repeated for 40 cycles including the denaturation at 95˚C (15 s) and a combined annealing and extending step at 60˚C (60 s). Assays were subsequently normalized using the NORMA-Gene approach as described by Heckman et al. [17] miRNA fold changes were calculated relative to the fasted group. Data were analyzed using Prism Version 7 (GraphPad Software, San Diego, CA, USA), and transformed to fit normal distribution when necessary. In normally distributed data, Grubb's outlier test was used to identify and remove possible single outliers in a treatment group. Data were subsequently analyzed using a one-tailed Welch's t-test. Significance was determined at a $p<0.05$ level.

Table 1. Real-time RT-PCR primer sequences and reaction parameters.

Gene target	Primer pair (5' to 3')	Annealing temperature (˚C)	Efficiency (%)	R^2	Reference
Canonical microRNA biogenesis pathway					
xpo5a GSONMT00065065001	F: AGTCAACTGGGTGGGGATTC R: TCCCACCTCAGACATGCTCA	59	104.1	0.98	
xpo5b GSONMT00007401001	F ACTCTCGAACACGGCTGATG R: CACACATATCAGCCACCGGT	59	103.6	0.98	
ago2a GSONMT00060791001	F: GTGGTGGGGTGGACTCATTT R: AAACCTTCAATCGGGCCCTT	59	107.5	0.99	
ago2b *GSONMT00025973001*	F : TGTCGCACGGTGTTAACATG R: AGCAATGCCGAGAAGAGCTA	58	99.3	0.98	
microRNAs					
fru-miR-21a-5p	F: TAGCTTATCAGACTGGTGTTGGC R: Taqman Universal Reverse Primer	60	95.7	0.98	
fru-miR-722	F: TTTTTTGCAGAAACGTTTCAGATT R: Taqman Universal Reverse Primer	60	98.1	0.99	
ssa-miR-26a-5p	F : TTCAAGTAATCCAGGATAGGCT R : Taqman Universal Reverse Primer	60	103.2	0.98	
fru-miR-let-7a	F: TGAGGTAGTAGGTTGTATAGTT R: Taqman Universal Reverse Primer	60	99.3	0.98	
fru-miR-152	F: TCAGTGCATAACAGAACTTTGT R: Taqman Universal Reverse Primer	60	107.9	0.99	
Hepatic glucose metabolism					
pck1 *GSONMG00082468001*	F: ACAGGGTGAGGCAGATGTAGG R: CTAGTCTGTGGAGGTCTAAGGGC	55	104.1	0.99	
pck2 *GSONMG00059643001*	F: ACAATGAGATGATGTGACTGCA R: TGCTCCATCACCTACAACCT	56	105.1	0.99	
g6pca *GSONMG00076843001*	F: GATGGCTTGACGTTCTCCT R: AGATCCAGGAGAGTCCTCC	55	91.0	0.98	[33]
g6pcb1a *GSONMG00076841001*	F: GCAAGGTCCAAAGATCAGGC R: GCCAATGTGAGATGTGATGGG	59	108.1	0.99	[33]
g6pcb1b *GSONMG00066036001*	F: GCTACAGTGCTCTCCTTCTG R: TCACCCCATAGCCCTGAAA	55	95.0	0.98	[33]
g6pcb2a *GSONMG00013076001*	F: ATCGGACAATACACACAGAACT R: CAACTGATCTATAGCTGCTGCCT	55	93.4	0.99	[33]
g6pcb2b *GSONMG00014864001*	F: CCTCTGCTCTTCTGACGTAG R: TGTCCATGGCTGCTCTCTAG	56	103.7	0.98	[33]
pygl *GSONMT00046884001*	F : TCAAGAACATCGCTGCGTCT R : TAACTTCACCCTGGTCACGC	59	100.3	0.99	
pygb *GSONMT00041162001*	F : GTGATCCCTGCAGCTGACTT R : TCCTCTACCCTCATGCCGAA	55	100.4	0.98	
Hepatic lipid metabolism					
hsl *GSONMT00023441001*	F : TGCCTTCCTGTACTCGCAAG R : GCAAGAAAGGCAAGGGTGTT	55	101.1	0.99	
Mitochondrial dynamics					
mfn1 *GSONMT00027395001*	F: AGGGAGCTGGAGGGAGAAAT R: CCAAGACAGGCTCCAGTGAA	55	106.4	0.99	
mfn2 *GSONMT00004526001*	F :ACTGCTCCGGAATAAGGCTG R: GTGGTCTTTTCGCGGTCAAC	55	106.5	0.99	
fis1 *GSONMT00039888001*	F : GGTTTGGTTGGCATGGCAAT R: TTCTCATCTTGGGGAACGGC	55	95.1	0.99	
Reference genes					

(*Continued*)

Table 1. (Continued)

Gene target	Primer pair (5' to 3')	Annealing temperature (˚C)	Efficiency (%)	R^2	Reference
ef1a	F: CATTGACAAGAGAACCATTGA R: CCTTCAGCTTGTCCAGCAC	56	91.9	0.99	[7]
snoRNA-U23	F :GCCCATGTCTGCTGTGAAACAAT R : Taqman Universal Primer	61	105.6	0.98	[7]

https://doi.org/10.1371/journal.pone.0217978.t001

2.3. Protein extraction and Ago2 protein quantification

Fractions (~100mg) of frozen livers (n = 6 per treatment group) were weighted into 1 mL of lysis buffer 150mM NaCl, 10 mM Tris HCl, 1 mM EGTA, 1mM EDTA (pH 7.4), 100 mM sodium fluoride, 4mM sodium pyrophosphate, 2mM sodium orthovanadate, 1% Triton X-100, 0.5% NP-40-IGEPAL (all Sigma-Aldrich), and a protease inhibitor cocktail (Roche, Basel, Switzerland) and homogenized using a sonicator model 100 (Thermo-Fisher Scientific, Mississauga, ON, Canada). Homogenates were centrifuged at 15000 g for 30 min at 4˚C, and the recovered supernatant stored at -80˚C. Protein concentrations were determined using the Bio-Rad protein assay kit (Bio-Rad) with BSA (bovine serum albumin) as the standard. Lysates (20 μg of the total protein) were subjected to SDS-PAGE and wet-transfer Blotting. Membranes were incubated with a rabbit polyclonal antibody raised against a human AGO2 epitope (Proteintech, Chicago, IL, USA) at 4˚C overnight. The next day, following blocking and washing steps, membranes were incubated with an IRDye infrared secondary anti-rabbit antibody (LI-COR Biosciences, Lincoln, NE, USA). The bands were visualized by infrared fluorescence using the Odyssey Imaging System (LI-COR Biosciences) and quantified by Odyssey infrared Imaging System software (version 3.0, LI-COR biosciences) using total protein stain as normalization method. A single band of expected size was detected and data were analyzed using Prism Version 7 following transformation to fit a normal distribution. Grubb's outlier test was used to identify and remove possible single outliers in a treatment group. Data were subsequently analyzed using a one-way ANOVA followed by Tukey's post-hoc test. Significance was determined at a $p<0.05$ level.

2.4. Small RNA next generation sequencing and differential expression analysis

The quality of Trizol-extracted total RNA was confirmed by RNA Integrity Numbers between 8.3 and 9.6, using an Agilent Technologies 2100 Bioanalyzer. Small RNA sequencing was performed by LC Sciences (Houston, TX, USA) using three randomly selected samples from each treatment group. Nucleotide fractions (15–50 nt) of small RNAs were isolated from the total RNA using polyacrylamide gel electrophoresis and were ligated to a 30 nt adapter followed by a 50 nt adapter (Illumina, San Diego, CA, USA). The small RNA ligated to the adaptors was reverse transcribed to cDNA, PCR amplified, and gel purified. The gel-extracted cDNA was used for library preparation, followed by cluster generation on Illumina's Cluster Station before sequencing using Illumina GAIIx. Raw sequence data were obtained from image data using Illumina's Sequencing Control Studio software version 2.8 following real-time sequencing image analysis and base-calling by Illumina's Real-Time Analysis version 1.8.70, and were deposited in the NCBI Gene expression Omnibus (GEO) under accession number GSE112815 with specific files (n = 3) for SS (GSM3084233-GSM3084235) and SD (GSM3084236-GSM3084238) rainbow trout liver samples.

Briefly, sequences were initially filtered with the proprietary LC Science ACGT10-miR v4.2 pipeline to remove low quality sequences, low complexity sequences, and sequences corresponding to common RNA families (mRNA, RFam, Repbase, piRNA), as described by Ma and colleagues [18]. Retained high quality sequences were then submitted to a bowtie search against all fish miRNA gene sequences deposited in miRbase v21.0 (1 mismatch allowed in the first 16 nt) and compared to published miRNAs from rainbow trout [19–21]. In cases where unique sequences mapped to the miRbase-deposited fish miRNA genes, the obtained miRbase hits were subsequently mapped to the rainbow trout genome to determine genomic locations (**S1 Table**). Any alignment that had already previously been characterized as a genomic location for this specific microRNA in the rainbow trout genome (**Table 2**) was identified as known rainbow trout miRNA (gp1a). All miRNAs that were successfully aligned to miRbase deposited fish species miRNA genes, and had not been described in the rainbow trout miRNA repertoire, but mapped to the rainbow trout genome, were retained as trout microRNAs (gp1b). The remaining miRbase hits from both gp1a and gp1b that in addition to known miRNA loci also mapped to other rainbow trout genome loci were designated as gp1c.

High quality sequences that could be matched to fish species miRNA genes in miRbase, which in turn could not be mapped to the rainbow trout genome, were further analyzed as follows: The high quality short sequence was directly mapped onto the rainbow trout genome, and the locus further analyzed for its possibility to generate hairpin transcripts. This was achieved by retrieving 80 nt flanking sequences of mapped high quality sequences. Retrieved sequence were then analyzed for their propensity to form hairpin structures using RNA-fold software (http://rna.tbi.univie.ac.at/cgi-bin/RNAfold.cgi) with the following criteria: (1) $\leq$ 12 nt in one bulge in stem; (2) $\geq$ 16 bp in the stem region of the predicted hairpin; (3) $\leq$ -15 kCal/mol cutoff of ΔG; (4) $\geq$ 50 hairpin length which contains up- and down stems and hairpin loop; (5) a $\leq$ 200 nt hairpin loop length; (6) $\leq$4 nt in one bulge in the mature miRNA region; (7) $\leq$2 errors in one bulge in mature region; (8) $\leq$2 biased bulges in mature region; (9) $\leq$4 errors in the mature miRNA region;(10) $\geq$ 12 bp in the mature region of the predicted hairpin; (11) >80% of mature miRNA is in located in the stem. Sequences in located in loci predicted to form hairpins were grouped as gp2a, and sequences mapped to loci not predicted to form hairpins were designated as gp2b. High quality sequences mapped to fish miRNA genes deposited in miRbase, which did neither map to the rainbow trout genome as fish miRbase gene hit, nor as mature sequence, but had been identified as mature miRNA in rainbow trout were designated gp3a. Conversely, high quality sequences mapped to fish miRNA genes deposited in miRbase, which did neither map to the rainbow trout genome as fish miRbase gene hit, nor as mature sequence, and had not been identified as mature miRNA in rainbow trout were designated gp3b. Finally, remaining sequences that could not be matched to miRbase fish species, but could be mapped to the rainbow trout genome, were again tested for the

Table 2. Reference databases used for rainbow trout miRNA annotation.

Reference databases	WEBlink and Information	Version or Built Date
miRNA (miRs) database	ftp://mirbase.org/pub/mirbase/CURRENT/; Specific species: dre; Selected species: fru, ola, tni, ccr, hhi, ipu, pol, ssa	v21
Pre-miRNA (mirs) database	ftp://miRbase.org/pub/mirbase/CURRENT/; Specific species: dre; Selected species fru, ola, tni, ccr, hhi, ipu, pol, ssa	v21
Genome database	http://www.genoscope.cns.fr/trout/data/Oncorhynchus_mykiss_chr.fa.gz	04/28/2014
mRNA database	http://www.genoscope.cns.fr/trout/data/Oncorhynchus_mykiss_mRNA.fa.gz	04/28/2014

https://doi.org/10.1371/journal.pone.0217978.t002

potential to form hairpin structures with flanking sequences. Sequences predicted to be able to form hairpins were designated as gp4a, sequences predicted to be unable to form hairpins were designated as gp4b. Details of the miRNAs and their respective groups are presented in **S2 Table**. Differentially expressed miRNAs were identified using the statistical software R (Version 3.2.2) package DESeq2 for t-test comparisons of SD versus SS groups.

2.5. In silico miRNA-target analysis

To predict rainbow trout specific mRNA targets of differentially regulated miRNAs, we utilized the miRanda package initially developed in the Enright lab [22]. The miRanda algorithm places emphasis on seed match and free energy of the duplex structure, two of the most relevant aspects in miRNA-target interaction [23–24]. Among the available miRNA target prediction algorithms [25–26], we chose the miRanda algorithm based on its increased sensitivity compared to other predictive algorithms [27], as well as its previous application across several rainbow trout transcriptome level miRNA target prediction studies [28,29], in an effort to facilitate comparison among studies. Because increased sensitivity occurs at the cost of an increased rate of false positive predictions, we used a stringent cut-off with a miRanda pairing score $S > 140$, and a free-energy score ΔG cut-off < -20, where S is the sum of single residue-pair match scores over the alignment trace, and ΔG is the free energy of duplex formation calculated by the Vienna package [30]. Annotated 3'UTRs were taken from the microTrout database [21].

2.6. Gene ontology enrichment, pathway, and sub-network enrichment analysis

Gene ontology enrichment of transcripts predicted to be targeted by differentially regulated miRNAs is a widely used approach to infer biological responses at the genome regulation level in rainbow trout and mammalian models [28,29,31]. We performed gene ontology enrichment in JMP Genomics V8.1. Parametric analysis of gene expression (PAGE) was conducted to determine which gene ontologies were significantly enriched in the dataset based upon predicted targets of miRNAs. The rainbow trout genome was used as a background list for comparison. Genes were considered to be miRNA targets if transcript-miRNA was predicted by the miRanda algorithm with cut-off values of $S > 140$ and $\Delta G < -20$. The p-value for each gene ontology was corrected using the false discovery rate. To build pathways for gene targets, we imported the short list of genes within a group of gene ontology categories (i.e. those related to "glucose metabolism") into Pathway Studio 11.4 (Elsevier, Amsterdam, Netherlands). The software uses known relationships (i.e. based on expression, binding, common pathways) between genes to create networks focused around a cell process. The miRNA targets were imported into the program using "Name + Alias" and rainbow trout genes were mapped to their mammalian homologues. Lastly, the miRNA targets were subjected to a subnetwork enrichment analysis in Pathway Studio for "Cell Process". This approach was used to achieve a general overview of what cell processes were those most relevant to hepatic regulation of glucose and intermediary metabolism based on the miRNA targets. These biological functions are those most likely controlled post-transcriptionally by the regulated miRNA network.

2.7. Correlative analysis of miRNA-mRNA targets

Specific mRNA targets belonging to enriched pathways that were predicted to be regulated by differentially expressed miRNAs were quantified to elucidate a potential involvement in the physiological consequences of social interactions in the liver of rainbow trout, and to determine correlations between expression of miRNA and targeted mRNA transcripts. Although

this approach does not indicate a functional relationship, such correlations act to prioritize specific miRNA-mRNA target pairs for future functional studies. The strength of correlations between differentially expressed miRNAs and the expression of their predicted specific targets was assessed using the Pearson correlation coefficient computed in Prism Version 7 (GraphPad Software, San Diego, CA, USA).

2.8. Glucose assay

Plasma glucose concentration in SD and SS fish were measured indirectly using a Spectra Max Plus384 Absorbance Microplate reader (Molecular Devices, Sunnyvale, CA, USA). Briefly, G6P-DH, NAD+ and ATP (all Sigma-Aldrich) were added to each undiluted plasma sample and a background measurement was taken. Hexokinase (Sigma-Aldrich) is then added, and the solution was incubated at room temperature for 30 min before measurement. Collectively, D-Glucose is converted to G-6-P by hexokinase and then to 6-phosphogluconate by G6P-DH and the resulting NADH allows for the indirect colorimetric measurement of glucose concentration. All spectrophotometric measurements were taken at 340nm. Data were normally distributed, but not homoscedastic, and were analyzed by Welch's t-test using Prism Version 7 (GraphPad Software, San Diego, CA, USA).

3. Results

3.1. Induction of hepatic canonical miRNA biogenesis pathway components in a trout social hierarchy

Responsiveness of the hepatic canonical miRNA biogenesis pathway to social interaction was probed at the mRNA abundance and protein levels in SI, SD, and SS rainbow trout (Fig 2). Specifically, transcript abundances of the two salmonid paralogues of exportin 5, *xpo5a* (Fig 2A) and argonaute 2, *ago2a* and *ago2b* (Fig 2B and 2C), were quantified, and Ago2 was also assessed at the protein level (Fig 2D). The hepatic mRNA abundance of *xpo5a* ($F_{2,15} = 0.24$, $p = 0.7885$; Fig 2A) did not change significantly compared to the SI in SD and SS fish, but *xpo5b* abundance was too low to be reliably quantified. Although the hepatic abundance of *ago2a* mRNA did not change significantly among groups ($F_{2,16} = 0.22$, $p = 0.2215$; Fig 2B), significant changes were observed in *ago2b* ($F_{2,16} = 10.58$, $p = 0.0012$; Fig 2C), which increased significantly in SS trout compared to SD or SI trout ($p < 0.05$). At the protein level, Ago2 quantification ($F_{2,16} = 16.13$, $p = 0.0001$; Fig 2D) revealed significant increases between SI and both SD and SS groups ($p < 0.05$ in both cases).

3.2. Small RNA next generation sequencing and identification of social status dependent regulation of hepatic miRNAs in rainbow trout

Of the overall ~55.18 M raw reads, 36.26 M reads (56.5%) were excluded firstly owing to a lack of 3'adaptor or 3'ADT (~25.01 M or 45.3%), and secondly because of nucleotide size outside the targeted range of 15–32 nt (~6.20 M or 11.2%) after 3'ADT sequence screening, resulting in ~40.60 M mappable reads (Fig 3A), of which 78% exhibited a size between 19 and 23 nt (Fig 3B). The Phred Score distribution of reads was larger than 30 (Fig 3C), indicating a probability of incorrect base calls of less than 1 in 1000 reads (or 99.9% accuracy). With regard to individual sample sequencing depth, a range between ~2.42 M and ~6.06 M mappable reads per sample was obtained (S3 Table). Following quality assurance of small RNA sequencing, the total of ~23.95 M mappable reads (Fig 3A) was annotated into specific groups according to the described pipeline (S1 Table). In this process, ~14.73 M or 61.5% of reads were annotated as 591 known miRNAs (Group 1), whereas ~2.42 M or 10.1% of reads were annotated as 983

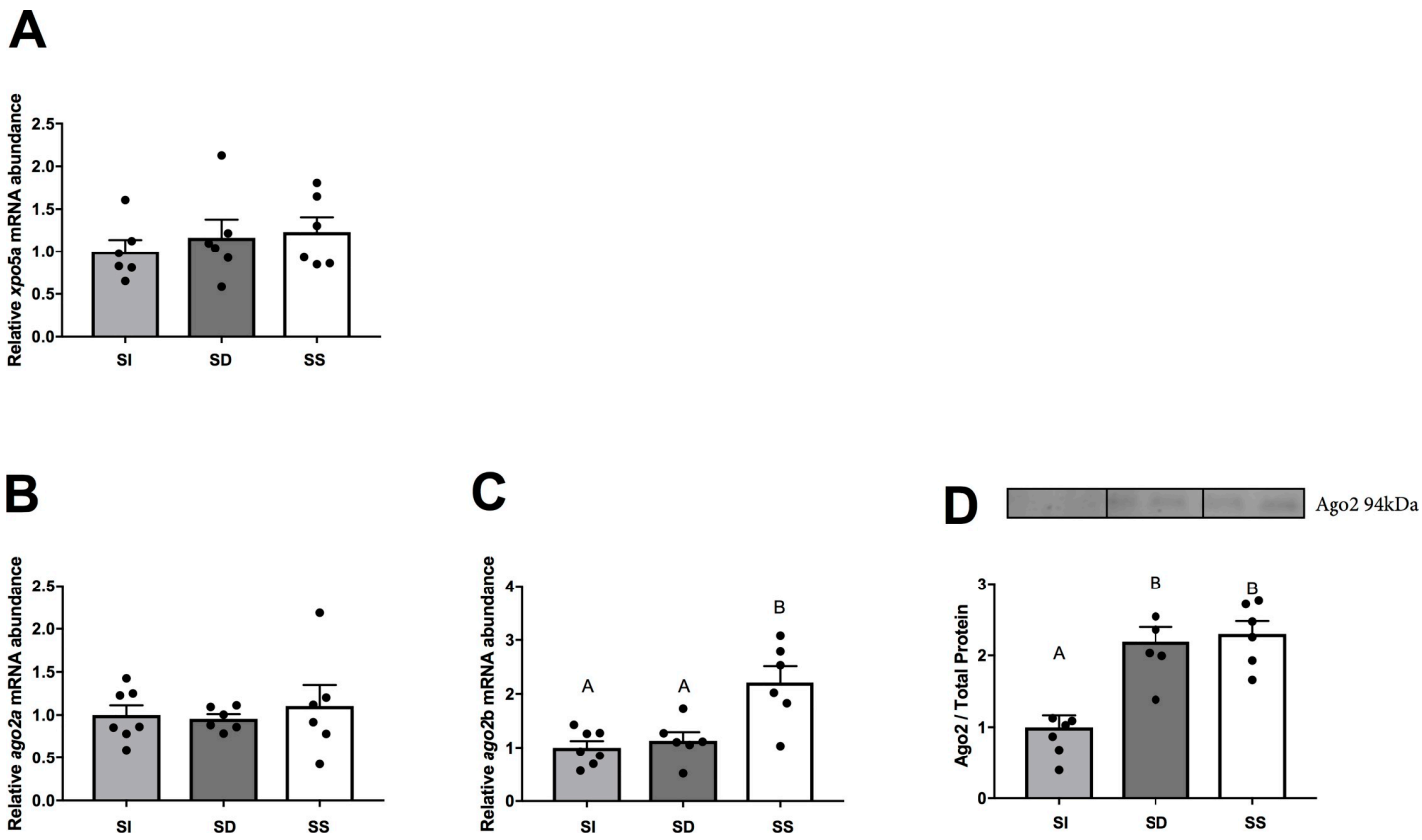

Fig 2. Relative steady-state mRNA abundance (+S.E.M.) of hepatic canonical miRNA biogenesis components exportin 5a (**A**), and argonaute 2a and argonaute 2b (**B**-**C**), as well as representative bands of argonaute protein abundance (**D**) in SI, SD and SS rainbow trout, *Oncorhynchus mykiss*. The mRNA abundance data were initially normalized using the Normagene approach, and protein data were initially normalized to total protein. Both mRNA abundance and protein data were then normalized to the SI group values to visualize relative fold-changes in SS and SD trout. Filled circles representing individual datapoints are additionally plotted for each group. A one-way ANOVAs followed by Tukey's test was used for analysis. A p-value of $p < 0.05$ was used as cut-off for significant effects.

https://doi.org/10.1371/journal.pone.0217978.g002

predicted miRNAs (Groups 2–4). A total of ~7.53 M or 31.4% of mappable reads was annotated as other RNA species or did not yield a hit (Table 3 and Table 4). Thus, we identified a total of 1574 unique miRNAs, the specific sequences of which are available in S2 Table.

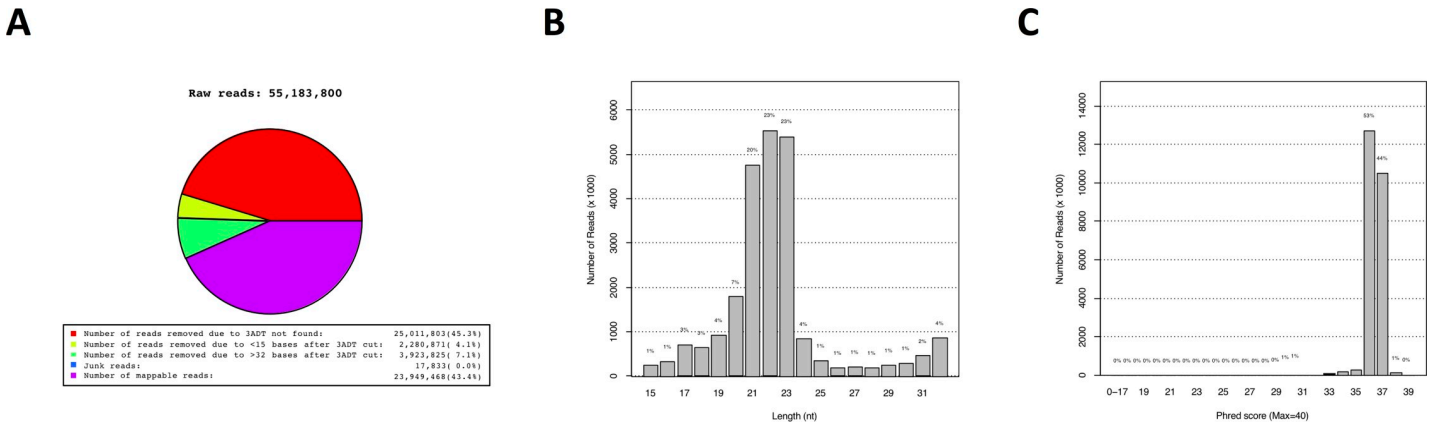

Fig 3. Number of raw reads, removed reads and mappable reads used in the small RNA next generation sequencing analysis (**A**), length distribution of reads (**B**), and Phred Score (**C**), an indicator of base call accuracy. A Phred score > 30 indicates 99.9% accuracy, or a 1:1000 probability of a false base call.

https://doi.org/10.1371/journal.pone.0217978.g003

Table 3. Number of annotated small RNA sequences by group as defined in the bioinformatics analysis pipeline flow chart in Fig 2.

Group	# Sequences	% Mappable Sequences
Raw	55,183,800	
Total mappable reads	23,949,468	100
Group 1a	9,747,348	40.7
Group 1b	4,977,912	20.8
Group 2a	235,217	1
Group 2b	92,526	0.4
Group 3a	3,393	0
Group 3b	4,573	0
Group 4a	32,125	0.1
Group 4b	1,844,196	8.6
Mapped to mRNA	3,374,845	7.7
Mapped to other RNAs (RFam: rRNA, tRNA, snRNA, snoRNA and others)	3,380,212	14.1
Mapped to Repbase	165,394	0.7
Nohit	2,141,579	8.9

https://doi.org/10.1371/journal.pone.0217978.t003

Analysis by t-tests ($p < 0.05$), revealed a total of 24 differentially expressed miRNAs between SD and SS trout, with 9 miRNAs that were expressed more abundantly in the liver of SD rainbow trout, and, conversely, 15 miRNAs that exhibited significantly higher abundance in SS trout (Fig 4). A detailed list of the differential expression analysis can be found in S3 Table. To validate miRNA abundance identified by small RNA next generation sequencing, we quantified the most abundant differentially regulated miRNA, *miRNA-21-5p* (S3 Table), by a Taqman based real-time RT-PCR, and found significantly higher hepatic *miRNA-21-5p* abundance (One-tailed Welch's t test: df = 5.229, t = 4.184, p = 0.0039, Fig 5A) in SS rainbow trout

Table 4. Number of annotated mature miRNA sequences by group as defined in the flow chart depicted in Fig 2.

miRNAs	Group	# Unique miRs
Known miRs		
of specific species[1]	Group 1a	150
of selected species, but novel to specific species[2]	Group 1b	441
Predicted miRs		
Mapped to known miRs of selected species and genome; with hairpins	Group 2a	251
Mapped to known miRs of selected species and genome; no hairpins	Group 2b	130
Mapped to known miRs and miRs of selected species but not mapped to genome	Group 3a	83
Mapped to known miRs of selected species, but not mapped to genome	Group 3b	313
Not mapped to known miRs but mapped to genome and with hairpins	Group 4a	582
Overall (Unique miRs)		1574

https://doi.org/10.1371/journal.pone.0217978.t004

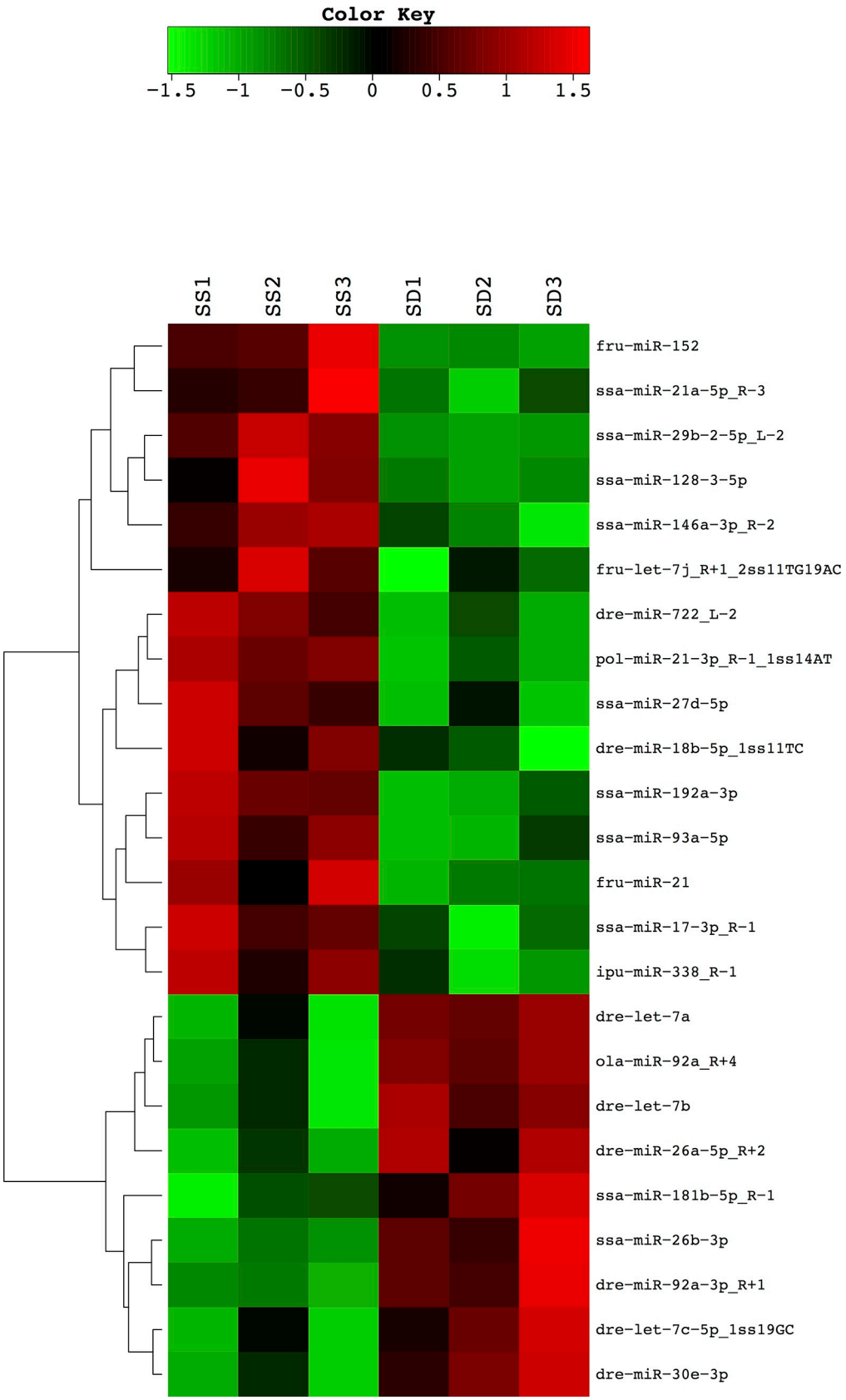
Color Key
−1.5
−1
−0.5
0
0.5
1
1.5
SS1
SS2
SS3
SD1
SD2
SD3
fru-miR-152
ssa-miR-21a-5p_R-3
ssa-miR-29b-2-5p_L-2
ssa-miR-128-3-5p
ssa-miR-146a-3p_R-2
fru-let-7j_R+1_2ss11TG19AC
dre-miR-722_L-2
pol-miR-21-3p_R-1_1ss14AT
ssa-miR-27d-5p
dre-miR-18b-5p_1ss11TC
ssa-miR-192a-3p
ssa-miR-93a-5p
fru-miR-21
ssa-miR-17-3p_R-1
ipu-miR-338_R-1
dre-let-7a
ola-miR-92a_R+4
dre-let-7b
dre-miR-26a-5p_R+2
ssa-miR-181b-5p_R-1
ssa-miR-26b-3p
dre-miR-92a-3p_R+1
dre-let-7c-5p_1ss19GC
dre-miR-30e-3p

Fig 4. Heatmap showing hierarchical clustering of differentially regulated hepatic miRNAs between SS (SUB1-3) and SD (DOM1-3) rainbow trout, analyzed by t-tests. See text for explanation.

https://doi.org/10.1371/journal.pone.0217978.g004

compared to SD animals. Additionally, we measured relative transcript abundance of *miRNA-722*, *miRNA-26a-5p*, *miRNA-let-7a*, and *miRNA-152* (Fig 5B–5E). Similarly, to *miRNA-21-5p*, we found significantly increased expression of *miRNA-722* in SS fish relative to SD fish (One-tailed Welch's t test: df = 9.363, t = 1.873, p = 0.0463, Fig 5B). Further validating the NGS data, *miRNA-26a-5p* (One-tailed Welch's t test: df = 7.203, t = 2.959, p = 0.0102, Fig 5C) and *miRNA-let-7a* (One-tailed Welch's t test: df = 5.608, t = 1.953, p = 0.0510 Fig 5D) demonstrated significantly and marginally significantly lower expression respectively in SS fish relative to SD fish. *miRNA-152* (One-tailed Welch's t test: df = 7.451, t = 0.4882, p = 0.3197 Fig 5E) did not show a significant difference in relative miRNA abundance between SS and SD rainbow trout.

3.3. In silico analysis of differentially regulated miRNA targets predicts glucose, lipid, and protein metabolic pathways as being post transcriptionally regulated

To gain initial insight into genome-wide consequences of differentially regulated hepatic miRNAs between SS and SD rainbow trout, targets were predicted based on their theoretical 3'UTR capacity to bind the 24 differentially regulated miRNAs (S4 Table). Based on annotated GO terms of the targets compared to whole genome GO terms, we identified several pathways that were predicted to be regulated by these differentially regulated miRNAs (S5 Table). The pathways most relevant to the differential regulation of hepatic metabolic pathways were related to glucose [4, 6], lipid [7] and to some extent, protein metabolism [7] in SD and SS

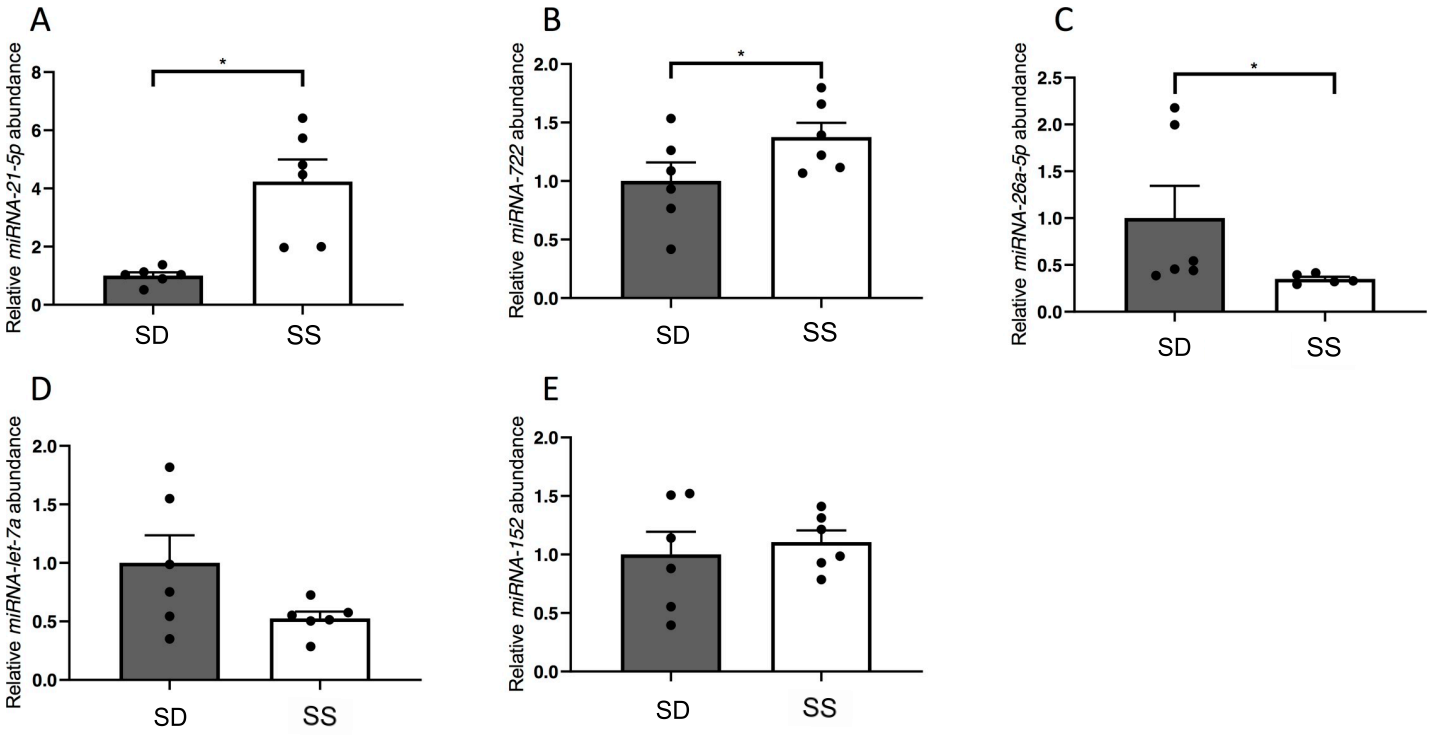

Fig 5. Relative steady-state abundance (+S.E.M.) of the most abundant differentially regulated hepatic miRNA, *miRNA-21-5p*, as well as *miRNA-722*, *miRNA-26a-5p*, *miRNA-let-7a* and *miRNA-152* in liver of SD and SS rainbow trout, *Oncorhynchus mykiss*. A one-tailed Welch's t-test was used for analysis, and a p-value of $p<0.05$ was used as cut-off for significant effects.

https://doi.org/10.1371/journal.pone.0217978.g005

Table 5. Significant metabolism-related GO-term enrichment of *in silico* predicted target mRNAs of miRNAs that were differentially regulated between dominant and subordinate rainbow trout. The full list of enriched GO terms can be consulted in S4 Table.

Targeted metabolic pathway or process	GO term	Fisher raw p-value
General intermediary metabolism		0.036
	GO:0097009 energy homeostasis	
Glucose metabolism		
	GO:0042149 cellular response to glucose starvation	0.019
	GO:0006094 gluconeogenesis	0.005
	GO:0006108 malate metabolic process	0.001
	GO:0004471 malate dehydrogenase (decarboxylating) (NAD +) activity	0.006
	GO:0006096 glycolytic process	0.031
	GO:0044262 cellular carbohydrate metabolic process	0.035
Lipid metabolism		
	GO:0034379 very-low-density lipoprotein particle assembly	0.001
Protein/AA metabolism		
	GO:0002181 cytoplasmic translation	0.001
	GO:0042274 ribosomal small subunit biogenesis	0.006
	GO:0006415 translational termination	0.009
	GO:0006622 protein targeting to lysosome	0.045
Mitochondria		
	GO:0008053 mitochondrial fusion	0.014
	GO:0042407 cristae formation	0.006
	GO:0060263 regulation of respiratory burst	0.006
	GO:0009055 electron carrier activity	0.009
	GO:0070469 respiratory chain	0.010
	GO:0008121 ubiquinol-cytochrome-c reductase activity	0.001
	GO:0005744 mitochondrial inner membrane presequence translocase complex	0.017

https://doi.org/10.1371/journal.pone.0217978.t005

rainbow trout liver. Additionally, pathways related to mitochondrial dynamics were predicted to be targeted by differentially regulated miRNAs between SS and SD fish. Results of the analysis are summarized in Table 5. In the case of glucose metabolism, we visualized individual genes and pathways predicted to be post-transcriptionally regulated by differentially regulated miRNAs using sub-network enrichment (SNEA) analysis (Fig 6, S1 Fig).

3.4. SS status induces *pck1* transcript in rainbow trout liver

Given the enrichment of intermediary metabolic pathways predicted to be post-transcriptionally regulated by differentially regulated miRNAs in SD and SS rainbow trout liver, and the well-described effects of social status on hepatic glucose metabolism, particularly gluconeogenesis and glycogen metabolism, we quantified mRNA abundances of gluconeogenic enzyme paralogues of phosphoenolcarboxykinase (*pck1* and *pck2*, Fig 7A and 7B), glucose-6-phosphatase (*g6pca*, *g6pcb1a*, *g6pcb1b*, *g6pcb2a*, and *g6pcb2b*, Fig 7C–7G), and glycogen phosphorylase (liver *pygl* and brain *pygb* forms, Fig 7H and 7I). The mRNA abundance of cytoplasmic *pck1* ($F_{2,15}$ = 132.10, p = 0.0001), but not mitochondrial *pck2* ($F_{2,16}$ = 2.84, p = 0.0880), was significantly higher in SS trout compared to both SI and SD rainbow trout ($p < 0.0001$). No changes were found in mRNA expression of *g6cpca* ($F_{2,16}$ = 1.04, p = 0.9414), *g6pcb1a* ($F_{2,16}$ = 0.7042,

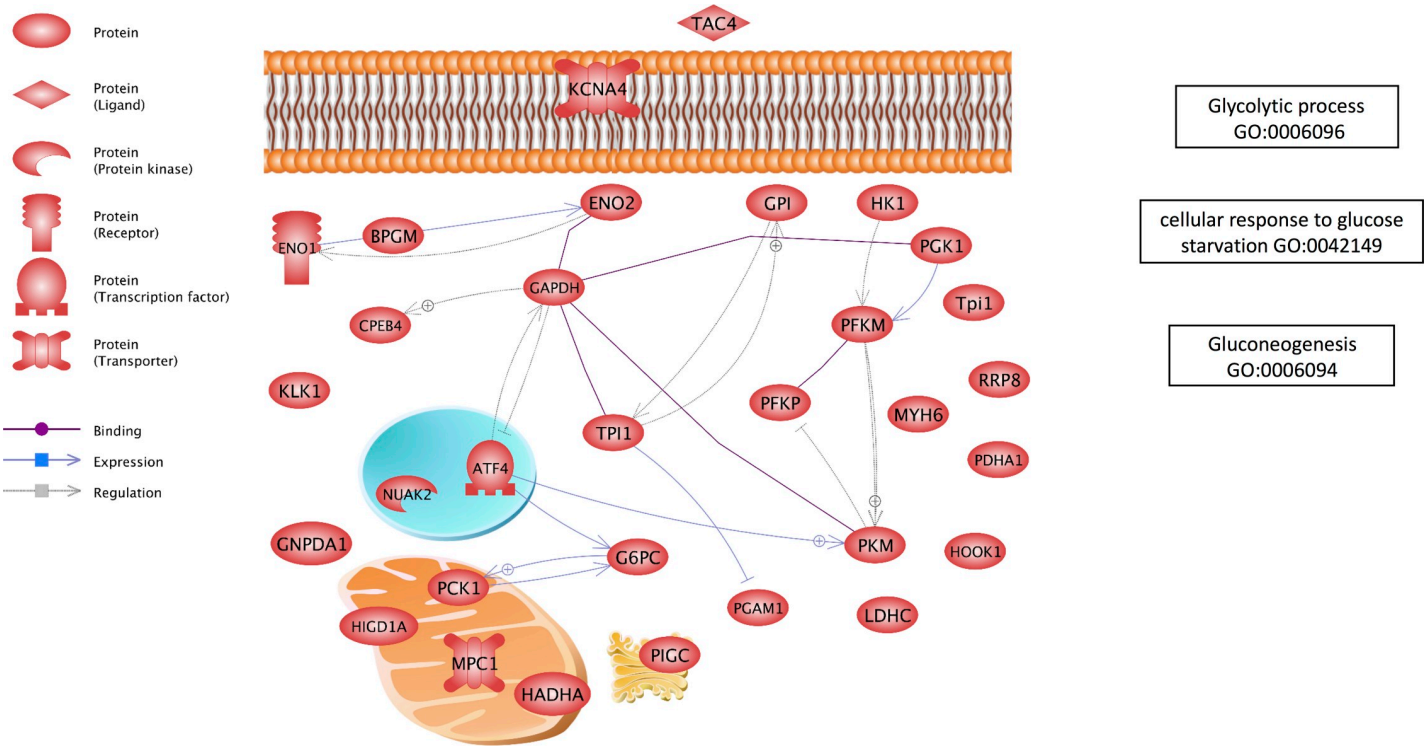

Fig 6. A gene network schematic depicting key predicted targets for miRNAs for gene ontology terms related to the theme of glucose regulation. Pathways were constructed in Pathway Studio. Each target in the pathway is predicted to be regulated by a hepatic miRNA that is differentially regulated between SS and SD rainbow trout.

https://doi.org/10.1371/journal.pone.0217978.g006

p = 0.5092) and *g6pcb1b* ($F_{2,16}$ = 0.2664, p = 0.7694).However, hepatic *g6pcb2a* ($F_{2,16}$ = 6.091, p = 0.0108) and *g6pc2b* ($F_{2,16}$ = 4.904, p = 0.0218) mRNA abundances were significantly higher in SD trout compared to SS trout (p = 0.0121 and p = 0.0290, respectively) and significantly or marginally higher than in SI trout (p = 0.0391 and p = 0.0502, respectively). The hepatic mRNA abundances of both *pygl* ($F_{2,16}$ = 18.59, p = 0.0001) and *pygb* ($F_{2,16}$ = 3.695, p = 0.0480) were lower in SS trout compared to SD trout (p = 0.0001 and p = 0.0469, respectively). In the case of *pygl*, the hepatic mRNA abundance in SS was also significantly reduced compared to SI animals (p = 0.0036).

3.5. Lipolytic and mitochondrial fission markers are elevated in SS rainbow trout

Hepatic expression of hormone sensitive lipase *hsl* ($F_{2,16}$ = 18.59, p = 0.0001, Fig 8A) was significantly higher in SS fish compared to SD (p = 0.005) and SI fish (p = 0.001). With regard to hepatic mRNA abundance of mitochondrial fusion proteins, *mfn1* ($F_{2,16}$ = 2,095 p = 0.1556, Fig 8B) did not differ among treatment groups, whereas *mfn2* ($F_{2,16}$ = 4.753, p = 0.0240, Fig 8C) was lower in SS trout compared to SD trout (p = 0.0194). Conversely, hepatic mRNA abundance of the mitochondrial fission protein, *fis1* ($F_{2,16}$ = 5.606, p = 0.0143, Fig 8D) was higher in SS trout compared to SD (p = 0.0417) and SI trout (p = 0.0175).

3.6. SS trout exhibit significantly increased circulating glucose concentration

To completely assess the SS phenotype at the metabolite level, we quantified circulating glucose concentrations to complement previously reported plasma lipid metabolite changes,

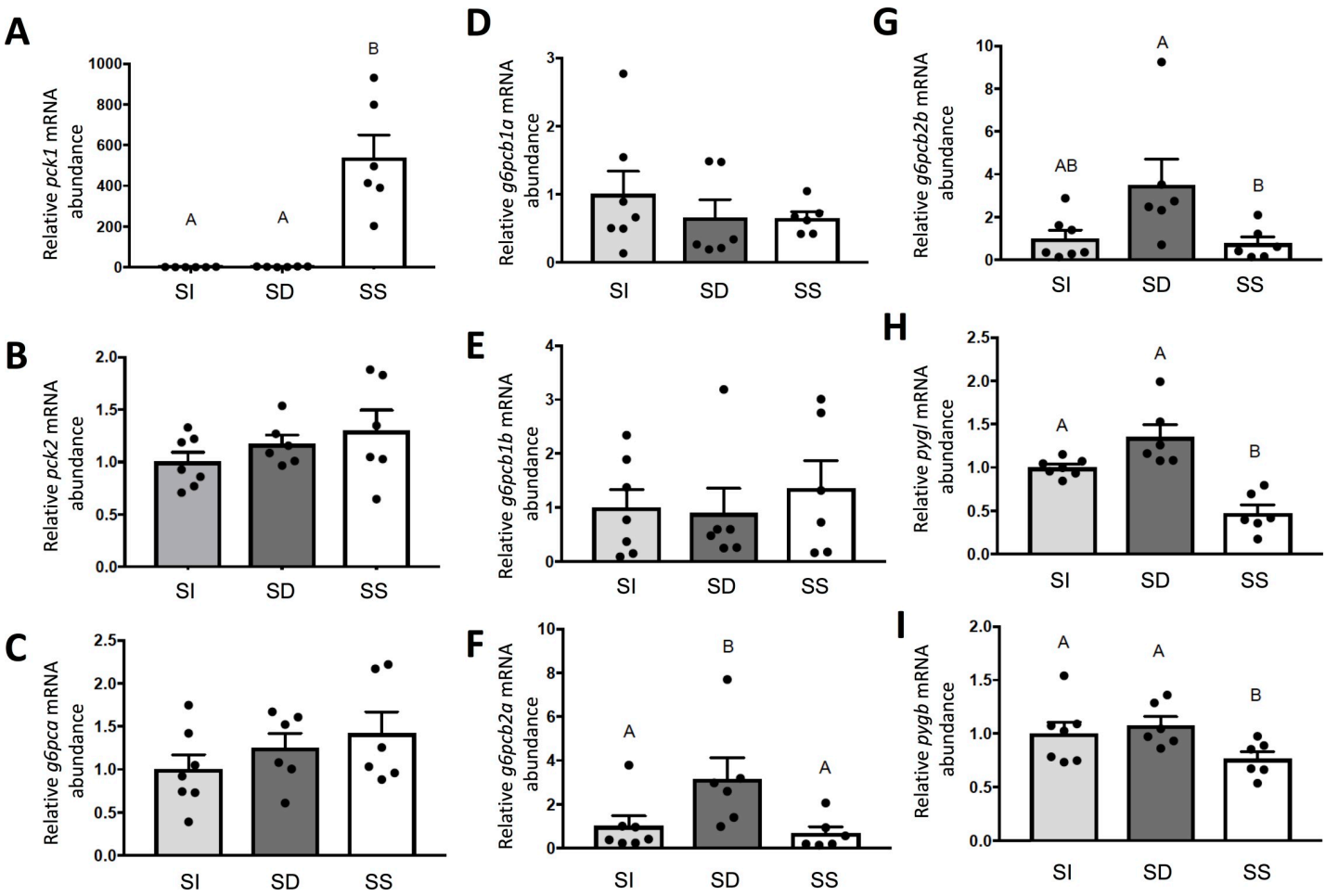

Fig 7. Steady state mRNA abundance (+S.E.M.) of genes involved in hepatic glucose metabolism, including gluconeogenic enzyme isoforms cytoplasmic phosphoenolpyruvate carboxykinase *pck1* (**A**), mitochondrial phosphoenolpyruvate carboxykinase *pck2* (**B**), gluconeogenic enzyme paralogues of glucose-6-phosphatase (**C-G**), and liver (**H**) and brain (**I**) isoforms of the glycogenolytic enzyme, glycogen phosphorylase. Data for SI, SD and SS rainbow trout (*Oncorhynchus muykiss*) were normalized using the Normagene algorithm, and then expressed relative to values for SI fish. A one-way ANOVAs followed by Tukey's post-hoc was used for analysis. A p-value of $p<0.05$ was used as cut-off for significant effects.

https://doi.org/10.1371/journal.pone.0217978.g007

specifically increases in triglyceride in SD rainbow trout and increases in free fatty acids in SS rainbow trout (7). SS trout exhibited significantly higher circulating glucose concentrations than SD rainbow trout ($t_{12} = 3.251$, $p < 0.01$; Fig 9).

3.7. miRNA-target gene relationships

Using correlative analysis of miRNA and predicted target gene expression, we identified several miRNA-mRNA expression pairs exhibiting significant correlation coefficients (Table 6). With regard to glucose metabolism, significant negative correlations between *miR-27d-5p* and *pck1*, and *miR-21-3p* and *pygb* were detected. With regard to lipid metabolism, the majority of miRNAs predicted to target *hsl* exhibited positive correlations with the *hsl* transcript, which was significant in the case of *miR-21-3p*. Exclusively negative relationships were identified for miRNAs predicted to target mitofusins, reaching significance for *miR-18b-5p*. Conversely, *miRNA-21-3p* and its predicted target *fis1* exhibit a significant positive correlation.

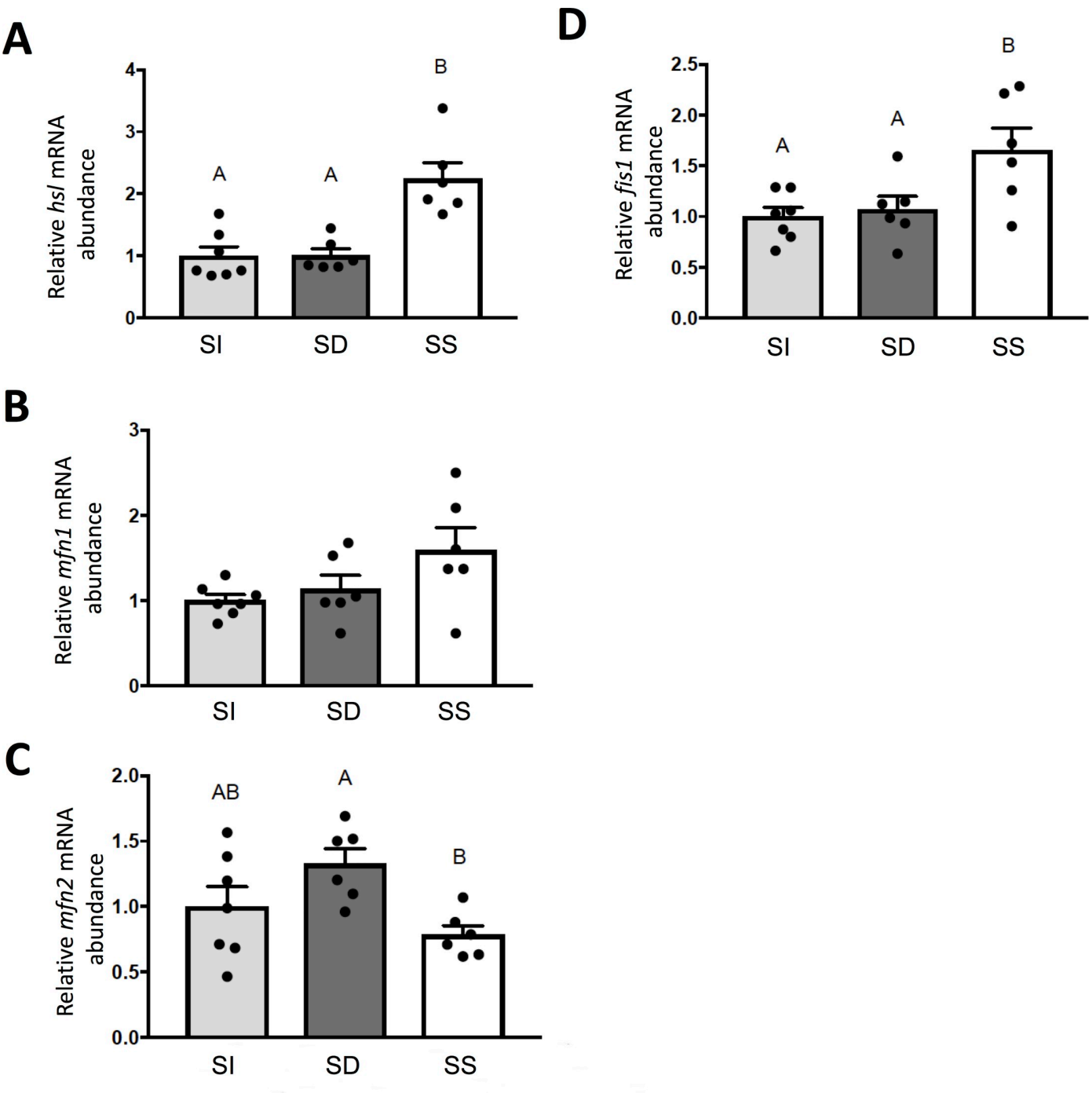

Fig 8. Steady state mRNA abundance (+S.E.M.) of genes involved in hepatic lipid metabolism, hormone sensitive lipase, *hsl* (**A**), and those involved in the regulation of mitochondrial dynamics including mitofusin 1, *mfn1* (**B**) mitofusin2, *mfn2* (**C**) and mitochondrial fission protein, *fis1* (D). Data for SI, SD and SS rainbow trout (*Oncorhynchus mykiss*) were normalized using the Normagene algorithm, and then expressed relative to values for SI fish. A one-way ANOVAs followed by Tukey's post-hoc was used for analysis. A p-value of $p<0.05$ was used as cut-off for significant effects.

https://doi.org/10.1371/journal.pone.0217978.g008

4. Discussion

The current study reveals that the hepatic miRNA biogenesis pathway is induced in interacting SD and SS juvenile rainbow trout compared to SI-treated trout that did not experience social

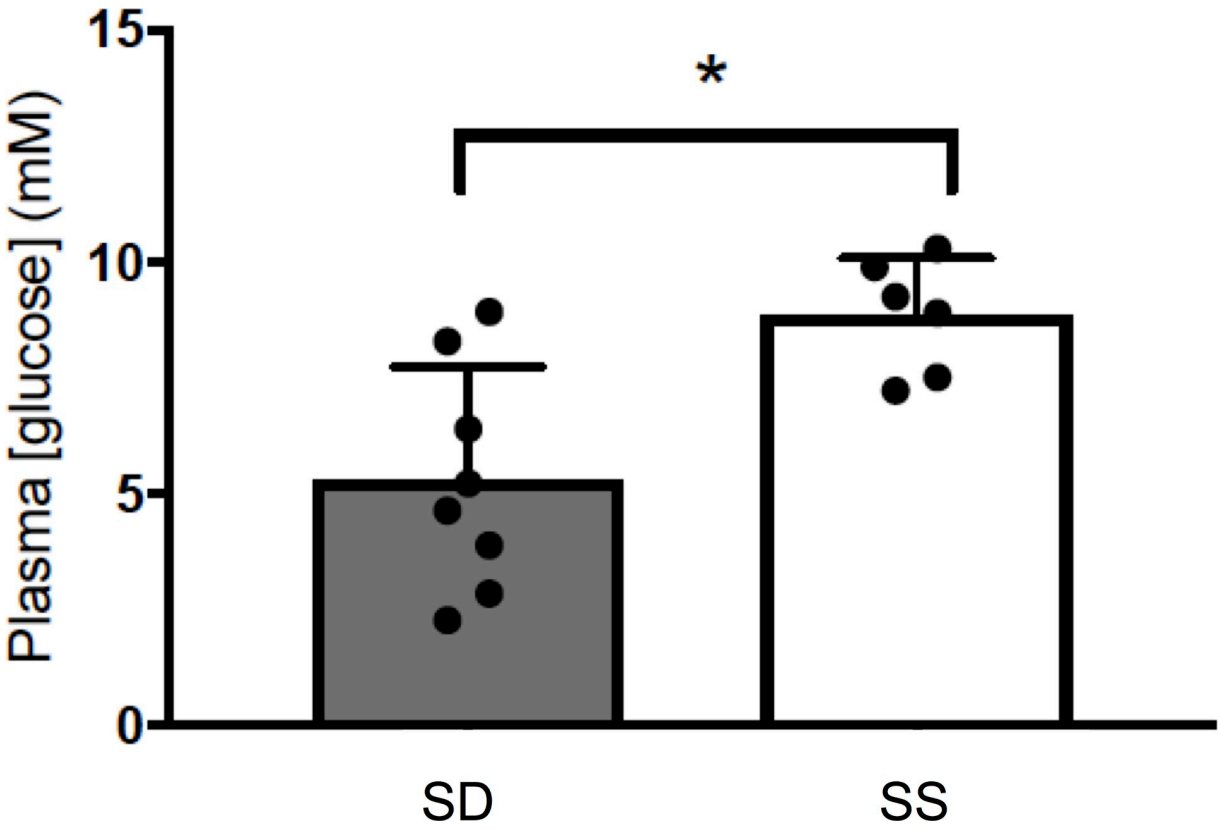

Fig 9. Circulating glucose concentrations in SD and SS rainbow trout (*Oncorhynchus mykiss*). Data were analyzed using Welch's t-test. A $p<0.05$ was used as cut-off for significant effect.

https://doi.org/10.1371/journal.pone.0217978.g009

interactions. In addition to the previously reported increase in *drosha* mRNA abundance [7], which is responsible for a crucial step in miRNA biogenesis [16, 32], we here report the elevation of Ago2 protein abundance in both SS and SD rainbow trout compared to individually housed SI trout, further supporting the notion of increased hepatic miRNA biogenesis and function in response to agonistic social interactions indicative of an enhanced functional role for miRNAs in post-transcriptional regulation of hepatic gene expression in socially antagonistic conditions.

To begin to delineate qualitative consequences of hepatic miRNA expression between SS and SD rainbow trout, we utilized a small miRNA next generation sequencing approach to identify 24 differentially regulated miRNAs, with 15 that exhibited increased expression, and 9 miRNAs that exhibited decreased expression in the liver of SS trout compared to SD trout. Differences in miRNA expression with social status may be mediated by differential biogenesis and/or turnover mechanisms [14,32]. While our experiment does not allow to resolve the relative contribution of each mechanism, the previously reported increase in *drosha* mRNA abundance in both SS and SD rainbow trout compared to individually housed SI controls [7] is indicative of at least a partial contribution of biogenesis to this differential expression. In order to explore the possible functional relevance of differentially expressed miRNAs, we used a genome-wide *in silico* approach [21] to predict specific targets and their enrichment by GO-term function. Because miRNAs play important roles in the regulation of (hepatic) energy metabolism not only in mammals (13,31), but also in fish, and in trout in particular [14,15] and social status-dependent regulation of hepatic glucose [4,6], lipid [7], and possibly protein

Table 6. Correlation of expression of differentially regulated miRNAs and predicted targets involved in pathways relevant to hepatic regulation of glucose metabolism.

Metabolic pathway and target gene	miRNA	Pearson correlation coefficient	Significance
Glucose metabolism			
pck1 GSONMT00082468001	*ssa-miR-27d-5p*	-0.75	$p<0.05$
pck2 GSONMT00059643001	*ssa-miR-128-3-5p*	0.19	n.s.
g6pca GSONMT00076843001	*ipu-miR-338_R-1*	-0.14	n.s.
g6pcb1.a GSONMT00076841001	*none*	none	none
g6pcb1.b GSNOMT00066036001	*ssa-miR-181b-5p_R-1*	0.13	n.s.
g6pcb2.a GSNOMT00013076001	*dre-miR-92a-3p_R+1*	0.62	n.s.
g6pcb2.b GSNOMT00014864001	*none*	none	n.s.
pygb GSNOMT00009821001	*pol-miR-21-3p_R-1_1ss14AT*	-0.84	$p<0.05$
Lipid metabolism			
hsl GSNOMT00023441001	*fru-miR-21*	0.58	n.s.
hsl GSNOMT00023441001	*pol-miR-21-3p_R-1_1ss14AT*	0.83	$p<0.05$
hsl GSNOMT00023441001	*fru-miR-152*	0.71	n.s.
hsl GSNOMT00023441001	*ssa-miR-93a-5p*	0.69	n.s.
hsl GSNOMT00023441001	*dre-miR-18b-5p_1ss11TC*	0.70	n.s.
hsl GSNOMT00023441001	*ipu-miR-338_R-1*	0.61	n.s.
hsl GSNOMT00023441001	*dre-miR-30e-3p*	-0.71	n.s.
Mitochondrial dynamics			
mfn1 GSNOMT00027395001	*dre-miR-let-7a*	-0.71	n.s.
mfn1 GSNOMT00027395001	*dre-miR-let7c-5p_1ss19GC*	-0.62	n.s.
mfn1 GSNOMT00027395001	*ssa-miR-27d-5p*	-0.62	n.s.
mfn2 GSNOMT00004526001	*dre-miR-18b-5p_1ss11TC*	-0.75	$p<0.05$
mfn2 GSNOMT00004526001	*fru-miR-152*	-0.44	n.s.
mfn2 GSNOMT00004526001	*pol-miR-21-3p_R-1_1ss14AT*	-0.73	n.s.
mfn2 GSNOMT00004526001	*ssa-miR-29b-2-5p_L-2*	-0.61	n.s.
fis1 GSNOMT00039888001	*pol-miR-21-3p_R-1_1ss14AT*	0.75	$p<0.05$

https://doi.org/10.1371/journal.pone.0217978.t006

metabolism [7] has been well described in SD versus SS rainbow trout, we focused our analysis of pathways predicted to be targeted by differentially regulated miRNAs on those relevant to hepatic glucose production, especially gluconeogenesis and glycogenolysis, lipolytic pathways, and pathways involved in protein synthesis. Additionally, pathways related to mitochondrial dynamics were examined because they were identified as being enriched targets of differentially regulated miRNAs in our *in silico* analysis, and have recently been linked to differential fuel utilization in response to nutrient availability and stress, at least in mammals [33–36].

With regard to gluconeogenesis target genes, we identified a very strong induction of *pck1*, the cytosolic form of phosphoenolpyruvate in SS fish, with no changes in the reported mitochondrial form of the enzyme, *pck2*. These results strongly suggest that the previously observed significant increase in global hepatic Pck activity in SS trout [4] is regulated at least in part, at the transcriptional and/or post-transcriptional level of the *pck1* gene. It is well documented that the SS trout phenotype is characterized by chronically elevated cortisol, as well as short term fasting [7], and both factors have been shown to contribute to increased *pck1* transcription in mammals. Indeed, cytosolic *pck1* is considered to be the principal target of endocrine and nutritional regulation [37]. This finding is in line with earlier studies investigating unspecified *pck* mRNA abundance before the publication of the rainbow trout genome facilitated paralogue specific *pck* transcript amplification. Our study clearly assigns this transcriptional response to the cytosolic *pck1* in rainbow trout, and the ability to distinguish between paralogues may have contributed to the much stronger fold-induction compared to pre-genome studies [38]. Additionally, the higher fold-induction may be explained by the fact that the current study investigated SS fish, which in addition to chronically elevated cortisol concentrations experienced a *de facto* short-term fast because of the monopolization of food by SD fish in the dyad [7]. Since it is well-described that cortisol interacts synergistically with glucagon in the regulation of *pck1* transcript abundance [37] future studies should investigate the role of fasting, glucagon and cortisol on the hepatic *pck1* transcript. Such synergism may also explain why both higher fold *pck1* mRNA abundance and global Pck activity are observed in SS trout, while cortisol injected trout reveal increased *pck* mRNA abundance but not activity [39]. Within the gluconeogenic pathway, we additionally probed *g6pc* paralogues and found no change in mRNA abundance of *g6pca* and *g6pcb1* paralogues. Unexpectedly, we identified a paradoxical increase in *g6pcb2* paralogues in SD fish, confirming an atypical regulation of these recently described novel members of the teleost *g6pc* family [40]. Because overall circulating glucose concentration was increased in SS fish compared to SD fish in our current study (**Fig 9**), our data suggest a functional contribution of gluconeogenesis, likely via transcriptional regulation of *pck1* in particular, to this phenotype. We found that *g6pcb2b* mRNA abundance is increased in SD, normoglycemic trout that monopolize food during social interactions, thereby acquiring a double ration. A similar, differential regulation of *g6pcb2b* paralogue mRNA abundance was reported previously in response to refeeding, especially with diets rich in carbohydrates [40]. With regard to glycogen phosphorylase paralogues, we identified lowered hepatic mRNA abundance of the liver and brain isoforms, *pygl* and *pygb*, in SS rainbow trout. SS rainbow trout exhibit significantly reduced hepatic glycogen content compared to both control and SD fish, with SS fish reaching concentrations of as low as 16% of hepatic glycogen content measured in SD fish [6]. This coincides with significant reductions in basal hepatic Gp activity, which is, however, likely limited by the decreased amount of glycogen, as total GP activity and GPα specific activity (assessed by adding additional glycogen or glycogen and caffeine, respectively) is lower in SS fish compared to controls, but exhibits the lowest values in SD fish [6]. This reported lowered GP activity compared to control fish has been interpreted to protect already depleted hepatic glycogen storage in SS fish from further glycogenolysis in the face of low food intake and chronic stress, and our current results indicate that this process

in SS fish is, at least in part, regulated at the mRNA abundance level of the hepatically expressed paralogues *pygl* and *pygb*. Conversely, the reported lowest total and GPα activity in SD trout interpreted to be reflective of rapid restocking of hepatic glycogen reserves following the initial acute stress of social hierarchy establishment do not appear to be linked to transcriptional regulation of these transcripts, as indicated by similar transcript abundances between control and SD fish. It is possible that chronically elevated cortisol levels are responsible for a mRNA based regulation as opposed to well described posttranslational regulation of glycogen phosphorylase activities. Indeed, conflicting results of cortisol on hepatic glycogen in rainbow trout have been reported [39], likely pointing to different baseline conditions, duration of the cortisol signaling and/or interaction between different regulating factors as mechanisms in the regulation of hepatic glycogen content in response to cortisol.

In addition to glucose metabolism, lipid metabolism exhibits pronounced differences between SD and SS rainbow trout [7]. Increased circulating triglycerides in SD rainbow trout correlate with increased hepatic indices of *de novo* lipogenesis, whereas elevated circulating free fatty acids correlate with indices of fatty acid β-oxidation in SS rainbow trout [7]. These results suggest that SD trout, which monopolize food use the energetically costly process of *de novo* lipogenesis to contribute to storage of lipid reserves, whereas SS fish rely on lipolytic processes to fuel metabolism, including hepatic metabolism [7]. Here, we report a significant increase in hepatic mRNA abundance of a paralogue of hormone sensitive lipase (*hsl*), providing further evidence for lipolytic activity in SS fish. In rainbow trout, hepatic *hsl* has been shown to be strongly regulated by nutritional and endocrine stimuli [41–42], and our finding of *hsl* upregulation in SS fish, which experience little or no food intake during social interactions, is consistent with data previously reported for *hsl* paralogues observed in trout in a comparable fasted state [41–42].

Because pathways linked to mitochondrial dynamics were predicted as being targeted by miRNA and are, at least in mammals, regulated by stress and nutritional status and functionally linked to oxidative glucose and lipid metabolism [33–36], we profiled markers of mitochondrial fusion and fission. We identified a decrease in mRNA abundance of *mfn2* in the liver of SS fish and, conversely, an increase in *fis1* transcript abundance, consistent with the opposing regulation often observed in these markers to coordinate mitochondrial dynamics [34]. Cortisol, the end-product of the stress axis, has been shown to increase mitochondrial fission, which, in turn, is functionally linked to increased gluconeogenesis in hepatoma cells [35]. Interestingly, liver-specific ablation of *mfn2* also contributes to increased gluconeogenesis [36], suggesting that in our model system, glucose liberation in SS fish may, at least in part, also mediated at the level of mitochondrial dynamics. Functional studies at the cellular level clearly are needed to support these gene expression findings.

Collectively, our findings at the gene expression level for paralogues involved in glucose metabolism, lipid metabolism and mitochondrial dynamics are consistent with previously reported metabolic changes [4,6,7], and suggest an important role for transcriptional and/or post-transcriptional regulation of gene expression in eliciting SD versus SS metabolic phenotypes. Because the specific transcript targets examined in this study were components of metabolic pathways identified as being regulated by differentially expressed miRNAs, and indeed predicted to be specifically targeted by differentially regulated miRNAs (**Table 5**), we investigated whether specific miRNA-mRNA target abundances were correlated (**Table 6**). Although significant correlations do not provide proof of functional interactions, the significant relationships in miRNA-target mRNA abundances that we observed prioritize these components for future functional studies.

A recent study has linked *miRNA-27* family members to the regulation of hepatic gluconeogenic enzymes, including PCK, suggesting that the predicted *miRNA-27d-5p-pck1* interaction in our study may be linked to evolutionarily deeply conserved roles of *miRNA-27* family

members in the regulation of gluconeogenesis [43]. Through predictions and significant inverse relationships in abundance, we identified *miRNA-27d-5p*, *miRNA-21-3p* and *miRNA-18b-5p* as potential regulators of glucose liberation, lipolysis and mitochondrial dynamics. In rodent models, functional roles for *miR-21-3p* in hepatic carbohydrate and lipid metabolism in response to nutritional stress have been described [44]. However, these effects are mediated via different primary targets compared to those predicted in rainbow trout, likely reflecting the low degree of deeply conserved miRNA-mRNA relationships, which have undergone extensive rewiring between fish and mammals [45]. With regard to protein metabolism, our current study predicts a convergent regulation on different paralogues of S6 kinase, a translational regulator, by multiple miRNAs (*let-7a*, *let-7b*, *let-7c*, *miRNA-92a-3p*, *miRNA-181-5p*) that are downregulated in the liver of SS trout compared to SD trout (**S4 Table**). This situation is suggestive of a post-transcriptionally-regulated increase in S6K. Consistent with this scenario, ribosomal S6 phosphorylation, an indicator of translational activity, was strongly induced in the liver of SS trout in our experimental animals [7], in line with the unexpected measurement of elevated rates of protein synthesis in the liver of SS rainbow trout (R.J. Saulnier, C. Best, D.J. Kostyniuk, K.M. Gilmour and S.G. Lamarre, unpublished results).

5. Conclusions, limitations and future perspectives

Overall, our study identifies increased protein abundance of Ago2 in dyad paired trout, suggesting that the miRNA pathway is important in the mediating posttranscriptional control of hepatic gene expression in both SS and SD rainbow trout. The nature of posttranscriptional regulation is differential between SS and SD rainbow trout, and differentially regulated miRNAs are predicted to target specific transcripts of important intermediary metabolic pathways of glucose, lipid and protein metabolism previously shown to be social status dependent in rainbow trout. Concerning the SI group, it is important to mention that a negative growth rate was observed, which, while not significantly different from growth rate observed in SD as is the case in SS, might be linked to catabolic reactions in this group, thereby affecting endpoints assessed in this group. Because the SS phenotype is associated with fasting, a chronic stress response and negative somatic growth, while the SD phenotype is associated with increased feed intake as it monopolizes food in dyads, the specific contribution of each of these factors to the observed hepatic miRNA regulation and their functional roles in mediating metabolic changes warrant further study.

Our framework therefore defines testable hypothesis for the involvement of specific miRNA-target mRNA pairs in the well-established metabolic differences in hepatic macronutrients metabolism, and identifies rainbow trout mitochondrial dynamics as a potential miRNA-regulated system that may contribute to differences in hepatic metabolism between SS and SD rainbow trout. Future studies are needed to functionally assess the role of specific miRNA-mRNA target pairs identified in our current study in the regulation of hepatic metabolism in rainbow trout. Specifically, the use of rainbow trout primary hepatocytes or cell lines transfected with plasmids containing 3'UTR and luciferase assays will allow to investigate physical interaction of miRNA and 3'UTR, while miRNA modulation approaches in the same systems allow to probe metabolic function, respectively (14). These assays are a necessary next step to validate identified candidates functionally, especially since *in silico* predictions suffer from false positives [25], and negative and positive correlations at a single sampling time only point towards possible modes of miRNA-mRNA interaction across time [46,47].

Supporting information

S1 Table. Flowchart representing the bioinformatics pipeline used to annotate and group miRNAs identified from small RNA next generation sequencing results. See text for

explanation.
(XLSX)

S2 Table. Next generation sequencing read summary, sequences and normalized counts.
(XLSX)

S3 Table. Differential hepatic miRNA expression between SS and SD trout (n = 3 per group) as determined by t-test.
(XLSX)

S4 Table. miRanda based annotated 3'UTR target prediction of differentially expressed miRNAs identified as being differentially expressed between SS and SD rainbow trout. Colours match heatmap designation in Fig 4, with green indicating predicted targets of miRNAs that have higher expression in SS rainbow trout liver, and red indicating predicted targets of miRNAs with higher expression in SD trout liver.
(XLSX)

S5 Table. GO-term enrichment analysis of target genes predicted to be targeted by differentially expressed miRNAs between treatment groups and Pathway Studio Sub-Network Enrichment Analysis (SNEA) results.
(XLSX)

S1 Fig. Detailed Pathway Studio Sub-Network Enrichment Analysis (SNEA) results for over-represented GO-term processes related to glucose metabolism, as results visualized in Fig 7.
(PDF)

Acknowledgments

Funding for this project was provided through NSERC-DG (#147476) and Canadian Foundation of Innovation (#35859) grants to JAM, and an NSERC-DG grant to KMG. Thanks are extended to Brett Culbert for his help in generating the tissues used for this study.

Author Contributions

Conceptualization: Christopher J. Martyniuk, Jan A. Mennigen.

Data curation: Daniel J. Kostyniuk, Christopher J. Martyniuk, Jan A. Mennigen.

Formal analysis: Daniel J. Kostyniuk, Dapeng Zhang, Christopher J. Martyniuk, Jan A. Mennigen.

Funding acquisition: Kathleen M. Gilmour, Jan A. Mennigen.

Investigation: Daniel J. Kostyniuk, Dapeng Zhang, Jan A. Mennigen.

Methodology: Daniel J. Kostyniuk, Dapeng Zhang, Kathleen M. Gilmour, Jan A. Mennigen.

Project administration: Jan A. Mennigen.

Resources: Dapeng Zhang, Christopher J. Martyniuk, Kathleen M. Gilmour, Jan A. Mennigen.

Software: Daniel J. Kostyniuk, Dapeng Zhang, Christopher J. Martyniuk, Jan A. Mennigen.

Supervision: Jan A. Mennigen.

Validation: Daniel J. Kostyniuk, Jan A. Mennigen.

Visualization: Daniel J. Kostyniuk, Christopher J. Martyniuk, Jan A. Mennigen.

Writing – original draft: Daniel J. Kostyniuk, Kathleen M. Gilmour, Jan A. Mennigen.

Writing – review & editing: Daniel J. Kostyniuk, Dapeng Zhang, Christopher J. Martyniuk, Kathleen M. Gilmour, Jan A. Mennigen.

References

1. Abbott JC, Dill LM. Patterns of Aggressive Attack in Juvenile Steelhead Trout (Salmo gairdneri). Can J Fish Aquat Sci. 1985 Nov 1; 42(11):1702–6.
2. Elliott JM. Mechanisms Responsible for Population Regulation in Young Migratory Trout, Salmo trutta. III. The Role of Territorial Behaviour. Journal of Animal Ecology. 1990; 59(3):803–18.
3. Metcalfe NB. Intraspecific variation in competitive ability and food intake in salmonids: consequences for energy budgets and growth rates J Fish Biol. 1986 May 28: 525–531.
4. DiBattista JD, Levesque HM, Moon TW, Gilmour KM. Growth Depression in Socially Subordinate Rainbow Trout Oncorhynchus mykiss: More than a Fasting Effect. Physiological and Biochemical Zoology. 2006 Jul 1; 79(4):675–87. https://doi.org/10.1086/504612 PMID: 16826494
5. Gilmour KM, DiBattista JD, Thomas JB. Physiological Causes and Consequences of Social Status in Salmonid Fish. Integr Comp Biol. 2005 Apr 1; 45(2):263–73. https://doi.org/10.1093/icb/45.2.263 PMID: 21676770
6. Gilmour KM, Kirkpatrick S, Massarsky A, Pearce B, Saliba S, Stephany C-É, et al. The Influence of Social Status on Hepatic Glucose Metabolism in Rainbow Trout Oncorhynchus mykiss. Physiological and Biochemical Zoology. 2012 Jul 1; 85(4):309–20. https://doi.org/10.1086/666497 PMID: 22705482
7. Kostyniuk DJ, Culbert BM, Mennigen JA, Gilmour KM. Social status affects lipid metabolism in rainbow trout, Oncorhynchus mykiss. Am J Physiol Regul Integr Comp Physiol. 2018 Mar 21;
8. Mommsen TP, Moon TW. Metabolic response of teleost hepatocytes to glucagon-like peptide and glucagon. J Endocrinol. 1990 Jul; 126(1):109–18. PMID: 2166124
9. Vijayan MM, Reddy PK, Leatherland JF, Moon TW. The effects of cortisol on hepatocyte metabolism in rainbow trout: a study using the steroid analogue RU486. Gen Comp Endocrinol. 1994 Oct; 96(1):75–84. https://doi.org/10.1006/gcen.1994.1160 PMID: 7843570
10. Culbert BM, Gilmour KM. Rapid recovery of the cortisol response following social subordination in rainbow trout. Physiology & Behavior. 2016 Oct 1; 164:306–13.
11. Polakof S, Panserat S, Soengas JL, Moon TW. Glucose metabolism in fish: a review. J Comp Physiol B, Biochem Syst Environ Physiol. 2012 Dec; 182(8):1015–45. https://doi.org/10.1007/s00360-012-0658-7 PMID: 22476584
12. Moon TW. Glucose intolerance in teleost fish: fact or fiction? Comp Biochem Physiol B, Biochem Mol Biol. 2001 Jun; 129(2–3):243–9. PMID: 11399456
13. Rottiers V, Näär AM. MicroRNAs in metabolism and metabolic disorders. Nat Rev Mol Cell Biol. 2012 Mar 22; 13(4):239–50. https://doi.org/10.1038/nrm3313 PMID: 22436747
14. Mennigen JA. Micromanaging metabolism-a role for miRNAs in teleost energy metabolism. Comp Biochem Physiol B, Biochem Mol Biol. 2016 Sep; 199:115–25. https://doi.org/10.1016/j.cbpb.2015.09.001 PMID: 26384523
15. Mennigen JA, Martyniuk CJ, Seiliez I, Panserat S, Skiba-Cassy S. Metabolic consequences of microRNA-122 inhibition in rainbow trout, Oncorhynchus mykiss. BMC Genomics. 2014 Jan 27; 15:70. https://doi.org/10.1186/1471-2164-15-70 PMID: 24467738
16. Kim Y-K, Kim B, Kim VN. Re-evaluation of the roles of DROSHA, Exportin 5, and DICER in microRNA biogenesis. Proc Natl Acad Sci U S A. 2016 Mar 29; 113(13):E1881–9. https://doi.org/10.1073/pnas.1602532113 PMID: 26976605
17. Heckmann L-H, Sørensen PB, Krogh PH, Sørensen JG. NORMA-Gene: A simple and robust method for qPCR normalization based on target gene data. BMC Bioinformatics. 2011 Jun 21; 12(1):250.
18. Ma H, Weber GM, Hostuttler MA, Wei H, Wang L, Yao J. MicroRNA expression profiles from eggs of different qualities associated with post-ovulatory ageing in rainbow trout (Oncorhynchus mykiss). BMC Genomics. 2015; 16:201. https://doi.org/10.1186/s12864-015-1400-0 PMID: 25885637
19. Berthelot C, Brunet F, Chalopin D, Juanchich A, Bernard M, Noël B, et al. The rainbow trout genome provides novel insights into evolution after whole-genome duplication in vertebrates. Nat Commun. 2014 Apr 22; 5:3657. https://doi.org/10.1038/ncomms4657 PMID: 24755649

20. Juanchich A, Bardou P, Rué O, Gabillard J-C, Gaspin C, Bobe J, et al. Characterization of an extensive rainbow trout miRNA transcriptome by next generation sequencing. BMC Genomics. 2016 Mar 1; 17:164. https://doi.org/10.1186/s12864-016-2505-9 PMID: 26931235

21. Mennigen JA, Zhang D. MicroTrout: A comprehensive, genome-wide miRNA target prediction framework for rainbow trout, Oncorhynchus mykiss. Comp Biochem Physiol Part D Genomics Proteomics. 2016 Dec; 20:19–26. https://doi.org/10.1016/j.cbd.2016.07.002 PMID: 27494513

22. Enright AJ, John B, Gaul U, Tuschl T, Sander C, Marks DS. MicroRNA targets in Drosophila. Genome Biol. 2003; 5(1):R1. https://doi.org/10.1186/gb-2003-5-1-r1 PMID: 14709173

23. Rehmsmeier M, Steffen P, Hochsmann M, Giegerich R. Fast and effective prediction of microRNA/target duplexes. RNA. 2004 Oct; 10(10):1507–17. https://doi.org/10.1261/rna.5248604 PMID: 15383676

24. Bartel DP. MicroRNAs: target recognition and regulatory functions. Cell. 2009 Jan 23; 136(2):215–33. https://doi.org/10.1016/j.cell.2009.01.002 PMID: 19167326

25. Peterson SM, Thompson JA, Ufkin ML, Sathyanarayana P, Liaw L, Congdon CB. Common features of microRNA target prediction tools. Front Genet. 2014; 5:23. https://doi.org/10.3389/fgene.2014.00023 PMID: 24600468

26. Fan X, Kurgan L. Comprehensive overview and assessment of computational prediction of microRNA targets in animals. Brief Bioinformatics. 2015 Sep; 16(5):780–94. https://doi.org/10.1093/bib/bbu044 PMID: 25471818

27. Witkos TM, Koscianska E, Krzyzosiak WJ. Practical Aspects of microRNA Target Prediction. Curr Mol Med. 2011 Mar; 11(2):93–109. https://doi.org/10.2174/156652411794859250 PMID: 21342132

28. Paneru BD, Al-Tobasei R, Kenney B, Leeds TD, Salem M. RNA-Seq reveals MicroRNA expression signature and genetic polymorphism associated with growth and muscle quality traits in rainbow trout. Scientific Reports. 2017 Aug 22; 7(1):9078. https://doi.org/10.1038/s41598-017-09515-4 PMID: 28831113

29. Koganti PP, Wang J, Cleveland B, Ma H, Weber GM, Yao J. Estradiol regulates expression of miRNAs associated with myogenesis in rainbow trout. Molecular and Cellular Endocrinology. 2017 Mar 5; 443:1–14. https://doi.org/10.1016/j.mce.2016.12.014 PMID: 28011237

30. Hofacker IL, Fontana W, Stadler PF, Bonhoeffer LS, Tacker M, Schuster P. Fast folding and comparison of RNA secondary structures. Monatsh Chem. 1994 Feb 1; 125(2):167–88.

31. Herrera BM, Lockstone HE, Taylor JM, Ria M, Barrett A, Collins S, et al. Global microRNA expression profiles in insulin target tissues in a spontaneous rat model of type 2 diabetes. Diabetologia. 2010 Jun; 53(6):1099–109. https://doi.org/10.1007/s00125-010-1667-2 PMID: 20198361

32. Best C, Ikert H, Kostyniuk DJ, Craig PM, Navarro-Martin L, Marandel L, et al. Epigenetics in teleost fish: From molecular mechanisms to physiological phenotypes. Comp Biochem Physiol B, Biochem Mol Biol. 2018 Jan 31

33. Wai T, Langer T. Mitochondrial Dynamics and Metabolic Regulation. Trends in Endocrinology & Metabolism. 2016 Feb; 27(2):105–17.

34. Schrepfer E, Scorrano L. Mitofusins, from Mitochondria to Metabolism. Molecular Cell. 2016 Mar; 61 (5):683–94. https://doi.org/10.1016/j.molcel.2016.02.022 PMID: 26942673

35. Hernández-Alvarez MI, Paz JC, Sebastián D, Muñoz JP, Liesa M, Segalés J, et al. Glucocorticoid Modulation of Mitochondrial Function in Hepatoma Cells Requires the Mitochondrial Fission Protein Drp1. Antioxidants & Redox Signaling. 2013 Aug; 19(4):366–78.

36. Sebastian D, Hernandez-Alvarez MI, Segales J, Sorianello E, Munoz JP, Sala D, et al. Mitofusin 2 (Mfn2) links mitochondrial and endoplasmic reticulum function with insulin signaling and is essential for normal glucose homeostasis. Proceedings of the National Academy of Sciences. 2012 Apr 3; 109 (14):5523–8.

37. Hanson RW, Reshef L. Regulation of phosphoenolpyruvate carboxykinase (GTP) gene expression. Annu Rev Biochem. 1997; 66:581–611. https://doi.org/10.1146/annurev.biochem.66.1.581 PMID: 9242918

38. Vijayan MM, Raptis S, Sathiyaa R. Cortisol treatment affects glucocorticoid receptor and glucocorticoid-responsive genes in the liver of rainbow trout. Gen Comp Endocrinol. 2003 Jun 15; 132(2):256–63. PMID: 12812773

39. Mommsen TP, Vijayan MM, Moon TW. Cortisol in teleosts: dynamics, mechanisms of action, and metabolic regulation. Reviews in Fish Biology and Fisheries. 1999 Sep 1; 9(3):211–68.

40. Marandel L, Seiliez I, Véron V, Skiba-Cassy S, Panserat S. New insights into the nutritional regulation of gluconeogenesis in carnivorous rainbow trout (Oncorhynchus mykiss): a gene duplication trail. Physiol Genomics. 2015 Jul; 47(7):253–63. https://doi.org/10.1152/physiolgenomics.00026.2015 PMID: 25901068

41. Kittilson JD, Reindl KM, Sheridan MA. Rainbow trout (Oncorhynchus mykiss) possess two hormone-sensitive lipase-encoding mRNAs that are differentially expressed and independently regulated by

nutritional state. Comp Biochem Physiol, Part A Mol Integr Physiol. 2011 Jan; 158(1):52–60. https://doi.org/10.1016/j.cbpa.2010.09.010 PMID: 20858550

42. Bergan-Roller HE, Ickstadt AT, Kittilson JD, Sheridan MA. Insulin and insulin-like growth factor-1 modulate the lipolytic action of growth hormone by altering signal pathway linkages. Gen Comp Endocrinol. 2017 01; 248:40–8. https://doi.org/10.1016/j.ygcen.2017.04.005 PMID: 28410970

43. Ma M, Yin Z, Zhong H, Liang T, Guo L. Analysis of the expression, function, and evolution of miR-27 isoforms and their responses in metabolic processes. Genomics. In Press https://doi.org/10.1016/j.ygeno.2018.08.004.

44. Calo N, Ramadori P, Sobolewski C, Romero Y, Maeder C, Fournier M, et al. Stress-activated miR-21/miR-21* in hepatocytes promotes lipid and glucose metabolic disorders associated with high-fat diet consumption. Gut. 2016; 65(11):1871–81. https://doi.org/10.1136/gutjnl-2015-310822 PMID: 27222533

45. Xu J., Zhang R., Shen Y., Liu G., Lu X., Wu C.I., 2013a. The evolution of evolvability in microRNA target sites in vertebrates. Genome Res. 23, 1810–1816 https://doi.org/10.1101/gr.148916.112 PMID: 24077390

46. Cora' D, Re A, Caselle M, Bussolino F. MicroRNA-mediated regulatory circuits: outlook and perspectives. Physical Biology. 2017 Jun 6; 14(4):045001. https://doi.org/10.1088/1478-3975/aa6f21 PMID: 28586314

47. Zhang H-M, Kuang S, Xiong X, Gao T, Liu C, Guo A-Y. Transcription factor and microRNA co-regulatory loops: important regulatory motifs in biological processes and diseases. Briefings in Bioinformatics. 2015 Jan 1; 16(1):45–58. https://doi.org/10.1093/bib/bbt085 PMID: 24307685

Chapter 5: Discussion

Cross-study comparison of differentially regulated hepatic miRNAs and their predicted glucoregulatory targets

This chapter will form the basis for a submission of a review paper to be submitted to the special issue "Integrating Epigenomics into the omics of animal Physiology' in The Journal of Comparative Biochemistry and Physiology – Part D: Genomics and Proteomics.

***Statement of contribution**: The social status experimental samples were generated in a collaborative study with Dr. Gilmour at uOttawa. The feeding experimental samples were generated at INRA St.Pée-sur-Nivelle, France. I conducted and analyzed all real-time RT-PCR assays, as well as in silico target prediction analysis of small RNA next generation sequence data.*

5.1. Novel insight into global regulation of hepatic miRNA biogenesis pathway components in rainbow trout

By using *real-time* RT-PCR and Western Blotting approaches, I provided novel evidence of a regulation of the highly conserved miRNA biogenesis pathway under two experimental conditions linked to, among other physiological changes, alterations in glucose metabolism. In general, dietary carbohydrates significantly increased the expression of all profiled miRNA biogenesis components in the liver compared to control, with the exception of *ago2b*. This response is partially, but not fully mimicked by administration of a protein-rich diet devoid of carbohydrates, suggesting that diet composition has an effect different from the process of feeding alone. To our knowledge, rainbow trout and salmonids are the only species described to-date which possess miRNA biogenesis pathway paralogues, since no duplicated miRNA biogenesis genes were retained following teleost-specific genome duplication events (Best *et al.* 2018). We here describe, for the first time a paralogue-specific transcript regulation of miRNA biogenesis genes, which is particularly evident in *xpo5* expression, whose transcripts code for an ATP-dependent transporter involved in *pre-miRNA* export from the nucleus to the cytoplasm. Interestingly, the genome sequences of *xpo5a* and *xpo5b* suggest functional differences in key amino acids forming the pre-miRNA binding pocket, suggesting differential regulation of these paralogues may functionally discriminate and modulate pre-miRNA export to the cytoplasm, the site of final miRNA maturation and target inhibition (Kostyniuk, Marandel, *et al.* 2019). This hypothesis however warrants functional validation. Because dietary carbohydrates are increased at the expense of proteins in the diet, the experimental design is unable to distinguish whether the significant induction of most canonical miRNA biogenesis components is indeed reflective of an increase in circulating glucose or a reduction in dietary protein. However, it is important to note

that both diets were isoenergetic and met rainbow trout protein requirements. If specific changes were indeed predominantly and potently linked to increased carbohydrate levels, then similar changes should be observed in physiological conditions inducing hyperglycemia. When comparing rainbow trout livers of subordinate to dominant fish, an induction of *ago2b* transcript and total Ago2 protein was evident. Interestingly during the preparation of both manuscripts (Kostyniuk, Marandel, *et al.* 2019, Kostyniuk, Zhang, *et al.* 2019), novel evidence implicated hepatic AGO2 levels to be controlled by extracellular glucose levels (Yan *et al.* 2018, Zhang *et al.* 2018). Our hepatic gene expression and protein quantification in rainbow trout experiencing elevated circulating glucose level following nutritional or social stimuli support these findings and suggest this mechanism may be conserved in rainbow trout. However, given the fact that differential paralogues are induced in rainbow trout fed a carbohydrate-rich diet and that protein abundance was not quantified in the nutritional experiment (Kostyniuk, Marandel, *et al.* 2019, Kostyniuk, Zhang, *et al.* 2019), additional experiments are necessary to fully validate this finding. Glucose injection or infusion experiments represent a more direct approach to assess glucose-dependency of Ago2 regulation. Interestingly, hepatic AGO2 does not only appear to be dependent on extracellular glucose concentrations but acts to inhibit the catalytic AMPKα1 subunit expression, thus reducing expression and function of the energy sensor AMPK (Yan *et al.* 2018, Zhang *et al.* 2018). Conversely DROSHA, the rate-limiting enzyme in miRNA biogenesis, has been shown to increase in response to glucose deprivation in an mTOR-dependent manner in human and mouse cell lines (Ye *et al.* 2015), suggesting further interaction between glucose and the canonical miRNA biogenesis pathway. In our nutritional study (Kostyniuk, Marandel, *et al.* 2019), we identified an increase in hepatic *drosha* transcript abundance in response to dietary carbohydrates, suggesting a different response in rainbow trout, possibly linked to the increased

responsiveness of the rainbow trout Tor pathway to proteins compared to carbohydrates (Seiliez *et al.* 2011, Dai *et al.* 2016). Clearly, future studies directly probing the role of the crosstalk between carbohydrates, miRNA biogenesis components energy- and nutrient-sensors are warranted in rainbow trout.

5.2. Conservation of hepatic miRNA regulation under hyperglycemic conditions

In order to determine potentially conserved glucose-responsive hepatic miRNAs in fish, I compared the rainbow trout hepatic miRNA expression profile following dietary modulation of carbohydrates to a hepatic miRNA expression profile in the blunt snout seabream reared on diets differing in digestible carbohydrates (Miao *et al.* 2017). Because the herbivorous blunt snout seabream exhibits, compared to the carnivorous rainbow trout, a higher glucose-tolerance, this comparison is also useful to begin to uncover potential differences in glucose-dependent hepatic miRNA regulation linked to different glucose utilization in fish with different feeding strategies. A total number of 49 differentially expressed miRNA were identified as responsive to dietary carbohydrates in rainbow trout (Kostyniuk, Marandel, *et al.* 2019), while a total of 124 miRNAs were identified as being differentially expressed in response to dietary carbohydrates in Blunt Snout Seabream (Miao *et al.* 2017). In spite of experimental differences, especially the length of the dietary treatment (4 d in rainbow trout, 8 weeks in blunt snout seabream), a total of n=22 miRNAs were identified as being commonly regulated in response to dietary carbohydrates in both species, the equivalent of almost half (45%) of differentially expressed miRNAs in rainbow trout. Together, these data suggest a high degree of conservation of gluco-responsive miRNAs between both fish species, a fact which is further reinforced by the matching directional changes in n=19 of the commonly regulated 22 miRNAs. Three hepatic miRNAs (*ssa-miR-145-3p*; *dre-miR-181a-*

2-3p, *dre-miR-125b-2-3p_L+1_2ss8GA11*) were identified as being differentially regulated by dietary carbohydrates in both rainbow trout and blunt snout bream, making them potential candidates to probe functional differences in gluco-regulation between both fish species. In addition to the regulatory level, it is possible that functional differences of commonly regulated miRNAs arise from rewiring of miRNA-target networks, the divergence of which is currently unknown in fish. In order to further probe the conservation of gluco-responsiveness of identified differentially expressed hepatic miRNAs in rainbow trout, I used additional hepatic small RNA next generation sequencing datasets from obtained mammalian models of hyperglycemia. Of the 22 miRNAs identified as gluco-responsive in both rainbow trout and blunt snout seabream, 11 had previously been identified as being regulated in hyperglycemic conditions in the rodent liver (Kostyniuk, Marandel, *et al.* 2019). Four of those miRNAs exhibit consistent miRNA expression changes (*miRNA-29b-3p*, *miR-30a-5p*, *miRNA-27b-3p*, *miRNA-200-5p*). Interestingly, a role of *miRNA-27b-3p* in gluconeogenic gene regulation has recently been described in alpha mouse liver 12 (AML-12) cells, were transfection with *miRNA-27b-3p* significantly reduced phosphoenolpyruvate carboxykinase and glucose-6 phosphatase protein abundance (Ma *et al.* 2018). Furthermore, increased abundance of circulating *miRNA-27b-3p* has been identified in obese mice and is functionally involved in mediating obese exosome-dependent glucose intolerance in lean animals (Castaño *et al.* 2018). In rainbow trout, the glucose-6-phosphatase paralogue *g6pcb1a* is predicted to be targeted by *miRNA-27b-3p*, suggesting an evolutionarily conserved mode-of action. Indeed, while *miRNA-27b-3p* is induced by high dietary carbohydrate content, its predicted target miRNA *g6pcb1a* is significantly reduced in the same sample (Marandel *et al.* 2015). However future functional studies in rainbow trout are necessary to evaluate this paralogue-specific regulation and its functional significance.

5.3. *In silico*-based prediction of hepatic gluconeogenic target rainbow trout prioritize miRNA-mRNA pairs for future functional validation

Across experiments, differentially regulated hepatic miRNAs were predicted *in silico* to target transcripts enriched in gluconeogenesis function (GO:0006094), indicating that hepatic miRNAs are likely involved in regulating gluconeogenic gene transcript abundance in rainbow trout under physiological conditions linked to an induction in hepatic *de novo* gluconeogenesis. Since the same experimental platform and pipeline was used for small RNA sequencing, a particular advantage of the experimental approach is the possibility to compare miRNA and *in silico*-predicted target gluconeogenesis transcript profiles across nutritional and social status experiments described in Chapters 3 and 4, thus strengthening the evidence for a potential involvement of specific miRNAs in hepatic gluconeogenesis regulation in rainbow trout. Using this approach (**Fig. 5.1**), I identified n=3 specific liver miRNAs (*dre-let-7c-5p*, *dre-miR-92a-3p_R+1*, *ssa-miR-27d-5p*) which are differentially regulated in response to dietary carbohydrates and social stress and are predicted to target at least one gluconeogenic transcript paralogue when using a ΔG cut-off score of -20 kcal/mol.

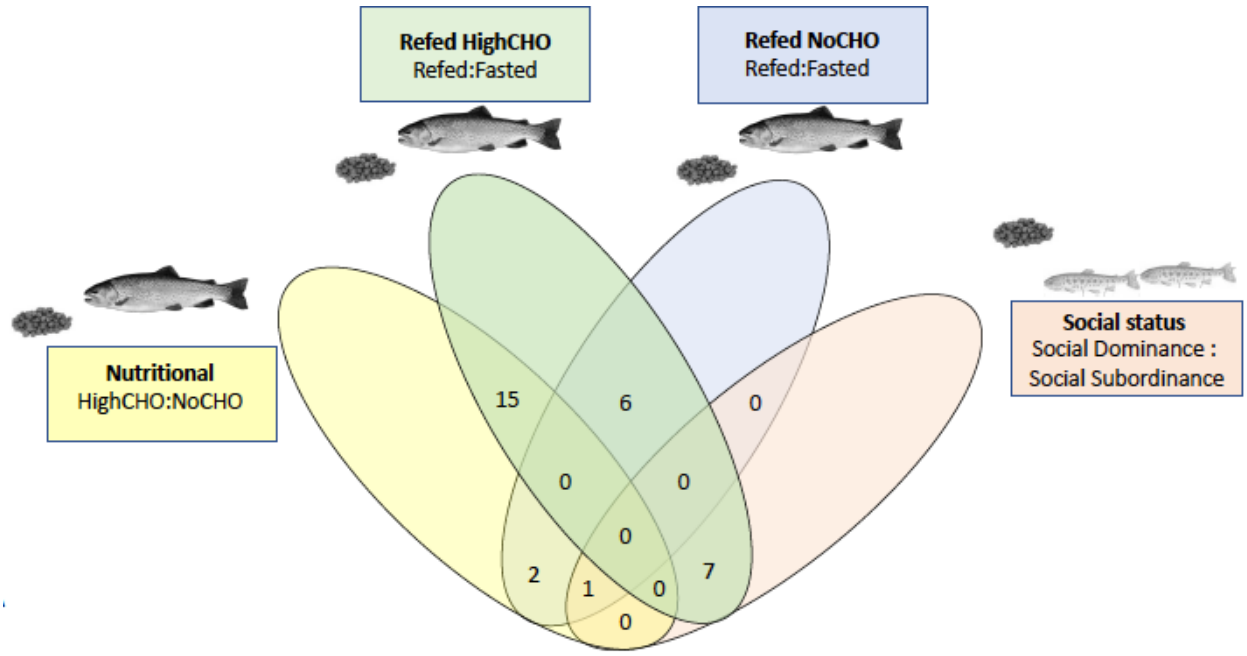

Figure 1. *Venn diagram showing the number of common differentially expressed hepatic miRNAs in rainbow trout in nutritional and social status experiments described in Chapters 3 and 4.*

miRNA *let-7c-5p* is significantly upregulated in both fish fed a carbohydrate rich diet compared to fasted fish and in dominant fish compared to subordinate fish. In the liver samples of diet-induced hyperglycemic fish, in which I identified an induction of *dre-let-7c-5p*, a significant downregulation of the predicted gluconeogenic target *fbp1b1* was observed (Marandel *et al.* 2015), suggesting miRNA-mediated repression of this transcript by *dre-let-7c-5p*. While an induction of *dre-let-7c-5p* was equally observed in dominant fish liver compared to subordinate fish, the quantification of *fbp1b1* in this sample set was not possible because of limitations in RNA availability. Future studies should focus on investigating expression profiles of the *dre-let-7c-5p* and *fbp1b1* pair to further confirm possible consistent posttranscriptional regulation. The *let-7* family of miRNAs (Zhao *et al.* 2017) is one of the first two discovered miRNAs, originally characterized in *C. elegans* (Reinhart *et al.* 2000), and has since been identified to be present in

multiple copies with slight sequence differences (Roush and Slack 2008). The seed region GAGGUAG of the *let-7* family is well conserved not just in fish species but in mammalian models also (Frost and Olson 2011, Lee *et al.* 2016). Members of the *let-7* family differ by one or two nucleotides in positions 10 - 12 and 16 – 19. Due to the conserved seed region, they are nevertheless predicted to share the same targets. Let-7 miRNAs are found in various clusters, where *let-7a*, *miR-100* and *miR-125* form cluster 1, *let-7a*, *let-7d* and *let-7f* form cluster 2 and *let-7a* and *let-7b* form cluster 3 in *H. sapiens* and *D. melanogaster* (Lee *et al.* 2016). These clusters are believed to be the result of vertebrate-specific whole genome duplication events, likely conferring proper regulation and biogenesis of these miRNA (Hertel *et al.* 2012). In Atlantic salmon, the only salmonid species with miRbase deposited sequences reveals the presence of 10 confirmed mature *let-7* miRNA which derive from separate genomic loci.

```
ssa-let-7a-5p      UGAGGUAGUAGGUUGUAUAGUU  22
ssa-let-7b-5p      UGAGGUAGUAGGUUGUGUGGUU  22
ssa-let-7c-5p      UGAGGUAGUAGGUUGUAUGGUU  22
ssa-let-7d-5p      UGAGGUAGUUGGUUGUAUGGUU  22
ssa-let-7e-5p      UGAGGUAGUAGAUUGAAUAGUU  22
ssa-let-7f-5p      UGAGGUAGUAGAUUGUAUUGUU  22
ssa-let-7g-5p      UGAGGUAGUAGUUUGUAUAGUU  22
ssa-let-7h-5p      UGAGGUAGUAAGUUGUGUUGUU  22
ssa-let-7i-5p      UGAGGUAGUAGUUUGUGCUGUU  22
ssa-let-7j-5p      UGAGGUAGUAGGUUGGAUAGUU  22
```

Figure 2. *Atlantic salmon let-7 sequences as retrieved from in miRBase (www.mirbase.org).*

In terms of a regulatory role of *let-7 miRNAs* in gluconeogenesis, *let-7* has, to my knowledge, not been reported to directly regulate gluconeogenic transcripts in more widely studied mammalian species. In trout fed a carbohydrate-rich diet, a significant increase in *dre-let-7c-5p_1_ss19GC* coincides with a decrease in *fbp1b1*. It is therefore unknown, whether the predicted posttranscriptional regulation of gluconeogenic transcripts of *fbp1b1* and *g6pcb2a* is functional

and specific to rainbow trout liver. However potent negative feedback roles on the insulin pathway have been described in mammals in multiple tissues (Frost and Olson 2011, Zhu *et al.* 2011, Gao *et al.* 2014, Kim *et al.* 2017), and potential evolutionarily conserved indirect roles of rainbow trout *let-7* in gluconeogenesis via insulin pathway regulation are discussed in the subsequent section. Of note *dre-let-7c-5p_1_ss19GC* appears to be induced by feeding status (higher in both protein and carbohydrate-fed fish and dominant compared to subordinate fish) rather than glycemic status as previously reported in central and peripheral mammalian tissues (Sangiao-Alvarellos *et al.* 2014, Katayama *et al.* 2015), suggesting a global role in postprandial hepatic energy metabolism regulation following nutritional stimuli.

miRNA *dre-miR-92a-3p_R+1* is significantly downregulated in response to protein-rich diet entirely devoid of carbohydrates and upregulated in the liver of dominant rainbow trout compared to subordinate rainbow trout. Thus, it appears *dre-miR-92a-3p_R+1* abundance is neither directly related to hyperglycemia nor feeding status. The *dre-miR-92a-3p_R+1* transcript is predicted to target the 3'UTR of the *g6pcb2a* transcript, which is increased in response to protein-rich diet and even more in response to a carbohydrate-rich diet. In dominant rainbow trout liver, both *dre-miR-92a-3p_R+1* and *g6pcb2a* transcript are induced. To our knowledge, no report for a direct regulation of gluconeogenic targets exists for *miRNA-92a-3p,* and functional studies are needed to validate a functional role in this context in rainbow trout liver.

miRNA-27d-5p was significantly increased in the liver of both carbohydrate-induced hyperglycemic trout and socially subordinate rainbow trout exhibiting significantly increased glucose concentrations compared to dominant rainbow trout. While the *miRNA-27a* and *miRNA-27b* family is present in most vertebrates, the *miRNA-27* family underwent a teleost-lineage specific expansion yielding additional genes termed *miRNA-27c*, *miRNA-27d* and *miRNA-27e* (Ma

et al. 2018). While regulation by glucose and glucoregulatory roles have been described for *miRNA-27* family members in mammals (Ma *et al.* 2018), my experiments are the first to reveal a consistent induction of the teleost-specific *miRNA-27d-5p* in the liver of rainbow trout exposed to experimental conditions which induce hyperglycemia. Teleost-specific *miRNA-27d-5p* is predicted to post-transcriptionally regulate *pck1*, which is transcriptionally the most responsive gluconeogenic gene paralogue across our experiments, in line with reported transcriptional regulation of cytosolic *pck1* across many species. I propose a negative feedback loop involving *miRNA-27d-5p* which acts to limit gluconeogenesis under hyperglycemic conditions by targeting transcript abundance of *pck1*, the rate-limiting and transcriptionally controlled gluconeogenic enzyme. In my experiments increased expression of *miRNA-27d-5p* correlated with decreased expression of *pck1* in rainbow trout fed a hyperglycemic diet, suggesting active repression. In subordinate rainbow trout a concurrent induction of *miRNA-27d-5p* and *pck1* was observed, and future time-course experiments as well as functional inhibition experiments are warranted to validate this hypothesis. Overall, we report carbohydrate responsiveness of multiple members of the teleost *miRNA-27* family in rainbow trout liver. In addition to *miRNA-27b-3p* and *miRNA-27d-5p*, *miRNA-27c-5p* is also carbohydrate responsive, as it induced in high carbohydrate fed trout liver. Future studies are clearly warranted to dissect the role and function of specific *miRNA-27* family members, especially given the divergence in their target determining seed sequence (**Fig 3**).

A summary of predicted gluconeogenic targets of differentially regulated hepatic miRNAs across experiments is presented in **Table 1**. It is however important to keep in mind that factors other than posttranscriptionally acting miRNAs are at play in physiological situations, and experiments extending to multiple specific timepoints may be needed to resolve kinetics of

miRNA-mRNA target interaction. Finally, miRNAs may, especially in interaction with other factors, result in target mRNA expression patterns other than a downregulation of the target transcript (Best *et al.* 2018).

```
ssa-miR-27a-5p      AGGACUUAGCCAGCUUUGUGAAC-    23
ssa-miR-27d-5p      AGGACUUAG-CACACAUGUGAACA    23
ssa-miR-27b-5p      AGAGCUUAG-CUGAUUGGUGAAC-    22
ssa-miR-27c-5p      AGAGCUUAG-CUAAUUGGUGAG--    21
```

Figure 3. *Atlantic salmon mir-27 sequences as retrieved from in miRBase (www.mirbase.org).*

Table 1. *Predicted gluconeogenic paralogue targets of differentially regulated miRNAs across experiments. 3'UTRs target sequences were retrieved from the MicroTrout database* (Mennigen and Zhang 2016) *and predictions between differentially regulated miRNAs and gluconeogenic target transcripts were generated using the miRanda algorithm with a ΔG cut-off of -20 kcal/mol. Colours indicate directional changes of differentially regulated miRNAs in specific experimental comparisons, where blue indicates a significant down-regulation and red indicates a significant upregulation.*

Experiment	miRNA ID	Target mRNA ID	Score (miRanda)	ΔG (kcal/mol)	miRNA length (nt)	3'UTR length (nt)	Binding Site location in 3'UTR	Target mRNA name
HighCHO vs Fasted	ccr-miR-15a	GSONMT00059643001	158	-20.39	21	571	52	pck2a
HighCHO vs NoCHO	ccr-miR-15a	GSONMT00059643001	158	-20.39	21	571	52	pck2a
NoCHO vs Fasted	dre-let-7c-5p_1ss19GC	GSONMT00063051001	282	-35.06	22	628	508 257	fbp1b1
HighCHO vs Fasted	dre-let-7c-5p_1ss19GC	GSONMT00063051001	282	-35.06	22	628	508 257	fbp1b1
Dom vs Sub	dre-let-7c-5p_1ss19GC	GSONMT00063051001	282	-35.06	22	628	508 257	fbp1b1
HighCHO vs Fasted	dre-miR-130a	GSONMT00063051001	153	-21.17	22	628	563	fbp1b1
HighCHO vs Fasted	dre-miR-142a-3p_L-1R-1	GSONMT00076841001	295	-23.8	21	580	195 554	g6pcb1a
NoCHO vs Fasted	dre-miR-181b-5p_R+1	GSONMT00013076001	303	-34.02	23	2128	1133 1470	g6pcb2a
HighCHO vs Fasted	dre-miR-190a_R+1	GSONMT00076843001	590	-42.05	23	1834	54 419 549 249	g6pca
HighCHO vs NoCHO	dre-miR-190a_R+1	GSONMT00076843001	590	-42.05	23	1834	54 419 549 249	g6pca
HighCHO vs Fasted	dre-miR-190a_R+1	GSONMT00013076001	287	-35.21	23	2128	1643 1037	g6pcb2a
HighCHO vs NoCHO	dre-miR-190a_R+1	GSONMT00013076001	287	-35.21	23	2128	1643 1037	g6pcb2a
HighCHO vs Fasted	dre-miR-27b-3p_R-1	GSONMT00076841001	150	-20.04	21	580	244	g6pcb1a
HighCHO vs NoCHO	dre-miR-27b-3p_R-1	GSONMT00076841001	150	-20.04	21	580	244	g6pcb1a
NoCHO vs Fasted	dre-miR-92a-3p_R+1	GSONMT00013076001	446	-65.4	23	2128	1088 421 1417	g6pcb2a
Dom vs Sub	dre-miR-92a-3p_R+1	GSONMT00013076001	446	-65.4	23	2128	1088 421 1417	g6pcb2a

Dom vs Sub	fru-let-7j_R+1_2ss11TG19AC	GSONMT00063051001	153	-23.32	23	628	506	fbp1b1
HighCHO vs Fasted	fru-miR-221_R-1	GSONMT00076843001	142	-26.06	22	1834	1286	g6pca
NoCHO vs Fasted	fru-miR-7_R+2	GSONMT00014864001	143	-21.87	23	190	13	g6pcb2b
HighCHO vs Fasted	ipu-miR-222a_1ss11TG	GSONMT00013076001	145	-21.9	22	2128	987	g6pcb2a
Dom vs Sub	ipu-miR-338_R-1	GSONMT00076843001	296	-36.94	21	1834	1704 1597	g6pca
NoCHO vs Fasted	ola-miR-101b-5p	GSONMT00015701001	152	-22.93	23	425	297	fbp1b2
HighCHO vs Fasted	ola-miR-101b-5p	GSONMT00015701001	152	-22.93	23	425	297	fbp1b2
NoCHO vs Fasted	ola-miR-101b-5p	GSONMT00013076001	150	-22.23	23	2128	1131	g6pcb2a
HighCHO vs Fasted	ola-miR-101b-5p	GSONMT00013076001	150	-22.23	23	2128	1131	g6pcb2a
NoCHO vs Fasted	ola-miR-101b-5p	GSONMT00063051001	145	-20.24	23	628	199	fbp1b1
HighCHO vs Fasted	ola-miR-101b-5p	GSONMT00063051001	145	-20.24	23	628	199	fbp1b1
HighCHO vs Fasted	ola-miR-27c-5p_L+1R+1_1ss12CA	GSONMT00082468001	151	-20.88	24	660	520	pck1
HighCHO vs Fasted	PC-5p-219_12291	GSONMT00013076001	144	-20.39	18	2128	1114	g6pcb2a
HighCHO vs NoCHO	PC-5p-219_12291	GSONMT00013076001	144	-20.39	18	2128	1114	g6pcb2a
NoCHO vs Fasted	ssa-let-7e-3p_1ss22CT	GSONMT00076843001	148	-20.52	22	1834	713	g6pca
HighCHO vs Fasted	ssa-miR-101b-5p	GSONMT00013076001	292	-37.83	24	2128	1129 1606	g6pcb2a
HighCHO vs Fasted	ssa-miR-101b-5p	GSONMT00015701001	148	-26.03	24	425	294	fbp1b2
HighCHO vs Fasted	ssa-miR-101b-5p	GSONMT00063051001	140	-20.16	24	628	197	fbp1b1
Dom vs Sub	ssa-miR-181b-5p_R-1	GSONMT00066036001	156	-21.13	23	553	316	g6pcb1b
HighCHO vs Fasted	ssa-miR-27d-5p	GSONMT00082468001	146	-21.48	23	660	520	pck1
Dom vs Sub	ssa-miR-27d-5p	GSONMT00082468001	146	-21.48	23	660	520	pck1
HighCHO vs Fasted	ssa-miR-30a-5p	GSONMT00059643001	315	-30.42	23	571	325 458	pck2a
HighCHO vs Fasted	ssa-miR-30a-5p	GSONMT00076843001	150	-21.6	23	1834	990	g6pca
NoCHO vs Fasted	ssa-miR-30c-5p_R+1_1ss24TC	GSONMT00059643001	303	-31.52	25	571	322 457	pck2a
HighCHO vs Fasted	ssa-miR-30e-5p	GSONMT00059643001	315	-31.34	22	571	326 457	pck2a
HighCHO vs NoCHO	ssa-miR-30e-5p	GSONMT00059643001	315	-31.34	22	571	326 457	pck2a
HighCHO vs Fasted	ssa-miR-30e-5p	GSONMT00076843001	145	-20.63	22	1834	991	g6pca
HighCHO vs NoCHO	ssa-miR-30e-5p	GSONMT00076843001	145	-20.63	22	1834	991	g6pca

5.4. Potential post-transcriptional regulation of additional pathways involved in hepatic gluconeogenesis in rainbow trout

In addition to direct effects of hepatic gluconeogenesis gene paralogue expression, differentially expressed miRNAs may affect additional upstream pathways involved in the regulation of gluconeogenesis. Indeed, GO-term based analysis of predicted targets of differentially regulated miRNAs in rainbow trout fed high carbohydrates revealed the insulin signaling pathway as a target (GO:0032868: Response to insulin; GO:0051896: Regulation of Protein Kinase B signaling; GO:0032007: down regulation of TOR signaling pathway) (Kostyniuk, Marandel, *et al.* 2019). In subordinate trout, transcripts with a function in mitochondrial dynamics (GO:0008053: Mitochondrial Fusion) were identified as being targeted by differentially regulated hepatic miRNAs. Because insulin (-pathway)-dependent regulation of hepatic gluconeogenic paralogue gene expression has been described in rainbow trout *in vivo* and

in vitro (Dai *et al.* 2014, 2015, Marandel, Lepais, *et al.* 2016), I correlatively investigated a potential contribution of differentially regulated miRNAs in the regulation of the hepatic insulin pathway. The functionality of the insulin pathway in rainbow trout under different dietary regimes and social status has been partially assessed at the level of cell signaling and gene expression (Kostyniuk, Marandel, *et al.* 2019, Kostyniuk, Zhang, *et al.* 2019). With regard to differentially expressed miRNAs predicted to target specific components of the insulin signaling pathway, the miRNA *let-7*, while predicted to target insulin receptor transcript 3'UTRs in rainbow trout, did not exceed the consistently used ΔG threshold of -20kcal/mol, and functional studies will be necessary to confirm an evolutionarily conserved role of *let-7* in insulin pathway regulation in rainbow trout. The miRNA *dre-miR-181a-2-3p_R+1_1ss20AG* was identified as being upregulated in response to refeeding when comparing both carbohydrate-rich and protein-rich diets to the fasted group and is predicted to target insulin receptor GSONMT00041258001 (ir.3). While this paralogue was not measured, the predicted expression pattern would match the measured transcript abundance pattern of insulin receptor GSONMT00026581001 (ir.1) where the target mRNA was decreased in response to refeeding when comparing both carbohydrate-rich and protein-rich diets to the fasted group, thus suggesting a possible role for *dre-miR-181a-2-3p_R+1_1ss20AG* in the regulation of this transcript (**Table 2**).

Table 2. *Predicted paralogues of genes involved in upstream regulation of gluconeogenesis via the insulin pathway of differentially regulated miRNAs across experiments. 3'UTRs target sequences were retrieved from the MicroTrout database* (Mennigen and Zhang 2016) *and predictions between differentially regulated miRNAs and insulin pathway target transcripts were generated using the miRanda algorithm with a ΔG cut-off of -20 kcal/mol. Colours indicate*

directional changes of differentially regulated miRNAs in specific experimental comparisons, where blue indicates a significant down-regulation and red indicates a significant upregulation

Experiment	miRNA ID	Target mRNA ID	Score (miRanda)	ΔG (kcal/ mol)	miRNA length (nt)	3'UTR length (nt)	Binding Site location in 3'UTR	Target mRNA name
HighCHO vs Fasted	ccr-miR-15a	GSONMT00004538001	142	-20.06	21	2174	2142	tor.2
NoCHO vs Fasted	dre-miR-122_R-1	GSONMT00020383001	149	-20.95	21	711	36	akt2.1
HighCHO vs Fasted	dre-miR-140-3p	GSONMT00020383001	420	-73.86	23	711	345 388 431	akt2.1
HighCHO vs Fasted	dre-miR-140-3p	GSONMT00074353001	285	-34.87	23	1677	1274 182	akt1
HighCHO vs Fasted	dre-miR-140-3p	GSONMT00048327001	161	-21.62	23	406	219	ampk
NoCHO vs Fasted	dre-miR-181a-2-3p_R+1_1ss20AG	GSONMT00041258001	140	-21.51	23	746	230	ir.3
HighCHO vs Fasted	dre-miR-181a-2-3p_R+1_1ss20AG	GSONMT00041258001	140	-21.51	23	746	230	ir.3
NoCHO vs Fasted	dre-miR-181b-5p_R+1	GSONMT00004532001	146	-23.77	23	1440	1380	tor.1
HighCHO vs Fasted	dre-miR-18b-5p_1ss11TC	GSONMT00026581001	307	-42.8	22	1537	1490 553	ir.1
HighCHO vs NoCHO	dre-miR-18b-5p_1ss11TC	GSONMT00026581001	307	-42.8	22	1537	1490 553	ir.1
HighCHO vs Fasted	dre-miR-190a_R+1	GSONMT00026581001	432	-35.09	23	1537	1402 143 72	ir.1
HighCHO vs NoCHO	dre-miR-190a_R+1	GSONMT00026581001	432	-35.09	23	1537	1402 143 72	ir.1
HighCHO vs Fasted	dre-miR-199-3p_L-1	GSONMT00020383001	442	-40.03	21	711	621 672 284	akt2.1
HighCHO vs NoCHO	dre-miR-199-3p_L-1	GSONMT00020383001	442	-40.03	21	711	621 672 284	akt2.1
HighCHO vs Fasted	dre-miR-19a-3p_L+1R-2	GSONMT00004538001	307	-28.25	22	2174	297 53	tor.2
HighCHO vs NoCHO	dre-miR-19a-3p_L+1R-2	GSONMT00004538001	307	-28.25	22	2174	297 53	tor.2
HighCHO vs NoCHO	dre-miR-22a-3p	GSONMT00004538001	295	-34.89	22	2174	511 1942	tor.2
HighCHO vs Fasted	dre-miR-22b-3p	GSONMT00004538001	441	-57.71	22	2174	508 1941 119	tor.2
HighCHO vs NoCHO	dre-miR-22b-3p	GSONMT00004538001	441	-57.71	22	2174	508 1941 119	tor.2
Dom vs Sub	dre-miR-30e-3p	GSONMT00004532001	290	-20.26	22	1440	1 2	tor.1
NoCHO vs Fasted	dre-miR-92a-3p_R+1	GSONMT00074353001	159	-24.27	23	1677	856	akt1
Dom vs Sub	dre-miR-92a-3p_R+1	GSONMT00074353001	159	-24.27	23	1677	856	akt1
NoCHO vs Fasted	fru-miR-200a_R-1	GSONMT00074353001	306	-27.2	21	1677	1556 225	akt1
HighCHO vs NoCHO	fru-miR-200a_R-1	GSONMT00074353001	306	-27.2	21	1677	1556 225	akt1
NoCHO vs Fasted	fru-miR-200a_R-1	GSONMT00004532001	289	-25.86	21	1440	1159 789	tor.1
HighCHO vs NoCHO	fru-miR-200a_R-1	GSONMT00004532001	289	-25.86	21	1440	1159 789	tor.1
NoCHO vs Fasted	fru-miR-200a_R-1	GSONMT00036283001	156	-22.33	21	598	560	akt2.3
HighCHO vs NoCHO	fru-miR-200a_R-1	GSONMT00036283001	156	-22.33	21	598	560	akt2.3
NoCHO vs Fasted	fru-miR-7_R+2	GSONMT00004538001	292	-36.27	23	2174	1565 1294	tor.2
NoCHO vs Fasted	fru-miR-7_R+2	GSONMT00015115001	155	-24.11	23	579	480	irs2.3
HighCHO vs Fasted	ipu-miR-125a	GSONMT00004538001	145	-20.29	22	2174	1051	tor.2
HighCHO vs NoCHO	ipu-miR-125a	GSONMT00004538001	145	-20.29	22	2174	1051	tor.2
NoCHO vs Fasted	ipu-miR-1388_R-1	GSONMT00048327001	144	-25.6	22	406	203	ampk
NoCHO vs Fasted	ola-miR-101a-5p_1ss12AT	GSONMT00038606001	156	-25.4	22	234	31	ir.2
Dom vs Sub	ola-miR-92a_R+4	GSONMT00074353001	160	-24.75	25	1677	853	akt1
HighCHO vs Fasted	ssa-miR-214-3p_L-1_1ss23AT	GSONMT00039521001	159	-24.48	22	451	115	irs1.2
HighCHO vs Fasted	ssa-miR-30a-5p	GSONMT00026581001	425	-25.33	23	1537	1254 1238 1379	ir.1
HighCHO vs Fasted	ssa-miR-30e-5p	GSONMT00026581001	427	-27.69	22	1537	1255 1238 1380	ir.1
HighCHO vs NoCHO	ssa-miR-30e-5p	GSONMT00026581001	427	-27.69	22	1537	1255 1238 1380	ir.1
HighCHO vs Fasted	ssa-miR-7132a-5p	GSONMT00004532001	284	-23.02	22	1440	23 414	tor.1
Dom vs Sub	ssa-miR-7132a-5p	GSONMT00004532001	284	-23.02	22	1440	23 414	tor.1
HighCHO vs Fasted	ssa-miR-722-5p_L-1R+1	GSONMT00026581001	302	-30.15	21	1537	647 854	ir.1

With regard to mitochondrial factors involved in regulating fusion and fission, a consistent induction of *fis1* was observed in fish fed a carbohydrate-rich diet and subordinate fish, both of which exhibit significantly increased circulating glucose levels in comparison to control fish. Indeed, a glucose dependent induction for *fis1* and mitochondrial fission has been observed in

hyperglycemic conditions in mammals (Williams and Caino 2018), suggesting a conserved mechanism in rainbow trout, although functional consequences at the level of mitochondrial dynamics warrant future confirmation. Interestingly, increased mitochondrial fission has been linked to promotion of gluconeogenesis (Hernández-Alvarez *et al.* 2013). Rainbow trout *fis1* (and the mitochondrial fusion factor mitofusin2) are predicted to be targeted by *miRNA-152*, which in turn is differentially expressed in carbohydrate-fed fish and subordinate fish compared to fasted control fish and dominant fish, respectively (**Table 3**). Interestingly, *miRNA-152* has been described to be downregulated in response to glucose in hepatocytes (Zhao *et al.* 2014). Future studies should therefore investigate a role for *miRNA-152* in glucose-dependent regulation of mitochondrial dynamics in rainbow trout and other species.

Table 3. *Predicted paralogues of genes involved in mitochondrial dynamics of differentially regulated miRNAs across experiments. 3'UTRs target sequences were retrieved from the MicroTrout database* (Mennigen and Zhang 2016) *and predictions between differentially regulated miRNAs and mitochondrial dynamics related target transcripts were generated using the miRanda algorithm with a ΔG cut-off of -20 kcal/mol. Colours indicate directional changes of differentially regulated miRNAs in specific experimental comparisons, where blue indicates a significant down-regulation and red indicates a significant upregulation of miRNA abundance.*

Experiment	miRNA ID	Target mRNA ID	Score (miRanda)	ΔG (kcal/ mol)	miRNA length (nt)	3'UTR length (nt)	Binding Site location in 3'UTR	Target mRNA name
HighCHO vs Fasted	ccr-miR-15a	GSONMT00004526001	306	-28.45	21	2325	1409 785	mfn2
HighCHO vs Fasted	ccr-miR-15a	GSONMT00009126001	141	-20.78	21	365	165	opa1
HighCHO vs Fasted	dre-let-7a	GSONMT00027395001	143	-21.89	22	1565	1474	mfn1.1
Dom vs Sub	dre-let-7a	GSONMT00027395001	143	-21.89	22	1565	1474	mfn1.1
HighCHO vs Fasted	dre-let-7c-5p_1ss19GC	GSONMT00027395001	144	-20.37	22	1565	1475	mfn1.1
Dom vs Sub	dre-let-7c-5p_1ss19GC	GSONMT00027395001	144	-20.37	22	1565	1475	mfn1.1
NoCHO vs Fasted	dre-let-7d-5p	GSONMT00027395001	149	-24.31	22	1565	1475	mfn1.1
HighCHO vs Fasted	dre-let-7d-5p	GSONMT00027395001	149	-24.31	22	1565	1475	mfn1.1
NoCHO vs Fasted	dre-miR-181b-5p_R+1	GSONMT00004526001	288	-27.3	23	2325	151 1928	mfn2

HighCHO vs Fasted	dre-miR-18b-5p_1ss11TC	GSONMT00004526001	165	-24.7	22	2325	2254	mfn2
HighCHO vs NoCHO	dre-miR-18b-5p_1ss11TC	GSONMT00004526001	165	-24.7	22	2325	2254	mfn2
NoCHO vs Fasted	dre-miR-19d-3p_1ss13TA	GSONMT00066804001	290	-22.16	23	1730	948 1407	fis1.2
HighCHO vs Fasted	dre-miR-19d-3p_1ss13TA	GSONMT00066804001	290	-22.16	23	1730	948 1407	fis1.2
HighCHO vs Fasted	dre-miR-27b-3p_R-1	GSONMT00066804001	155	-22.15	21	1730	603	fis1.2
HighCHO vs NoCHO	dre-miR-27b-3p_R-1	GSONMT00066804001	155	-22.15	21	1730	603	fis1.2
NoCHO vs Fasted	dre-miR-456_1ss22AT	GSONMT00066804001	288	-47.55	22	1730	1344 906	fis1.2
HighCHO vs Fasted	fru-miR-152	GSONMT00004526001	435	-39.75	22	2325	745 305 723	mfn2
HighCHO vs NoCHO	fru-miR-152	GSONMT00004526001	435	-39.75	22	2325	745 305 723	mfn2
Dom vs Sub	fru-miR-152	GSONMT00004526001	435	-39.75	22	2325	745 305 723	mfn2
HighCHO vs Fasted	fru-miR-152	GSONMT00066804001	306	-31.71	22	1730	1155 1411	fis1.2
HighCHO vs NoCHO	fru-miR-152	GSONMT00066804001	306	-31.71	22	1730	1155 1411	fis1.2
Dom vs Sub	fru-miR-152	GSONMT00066804001	306	-31.71	22	1730	1155 1411	fis1.2
NoCHO vs Fasted	fru-miR-200a_R-1	GSONMT00039888001	290	-29.43	21	1035	720 986	fis1.1
HighCHO vs NoCHO	fru-miR-200a_R-1	GSONMT00039888001	290	-29.43	21	1035	720 986	fis1.1
HighCHO vs Fasted	fru-miR-221_R-1	GSONMT00066804001	284	-27.78	22	1730	332 1708	fis1.2
NoCHO vs Fasted	fru-miR-7_R+2	GSONMT00078240001	296	-36	23	749	174 715	mfn1.2
NoCHO vs Fasted	fru-miR-7_R+2	GSONMT00027395001	298	-32.66	23	1565	145 1	mfn1.1
NoCHO vs Fasted	fru-miR-7_R+2	GSONMT00066804001	286	-31.5	23	1730	295 940	fis1.2
NoCHO vs Fasted	hhi-let-7j	GSONMT00027395001	147	-21.51	22	1565	1474	mfn1.1
HighCHO vs Fasted	ipu-miR-222a_1ss11TG	GSONMT00009126001	140	-21.08	22	365	167	opa1
HighCHO vs NoCHO	ipu-miR-222a_1ss11TG	GSONMT00009126001	140	-21.08	22	365	167	opa1
HighCHO vs Fasted	ola-miR-27c-5p_L+1R+1_1ss12CA	GSONMT00027395001	155	-20.37	24	1565	1499	mfn1.1
HighCHO vs NoCHO	ola-miR-27c-5p_L+1R+1_1ss12CA	GSONMT00027395001	155	-20.37	24	1565	1499	mfn1.1
Dom vs Sub	ola-miR-27d-3p_R+3	GSONMT00078240001	153	-20.64	21	749	389	mfn1.2
Dom vs Sub	pol-miR-21-3p_R-1_1ss14AT	GSONMT00004526001	300	-39.33	21	2325	394 1540	mfn2
Dom vs Sub	pol-miR-21-3p_R-1_1ss14AT	GSONMT00039888001	287	-22.93	21	1035	464 608	fis1.1
HighCHO vs Fasted	ssa-let-7h-3p	GSONMT00004526001	282	-30.22	22	2325	1645 1702	mfn2
HighCHO vs Fasted	ssa-miR-101b-5p	GSONMT00004526001	298	-34.22	24	2325	625 1906	mfn2
HighCHO vs Fasted	ssa-miR-106a-5p	GSONMT00004526001	285	-28.43	22	2325	1392 723	mfn2
HighCHO vs NoCHO	ssa-miR-15a-5p_L-2R+1_1ss18GA	GSONMT00004526001	295	-25.35	22	2325	1408 785	mfn2
HighCHO vs NoCHO	ssa-miR-15a-5p_L-2R+1_1ss18GA	GSONMT00009126001	150	-20.82	22	365	164	opa1
HighCHO vs Fasted	ssa-miR-15b-5p	GSONMT00004526001	293	-22.78	21	2325	1409 785	mfn2
HighCHO vs NoCHO	ssa-miR-16c-5p_R-1	GSONMT00004526001	448	-39.93	21	2325	1408 785 835	mfn2
HighCHO vs Fasted	ssa-miR-17-5p_R-1	GSONMT00004526001	285	-27.34	22	2325	1392 723	mfn2
HighCHO vs Fasted	ssa-miR-214-3p_L-1_1ss23AT	GSONMT00004526001	283	-43.74	22	2325	778 757	mfn2
HighCHO vs Fasted	ssa-miR-214-3p_L-1_1ss23AT	GSONMT00066804001	148	-25.31	22	1730	843	fis1.2
HighCHO vs Fasted	ssa-miR-27d-5p	GSONMT00027395001	143	-20.57	23	1565	1499	mfn1.1
Dom vs Sub	ssa-miR-27d-5p	GSONMT00027395001	143	-20.57	23	1565	1499	mfn1.1
HighCHO vs Fasted	ssa-miR-29b-2-5p_L-2	GSONMT00004526001	290	-24.19	23	2325	797 128	mfn2
Dom vs Sub	ssa-miR-29b-2-5p_L-2	GSONMT00004526001	290	-24.19	23	2325	797 128	mfn2
HighCHO vs Fasted	ssa-miR-29b-2-5p_L-2	GSONMT00078240001	143	-20.52	23	749	572	mfn1.2
Dom vs Sub	ssa-miR-29b-2-5p_L-2	GSONMT00078240001	143	-20.52	23	749	572	mfn1.2
HighCHO vs Fasted	ssa-miR-30a-5p	GSONMT00066804001	301	-34.52	23	1730	661 808	fis1.2
HighCHO vs Fasted	ssa-miR-30e-5p	GSONMT00066804001	294	-28.76	22	1730	666 810	fis1.2
HighCHO vs NoCHO	ssa-miR-30e-5p	GSONMT00066804001	294	-28.76	22	1730	666 810	fis1.2
Dom vs Sub	ssa-miR-93a-5p	GSONMT00009126001	155	-22.38	23	365	178	opa1

5.5. Conclusions

In my thesis, I characterized differentially expressed hepatic miRNAs in rainbow trout exposed to nutritional and social stimuli and employed an *in silico* algorithm in conjunction with correlative target mRNA transcript abundance quantification to infer potential roles for miRNAs in the regulation of hepatic gluconeogenesis via modulation of gluconeogenesis enzyme gene paralogue transcript abundance in rainbow trout. I characterized, for the first time in any species,

a salmonid-specific *pck2* paralogue termed *pck2b*, which is differentially regulated compared to the second mitochondrial *pck* paralogue *pck2a* and the cytoplasmic paralogue *pck1*. The differential regulation of *pck2b* transcript abundance in response to environmental stimuli (dietary carbohydrates, social status, hypoxia) is indicative of potential sub- or neofunctionalization. While physiological consequences of this differential regulation warrant further study, induction of *pck2b* by dietary carbohydrates suggest a contribution of this transcript to the glucose-intolerant phenotype, similarly to the proposed contribution of previously uncharacterized and similarly atypically regulated *g6pcb2* paralogues (Marandel *et al.* 2015).

While miRNAs have been shown to play a crucial role in glucoregulation in mammals (Mirra *et al.* 2018), comparative evidence in other vertebrate species is almost completely lacking. Rainbow trout represent a particularly interesting comparative model to begin to probe miRNA-dependent glucoregulation, as rainbow trout firstly possess a phenotype characterized by a poor utilization of dietary carbohydrates (Panserat *et al.* 2013), and secondly possess a complex genome with several gluconeogenic gene paralogues, whose differential regulation in the liver has been hypothesized to contribute to the observed lack of gluconeogenic repression in response to dietary carbohydrates (Marandel *et al.* 2015, Kostyniuk, Marandel, *et al.* 2019). Because the publication of the rainbow trout genome (Berthelot *et al.* 2014) has made it feasible to probe miRNA regulation (Juanchich *et al.* 2016) and infer potential effects on targeted protein coding transcripts *in silico* (Mennigen 2016, Mennigen and Zhang 2016), the current thesis used a descriptive approach to begin elucidating the regulation and function of hepatic miRNAs in physiological contexts linked to a regulation of hepatic gluconeogenesis. Using this approach, I identified both common and different hepatic miRNAs with predicted gluconeogenesis paralogue as being regulated in rainbow trout liver in nutritional and social contexts linked increased gluconeogenesis and hyperglycemia

(**Table 1**). These results indicate that while some specific miRNA-target gene pairs, such as *miR-27d-5p* and *pck1,* may act as key posttranscriptional switches controlling gluconeogenesis across different physiological conditions in rainbow trout, additional miRNAs may provide a context-specific regulation of the gluconeogenic pathway. This notion is supported by the fact that predicted targets of all miRNAome profiles in the liver are enriched for gluconeogenesis function, in spite of only a relatively small subset of commonly regulated miRNAs (**Table 1**). Interestingly, both teleost-specific and newly described, rainbow trout-specific miRNAs (*PC-5p-219_12291*) were identified as being regulated and predicted to target gluconeogenic mRNA transcripts, suggesting that infraclass- and species-specific miRNAs may contribute to hepatic glucoregulation in rainbow trout. Because miRNAs can regulate multiple targets simultaneously, specific miRNAs can converge on individual target 3'UTRs to additively or synergistically exert posttranscriptional regulation, as evidenced for example by *miRNA-30e-5p*, predicted to target both *pck1* and *g6pca*. Conversely, a single miRNA may potentiate its effect in glucoregulation by targeting additional upstream regulatory components of gluconeogenesis, such as the insulin pathway or components regulating mitochondrial dynamics, in addition to direct regulation of gluconeogenic targets. This scenario is suggested in the case of target predictions for *dre-miR-190a-R+1* predicted to target an insulin receptor transcript in addition to gluconeogenesis transcripts of *g6pca* and *g6pcb2a* **(Figure 4)**. While the current and future comparative analysis of miRNA regulation networks in evolutionarily distant species can simultaneously provide insight into deeply conserved miRNA-target pairs, as well as species-specific innovation via lineage or species-specific miRNAs and/or evolutionary rewiring of different miRNA-mRNA target pairs at the 3'UTR level, functional studies are the next necessary step to probe glucoregulatory function of candidate miRNAs mechanistically. Interestingly, our study as well recent evidence in mammals (Ye *et al.* 2015, Yan

et al. 2018, Zhang *et al.* 2018) suggest that carbohydrates, in addition to affecting differential expression of specific miRNAs, may regulate functional components of the miRNA biogenesis pathway, adding an additional level of complexity to miRNA-dependent glucoregulation. Together these data suggest that, in addition to specific miRNA regulation, global regulation of miRNA biogenesis occurs in response to carbohydrates.

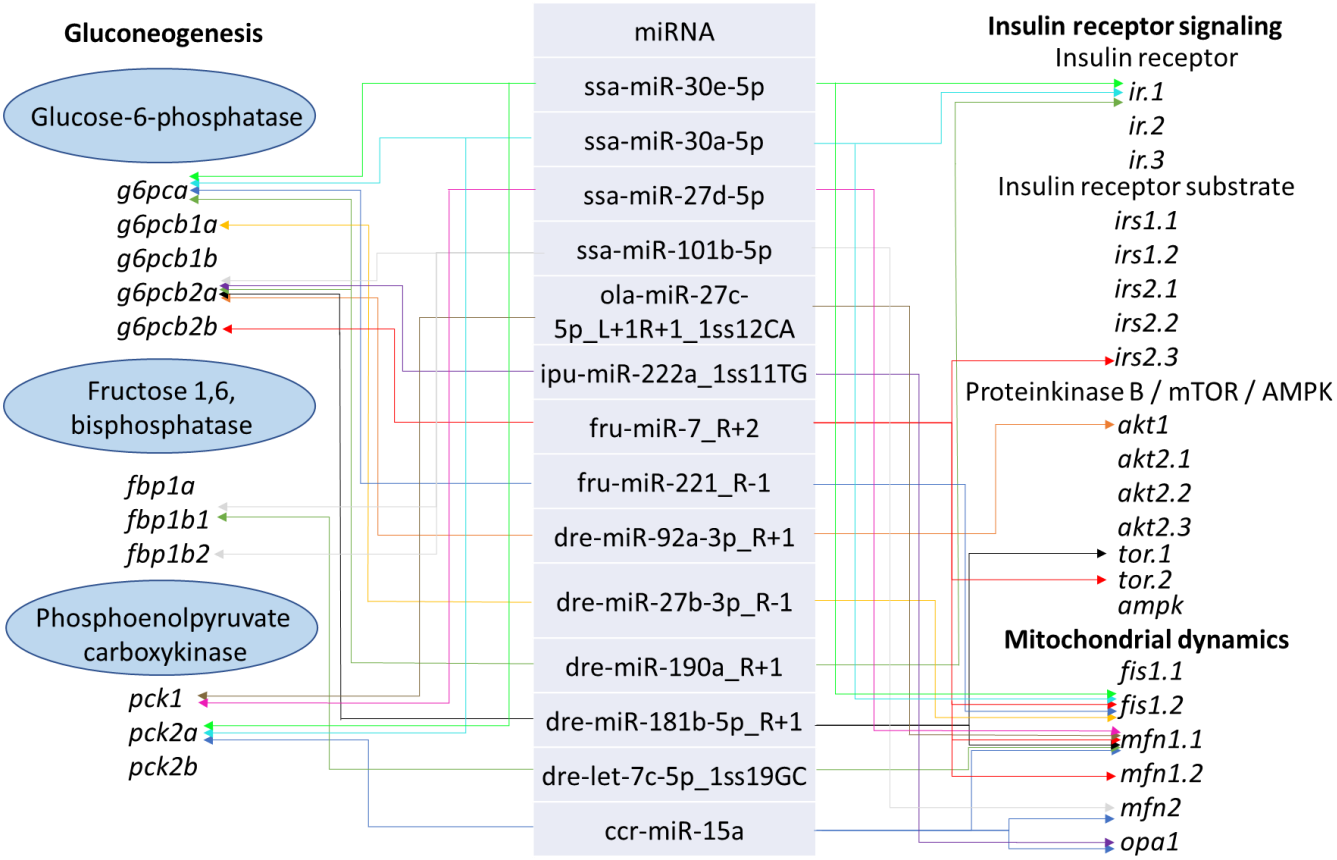

Figure 4. *Relational diagram showing differentially expressed hepatic miRNAs in rainbow trout in nutritional or social status experiments that are predicted to target at least one gluconeogenic and one insulin receptor signaling or mitochondrial dynamics related target mRNA.*

Table 4. *NCBI database accession numbers of described gluconeogenesis, upstream insulin signaling and mitochondrial dynamics paralogues.*

Pathway	Subtype	Target	ID
Gluconeogenesis	Phosphoenolpyruvate carboxykinase	*pck1*	GSONMT00082468001
Gluconeogenesis	Phosphoenolpyruvate carboxykinase	*pck2a*	GSONMT00059643001
Gluconeogenesis	Phosphoenolpyruvate carboxykinase	*pck2b*	GSONMT00051764001
Gluconeogenesis	Glucose-6-phosphatase	*g6pca*	GSONMT00076843001
Gluconeogenesis	Glucose-6-phosphatase	*g6pcb1a*	GSONMT00076841001
Gluconeogenesis	Glucose-6-phosphatase	*g6pcb1b*	GSONMT00066036001
Gluconeogenesis	Glucose-6-phosphatase	*g6pcb2a*	GSONMT00013076001
Gluconeogenesis	Glucose-6-phosphatase	*g6pcb2b*	GSONMT00014864001
Gluconeogenesis	Fructose 1,6, bisphosphatase	*fbp1a*	GSONMT00001932001
Gluconeogenesis	Fructose 1,6, bisphosphatase	*fbp1b1*	GSONMT00063051001
Gluconeogenesis	Fructose 1,6, bisphosphatase	*fbp1b2*	GSONMT00015701001
Insulin receptor signaling	Insulin receptor	*ir.1*	GSONMT00026581001
Insulin receptor signaling	Insulin receptor	*ir.2*	GSONMT00038606001
Insulin receptor signaling	Insulin receptor	*ir.3*	GSONMT00041258001
Insulin receptor signaling	Insulin receptor substrate	*irs1.1*	GSONMT00017704001
Insulin receptor signaling	Insulin receptor substrate	*irs1.2*	GSONMT00039521001
Insulin receptor signaling	Insulin receptor substrate	*irs2.1*	GSONMT00030752001
Insulin receptor signaling	Insulin receptor substrate	*irs2.2*	GSONMT00027021001
Insulin receptor signaling	Insulin receptor substrate	*irs2.3*	GSONMT00015115001
Insulin receptor signaling	Proteinkinase B	*akt1*	GSONMT00074353001
Insulin receptor signaling	Proteinkinase B	*akt2.1*	GSONMT00020383001
Insulin receptor signaling	Proteinkinase B	*akt2.2*	GSONMT00007396001
Insulin receptor signaling	Proteinkinase B	*akt2.3*	GSONMT00036283001
Insulin receptor signaling	TOR	*tor.1*	GSONMT00004532001
Insulin receptor signaling	TOR	*tor.2*	GSONMT00004538001
Insulin receptor signaling	AMPK	*ampk*	GSONMT00048327001
Mitochondrial dynamics	Mitochondrial fission	*fis1.1*	GSONMT00039888001
Mitochondrial dynamics	Mitochondrial fission	*fis1.2*	GSONMT00066804001
Mitochondrial dynamics	Mitofusin	*mfn1.1*	GSONMT00027395001
Mitochondrial dynamics	Mitofusin	*mfn1.2*	GSONMT00078240001
Mitochondrial dynamics	Mitofusin	*mfn2*	GSONMT00004526001
Mitochondrial dynamics	Mitochondrial dynamin like GTPase	*opa1*	GSONMT00009126001

5.6. Limitations and future directions

While I identified several hepatic miRNA with predicted roles in glucoregulation for future functional validation in my thesis, several limitations should be acknowledged. Firstly, while cross comparison across experiments can serve to strengthen the identification of miRNAs predicted to regulate gluconeogenesis, the question of whether commonly regulated miRNAs are directly glucose-dependent cannot be determined by this experimental approach. Indeed, while both dietary carbohydrates and subordinate social status induce a significant increase in circulating dietary carbohydrates, additional factors change in both experiments. For example, the increase in dietary carbohydrates occurs at the expense of a reduction in dietary proteins, and while diets are isoenergetic and minimum protein requirements are met in either case, it remains possible that the reduction in proteins / amino acids plays, at least in part, a role in the differential regulation of hepatic miRNAs. Similarly, in addition to an increase in circulating glucose due to gluconeogenesis in subordinate trout, several other factors are significantly altered in subordinate trout compared to dominant counterparts, including a significant reduction in feed intake and a significant increase in circulating cortisol. Therefore, in order to provide additional support for a direct glucose-dependent regulation of identified specific miRNAs, i.p injection of glucose *in vivo* or glucose application to rainbow trout primary hepatocytes or rainbow trout hepatic cell lines such as SOB-15 (Castro *et al.* 2014, Bols *et al.* 2017) *in vitro* should be coupled with targeted miRNA *real-time* RT-PCR approaches.

A second current limitation depends on the functional interaction between differentially regulated miRNAs and glucoregulatory targets. Because miRNA-target interactions are promiscuous, transcriptome level computational approaches have become a popular choice to gain

insight into miRNA-dependent posttranscriptional regulation. While circumventing the problem of the unfeasibility to experimentally probe all possible miRNA-target interactions, it is well known that *in silico* based prediction methods inevitably suffer from limitations related to accuracy and/or precision (Peterson *et al.* 2014). With regard to experimental designs, a single time-point may not capture complex miRNA target transcript temporal dynamics, especially given recent observations of different half-lives in the miRNA population (Marzi *et al.* 2016). Additionally, as one of many processes regulating transcript abundance, additional well-known (e.g. transcription factors) and emerging (epigenetic mechanisms such as DNA methylation and histone modifications) mechanisms cannot be excluded. Indeed, recent studies reveal that simple feedback loops that include transcription factors can result, in addition to an inverse correlation in expression between miRNA and mRNA pair, result in stabilizing or even positive correlation in miRNA and target mRNA expression (Zhang *et al.* 2015, Cora *et al.* 2017). Additionally, miRNAs may, depending on the time of the interaction, affect protein translation prior to mRNA abundance (Wilczynska and Bushell 2015). Therefore, while the scope of the current thesis was to identify and prioritize miRNAs for future investigation in hepatic rainbow trout glucoregulation, functional studies are clearly warranted to unequivocally demonstrate a functional involvement of specific identified hepatic miRNAs in rainbow trout glucoregulation. Several approaches are available to do so. Firstly, especially given the recently reported link between AGO2 and circulating glucose concentrations (Zeng *et al.* n.d., Yan *et al.* 2018) which is in line with our reported increases in *ago2* transcript abundance and or Ago2 protein level in carbohydrate-fed and subordinate trout characterized by increased glucose concentrations, a RIP-ChiP based approach (Wang *et al.* 2010) would provide an elegant approach to probe which specific miRNAs and mRNAs are actively bound to Ago2 in dietary and social status experiments. Enrichment of bound miRNAs and

mRNAs can be assessed both globally at the transcriptome levels, however given the predicted relationship a targeted real-time RT-PCR based approach would be warranted.

In order to probe physical interaction of miRNA and mRNA targets through complimentary binding, *in vitro* approaches using commercially available rainbow trout cell lines such as SOB15 should be used in a luciferase approach. As rainbow trout 3'UTRs are available (Mennigen 2016) cloning these elements into specific luciferase reporter plasmids to probe miRNA inhibition through transfection assays represents a logical next step. Finally, in order to probe not only interaction, but also functional roles of candidate miRNAs in regulation of gluconeogenesis, miRNA mimics or antagonists can be used in rainbow trout hepatocyte transfection and mRNA, protein levels, enzymatic activities and glucose secretion in the medium can be profiled. This approach is equally useful to profile potential upstream involvement of the insulin signaling pathway, since insulin cell signaling markers have been widely used both *in vivo* and *in vitro* in rainbow trout (Plagnes-Juan *et al.* 2008, Mennigen, Plagnes-Juan, *et al.* 2014). Finally, because other tissues are crucially involved in rainbow trout glucoregulation, longer-term studies should investigate miRNA-dependent regulation of glucose metabolism in additional tissues, such as muscle, adipose tissue, Brockmann bodies and the brain (Mennigen 2016). Since circulating miRNAs, including *miRNA-27b-3p*, have recently been shown to coordinate glucoregulation in obese mice by acting as endocrine signal (Castaño *et al.* 2018), available rainbow trout double cannulation infusion approaches (Forbes *et al.* 2019) have the potential to address this novel type of endocrine regulation in this species in real-time.

References

Bartel, D.P., 2009. MicroRNAs: Target Recognition and Regulatory Functions. *Cell*, 136 (2), 215–233.

Bergot, F., 1979. Effects of dietary carbohydrates and of their mode of distribution on glycaemia in rainbow trout (Salmo gairdneri richardson). *Comparative Biochemistry and Physiology Part A: Physiology*, 64 (4), 543–547.

Berthelot, C., Brunet, F., Chalopin, D., Juanchich, A., Bernard, M., Noël, B., Bento, P., Da Silva, C., Labadie, K., Alberti, A., Aury, J.-M., Louis, A., Dehais, P., Bardou, P., Montfort, J., Klopp, C., Cabau, C., Gaspin, C., Thorgaard, G.H., Boussaha, M., Quillet, E., Guyomard, R., Galiana, D., Bobe, J., Volff, J.-N., Genêt, C., Wincker, P., Jaillon, O., Crollius, H.R., and Guiguen, Y., 2014. The rainbow trout genome provides novel insights into evolution after whole-genome duplication in vertebrates. *Nature Communications*, 5 (1), 3657.

Best, C., Ikert, H., Kostyniuk, D.J., Craig, P.M., Navarro-Martin, L., Marandel, L., and Mennigen, J.A., 2018. Epigenetics in teleost fish: From molecular mechanisms to physiological phenotypes. *Comparative Biochemistry and Physiology Part B: Biochemistry and Molecular Biology*, 224, 210–244.

Blasco, J., Marimón, I., Viaplana, I., and Fernández-Borrás, J., 2001. Fate of plasma glucose in tissues of brown trout in vivo: effects of fasting and glucose loading. *Fish Physiology and Biochemistry*, 24 (3), 247–258.

Bobe, J., Marandel, L., Panserat, S., Boudinot, P., Berthelot, C., Quillet, E., Volff, J.N., Genêt, C., Jaillon, O., Crollius, H.R., and Guiguen, Y., 2016. The rainbow trout genome, an important landmark foraquaculture and genome evolution. *In*: *Genomics in Aquaculture*. Elsevier Inc., 21–43.

Bols, N.C., Pham, P.H., Dayeh, V.R., and Lee, L.E.J., 2017. Invitromatics, invitrome, and invitroomics: introduction of three new terms for in vitro biology and illustration of their use with the cell lines from rainbow trout. *In Vitro Cellular and Developmental Biology - Animal*.

Bucking, C. and Wood, C.M., 2005. Renal regulation of plasma glucose in the freshwater rainbow trout. *The Journal of experimental biology*, 208 (Pt 14), 2731–9.

Castaño, C., Kalko, S., Novials, A., and Párrizas, M., 2018. Obesity-associated exosomal miRNAs modulate glucose and lipid metabolism in mice. *Proceedings of the National Academy of Sciences of the United States of America*, 115 (48), 12158–12163.

Castro, R., Abós, B., Pignatelli, J., von Gersdorff Jørgensen, L., González Granja, A., Buchmann, K., and Tafalla, C., 2014. Early Immune Responses in Rainbow Trout Liver upon Viral Hemorrhagic Septicemia Virus (VHSV) Infection. *PLoS ONE*, 9 (10), e111084.

Chen, P.-S., Su, J.-L., Cha, S.-T., Tarn, W.-Y., Wang, M.-Y., Hsu, H.-C., Lin, M.-T., Chu, C.-Y., Hua, K.-T., Chen, C.-N., Kuo, T.-C., Chang, K.-J., Hsiao, M., Chang, Y.-W., Chen, J.-S., Yang, P.-C., and Kuo, M.-L., 2011. miR-107 promotes tumor progression by targeting the let-7 microRNA in mice and humans. *The Journal of Clinical Investigation*, 121 (9).

Choi, K. and Weber, J.-M.J.-M., 2015. Pushing the limits of glucose kinetics: how rainbow trout cope with a carbohydrate overload. *The Journal of experimental biology*, 218 (18), 2873–80.

Cora, D., Re, A., Caselle, M., and Bussolino, F., 2017. MicroRNA-mediated regulatory circuits: outlook and perspectives. *Physical Biology*, 14 (4), 045001.

Culbert, B.M. and Gilmour, K.M., 2016. Rapid recovery of the cortisol response following social subordination in rainbow trout. *Physiology & Behavior*, 164, 306–313.

Dai, W., Panserat, S., Kaushik, S., Terrier, F., Plagnes-Juan, E., Seiliez, I., and Skiba-Cassy, S., 2016. Hepatic fatty acid biosynthesis is more responsive to protein than carbohydrate in rainbow trout during acute stimulations. *American journal of physiology. Regulatory, integrative and comparative physiology*, 310 (1), R74-86.

Dai, W., Panserat, S., Mennigen, J.A., Terrier, F., Dias, K., Seiliez, I., and Skiba-Cassy, S., 2013. Post-prandial regulation of hepatic glucokinase and lipogenesis requires the activation of TORC1 signalling in rainbow trout (Oncorhynchus mykiss). *The Journal of experimental biology*, 216 (Pt 23), 4483–4492.

Dai, W., Panserat, S., Plagnes-Juan, E., Seiliez, I., and Skiba-Cassy, S., 2015. Amino Acids Attenuate Insulin Action on Gluconeogenesis and Promote Fatty Acid Biosynthesis via mTORC1 Signaling

Pathway in trout Hepatocytes. *Cellular Physiology and Biochemistry*, 36 (3), 1084–1100.

Dai, W., Panserat, S., Terrier, F., Seiliez, I., and Skiba-Cassy, S., 2014. Acute rapamycin treatment improved glucose tolerance through inhibition of hepatic gluconeogenesis in rainbow trout (*Oncorhynchus mykiss*). *American Journal of Physiology-Regulatory, Integrative and Comparative Physiology*, 307 (10), R1231–R1238.

Desvergne, B., Michalik, L., and Wahli, W., 2006. Transcriptional Regulation of Metabolism. *Physiological Reviews*, 86 (2), 465–514.

DiBattista, J.D.D., Levesque, H.M.M., Moon, T.W.W., and Gilmour, K.M.M., 2006. Growth Depression in Socially Subordinate Rainbow Trout *Oncorhynchus mykiss* : More than a Fasting Effect. *Physiological and Biochemical Zoology*, 79 (4), 675–687.

Dumortier, O., Hinault, C., and Van Obberghen, E., 2013. MicroRNAs and Metabolism Crosstalk in Energy Homeostasis. *Cell Metabolism*, 18 (3), 312–324.

Fabian, M.R., Sonenberg, N., and Filipowicz, W., 2010. Regulation of mRNA Translation and Stability by microRNAs. *Annual Review of Biochemistry*, 79 (1), 351–379.

Forbes, J.L.I.I., Kostyniuk, D.J., Mennigen, J.A., and Weber, J.-M., 2019. Unexpected effect of insulin on glucose disposal explains glucose intolerance in trout. *American Journal of Physiology-Regulatory, Integrative and Comparative Physiology*, 316 (4), ajpregu.00344.2018.

Frost, R.J.A. and Olson, E.N., 2011. Control of glucose homeostasis and insulin sensitivity by the Let-7 family of microRNAs. *Proceedings of the National Academy of Sciences of the United States of America*, 108 (52), 21075–80.

Gao, Y., Wu, F., Zhou, J., Yan, L., Jurczak, M.J., Lee, H.-Y., Yang, L., Mueller, M., Zhou, X.-B., Dandolo, L., Szendroedi, J., Roden, M., Flannery, C., Taylor, H., Carmichael, G.G., Shulman, G.I., and Huang, Y., 2014. The H19/let-7 double-negative feedback loop contributes to glucose metabolism in muscle cells. *Nucleic Acids Research*, 42 (22), 13799–13811.

Gilmour, K.M., Craig, P.M., Dhillon, R.S., Lau, G.Y., and Richards, J.G., 2017. Regulation of energy metabolism during social interactions in rainbow trout: A role for AMP-activated protein kinase.

American Journal of Physiology - Regulatory Integrative and Comparative Physiology, 313 (5), R549–R559.

Gilmour, K.M., Dibattista, J.D., and Thomas, J.B., 2005. Physiological Causes and Consequences of Social Status in Salmonid Fish. *Intergrative and Comparative Biology*, 273 (2), 263–273.

Gilmour, K.M., Kirkpatrick, S., Massarsky, A., Pearce, B., Saliba, S., Lise, C.-É., Thomas, S., Moon, W., Stephany, C.-É., and Moon, T.W., 2012. The Influence of Social Status on Hepatic Glucose Metabolism in Rainbow Trout Oncorhynchus mykiss. *Physiological and Biochemical Zoology*, 85 (4), 309–320.

Hahn, M.W., 2009. Distinguishing Among Evolutionary Models for the Maintenance of Gene Duplicates. *Journal of Heredity*, 100 (5), 605–617.

Haman, F., Powell, M., and Weber, J., 1997. Reliability of continuous tracer infusion for measuring glucose turnover rate in rainbow trout. *Journal of Experimental Biology*, 200 (19).

He, L. and Hannon, G.J., 2004. MicroRNAs: small RNAs with a big role in gene regulation. *Nature Reviews Genetics*, 5 (7), 522–531.

Hernández-Alvarez, M.I., Paz, J.C., Sebastián, D., Muñoz, J.P., Liesa, M., Segalés, J., Palacín, M., and Zorzano, A., 2013. Glucocorticoid Modulation of Mitochondrial Function in Hepatoma Cells Requires the Mitochondrial Fission Protein Drp1. *Antioxidants & Redox Signaling*, 19 (4), 366–378.

Herrera, B.M., Lockstone, H.E., Taylor, J.M., Ria, M., Barrett, A., Collins, S., Kaisaki, P., Argoud, K., Fernandez, C., Travers, M.E., Grew, J.P., Randall, J.C., Gloyn, A.L., Gauguier, D., McCarthy, M.I., and Lindgren, C.M., 2010. Global microRNA expression profiles in insulin target tissues in a spontaneous rat model of type 2 diabetes. *Diabetologia*, 53 (6), 1099–1109.

Hertel, J., Bartschat, S., Wintsche, A., Otto, C., of the Bioinformatics Computer Lab, T.S., and Stadler, P.F., 2012. Evolution of the let-7 microRNA Family. *RNA Biology*, 9 (3), 231–241.

Horie, T., Ono, K., Horiguchi, M., Nishi, H., Nakamura, T., Nagao, K., Kinoshita, M., Kuwabara, Y., Marusawa, H., Iwanaga, Y., Hasegawa, K., Yokode, M., Kimura, T., and Kita, T., 2010. MicroRNA-33 encoded by an intron of sterol regulatory element-binding protein 2 (Srebp2)

regulates HDL in vivo. *Proceedings of the National Academy of Sciences of the United States of America*, 107 (40), 17321–6.

Juanchich, A., Bardou, P., Rué, O., Gabillard, J.-C., Gaspin, C., Bobe, J., and Guiguen, Y., 2016. Characterization of an extensive rainbow trout miRNA transcriptome by next generation sequencing. *BMC Genomics*, 17 (1), 164.

Katayama, M., Sjögren, R.J.O., Egan, B., and Krook, A., 2015. MiRNA let-7 expression is regulated by glucose and TNF-α by a remote upstream promoter. *Biochemical Journal*, 472 (2), 147–156.

Kim, J.D., Toda, C., Ramírez, C.M., Fernández-Hernando, C., and Diano, S., 2017. Hypothalamic ventromedial Lin28a enhances glucose metabolism in diet-induced obesity. *Diabetes*, 66 (8), 2102–2111.

Kirchner, S., Kaushik, S., and Panserat, S., 2003. Low Protein Intake Is Associated with Reduced Hepatic Gluconeogenic Enzyme Expression in Rainbow Trout (Oncorhynchus mykiss). *The Journal of Nutrition*, 133 (8), 2561–2564.

Kostyniuk, D.J., Culbert, B.M., Mennigen, J.A., and Gilmour, K.M., 2018. Social status affects lipid metabolism in rainbow trout, *Oncorhynchus mykiss*. *American Journal of Physiology-Regulatory, Integrative and Comparative Physiology*, 315 (2), R241–R255.

Kostyniuk, D.J., Marandel, L., Jubouri, M., Dias, K., de Souza, R.F., Zhang, D., Martyniuk, C.J., Panserat, S., and Mennigen, J.A., 2019. Profiling the rainbow trout hepatic miRNAome under diet-induced hyperglycemia. *Physiological Genomics*, 51 (9), 411–431.

Kostyniuk, D.J., Zhang, D., Martyniuk, C.J., Gilmour, K.M., and Mennigen, J.A., 2019. Social status regulates the hepatic miRNAome in rainbow trout: Implications for posttranscriptional regulation of metabolic pathways. *PLOS ONE*, 14 (6), e0217978.

Lai, X. and Vera, J., 2013. MicroRNA Clusters. *In*: *Encyclopedia of Systems Biology*. New York, NY: Springer New York, 1310–1314.

Lee, H., Han, S., Kwon, C.S., and Lee, D., 2016. Biogenesis and regulation of the let-7 miRNAs and their functional implications. *Protein & Cell*, 7 (2), 100–113.

Lee, Y., Han, J., Yeom, K.-H., Jin, H., and Kim, V.N., 2006. Drosha in primary microRNA processing. *Cold Spring Harbor symposia on quantitative biology*, 71, 51–7.

Legate, N.J., Bonen, A., and Moon, T.W., 2001. Glucose Tolerance and Peripheral Glucose Utilization in Rainbow Trout (Oncorhynchus mykiss), American Eel (Anguilla rostrata), and Black Bullhead Catfish (Ameiurus melas). *General and Comparative Endocrinology*, 122 (1), 48–59.

Li, K., Zhang, J., Yu, J., Liu, B., Guo, Y., Deng, J., Chen, S., Wang, C., and Guo, F., 2015. MicroRNA-214 suppresses gluconeogenesis by targeting activating transcriptional factor 4. *Journal of Biological Chemistry*, 290 (13), 8185–8195.

Li, S., Chen, X., Zhang, H., Liang, X., Xiang, Y., Yu, C., Zen, K., Li, Y., and Zhang, C.-Y., 2009. Differential expression of microRNAs in mouse liver under aberrant energy metabolic status. *Journal of Lipid Research*, 50 (9), 1756–1765.

Lien, S., Koop, B.F., Sandve, S.R., Miller, J.R., Kent, M.P., Nome, T., Hvidsten, T.R., Leong, J.S., Minkley, D.R., Zimin, A., Grammes, F., Grove, H., Gjuvsland, A., Walenz, B., Hermansen, R.A., von Schalburg, K., Rondeau, E.B., Di Genova, A., Samy, J.K.A., Olav Vik, J., Vigeland, M.D., Caler, L., Grimholt, U., Jentoft, S., Inge Våge, D., de Jong, P., Moen, T., Baranski, M., Palti, Y., Smith, D.R., Yorke, J.A., Nederbragt, A.J., Tooming-Klunderud, A., Jakobsen, K.S., Jiang, X., Fan, D., Hu, Y., Liberles, D.A., Vidal, R., Iturra, P., Jones, S.J.M., Jonassen, I., Maass, A., Omholt, S.W., and Davidson, W.S., 2016. The Atlantic salmon genome provides insights into rediploidization. *Nature*, 533 (7602), 200–205.

Ma, M., Yin, Z., Zhong, H., Liang, T., and Guo, L., 2018. Analysis of the expression, function, and evolution of miR-27 isoforms and their responses in metabolic processes. *Genomics*.

Macqueen, D.J., Primmer, C.R., Houston, R.D., Nowak, B.F., Bernatchez, L., Bergseth, S., Davidson, W.S., Gallardo-Escárate, C., Goldammer, T., Guiguen, Y., Iturra, P., Kijas, J.W., Koop, B.F., Lien, S., Maass, A., Martin, S.A.M., McGinnity, P., Montecino, M., Naish, K.A., Nichols, K.M., Ólafsson, K., Omholt, S.W., Palti, Y., Plastow, G.S., Rexroad, C.E., Rise, M.L., Ritchie, R.J., Sandve, S.R., Schulte, P.M., Tello, A., Vidal, R., Vik, J.O., Wargelius, A., and Yáñez, J.M., 2017.

Functional Annotation of All Salmonid Genomes (FAASG): An international initiative supporting future salmonid research, conservation and aquaculture. *BMC Genomics*.

Mannerstrom, M., Soivio, A., and Salama, A., 2001. Intestinal absorption and tissue distribution of glucose and isoleucine in rainbow trout (Oncorhynchus mykiss). *Aquaculture Nutrition*, 7 (4), 229–235.

Marandel, L., Dai, W., Panserat, S., and Skiba-Cassy, S., 2016. The five glucose-6-phosphatase paralogous genes are differentially regulated by insulin alone or combined with high level of amino acids and/or glucose in trout hepatocytes. *Molecular Biology Reports*, 43 (4), 207–211.

Marandel, L., Kostyniuk, D.J., Best, C., Forbes, J.L.I., Liu, J., Panserat, S., and Mennigen, J.A., 2019. Pck-ing up steam: Widening the salmonid gluconeogenic gene duplication trail. *Gene*, 698, 129–140.

Marandel, L., Lepais, O., Arbenoits, E., Véron, V., Dias, K., Zion, M., and Panserat, S., 2016. Remodelling of the hepatic epigenetic landscape of glucose-intolerant rainbow trout (Oncorhynchus mykiss) by nutritional status and dietary carbohydrates. *Scientific Reports*, 6 (1), 32187.

Marandel, L., Seiliez, I., Véron, V., Skiba-Cassy, S., and Panserat, S., 2015. New insights into the nutritional regulation of gluconeogenesis in carnivorous rainbow trout (*Oncorhynchus mykiss*): a gene duplication trail. *Physiological Genomics*, 47 (7), 253–263.

Marzi, M.J., Ghini, F., Cerruti, B., de Pretis, S., Bonetti, P., Giacomelli, C., Gorski, M.M., Kress, T., Pelizzola, M., Muller, H., Amati, B., and Nicassio, F., 2016. Degradation dynamics of microRNAs revealed by a novel pulse-chase approach. *Genome research*, 26 (4), 554–65.

Mennigen, J.A., 2016. Micromanaging metabolism—a role for miRNAs in teleost energy metabolism. *Comparative Biochemistry and Physiology Part - B: Biochemistry and Molecular Biology*, 199, 115–125.

Mennigen, J.A., Martyniuk, C.J., Seiliez, I., Panserat, S., and Skiba-Cassy, S., 2014. Metabolic consequences of microRNA-122 inhibition in rainbow trout, Oncorhynchus mykiss. *BMC Genomics*, 15 (70), 70.

Mennigen, J.A., Plagnes-Juan, E., Figueredo-Silva, C.A., Seiliez, I., Panserat, S., and Skiba-Cassy, S., 2014. Acute endocrine and nutritional co-regulation of the hepatic omy-miRNA-122b and the lipogenic gene fas in rainbow trout, Oncorhynchus mykiss. *Comparative Biochemistry and Physiology Part B: Biochemistry and Molecular Biology*, 169, 16–24.

Mennigen, J.A. and Zhang, D., 2016. MicroTrout: A comprehensive, genome-wide miRNA target prediction framework for rainbow trout, Oncorhynchus mykiss. *Comparative Biochemistry and Physiology Part D: Genomics and Proteomics*, 20, 19–26.

Metcalfe, N.B., 1986. Intraspecific variation in competitive ability and food intake in salmonids: consequences for energy budgets and growth rates. *Journal of Fish Biology*, 28 (5), 525–531.

Miao, L.-H., Lin, Y., Pan, W.-J., Huang, X., Ge, X.-P., Ren, M.-C., Zhou, Q.-L., Liu, B., Miao, L.-H., Lin, Y., Pan, W.-J., Huang, X., Ge, X.-P., Ren, M.-C., Zhou, Q.-L., and Liu, B., 2017. Identification of Differentially Expressed Micrornas Associate with Glucose Metabolism in Different Organs of Blunt Snout Bream (Megalobrama amblycephala). *International Journal of Molecular Sciences*, 18 (6), 1161.

Mirra, P., Nigro, C., Prevenzano, I., Leone, A., Raciti, G.A., Formisano, P., Beguinot, F., and Miele, C., 2018. The Destiny of Glucose from a MicroRNA Perspective. *Frontiers in Endocrinology*, 9, 46.

Miyamoto, T. and Amrein, H., 2017. Gluconeogenesis: An ancient biochemical pathway with a new twist. *Fly*, 11 (3), 218–223.

Moon, T.W., 2001. Glucose intolerance in teleost fish: fact or fiction? *Comparative Biochemistry and Physiology Part B: Biochemistry and Molecular Biology*, 129 (2–3), 243–249.

Naylor, R.L., Hardy, R.W., Bureau, D.P., Chiu, A., Elliott, M., Farrell, A.P., Forster, I., Gatlin, D.M., Goldburg, R.J., Hua, K., and Nichols, P.D., 2009. Feeding aquaculture in an era of finite resources. *Proceedings of the National Academy of Sciences of the United States of America*, 106 (36), 15103–10.

Nigi, L., Grieco, G., Ventriglia, G., Brusco, N., Mancarella, F., Formichi, C., Dotta, F., and Sebastiani, G., 2018. MicroRNAs as Regulators of Insulin Signaling: Research Updates and Potential

Therapeutic Perspectives in Type 2 Diabetes. *International Journal of Molecular Sciences*, 19 (12), 3705.

Panserat, S., Kaushik, S., and Médale, F., 2013. *Rainbow trout as a model for nutrition and nutrient metabolism studies. In: Trout: from physiology to conservation*. Saint-Pée-sur-Nivelle, France: Nova Science Publishers, Inc.

Panserat, S., Médale, F., Blin, C., Brèque, J., Vachot, C., Plagnes-Juan, E., Gomes, E., Krishnamoorthy, R., and Kaushik, S., 2000. Hepatic glucokinase is induced by dietary carbohydrates in rainbow trout, gilthead seabream, and common carp. *American Journal of Physiology-Regulatory, Integrative and Comparative Physiology*, 278 (5), R1164–R1170.

Panserat, S., Skiba-Cassy, S., Seiliez, I., Lansard, M., Plagnes-Juan, E., Vachot, C., Aguirre, P., Larroquet, L., Chavernac, G., Medale, F., Corraze, G., Kaushik, S., and Moon, T.W., 2009. Metformin improves postprandial glucose homeostasis in rainbow trout fed dietary carbohydrates: a link with the induction of hepatic lipogenic capacities? *American Journal of Physiology-Regulatory, Integrative and Comparative Physiology*, 297 (3), R707–R715.

Pereira, C., Vijayan, M.M., Storey, K.B., Jones, R.A., and Moon, T.W., 1995. Role of glucose and insulin in regulating glycogen synthase and phosphorylase activities in rainbow trout hepatocytes. *Journal of Comparative Physiology B*, 165 (1), 62–70.

Peterson, S.M., Thompson, J.A., Ufkin, M.L., Sathyanarayana, P., Liaw, L., and Congdon, C.B., 2014. Common features of microRNA target prediction tools. *Frontiers in Genetics*, 5, 23.

Phillips, A.M.J., Tunison, A.V., and Brockway, D.R., 1948. The utilisation of carbohydrates by trout. *Fisheries Resources Bulletin NY*, 11 (44).

Plagnes-Juan, E., Lansard, M., Seiliez, I., Médale, F., Corraze, G., Kaushik, S., Panserat, S., and Skiba-Cassy, S., 2008. Insulin regulates the expression of several metabolism-related genes in the liver and primary hepatocytes of rainbow trout (Oncorhynchus mykiss). *The Journal of experimental biology*, 211 (Pt 15), 2510–8.

Polakof, S., Mommsen, T.P., and Soengas, J.L., 2011. Glucosensing and glucose homeostasis: From fish

to mammals. *Comparative Biochemistry and Physiology Part B: Biochemistry and Molecular Biology*, 160 (4), 123–149.

Polakof, S., Panserat, S., Soengas, J.L., and Moon, T.W., 2012. Glucose metabolism in fish: A review. *Journal of Comparative Physiology B: Biochemical, Systemic, and Environmental Physiology*, 182 (8), 1015–1045.

Pratt, A.J. and MacRae, I.J., 2009. The RNA-induced Silencing Complex: A Versatile Gene-silencing Machine. *Journal of Biological Chemistry*, 284 (27), 17897–17901.

Reinhart, B.J., Slack, F.J., Basson, M., Pasquienelll, A.E., Bettlnger, J.C., Rougvle, A.E., Horvitz, H.R., and Ruvkun, G., 2000. The 21-nucleotide let-7 RNA regulates developmental timing in Caenorhabditis elegans. *Nature*, 403 (6772), 901–906.

Rottiers, V. and Näär, A.M., 2012. MicroRNAs in metabolism and metabolic disorders. *Nature Reviews Molecular Cell Biology*, 13 (4), 239–250.

Roush, S. and Slack, F.J., 2008. The let-7 family of microRNAs. *Trends in Cell Biology*, 18 (10), 505–516.

Rüegger, S. and Großhans, H., 2012. MicroRNA turnover: when, how, and why. *Trends in Biochemical Sciences*, 37 (10), 436–446.

Sangiao-Alvarellos, S., Pena-Bello, L., Manfredi-Lozano, M., Tena-Sempere, M., and Cordido, F., 2014. Perturbation of Hypothalamic MicroRNA Expression Patterns in Male Rats After Metabolic Distress: Impact of Obesity and Conditions of Negative Energy Balance. *Endocrinology*, 155 (5), 1838–1850.

Seiliez, I., Sabin, N., and Gabillard, J.-C., 2011. FoxO1 is not a key transcription factor in the regulation of *myostatin* (*mstn-1a* and *mstn-1b*) gene expression in trout myotubes. *American Journal of Physiology-Regulatory, Integrative and Comparative Physiology*, 301 (1), R97–R104.

Skiba-Cassy, S., Lansard, M., Panserat, S., and Médale, F., 2009. Rainbow trout genetically selected for greater muscle fat content display increased activation of liver TOR signaling and lipogenic gene expression. *American Journal of Physiology. Regulatory, integrative and comparative physiology*,

297 (5), R1421-9.

Subramaniam, M., Weber, L.P., Ching, J.C., Enns, C.B., Kilgour, A.B., Drew, M.D., and Loewen, M.E., 2016. Species Differences in Gastrointestinal Tract Glucose Transporters between Rainbow Trout (Oncorhynchus mykiss) and Nile Tilapia (Oreochromis niloticus) | The FASEB Journal. *Federation of American Societies for Experimental Biology*, 30.

Tijsterman, M. and Plasterk, R.H.., 2004. Dicers at RISC: The Mechanism of RNAi. *Cell*, 117 (1), 1–3.

Tsai, W.-C.C., Hsu, S.-D. Da, Hsu, C.-S.S., Lai, T.-C.C., Chen, S.-J.J., Shen, R., Huang, Y., Chen, H.-C.C., Lee, C.-H.H., Tsai, T.-F.F., Hsu, M.-T.T., Wu, J.-C.C., Huang, H.-D. Da, Shiao, M.-S.S., Hsiao, M., and Tsou, A.-P.P., 2012. MicroRNA-122 plays a critical role in liver homeostasis and hepatocarcinogenesis. *Journal of Clinical Investigation*, 122 (8), 2884–2897.

Wang, W.X., Wilfred, B.R., Hu, Y., Stromberg, A.J., and Nelson, P.T., 2010. Anti-Argonaute RIP-Chip shows that miRNA transfections alter global patterns of mRNA recruitment to microribonucleoprotein complexes. *RNA*, 16 (2), 394–404.

Weber, J.-M. and Shanghavi, D.S., 2000. Regulation of glucose production in rainbow trout: role of epinephrine in vivo and in isolated hepatocytes. *American Journal of Physiology-Regulatory, Integrative and Comparative Physiology*, 278 (4), R956–R963.

Wightman, F.F., Giono, L.E., Fededa, J.P., and de la Mata, M., 2018. Target RNAs Strike Back on MicroRNAs. *Frontiers in genetics*, 9, 435.

Wilczynska, A. and Bushell, M., 2015. The complexity of miRNA-mediated repression. *Cell Death & Differentiation*, 22 (1), 22–33.

Wilding, J.P.H., 2014. The role of the kidneys in glucose homeostasis in type 2 diabetes: Clinical implications and therapeutic significance through sodium glucose co-transporter 2 inhibitors. *Metabolism*, 63 (10), 1228–1237.

Williams, M. and Caino, M.C., 2018. Mitochondrial dynamics in type 2 diabetes and cancer. *Frontiers in Endocrinology*.

Xu, J., Zhang, R., Shen, Y., Liu, G., Lu, X., and Wu, C.-I., 2013. The evolution of evolvability in

microRNA target sites in vertebrates. *Genome research*, 23 (11), 1810–6.

Yan, X., Wang, Z., Bishop, C.A., Weitkunat, K., Feng, X., Tarbier, M., Luo, J., Friedländer, M.R., Burkhardt, R., Klaus, S., Willnow, T.E., and Poy, M.N., 2018. Control of hepatic gluconeogenesis by Argonaute2. *Molecular Metabolism*, 18, 15–24.

Ye, P., Liu, Y.Y., Chen, C., Tang, F., Wu, Q., Wang, X., Liu, C.-G.G., Liu, X., Liu, R., Liu, Y.Y., and Zheng, P., 2015. An mTORC1-Mdm2-Drosha axis for miRNA biogenesis in response to glucose- and amino acid-deprivation. *Molecular Cell*, 57 (4), 708–720.

Zeng, C., Xia, J., Chen, X., Zhou, Y., Peng, M., and Zhang, W., n.d. MicroRNA-like RNAs from the same miRNA precursors play a role in cassava chilling responses.

Zhang, C., Seo, J., Murakami, K., Salem, E.S.B., Bernhard, E., Borra, V.J., Choi, K., Yuan, C.L., Chan, C.C., Chen, X., Huang, T., Weirauch, M.T., Divanovic, S., Qi, N.R., Thomas, H.E., Mercer, C.A., Siomi, H., and Nakamura, T., 2018. Hepatic Ago2-mediated RNA silencing controls energy metabolism linked to AMPK activation and obesity-associated pathophysiology. *Nature Communications*, 9 (1), 3658.

Zhang, H.-M., Kuang, S., Xiong, X., Gao, T., Liu, C., and Guo, A.-Y., 2015. Transcription factor and microRNA co-regulatory loops: important regulatory motifs in biological processes and diseases. *Briefings in Bioinformatics*, 16 (1), 45–58.

Zhao, E., Keller, M.P., Rabaglia, M.E., Oler, A.T., Stapleton, D.S., Schueler, K.L., Neto, E.C., Moon, J.Y., Wang, P., Wang, I.-M., Lum, P.Y., Ivanovska, I., Cleary, M., Greenawalt, D., Tsang, J., Choi, Y.J., Kleinhanz, R., Shang, J., Zhou, Y.-P., Howard, A.D., Zhang, B.B., Kendziorski, C., Thornberry, N.A., Yandell, B.S., Schadt, E.E., and Attie, A.D., 2009. Obesity and genetics regulate microRNAs in islets, liver, and adipose of diabetic mice. *Mammalian Genome*, 20 (8), 476–485.

Zhao, L., Wan, H., Liu, Q., and Wang, D., 2017. Multi-walled carbon nanotubes-induced alterations in microRNA let-7 and its targets activate a protection mechanism by conferring a developmental timing control. *Particle and Fibre Toxicology*, 14 (1), 27.

Zhao, X., Lu, Y., Wang, F., Dou, L., Wang, L., Guo, J., and Li, J., 2014. High glucose reduces hepatic

glycogenesis by suppression of microRNA-152. *Molecular Medicine Reports*, 10 (4), 2073–2078.

Zhu, H., Shyh-Chang, N., Segrè, A. V., Shinoda, G., Shah, S.P., Einhorn, W.S., Takeuchi, A., Engreitz, J.M., Hagan, J.P., Kharas, M.G., Urbach, A., Thornton, J.E., Triboulet, R., Gregory, R.I., Altshuler, D., and Daley, G.Q., 2011. The Lin28/let-7 Axis Regulates Glucose Metabolism. *Cell*, 147 (1), 81–94.

Zhuo, S., Yang, M., Zhao, Y., Chen, X., Zhang, F., Li, N., Yao, P., Zhu, T., Mei, H., Wang, S., Li, Y., Chen, S., and Le, Y., 2016. MicroRNA-451 negatively regulates hepatic glucose production and glucose homeostasis by targeting glycerol kinase-mediated gluconeogenesis. *Diabetes*, 65 (11), 3276–3288.